NASA Conference Publication 3091

Second Conference on NDE for Aerospace Requirements

[illegible] of a conference held at
[illegible], Alabama
[illegible] 1989

NASA

NASA Conference Publication 3091

Second Conference on NDE for Aerospace Requirements

Compiled by
Kenneth W. Woodis
Craig C. Bryson
and Gary L. Workman
George C. Marshall Space Flight Center
Marshall Space Flight Center, Alabama

Proceedings of a conference sponsored by
NASA George C. Marshall Space Flight Center
and the University of Alabama
in Huntsville and held at the
Huntsville Marriott
Huntsville, Alabama
August 22–24, 1989

NASA

National Aeronautics and
Space Administration

Office of Management

Scientific and Technical
Information Division

1990

PREFACE

Marshall Space Flight Center and the University of Alabama in Huntsville are pleased to sponsor the Second Conference on NDE for Aerospace Requirements. We are indebted to the speakers and the attendees for their participation in making the conference highly successful in meeting its goals to foster discussion on NDE and its role in determining the integrity of aerospace systems. NASA and the aerospace industry certainly benefits from participating in such fora to truly proceed forward in providing synergism between the designers, the inspectors and the fabricators in order to provide safer and more reliable aerospace systems.

These proceedings represent only a small part of the information and discussion which occurred at the conference. We hope that those who were unable to attend will appreciate the diversity and significance of what transpired during the conference.

Thanks also go to the Conference Division of Continuing Education for its work in facilitating the conference and to the co-sponsors, the Huntsville Section of ASNT and the Aerospace Division of the Technical Council for ASNT, for their assistance in publicizing the conference.

Sincerely

Kenneth W. Woodis
EH13
Marshall Space Flight Center

Gary L. Workman
Johnson Research Center
University of Alabama in Huntsville

TABLE OF CONTENTS

Conference on NDE for Aerospace Requirements
August 22-24, 1989

We would like to believe that our capabilities to develop nondestructive evaluation and inspection procedures are improving rapidly in order to keep pace with corresponding advances being made in aerospace materials and systems. Thus in order that we maintain our ability to inspect and verify aerospace systems as new technologies emerge, we must allow communication between the materials scientists, designers and NDE engineers who produce current and future aerospace systems. This conference is intended to provide a forum such that communication and discussion between the critical groups in the aerospace industry can occur. The paper presenters and the ensuing discussion among the conference attendees then can stimulate a conscious desire that the new materials and structures be designed in such a way as to be inspectable both during manufacture and in service and to perform reliably over the life cycle of the system.

The aerospace community in Huntsville is proud to be the host for the Second Conference on NDE for Aersospace Requirements. The critical needs of the aerospace industry can be met only if we continue to participate in a objective forum of this magnitude for the benefit of industry and government.

Tuesday, August 22, 1989

8:15 A. M   Keynote Session

Welcoming Remarks: *George McDonough, Director*
Science & Engineering Directorate
Marshall Space Flight Center

Louis Padulo, President
The University of Alabama in Huntsville

Keynote Address: NDE for the Nineties
James Ehl, Deputy Associate Administrator
Safety, Reliability, Maintainabilility and Quality Assurance
NASA/Headquarters

Overview of NDE Research at Langley
Joe Heyman, NASA/Langley

NDE Applications Development at Marshall Space Flight Center
Ann F. Whitaker, NASA/MSFC

10:00 A. M. **Coffee Break**

10:15 A. M. **Session A-2**

A Summary of Computed Tomography Applications at MSFC
Lisa Hediger, NASA/MSFC

Tomography System for Inspection of Turbine Blades
John J. Munro III,R. E. McNuty, R.LInk, R.Grimm, W.Nuding, H.Wiaker
RTS Technology Inc.

Space Shuttle Main Engine Computed Tomography
Richard F. Sporny, Rocketdyne

12:00 **Lunch**

1:15 P. M. **Session A-3**

Review of Açousto-Ultrasonic NDE for Composites
Alex Vary, NASA/Lewis

Acousto-ultrasonic Nondestructive Evaluation of Materials using Laser Beam Generation and Detection
Robert D. Huber and R. E. Green Jr. The Johns Hopkins Universityand Alex Vary and Harold Kautz, NASA/Langley

A New Technique for Ultrasonic NDE of Damage in Thin Composite Laminates
V. K. Kinra and V. Dayal, Texas A&M University

3:00 P.M. **Break**

3:15 P.M. **Session A-4**

Quantitative Ultrasonic NDE of Flaws and Damages in Fiber Reinforced Polymer Composites
David K. Hsu, Iowa State University

Image Correlation NDE of Impact Damage in a Glass Fiber Reinforced Composite
Samuel S. Russell, University of South Carolina

Eddy Current Inspection of Shuttle Heat Exchanger Tube Welds
Casius V. Dodd, Martin-Marietta Energy Systems, Oak Ridge and G.W. Scott and L.D. Chitwood, Martin-Marietta Manned Space Systems

Wednesday, August 23, 1989

8:15 A. M. Keynote Session

Welcoming Remarks: **Larry W. Mixon, Director, Structures Laboratory**
Research, Development and Engineering Center
US Army Missile Command

Keynote Address: NDE and Total Quality Mangement (TQM) for Missile Systems
Truman Howard III, Director
Quality Assurance Directorate/MICOM

The New Army NDE Mantech Thrust Area
Alfred L. Broz and Walter Roy, US Army, Watertown Arsenal

US Air Force NDE Programs - Addressing Tomorrows Aeropace Needs
Charles Buynak, US Air Force, Wright Research & Development Center

10:00 A.M. Coffee Break

10:15 A. M. Session B-2

Acoustic Emission to Determine Air Frame Integrity
John Carlyle, Physical Acoustics Corporation

Predicting The Performance of CT Scanners for NDE Applications
Lowell D. Harris, Bio Imaging Research

Probability of Detection Analysis for X-ray Radiography and Penetrant Inspection Methods
Robert W. Polen, R. J. Brown, R. L. Moreau, and B. N. Ranganthan, Martin-Marietta Manned Space Systems

12:00 Lunch

1:15 P. M. Session B-3

An Automatic Gore Panel Mapping System
John D. Shiver, Martin-Marietta Manned Space Systems

Laser Acoustic Sensing for Inspection of Thermal Protection Tiles
Julio Rodriguez, EG&G Idaho National Energy Laboratory

Cavity Inspection Using Radial Metrology
P. Greguss, Technical U. of Budapest, D. Matthys, Marquette U., John Gilbert, D. Lehner, and A. Kransteuber,University of Alabama in Huntsville

3:00 P. M. Coffee Break

3:15 P. M. Session B-4

PC Based NDE Signal Acquisition and Analysis
Tony Mucciardi, Infometrics

Ultrasonic Correlator Technique for the Inspection of Thick Materials
Doran Kishoni, NASA-Langley/College of William & Mary

NDE of Composite Space Structures
Brian Lempriere, Boeing Aerospace

Requirements for NDE Advancement in Support of Space Systems
Robert W. Neuschaefer, NASA/MSFC

Thursday, August 23, 1989

8:30 A. M. Session C-1

Data Handling for SPIP Workstation
Richard White, Missa Gage, Ben Knutson, and Brian Lempriere, Boeing Aerospace Corporation

NDE Data Applications
Joe Hildreth, Edwards Air Force Base

The Determination of Material Property Values Using Ridge Regression Inversion
W. R. Petrick,L. H. Pearson and J.H. Hartman, Morton Thiokol Inc.

10:00 A. M. Coffee Break

10:15 A. M. Session C-2

Feature Enhanced UT Imaging of Bondlines
Glenn Andrew and Mitch Gregory, SAIC, Inc.

Advanced Technologies for Examination of Coatings
Robert McClung, Consultant

11:45 A. M. Lunch

After lunch there will be a tour of Marshall Space Flight Center NDE Facilities

NDE FOR THE NINETIES

JAMES H. EHL

DEPUTY ASSOCIATE ADMINISTRATOR
OFFICE OF SAFETY, RELIABILITY, MAINTAINABILITY
AND QUALITY ASSURANCE
NATIONAL AERONAUTICS AND SPACE ADMINISTRATION

Good morning, ladies and gentlemen.

It is a pleasure for me to be here today and speak to you on the subject of "NDE for the Nineties."

We know NDE as an indispensable part of modern technology. It is used to measure, analyze, and predict material behavior. It is also used to analyze systems and structures for safety, reliability, and mission assurance. Yet, the concept of NDE dates back to when people first used sight, sound, and other senses to inspect and check out objects for their use.

In this century, the first major event that signalled the advent of modern NDE occurred in the 1930's and 40's, when instruments were developed that enabled us to "see inside" materials. This created a whole new dimension for science and engineering disciplines as well as for human perception. The work of the late Dr. Shockley, Dr. Bardeen, and others on the semi-conductor and transistor were characteristic of the rapid developments that occurred in the electronics industry during and after WWII. These efforts provided the basis for many of the modern tools of NDE.

In the 50's, this new technology was applied to diverse materials, which dramatically increased the resolution of instruments used to measure the materials. These instruments were further refined in the 60's. Also, new passive NDE technologies were introduced in the 60's, including interferometric concepts.

In the 80's, modern NDE has made another leap forward with the applications to new, sophisticated materials--many of which are anisotropic; and with unique applications such as for the Shuttle. So today's NDE methods and their interpretations have become increasingly complex. This evolution has made NDE a vital part of the space program. The use of NDE techniques has provided information that could not have been obtained by any other means.

For example, NDE provides much of the data needed to satisfy launch safety requirements for critical systems on the Shuttle. Some of the NDE applications that have been used for the Shuttle include:

- An ultrasonic technique to measure bondline integrity for inhibitor insulation and fuel interface for the Shuttle solid rocket motors;

- An ultrasonic bolt monitor to measure preload in fasteners such as used on the Shuttle wheels, nozzle, and attachment bolts; and

- Thermal imaging technology to determine the integrity of the inhibitor in the solid rocket motor.

These applications reflect the use of NDE as primarily a detection and inspection tool. NDE is also emerging as a valuable tool in other areas including the evaluation of complex materials such as composites and the verification of aerospace systems.

NDE in the 90's and beyond will require a full understanding of the physical properties of complex materials. We will need to ensure that NDE testing parameters continue to produce quantifiable test results that are reliable and repeatable. We need to understand the underlying physical principles of what is occurring as we perform the test and evaluation. What do the results mean? How should we interpret the information? As the requirements for NDE change in response to emerging technologies, NDE will have to develop procedures to keep pace. NDE will have to function as a scientific discipline.

Less than one year ago, NASA dedicated the NDE Research Laboratory at the Langley Research Center. This facility is important because it represents NASA's commitment to the future of NDE as a science. The primary objective of the Laboratory's research staff is to advance the state-of-the-art by developing a quantitative base for NDE measurement sciences, process sensors, and material characterization.

As a scientific discipline, NDE findings will be based on an understanding of the underlying physics of the observed effects. Quantitative measurements will provide real engineering data about material and structural performance.

Our intent is to bring together the necessary expertise to integrate physical and measurement sciences in a multi-discipline approach, which will provide a national focus for NDE technology. Fortunately, the field of measurement sciences is making great progress in developing new techniques to acquire the information we need. The application of ultrasonics, thermal imaging, acoustic emissions, laser holography, and tomography are examples of some methods that are being developed.

We also intend to develop relationships with other research groups/individuals and users to promote and assist the application of laboratory concepts and techniques to real-world problems.

In meeting the real-world problems of the Shuttle, a great deal of space age NDE technology was developed in real-time. This required an extraordinary level of cooperation and teamwork on the part of Langley, Marshall, and the contractors working the problems. The interaction between these organizations and people in this context created an environment that led to advancements in NDE technology that perhaps would not have happened otherwise.

Cooperative efforts such as these will enable the transition to the next logical phase, which is on-orbit NDE. As we look to the near-term future in space, on-orbit NDE for the Space Station Program as well as for the manned expeditions projected by President Bush represents a significant challenge. It also presents a singular opportunity to be on the leading edge of our ability to understand the physics of observed phenomena and then to translate this understanding into the design process.

Extremely long in-space operating life-times, complex interactive systems and subsystems, and a hostile operating environment will require a level of engineering detail and understanding that previously has not been necessary. The challenge for NDE in satisfying this requirement is formidable.

The challenge for the 90's will be to apply NDE techniques to potential major and minor failures of structures and structural elements, leaks, and degradation of all systems and subsystems over time and under conditions with which we have a very limited experience base.

This challenge is magnified by constraints such as operating in the vacuum of space and under micro-gravity condition, outgassing limitations, portability, transportability, ease of operation, weight, size, sensitivity, and power requirements--to name a few. The challenge will require the application of novel NDE concepts, so that the playing field is wide open.

It really depends on you--your creativity, dedication, and resourcefulness. Scanning the topics to be discussed at this conference as well as the credentials of the participants, it is apparent that you have the expertise and the understanding needed to evolve NDE to the level of a science. This will not happen overnight or in one giant leap forward; it is much more likely to occur in increments. As 16th century philosopher, Montaigne (Mon-tanye) noted in his famous Essays:

> "...sciences are not cast in a mould, but are formed and perfected by degrees, by handling and polishing..."

It is a matter of setting our goals toward this end and dedicating ourselves to meeting the challenges as they arise.

It is apparent that to continue advancing NDE technology, you who are the acknowledged experts in the field, must have the dedicated support of NASA management. It also seems apparent that the critical need for NDE in the 90's and beyond is an integral part of what

NASA management views as the critical need to ensure the Safety, Reliability, Maintainability, and Quality Assurance aspects of future missions and systems.

NASA management's commitment to the total SRM&QA Program can be seen in the increases in the resource that NASA places the highest value on--the civil service workforce. The number of NASA personnel devoted to SRM&QA functions is almost 40 percent greater than in previous years. In addition, the NASA SRM&QA contractor workforce has increased substantially over the same time period.

Extensive organizational changes have been made throughout the Agency to clearly define SRM&QA roles and responsibilities as well as to enhance communication and cooperation at all levels. The objective is to maintain <u>long-range</u> policies and programs that speak to the future and also satisfy today's needs.

To this end, we are undertaking initiatives to identify key areas for improved technical capabilities and to develop projects in selected areas. Such projects will include materials treatments and processes, inspection and control of multi-layer board design and fabrication, inspection and quality control for microcircuits and semiconductors, methods for fracture control, and electronic packaging technology.

We are also encouraging the use of new NDE inspection and quality control techniques to evaluate the integrity of advanced designs, complex materials, integrated electronics, and manufacturing processes.

We are making this commitment because we recognize that current and future SRM&QA

requirements translate to the need for a strong and energetic NDE capability within the Agency.

In closing, I would like to salute each of you for what you have accomplished to date. I look forward to working with you in the future. With the increasing complexity of our missions particularly for the manned expeditions, it is imperative that we continue to stress NDE for NASA programs and projects.

To quote a modern philosopher, Robert Pirsig:

> "The whole purpose of scientific method is to make valid distinctions between the false and the true....so as to obtain an objective, true picture of reality."

This is the essence of NDE in the 90's and in the 21st century.

Thank you for your attention.

N91-18190

DEVELOPMENT AND APPLICATIONS OF NONDESTRUCTIVE EVALUATION AT MARSHALL SPACE FLIGHT CENTER

SURFACE INSPECTION FACILITY:

The Surface Inspection Facility provides magnetic particle, penetrant, and remote visual inspection capabilities. Both in-plant and field inspection capabilities exist for all three techniques. The permanent lab facilities include a large fixed magnetization station for magnetic particle inspection, a well-ventilated penetrant inspection station with dark room and microscopic viewing capability, and a photographic laboratory to provide documentation of any surface inspection performed. A wide variety of portable equipment is available for field inspections. These include: both stiff and flexible-leg magnetizing yokes and field strength instruments for magnetic particle inspection, portable penetrant systems, and more than two dozen flexible/rigid borescopes and fiberscopes.

TYPICAL INVESTIGATIONS:

* Detection of surface and near-surface cracks in weldments
* Detection of seams and foldovers in castings
* Monitoring of bearing wear during SSME operations
* Detection of structural failure in tie-down hardware

ADVANCED COMPUTED TOMOGRAPHY INSPECTION STATION (ACTIS) :

ACTIS is a state-of-the-art computed tomography facility which uses digital x-ray technology to produce cross-sectional images of space components nondestructively. ACTIS utilizes four x-ray sources, a high-speed array processing computer, and variable system geometry to allow optimization for virtually any test object up to 4 feet in diameter. Image processing capabilities include: solids modelling, multiplanar reconstruction, and a wide variety of statistical and data display options. Images may be archived to either 1600 bpi magnetic tape or 2 gigabyte optical disk as desired. Raw scan data may be archived to optical disk for later recall.

TYPICAL INVESTIGATIONS:

* Characterization of flaws in composite materials
* Detection of inhomogeneities in metal castings
* Verification of internal geometry
* Development of acceptance criteria for SRM nozzle

NDE DATA EVALUATION FACILITY:

The NDE Data Evaluation Facility provides the capability for mapping NDE data from any source (within or outside MSFC) and mapping it into a common frame of reference. The data may then be directly compared to each other or to other data sets, such as

ORIGINAL PAGE
BLACK AND WHITE PHOTOGRAPH

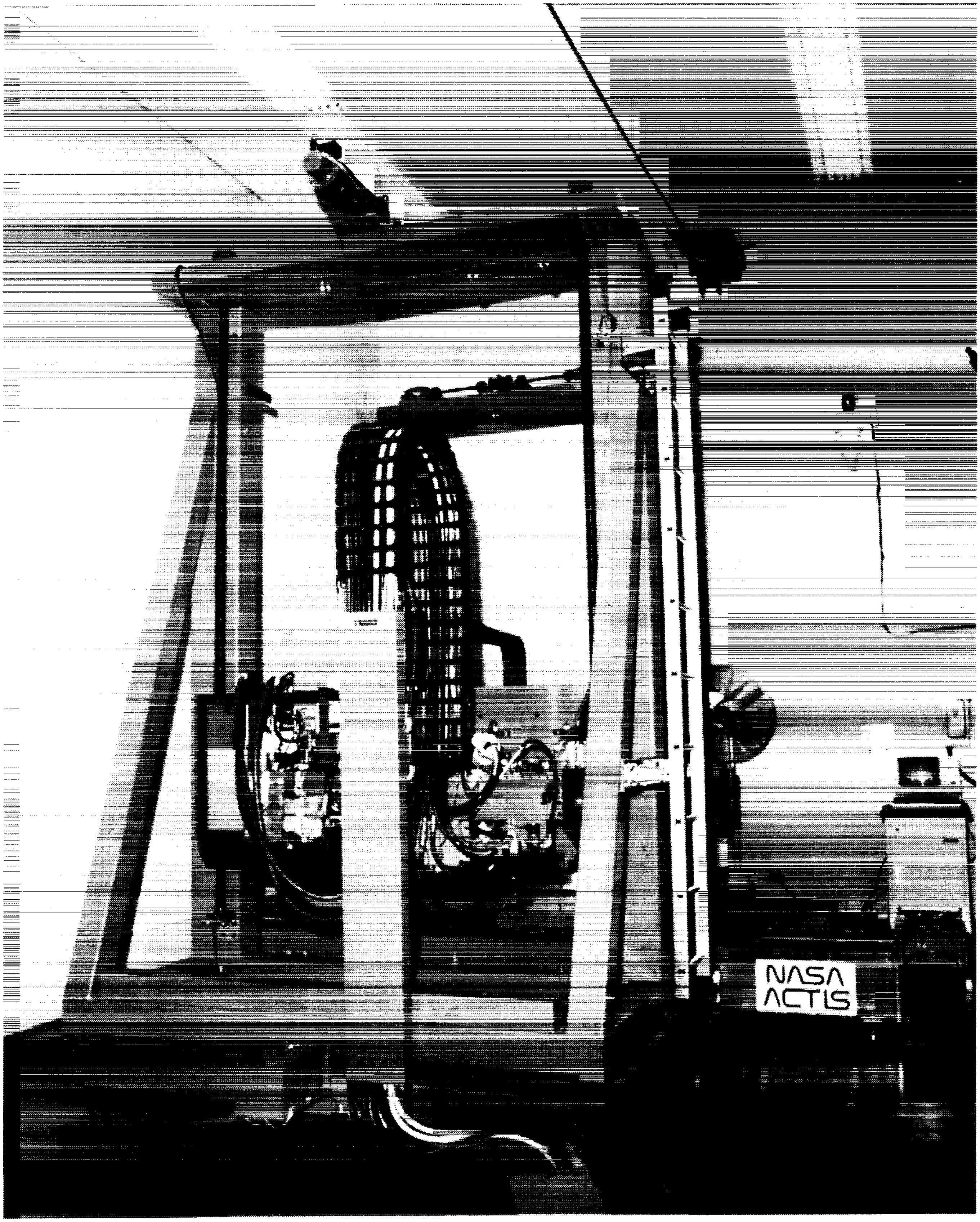

MSFC COMPUTED TOMOGRAPHY SYSTEM

mechanical test data. Additional capabilities such as mechanical test cutting plan development, statistical analyses, and the correlation of NDE to materials properties are also provided. These capabilities are provided primarily by the Integrated NDE Data Reduction System (INDERS), a network of three digital computers and specialized software. The center of the network is the MicroVAX II computer, which is capable of handling large data sets with relative speed. One IBM AT and one Tektronix 2330 Workstation allow some off-line processing of smaller data sets.

TYPICAL INVESTIGATIONS:

* Inspection of SSME turbine blades for microporosity
* Post-fire evaluation of PAM nozzles
* Development of acceptance criteria for SRM nozzle
* Development of materials properties for carbon-carbon

THERMOGRAPHIC TEST DEVELOPMENT FACILITY

Thermography is and NDE technique which makes use of an infrared camera system and digital image processor to monitor the infrared energy emission from the surface of a part under investigation. The system is capable of resolving minute temperature variations, of as little as 0.1 degrees C. The image processor utilizes a number of image enhancement techniques to increase temperature difference resolution.

TYPICAL INVESTIGATIONS:

* Detection of subsurface disbond conditions in samples representative of the SRM
* Detection of ice formation on the surface of the ET
* Detection of ice during warm up of cryo-cooled SSME turbopump shafts

RADIOGRAPHIC TEST FACILITY

The Radiographic Test Facility, comprised of a radiation-shielded cell and adjacent control room, film processing rooms, and a film reading area, provides the capability of radiographic evaluation of hardware. Portable lower energy x-ray generating units are located in the facility, as well as permanently mounted units capable of producing 150 kev and 320 kev x-rays. Processed film radiographs are analyzed in the film reading area to detect possible defects in the parts under investigation.

TYPICAL INVESTIGATIONS:

* Evaluation of welding processes
* Assessment of internal configuration
* Detection of materials anomalies
* Determination of structural integrity

REALTIME RADIOGRAPHIC TEST FACILITY

Realtime radiography (RTR) eliminates the use of film by replacing it with an image intensifying unit and video system, allowing viewing of a radiographic image on a video monitor while x-rays are passing through the test specimen. The specimen is placed within a radiation-shielded cabinet, and x-rays are generated by a microfocus x-ray tube with a maximum energy of 160 kev. The microfocus tube can be used to produce magnified images of up to 80X. A computer is also an integral part of the system and equips it with the capability of digitizing and enhancing images received from video.

TYPICAL INVESTIGATIONS:
* Detection of flaws in composite parts
* Examination of electrical components
* Determination of internal dimensions
* Failure analyses support

EDDY CURRENT RESEARCH FACILITY

The Eddy Current Research Facility provides the capability to perform critical development of eddy current applications for various aerospace components. Specific capabilities include: measurement of materials surface conductivity, determination of thickness of films and coatings, interrogation of material inhomogeneity, and detection of surface or near-surface crack-like flaws. Refinements in eddy current tooling and adapters have led to improved detection of flaws in previously inaccessible locations.

TYPICAL INVESTIGATIONS
* Nickel/Hydrogen battery cell girth weld investigations
* Weld wire material sorting
* Advances in SSME heat exchanger weld inspection
* Improved detection of flaws in clevis pins

ACOUSTIC EMISSION MONITORING SYSTEM

The Acoustic Emission Monitoring System makes use of transient electrical energy that is spontaneously released when materials deform, fracture, or are subjected to stress. Sensors are placed on the test object and are connected to an acoustic processor. The processor monitors both the amplitude and number of events (instances of energy releases) that occur during the test. The amplitude and number of events are displayed on the processors CRT and also in hardcopy form through a strip chart recorder.

TYPICAL INVESTIGATIONS
* FWC Structural Test Article Hydrostatic Test Monitoring
* OMV Composite Tank Test Monitoring
* Carbon-Carbon Nozzle Hydroburst Monitoring
* Monitoring of Test Stand Pressure Vessels and High

Pressure Lines

ADVANCED ULTRASONIC TEST STATION (AUTS)

AUTS was designed for ultrasonic inspection of composite material symmetrical components, with an operational envelope of 8" to 48" diameter and 2 to 15 foot length. Filament wound motor cases and bottles, wound in the adjacent Productivity Enhancement Facility and SRM sub-scale components were primary targets of capability development. The AUTS employs a dual water squirter coupling mode, as well as an air-coupling mode. The system has remote manipulation capability for both transducers and can be operated in the through-transmission or pulse-echo modes. Scan data is displayed in color or gray scale at the control console. Digital, amplitude, or time-of-flight information is displayed and stored, along with C-scan and depth data. Flaw resolution is 0.250" diameter in 3" of graphite epoxy.

TYPICAL INVESTIGATIONS

* PAM-D Exit Cone Evaluation
* Composite Ballistic Environment Generator (BEG) Motor Cases
* Solid Propulsion Processing Technology Investigations
* Materials Characterization Investigations

ULTRASONICS TEST FACILITY

The Ultrasonics Test Facility consists of both hand scan contact and immersion noncontact ultrasonics used in the interrogation of internal anomalies and bondline integrity. The immersion capability is quite versatile, providing a capability to perform either through-transmission or single-side pulse echo scanning of flat panels or cylindrical and conical shaped objects. The microprocessor controlled system produces hardcopy ultrasonic data displays in flat X-Y or polar scans. Portable contact ultrasonic inspection equipment provides a capability to ultrasonically interrogate hardware too large for the immersion tank, or materials that cannot be immersed.

TYPICAL INVESTIGATIONS

* Detection of cracks in weldments
* Characterization of anomalies
* Impact damage tolerance studies
* Internal characteristics of plates and castings

ORIGINAL PAGE
BLACK AND WHITE PHOTOGRAPH

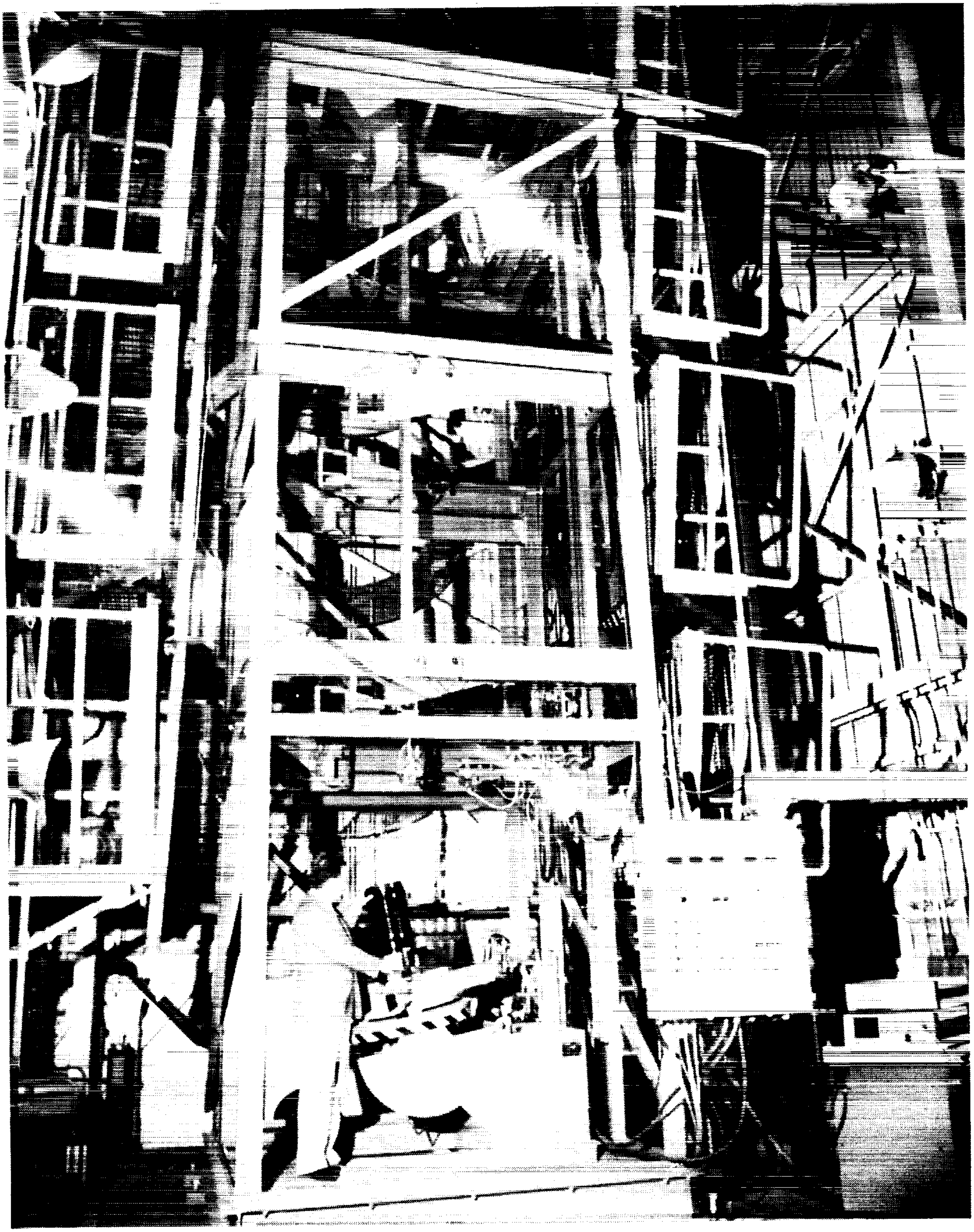

MSFC AUTOMATED ULTRASONICS STATION

COMPUTER CONTROLLED SCANNING/OPTICALLY STIMULATED ELECTRON EMISSION SURFACE CONTAMINATION MEASUREMENTS

Computer controlled contamination scanning (CONSCAN) is a system developed by MSFC utilizing the optically stimulated electron emission (OSEE) technique for scanning solid rocket motor (SRM) cases for surface contamination prior to critical bonding operations.

The CONSCAN system has the principal advantages of providing the sensitivity and spacial resolution necessary when scanning large areas, to ensure that surfaces are sufficiently free of contaminants that reduce bond strength.

Scanning the surface with the CONSCAN provides a map of surface contamination levels, which clearly identifies those areas that require further cleaning; rescanning after the additional cleaning operation provides results of that recleaning. This data provides a permanent record of surface cleanliness levels. This record may be used at a later date to help identify the specific process during which contamination occurred and to correlate surface cleanliness levels with subsequent debond locations.

Principle of operation of the OSEE may be briefly described as follows. When a surface is exposed to ultraviolet (UV) light of sufficient energy, photoelectrons will be released from the surface. Contaminants on the surface will normally reduce the number of these photoelectrons which are emitted. The OSEE sensor has two major components: the electron UV light source and the electron collector. The photoelectron current emitted from the irradiated surface is measured by the electron detector. This current can be calibrated to the contaminant level on the surface.

The technique as applied to measuring contaminants on surfaces was developed and reported by Tennyson Smith in April 1975. He demonstrated both the sensitivity of the technique to contaminant level and bond strength variation due to contamination.

The technique with MSFC support was utilized on the External Tank foam debond study in 1979. This technique was instrumental in identifying the surface contaminant causing debonds as being silicone which originated from simultaneous processing of other hardware in the same building.

Since the original instrument configuration in 1979, significant OSEE instrument improvements have been implemented, including: increased signal amplification, noise filtering, higher output UV light sources, compact sensor configurations, and computer data analysis.

MSFC initiated a study of the SRM debonds associated with propellant liner insulation to case, and the carbon and glass phenolics used in the nozzle. Research studies determined that the corrosion; protective HD-2 grease used on the SRM case has a significant effect on bond strength. Quantitative levels that affect bond strength and associated OSEE signal levels were determined by extensive laboratory testing. This calibration data was incorporated in the design, development, and implementation of the CONSCAN system.

ORIGINAL PAGE
BLACK AND WHITE PHOTOGRAPH

N91-18191

SPACE SHUTTLE MAIN ENGINE COMPUTED TOMOGRAPY APPLICATIONS*

R. F. Sporny
Rocketdyne Division, Rockwell International
Canoga Park, California 91304

ABSTRACT

For the past 2 yr, the Rocketdyne Division of Rockwell International, with the support of the Marshall Space Flight Center, has been evaluating the potential applications of computed tomography to the fabrication and overhaul of the Space Shuttle Main Engines. Application tests were performed at various government and manufacturer facilities with equipment produced by four different manufacturers. The hardware scanned varied in size and complexity from a small temperature sensor and turbine blades to an assembled heat exchanger and main injector oxidizer inlet manifold. The evaluation of capabilities included the ability to identify and locate internal flaws, measure the depth of surface cracks, measure wall thickness, compare manifold design contours to actual part contours, perform automatic dimensional inspections, generate 3-D computer models of actual parts, and image the relationship of the details in a complex assembly. The capabilities evaluated, with the exception of measuring the depth of surface flaws, demonstrated the existing and potential ability to perform many beneficial Space Shuttle Main Engine applications.

INTRODUCTION

The Computed Tomography (CT) effort at Rocketdyne began in 1987 with a special 1-yr task assignment from National Aeronautics and Space Administration Marshall Space Flight Center (NASA-MSFC) to evaluate current state-of-the-art industrial CT and its potential as a nondestructive test method for Space Shuttle Main Engine (SSME) hardware. Due to the very promising results of the initial task, a follow-on 1-yr task was assigned to continue evaluating the application of CT to the SSME hardware and to better define the capabilities and limitations of CT. As various applications were evaluated, the results highlighted another potential application. As a result, CT has, potentially, a much greater use on SSME hardware than initially expected.

This report contains an overview and highlights of the CT SSME application evaluations since 1987.

APPLICATIONS

TURBINE BLADES

Turbine blades were the first actual SSME hardware scanned with CT. The purpose of the evaluation initially was to determine whether a single Digital Radiography (DR) mode scan could replace our current film radiography, which requires eight exposures to inspect the various thicknesses of the blade material. This effort was very successful. It was determined that the CT system was able to locate all of the casting flaws that were detectable by the conventional method. Additionally, CT could distinguish between actual flaws and grain solidification patterns and locate microshrinkage that was undetected previously. Figure 1 shows a CT image of turbine blade casting microshrinkage and a 50X photograph of a metallographic cross section at the same location.

To evaluate the modeling capability, a turbine blade was scanned in 152 CT slices. These raw CT data were transferred to Rocketdyne's CAD-Computer Vision system. Figure 2 shows the initial 3-D model of the turbine blade and Fig. 3 shows the transparent model of the fir tree area containing microshrinkage porosity.

Although not initially considered as an application, results appeared to indicate that the CT system could perform dimensional inspections of the turbine blades. The system was calibrated using blades with known dimensions. The blades to be measured were then scanned in both the CT mode and DR mode as required to image the area to be measured. The dimensions were then taken by manually placing the cursors at the dimension end points and the system then calculated the distances. Figures 4, 5, 6, 7, and 8 show the various images of a turbine blade and the dimensions taken. The dimensional accuracy was found to be within 50.8 µm (0.002 in.) of the conventional measurements. It is believed that, when the CT software to automate the internal flaw detection and dimensioning is completed, the turbine blade inspection time will be reduced from the current 4 h per blade to approximately 4 min.

The turbine blade CT scanning was accomplished on a General Electric XIM system located in the GE NDE Systems and Services facility in Cincinnati, Ohio.

*This work was performed under Contract NAS8-40000 with NASA-MSFC in Huntsville, Alabama.

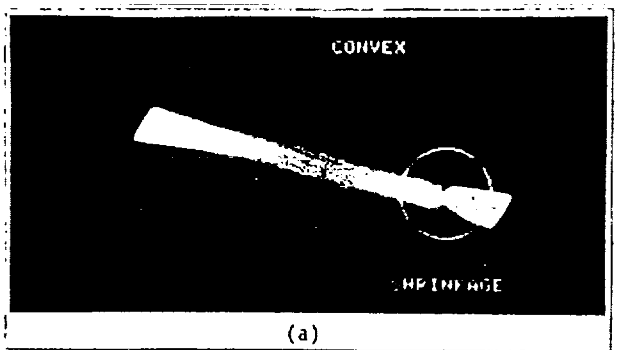

Figure 1a. CT Slice of Turbine Blade Showing Shrinkage and Metallographic Section at the Same Location

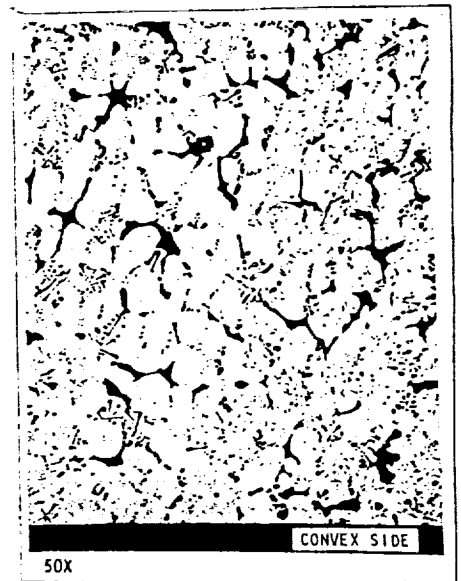

Figure 1b. CT Slice of Turbine Blade Showing Shrinkage and Metallographic Section at the Same Location

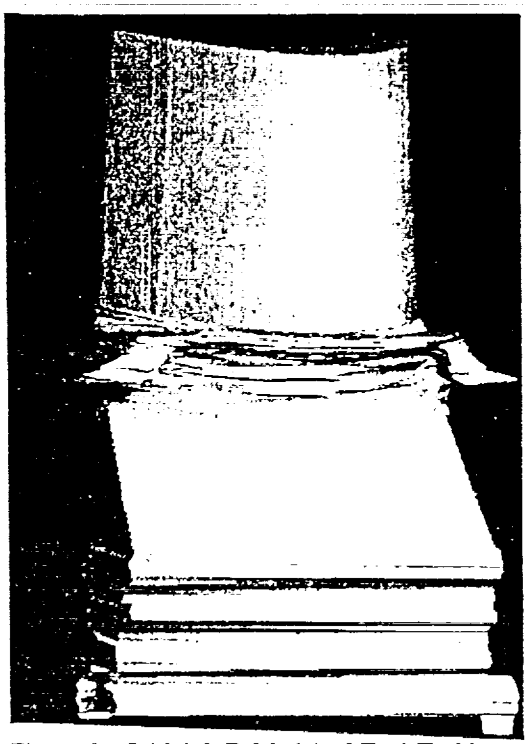

Figure 2. Initial 3-D Model of Fuel Turbine Blade on CAD/CAM System

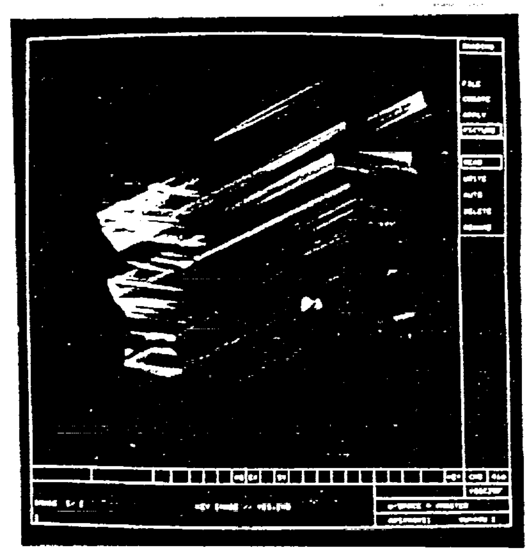

Figure 3. 3-D Model of the Fir Tree Area Containing Microshrinkage Porosity on CAD/CAM System

ORIGINAL PAGE IS OF POOR QUALITY

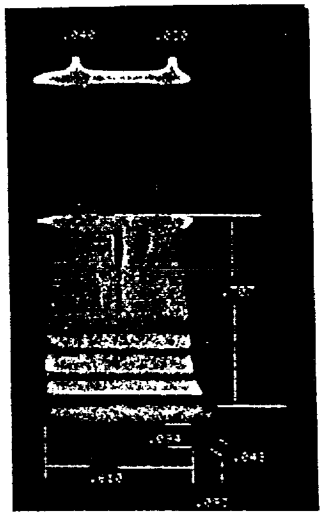

Figure 4. Digital Radiograph of Turbine Blade Used for Dimensional Measurements

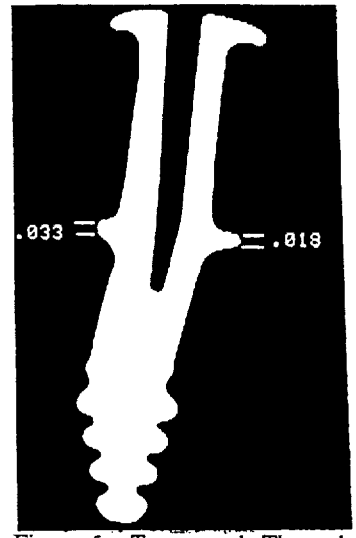

Figure 5. Tomograph Through Blade Vertical Axis With Platform Measurements

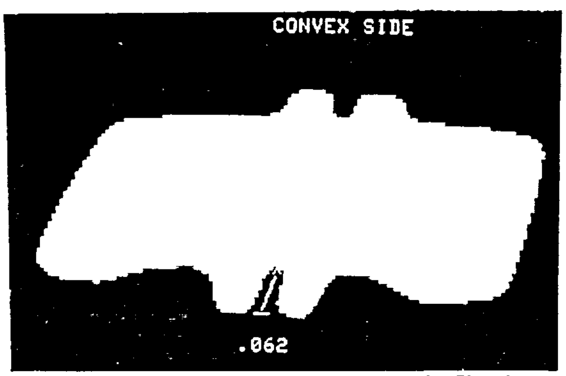

Figure 6. Tomograph Through Blade Shank Showing Damper Pocket Depth

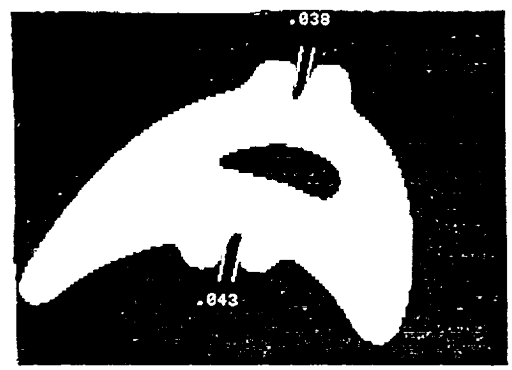

Figure 7. Tomograph Through Shank Showing Damper Pocket Widths

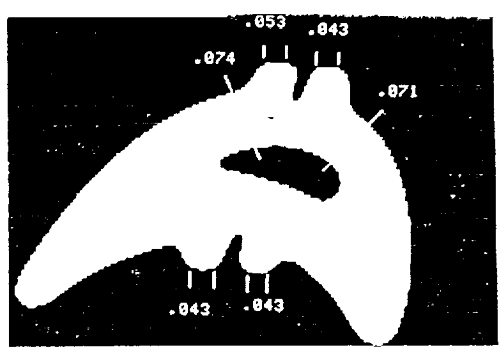

Figure 8. Tomograph Through Shank Showing Wall Thicknesses and Damper Pocket Sidewall Thicknesses

TEMPERATURE SENSOR

A sketch of the SSME hot gas temperature sensor is shown in Fig. 9. The active part of the sensor is the element, which consists of a 17.78-µm- (0.0007-in.-) dia platinum (Pt) wire wound around an aluminum oxide covered Pt tube and then covered with a Pt tubular cover. The spacing between the windings of the element is nominally 63.50 µm (0.0025 in.). The element is 1.52 mm (0.060 in.) dia and is installed in the sensor body, which is approximately 6.35 mm (0.250 in.) dia with a 1.27-mm (0.050-in.) wall. The sensor body is machined from Inconel 625 high nickel alloy.

One sensor developed an intermittent shorting condition during an engine test. Engineering believed that the failure might be caused by the element winding spacing being less than required, which allowed adjacent windings to touch. An attempt was made to identify a nondestructive test method to measure the element spacing prior to any disassembly of the part. Conventional radiographic and microfocus methods were unable to penetrate the element's Pt enclosure.

Inspection using CT was then attempted. The sensor was inspected by Scientific Measurement Systems, Inc., using their Model 101B CT scanner located in their Austin, Texas, facility. A 420-kV source was used to operate the system in the DR mode. Various columnator arrangements were tried until a combination was found to produce a spatial resolution of 12.20 µm (0.0005 in.), necessary to image the windings. Figure 10 shows the high-resolution DR image of the element windings. The spacing between the windings was then measured by making an opacity (density) trace through the windings, as shown in Fig. 11. The individual peaks in the trace correspond to the element wires. The results of the dimensional analysis of the wire spacing is shown in Table I. The accuracy of the measurements is ±2.54 µm (0.0001 in.). Spacings between the windings were found to be correct and, therefore, probably eliminate winding shorts as the source of the problem.

WELDED MANIFOLD PROFILE MEASUREMENT

The Rocketdyne Robotic Welding Development Group requested that CT be applied to measure the weld mismatch and profile on the sample assembly being used to qualify robotic welding for use on the SSME main injector oxidizer inlet manifold. Figure 12 shows a sketch of the assembly. The stress department was also concerned about the amount of distortion to the manifold shape that may have occurred as a result of the welding. The assembly was scanned in the CT laboratory at NASA-Kennedy Space Center. A CT scan was performed through the vertical centerline of the inlet flange. Figure 13 shows the CT image, and Fig. 14 shows

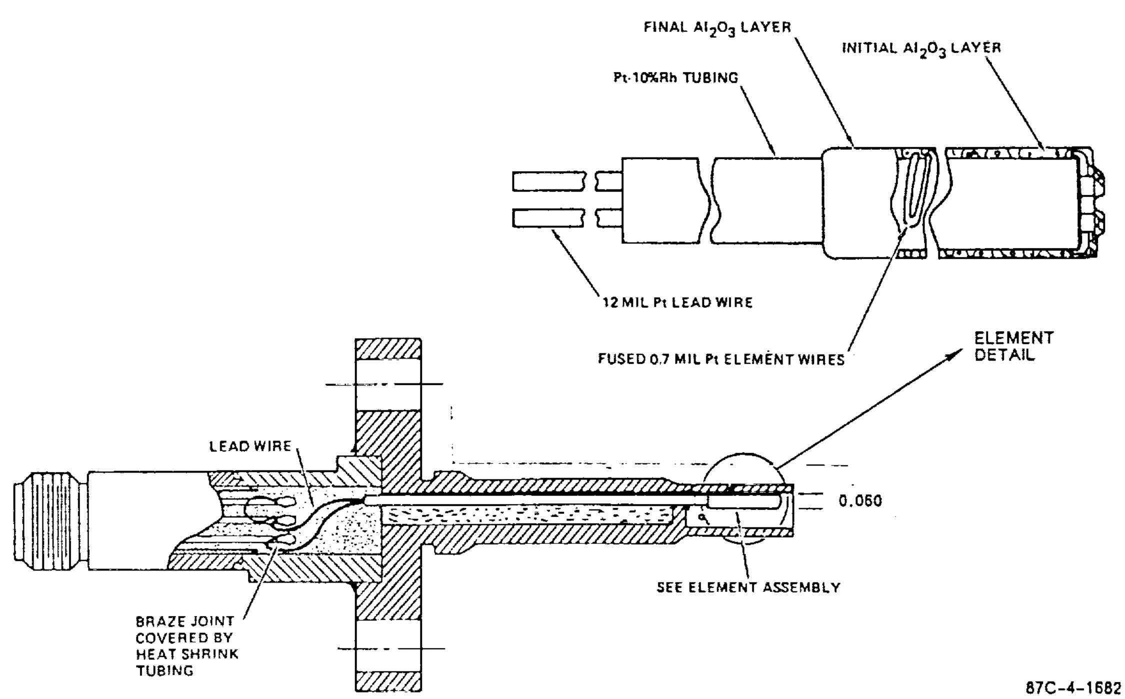

Figure 9. Temperature Sensor Sketch and Element Details

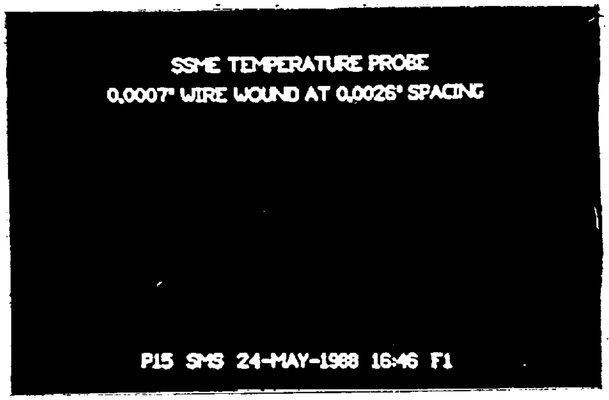

Figure 10. High Resolution DR Image of Element Showing Windings

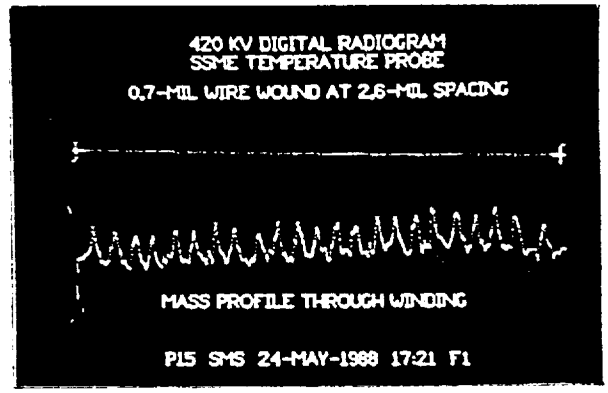

Figure 11. Opacity Scan Through Windings Used to Measure Spacing

Table I. Spacings Between Windings

Interval	Spacing	Interval	Spacing
1	77.978 µm = 0.00307 in.	12	69.342 µm = 0.00273 in.
2	72.644 µm = 0.00286 in.	13	72.644 µm = 0.00286 in.
3	63.754 µm = 0.00251 in.	14	74.168 µm = 0.00292 in.
4	81.280 µm = 0.00320 in.	15	66.294 µm = 0.00261 in.
5	63.500 µm = 0.00250 in.	16	70.612 µm = 0.00278 in.
6	77.470 µm = 0.00305 in.	17	57.150 µm = 0.00225 in.
7	65.278 µm = 0.00257 in.	18	87.376 µm = 0.00344 in.
8	86.614 µm = 0.00341 in.	19	70.612 µm = 0.00278 in.
9	69.088 µm = 0.00272 in.	20	67.310 µm = 0.00265 in.
10	70.612 µm = 0.00278 in.	21	70.104 µm = 0.00276 in.
11	68.072 µm = 0.00268 in.	22	101.600µm = 0.00400 in.

the enlarged detail of one of the two weld joints. Figure 15 shows the cross section reduced to a profile outline. It was determined that this CT-generated profile could be overlaid on the CAD profile data and used by the stress engineers to evaluate the presence and extent of any distortion of the manifold.

HEAT EXCHANGER ASSEMBLY

A heat exchanger assembly removed from an SSME was chosen to evaluate the capability of CT to image and measure details within a complicated assembly. Figure 16 shows a sketch of the heat exchanger assembly. The outer bowl is an Inconel 718 forging with an average thickness of 19.05 mm (0.750 in.). The liner is Inconel 903-formed sheet material 2.29 mm (0.090 in.) thick. The primary tube is 4.83 mm (0.190 in.) dia 316 CRES with 317.5 µm (0.0125 in.) wall, and the secondary tubes are 9.53 mm (0.375 in.) dia 316 CRES with 0.71 mm (0.028 in.) walls. The scans shown were made on an ARACOR system during its acceptance testing at Hill Air Force Base. The scans were made using a 2-MeV source and a scan time of 135 s. Figure 17 shows a CT slice through the assembly, including the threaded studs that mount one of the engines turbopumps. Figure 18 shows a CT section through the most critical area of the heat exchanger; i.e., primary tube weld RS008812 3 (see Fig. 16). This heat exchanger had been removed and scrapped due to known thinning of the tube wall in this weld area. Microfocus radiography had been used to locate and estimate the thinning. It was believed that the 317.5 µm (0.0125 in.) nominal wall thickness had been reduced to 152.4 µm (0.006 in.) on one side of the tube. A series of eight scans was made along the cursor line shown in Fig. 18 with the first and last scan through the opposite tube walls and the remaining scans spaced equally across the tube diameter; approximate scan spacing was 0.635 mm (0.025 in.) (see Fig. 19).

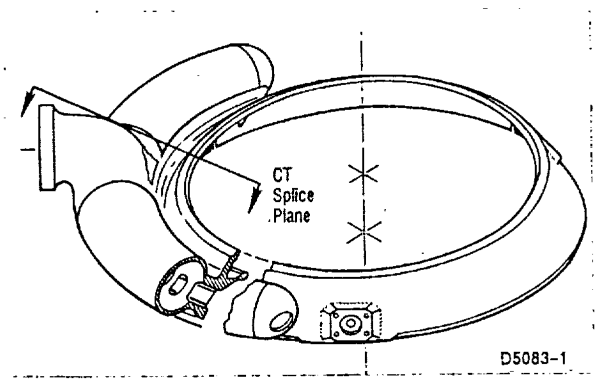

Figure 12. SSME Main Injector Manifold Assembly

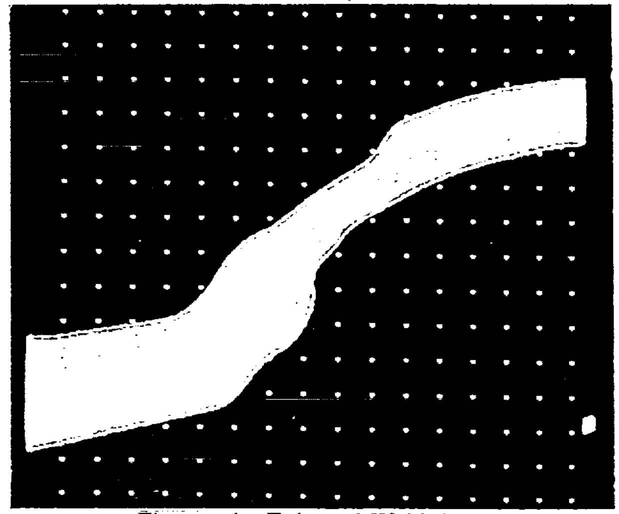

Figure 14. Enlarged Weld Area

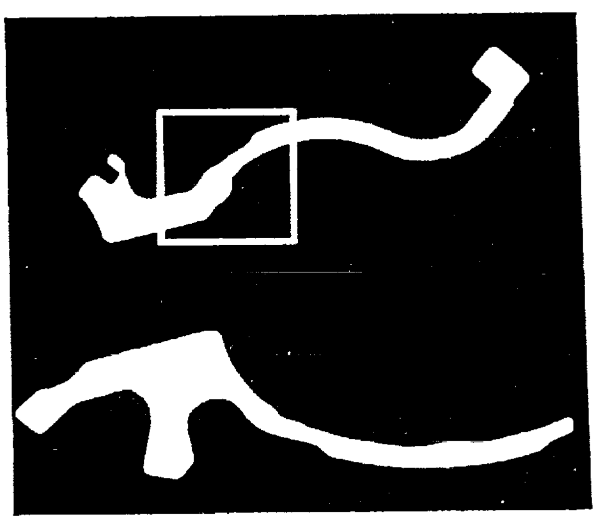

Figure 13. CT Image Through Flange Centerline

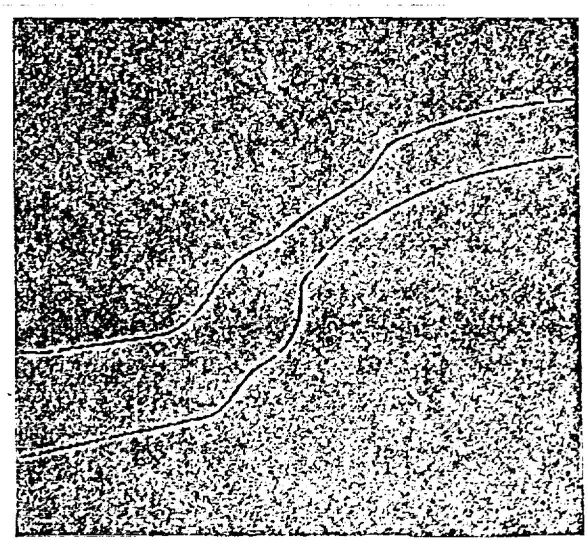

Figure 15. Image Reduced to Profile Outline

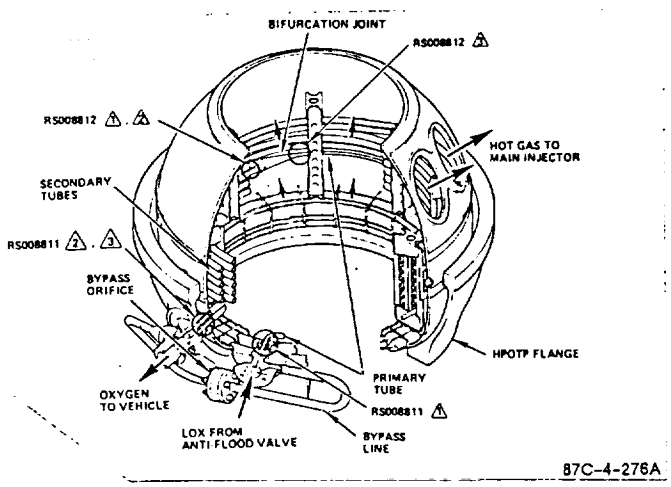

Figure 16. Sketch of Heat Exchanger Assembly

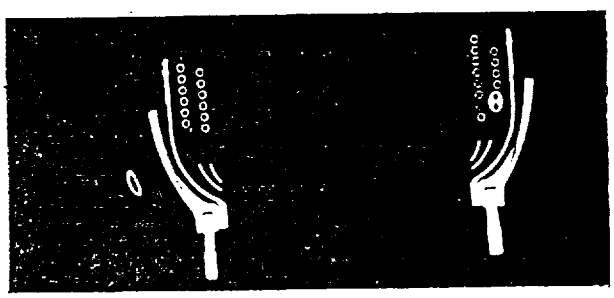

Figure 17. CT Slice Through SSME Heat Exchanger Assembly

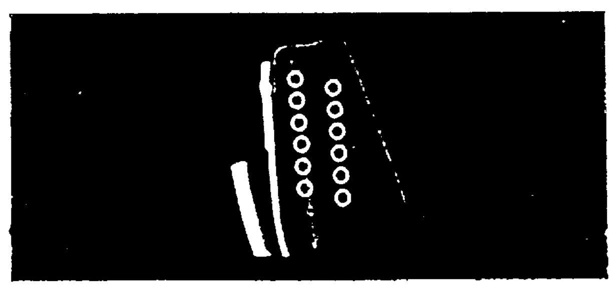

Figure 18. Enlarged Image of CT Scan Through Critical Weld Joint Area

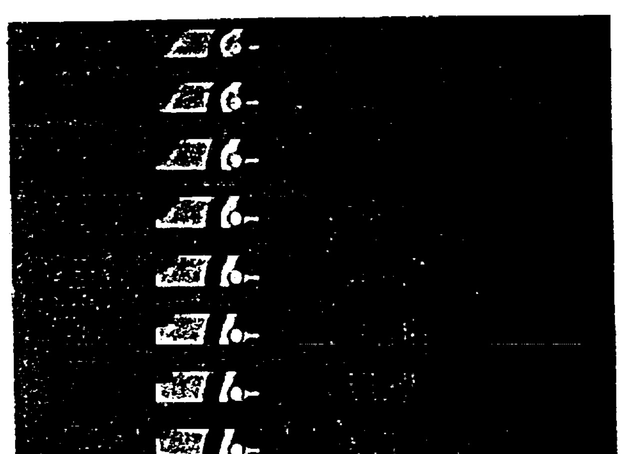

Figure 19. Series of CT Images at 0.635 μm (0.025 in.) Intervals Through Critical Weld Joint Showing Tube Wall Thinning

ORIGINAL PAGE IS
OF POOR QUALITY

Note the tube wall thinning apparent in the small tube toward the middle of the images. An analysis of the reconstructed images revealed the remaining tube wall to be 144.8 μm (0.0057 in.) at its thinnest point. Subsequent metallographic sectioning and measurements of the thinned tube determined the actual thickness to be 139.7 μm (0.0055 in.).

CONCLUSION

The 2-yr study of CT applications on the SSME hardware demonstrated the potential of CT as a very powerful diagnostic and inspection tool. The uses of the equipment seem to be limited only by the user's imagination and rapport with the CT equipment manufacturer. The relationship with the equipment manufacturer is vital, since many of the innovative applications require a software or hardware modification most effectively accomplished by working with the developer-supplier of the CT equipment. One of the most unexpected results of this study was the tremendous increase in value to the SSME program that evolved. Whereas CT was initially being evaluated as only an advanced flaw detector, its other capabilities to image, measure, and evaluate hardware characteristics that currently cannot be inspected by nondestructive means are of tremendous import to the SSME program.

N91-18192

Prepared for University of Alabama and ASNT Conference on
Nondestructive Evaluation for Aerospace Requirements
August 22-24, 1989, Huntsville Marriot, Huntsville, Alabama

REVIEW OF ACOUSTO-ULTRASONIC NDE FOR COMPOSITES

Alex Vary and Harold Kautz
NASA Lewis Research Center
Cleveland, Ohio 44135

Acousto-ultrasonics utilizes simulated stress waves to detect and quantify defect states, damage conditions, and variations of mechanical properties in fiber reinforced composites. The term "acousto-ultrasonics" denotes a combination of aspects of acoustic emission methodology with ultrasonic materials characterization. The acousto-ultrasonic approach was developed to deal primarily with evaluation of the integrated effect of minor flaws and diffuse flaw populations of subcritical flaws in composite and bonded structures. These factors singly and collectively also influence acousto-ultrasonic measurements that, in turn, correlate with dynamic response and mechanical property variations. Since it was first introduced, the acousto-ultrasonic approach has been successfully applied to a variety of materials, including polymeric, metallic, and ceramic matrix composites; adhesively bonded materials; paper and wood products; cable and rope; and also human bone. Examples of applications and limitations of the approach are reviewed. Basic methods and guidelines are discussed. The underlying hypothesis and theory development needs are indicated.

THE ACOUSTO-ULTRASONIC APPROACH

- COMBINES SOME ASPECTS OF ACOUSTIC EMMISION METHODOLOGY WITH ULTRASONIC SIMULATION OF STRESS WAVES
- CONCERNED PRIMARILY WITH ASSESSMENT OF COLLECTIVE EFFECTS OF DISCRETE AND DIFFUSE FLAW POPULATIONS
- CONCERNED WITH VARIATIONS IN AND CORRELATIONS WITH:

  MATERIAL MORPHOLOGY, MECHANICAL PROPERTIES, INTERLAMINAR AND INTERFACIAL BOND STRENGTH, DEGRADATION FROM FATIGUE, IMPACT, ETC.

CD-87-27473

CHALLENGES

- ONLY ONE SIDE ACCESS AVAILABLE
- PULSE-ECHO APPROACH AMBIGUOUS
- LATERAL STRENGTH PROPERTIES
- NO EDGES OR EDGES INACCESSIBLE
- OBLIQUE INCIDENCE IMPRACTICAL
- BOND-LINE STRENGTH EVALUATION
- EFFECT OF FLAWS AMBIGUOUS

CD-87-27472

QUANTITATIVE SIGNAL PROCESSING FOR ACOUSTO-ULTRASONICS

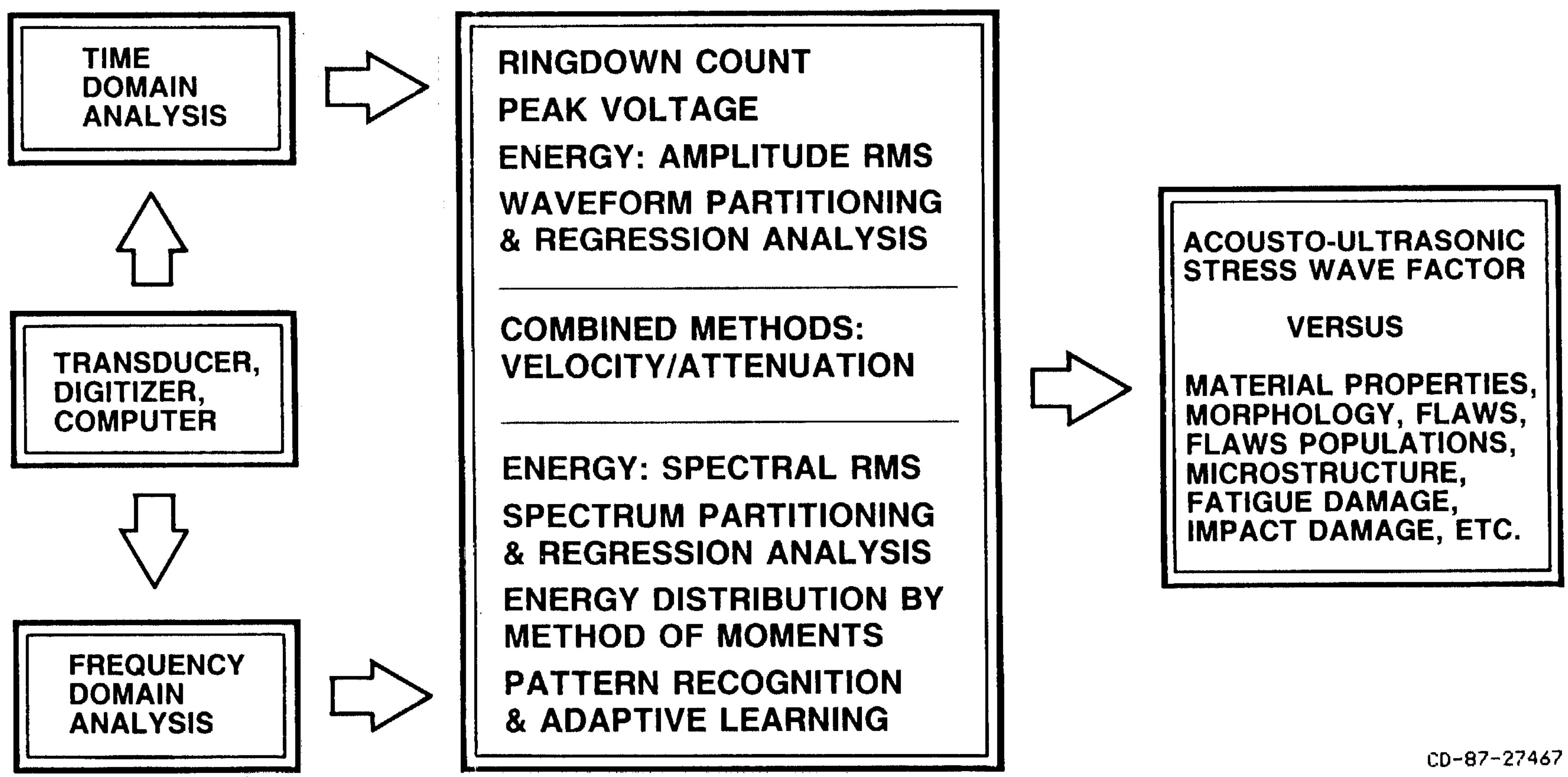

CD-87-27467

THE STRESS WAVE FACTOR

- STRESS WAVE FACTOR (SWF) QUANTIFIES ACOUSTO-ULTRASONIC SIGNALS
- DOMINANT EFFECT MEASURED BY (SWF) IS ULTRASONIC ATTENUATION
- HIGHER VALUES OF (SWF) GENERALLY CORRESPOND TO LOWER ATTENUATION

CD-87-27474

WORKING HYPOTHESES

- (SWF) MEASURES RELATIVE EFFICIENCY OF STRESS WAVE ENERGY FLOW
- BETTER ENERGY FLOW MEANS BETTER DYNAMIC STRAIN DISTRIBUTION
- PROMPT, EFFICIENT FLOW OF STRESS WAVE ENERGY AWAY FROM CRACK NUCLEATION SITES IS NEEDED TO AVOID CATASTROPIC FRACTURE WHEN THE ENERGY CANNOT BE ABSORBED LOCALLY

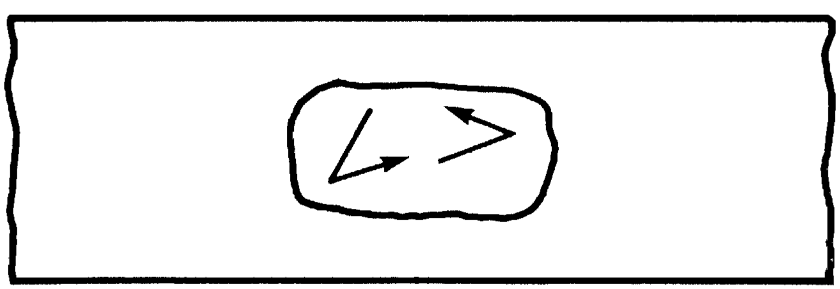

CRACK NUCLEATION ENERGY CONFINED

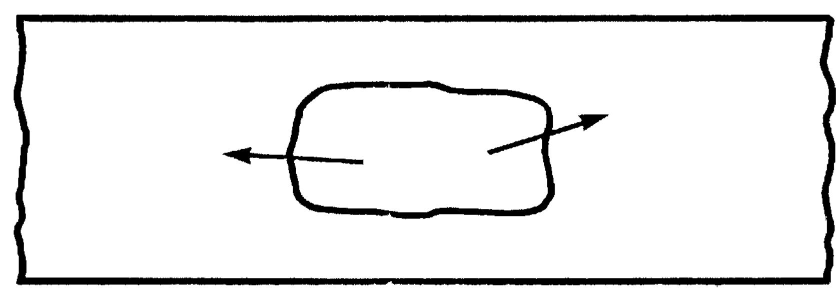

CRACK NUCLEATION ENERGY DISSIPATED

CD-87-27469

REPRESENTATIVE ECHO SYSTEMS FOR BASIC ACOUSTO-ULTRASONIC CONFIGURATION

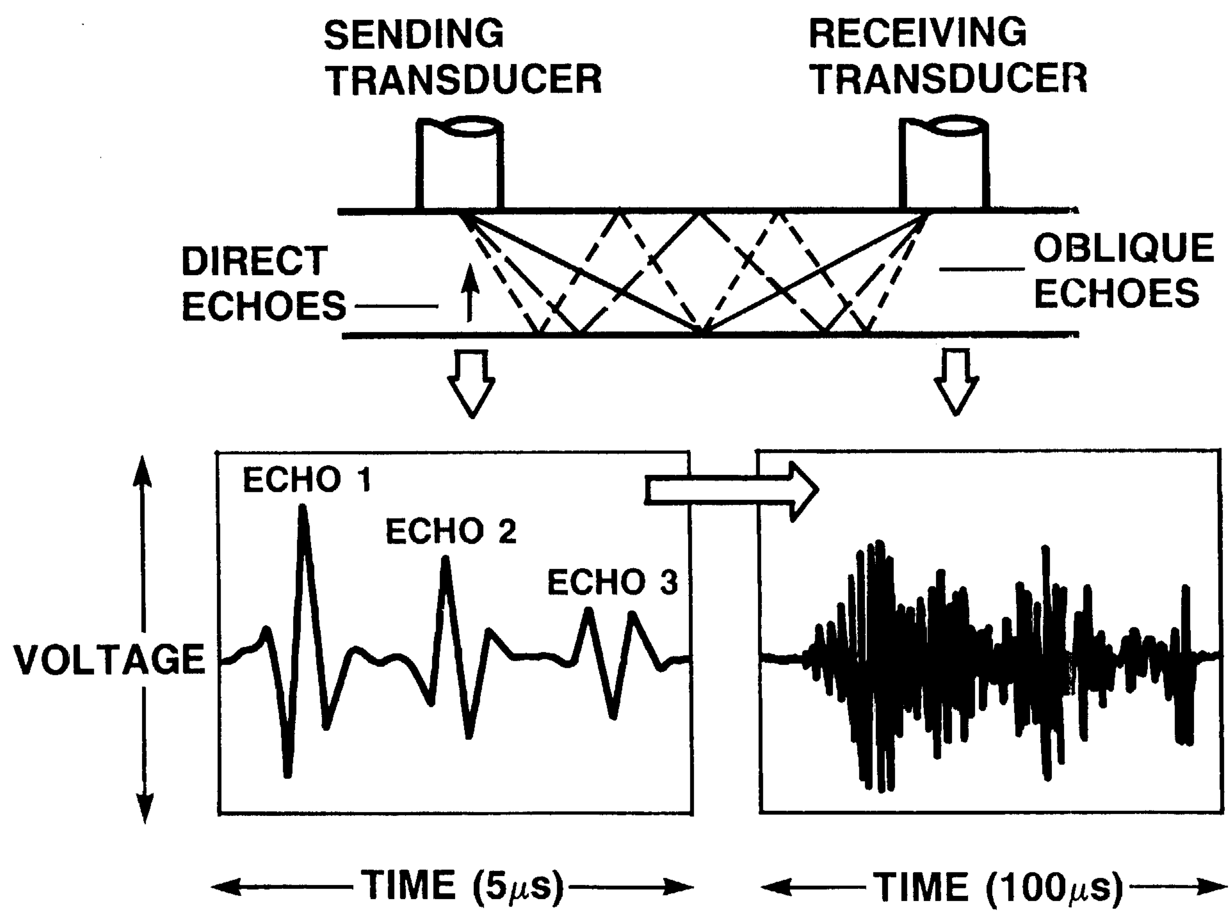

DIRECT ECHOES SEEN BY SENDING TRANSDUCER

OBLIQUE ECHOES SEEN BY RECEIVING TRANSDUCER

CD-87-27449

ACOUSTO-ULTRASONIC WAVEFORMS FROM ALUMINUM PLATES WITH TWO DIFFERENT THICKNESS

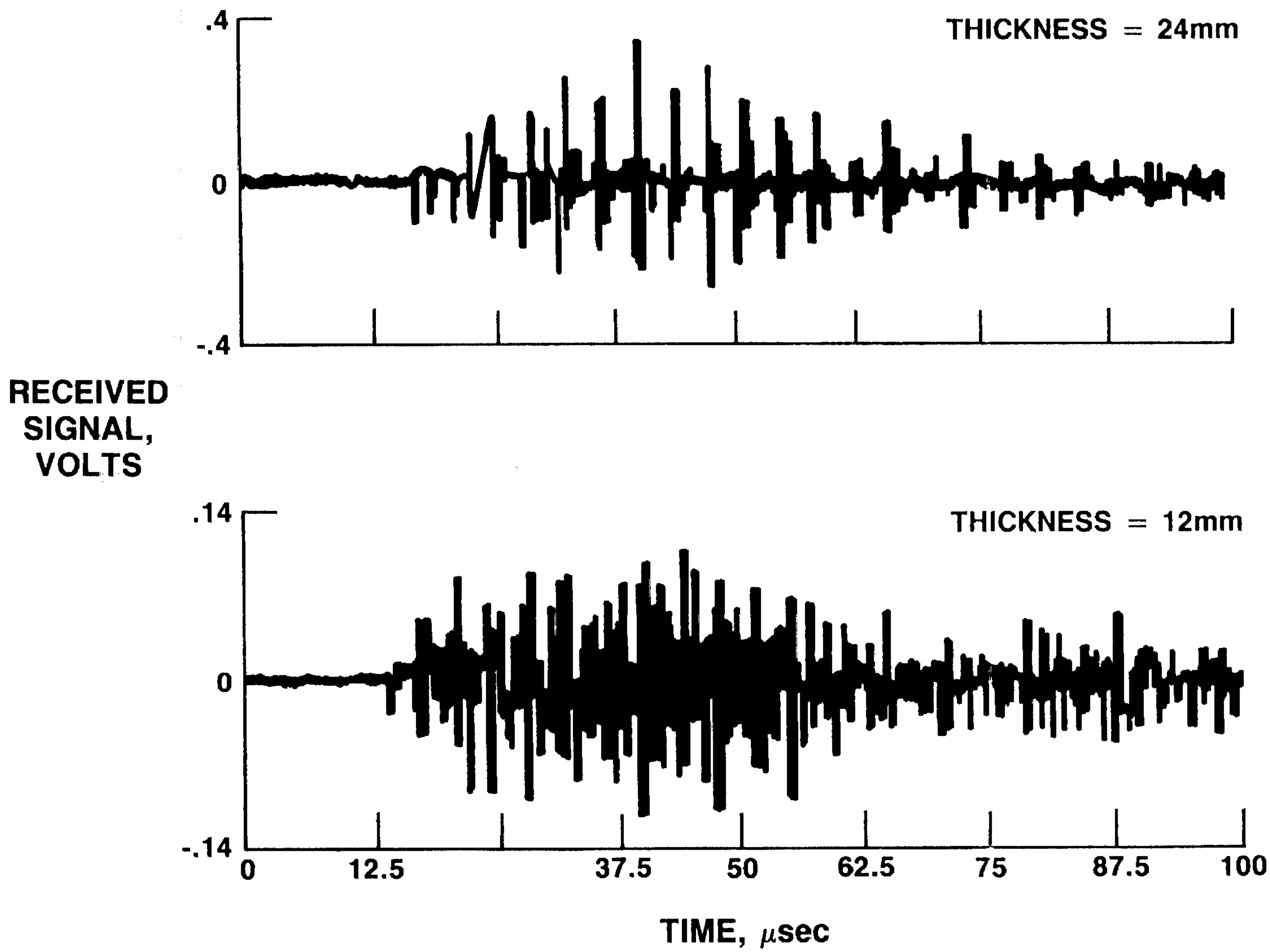

CD-87-27454

VARIATION OF ACOUSTO-ULTRASONIC SIGNAL RELATIVE TO FIBER DIRECTION IN UNDIRECTIONAL COMPOSITE LAMINATE

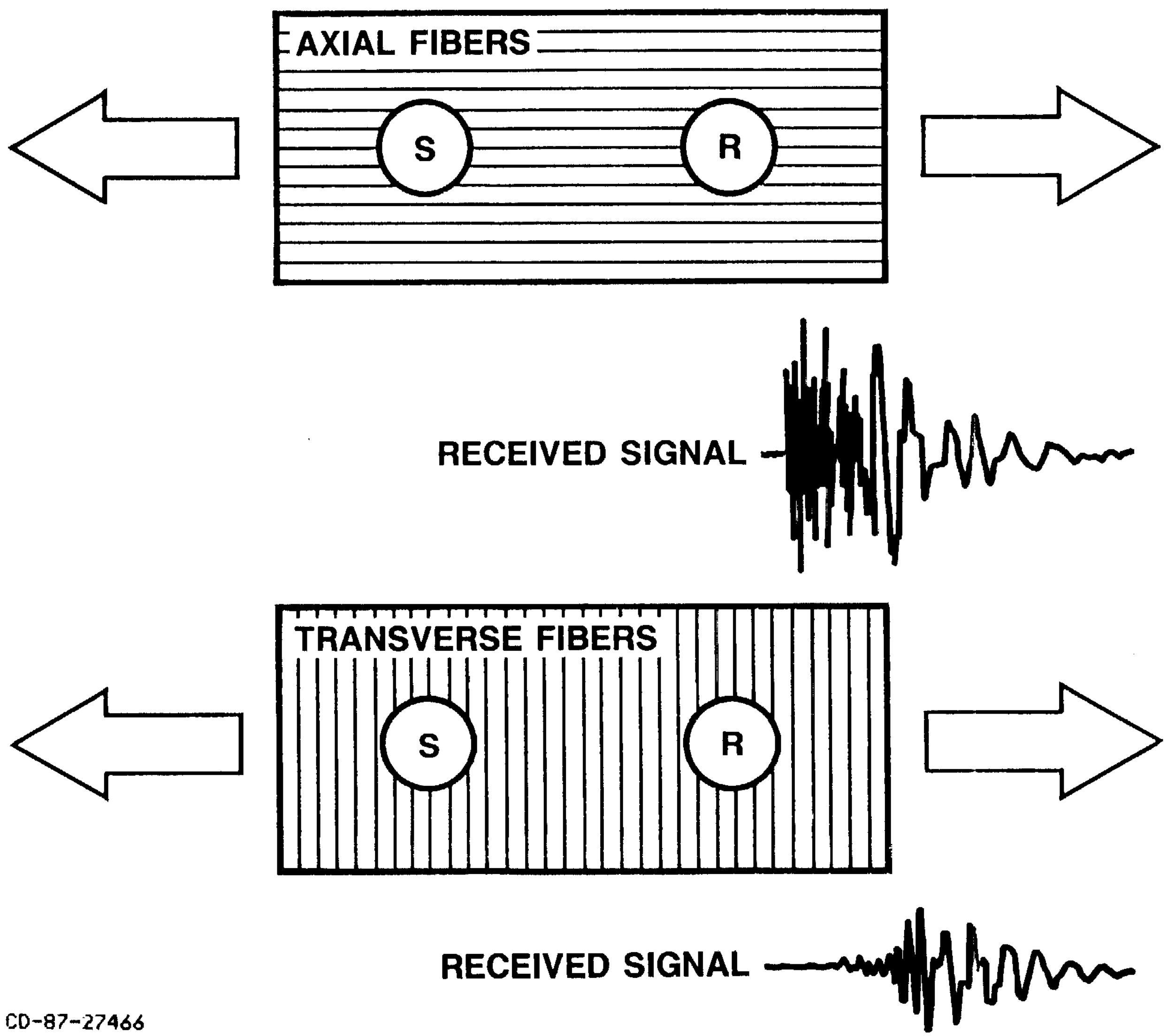

CD-87-27466

QUANTITATIVE SIGNAL PROCESSING FOR STRESS WAVE FACTOR (SWF) USING ACOUSTIC EMMISSION METHODOLOGY

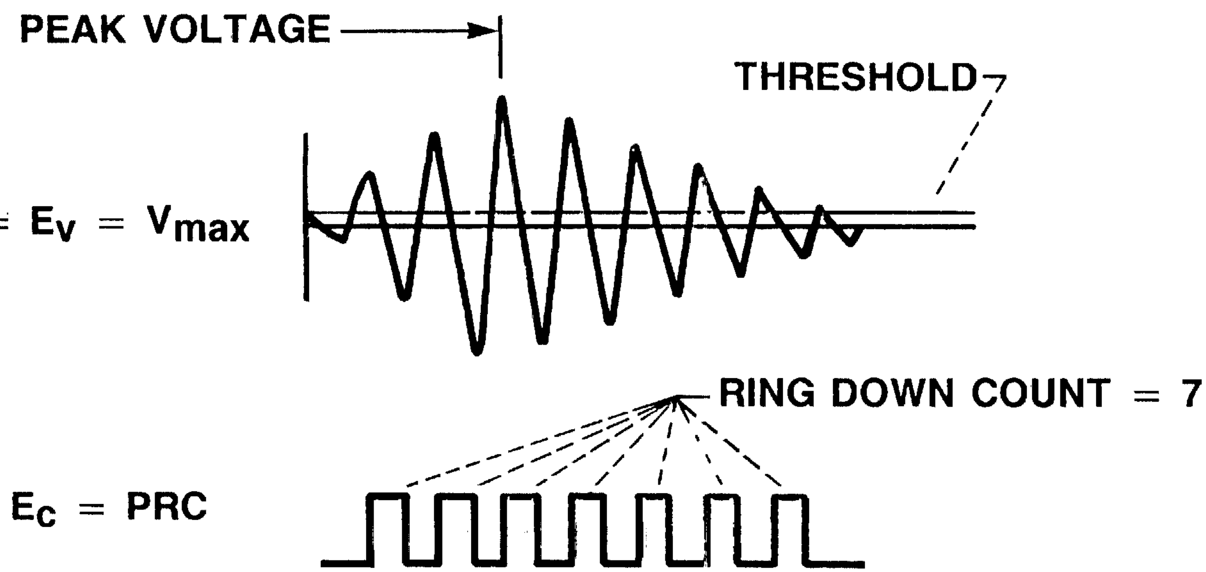

PEAK VOLTAGE (SWF) = E_V = V_{max}

RINGDOWN (SWF) = E_C = PRC

P = PULSE RATE, R = RESET TIME, C = RINGDOWN COUNT

CD-87-27448

QUANTITATIVE SIGNAL PROCESSING FOR STRESS WAVE FACTOR (SWF) BY PARTITIONING OF ROOT MEAN SQUARE (rms) ENERGY

$$\text{TIME DOMAIN (SWF)} = E_t = (V_{rms})^2 = \frac{1}{T}\int_{t_1}^{t_2} v^2\,dt$$

$$\text{FREQUENCY DOMAIN (SWF)} = E_f = (S_{rms})^2 = \frac{1}{F}\int_{f_1}^{f_2} s^2\,df$$

$T = t_2 - t_1$ AND $F = f_2 - f_1$

CD-87-27465

CORRELATION OF STRESS WAVE FACTOR WITH FAILURE SITES IN GRAPHITE/EPOXY TENSILE SPECIMENS

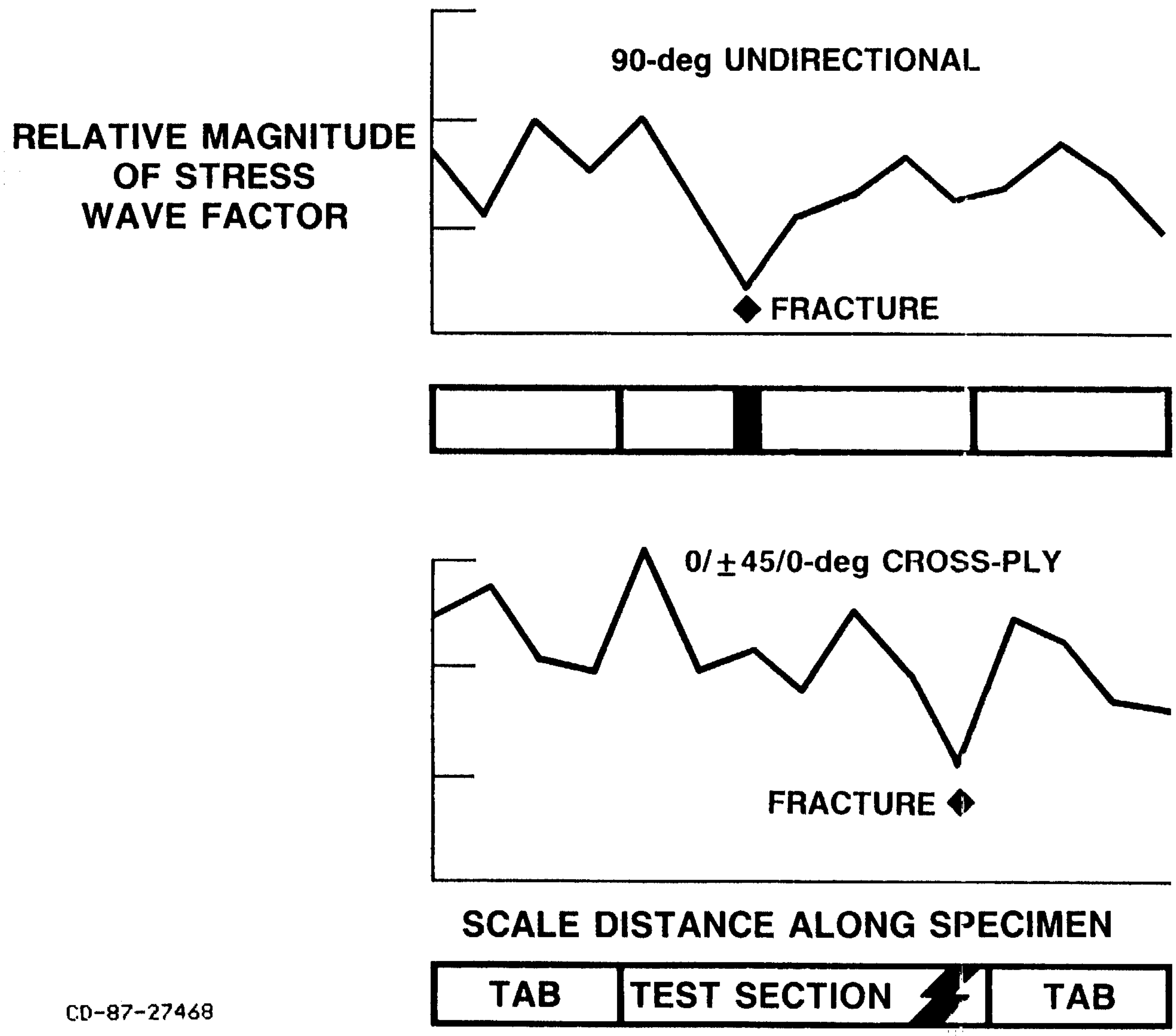

CD-87-27468

STRESS WAVE FACTOR (SWF) VERSUS THROUGH-TRANSMISSION ULTRASONIC ATTENUATION AT IMPACT SITE OF 10-PLY UNDIRECTIONAL GRAPHITE/ EPOXY COMPOSITE LAMINATE SPECIMENS

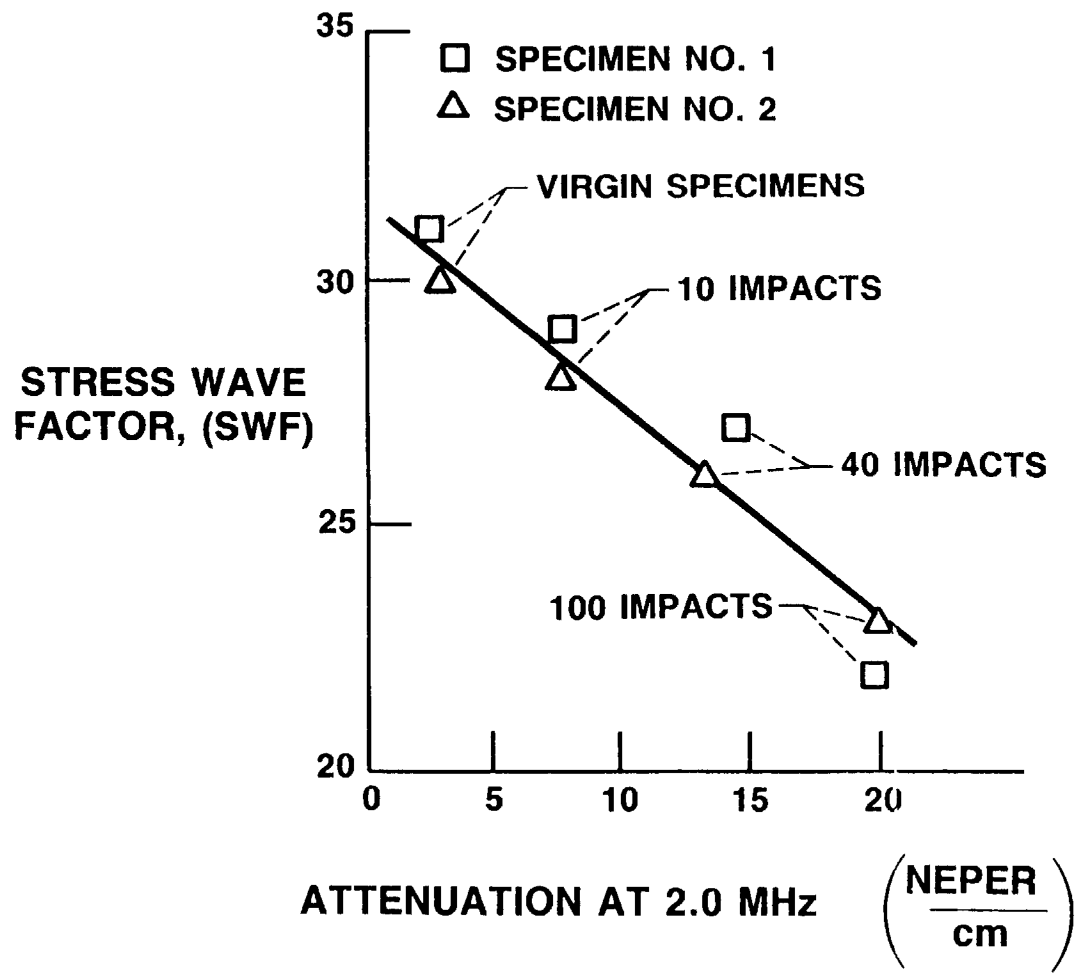

CD-87-27461

ACOUSTO-ULTRASONIC STRESS WAVE FACTOR AS CO-FUNCTION OF ULTIMATED TENSILE STRENGTH AND FIBER/PLY ANGLE IN COMPOSITE LAMINATE

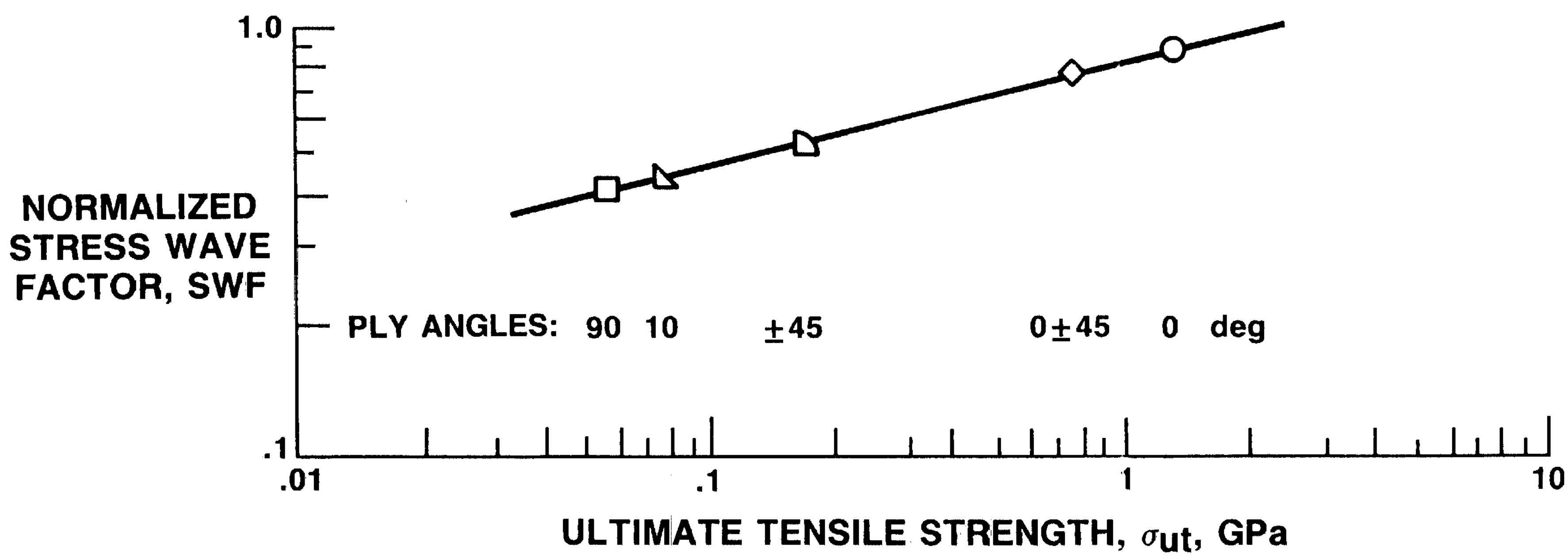

CD-87-27464

CORRELATION OF INTERLAMINAR SHEAR STRENGTH WITH THE ACOUSTO-ULTRASONIC ESTIMATOR FOR GRAPHITE/POLYIMIDE FIBER COMPOSITE LAMINATE

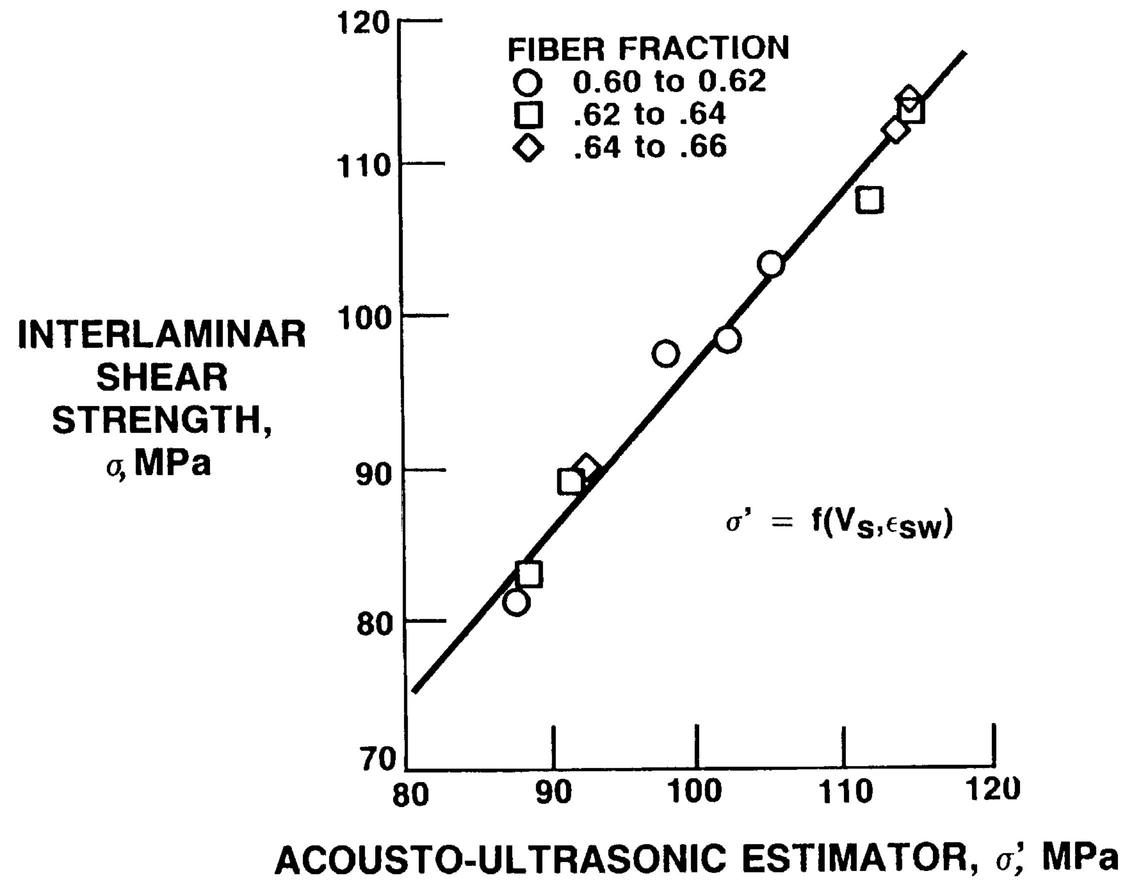

CD-87-27455

COVARIATION OF STRESS WAVE FACTOR AND LONGITUDINAL SECANT MODULUS WITH FATIGUE DAMAGE IN GRAPHITE/EPOXY FIBER COMPOSITE LAMINATE

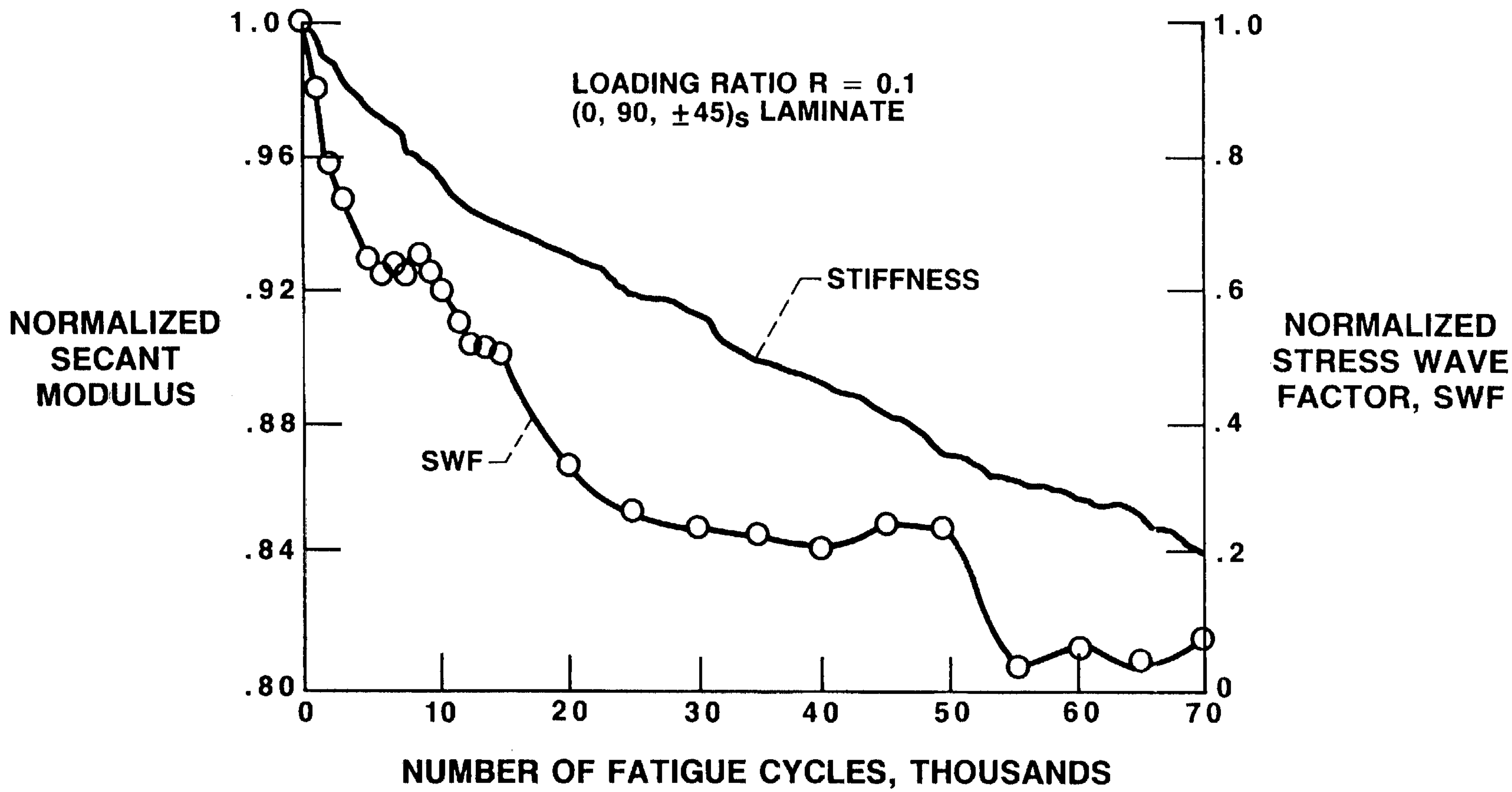

DIFFERENCE IN SLOPES IS BECAUSE SECANT MODULUS IS FOR FULL GAGE LENGTH WHILE (SWF) IS FOR LOCAL ZONE ON TEST SPECIMEN

CD-87-27451

CONCLUSIONS

- UNDERLYING (SWF) HYPOTHESIS APPEARS TO BE CONFIRMED
- CAPABILITY FOR PREDICTING POTENTIAL FAILURE SITES
- MEASUREMENT OF DEGRADATION DUE TO IMPACT, FATIGUE
- CORRELATIONS WITH INTERLAMINAR, ULTIMATE STRENGTH

CD-87-27475

ACOUSTO-ULTRASONIC NONDESTRUCTIVE EVALUATION OF MATERIALS USING LASER BEAM GENERATION AND DETECTION

Robert D. Huber and Robert E. Green Jr.
Center for Nondestructive Evaluation
The Johns Hopkins University
and
Alex Vary and Harold Kautz
NASA/Lewis Research Center

This work has been supported in part by
NASA/Lewis Research Center
Through NASA Grant #NAG3-728

RESEARCH OBJECTIVE

TO INVESTIGATE THE POSSIBILITY OF USING LASER GENERATION AND DETECTION OF ULTRASOUND TO REPLACE PIEZOELECTRIC TRANSDUCERS FOR THE ACOUSTO-ULTRASONIC TECHNIQUE.

ADVANTAGES OF LASER ACOUSTO-ULTRASONICS

- NON-CONTACT TESTING
- PIEZOELECTRIC TRANSDUCER COUPLING PROBLEMS ELIMINATED
  - CONTACT PRESSURE
  - COUPLANT
  - TESTING HOT SURFACES OR IN HOSTILE ENVIRONMENTS
- RESONANCE OF TRANSDUCERS ELIMINATED
- POINT DETECTION
- NARROW AND WIDE BAND DETECTION
- DETECTION NEAR MATERIAL EDGES

DISADVANTAGES OF LASER DETECTION

- SURFACE MUST BE REFLECTIVE
- NOT AS SENSITIVE AS PIEZOELECTRIC TRANSDUCERS
- OPTICAL SYSTEMS ARE OFTEN MORE EXPENSIVE

TYPES OF INTERFEROMETERS USED

- PATH STABILIZED BULK SYSTEM
- HETERODYNE FIBER OPTIC SYSTEM

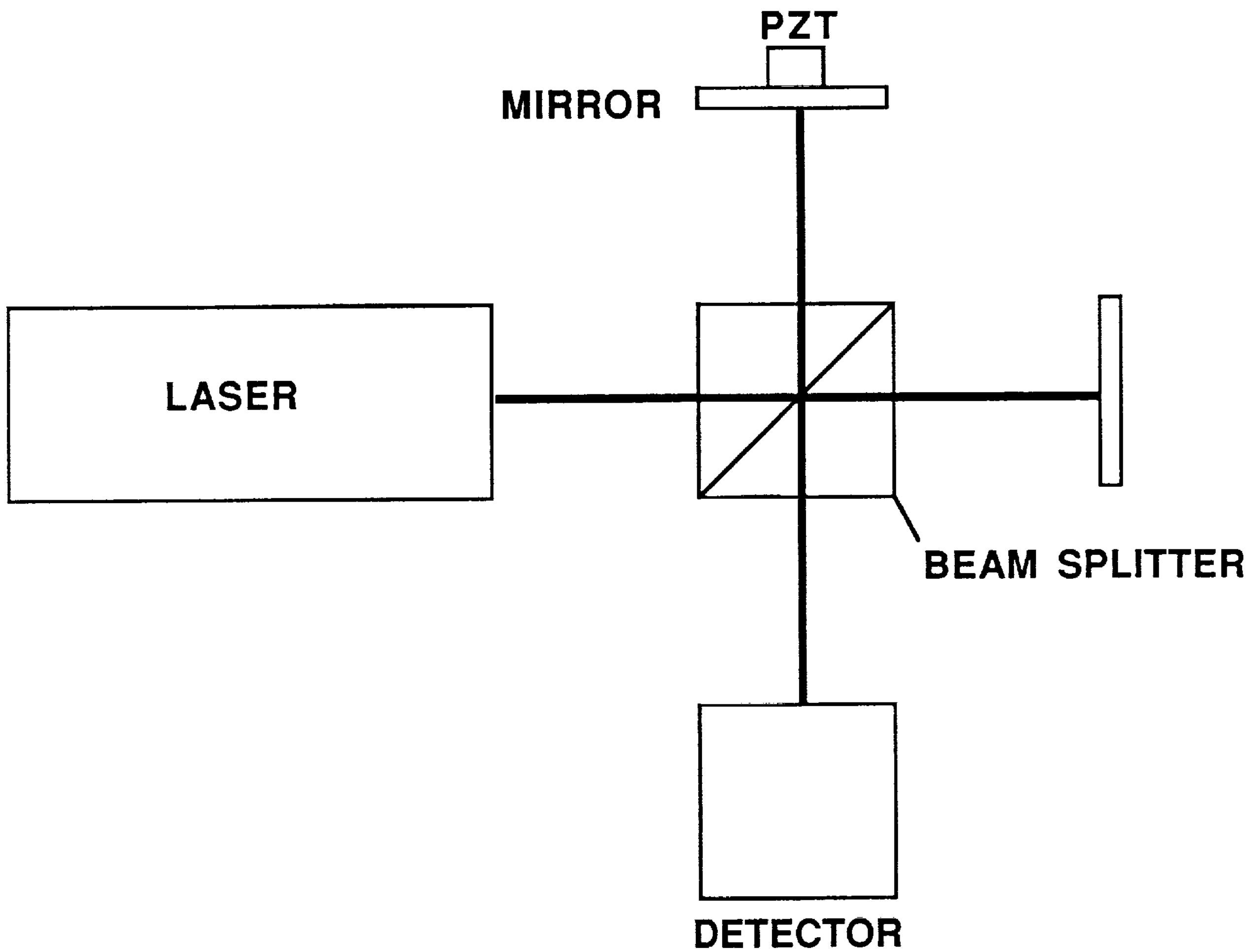

PATH STABILIZED INTERFEROMETER

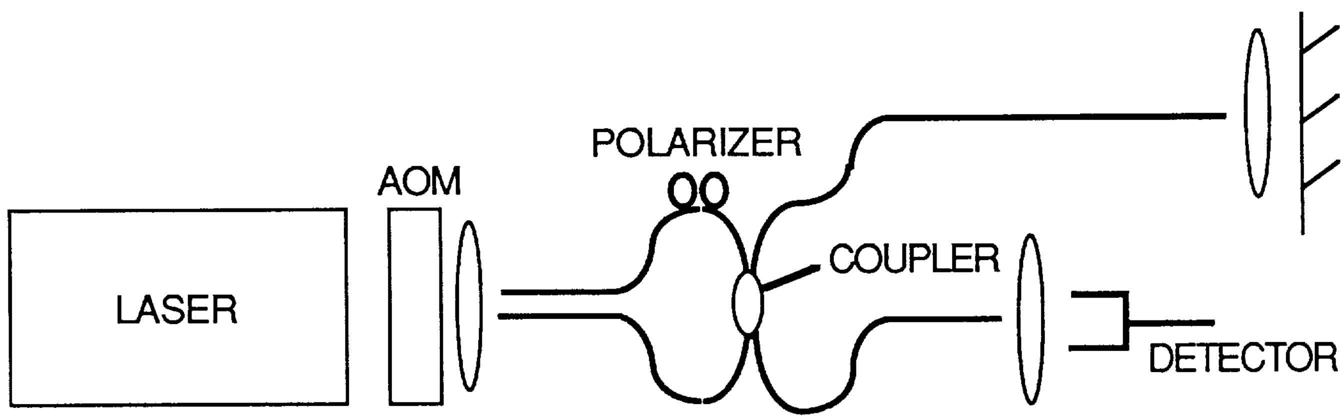

HETERODYNE FIBER OPTIC INTERFEROMETER

INTERFEROMETER SENSITIVITY CONSIDERATIONS

$$SNR \;\alpha\; \left[\frac{R\,P_O\,\eta}{h\,\nu\,\Delta\nu}\right]^{1/2} \frac{\delta}{\lambda}$$

h : PLANCK'S CONSTANT

λ : OPTICAL WAVELENGTH

η : DETECTOR QUANTUM EFFICIENCY

δ : SIGNAL AMPLITUDE

$\Delta\nu$: DETECTION BANDWIDTH

R : SAMPLE REFLECTIVITY

P_O : LASER POWER

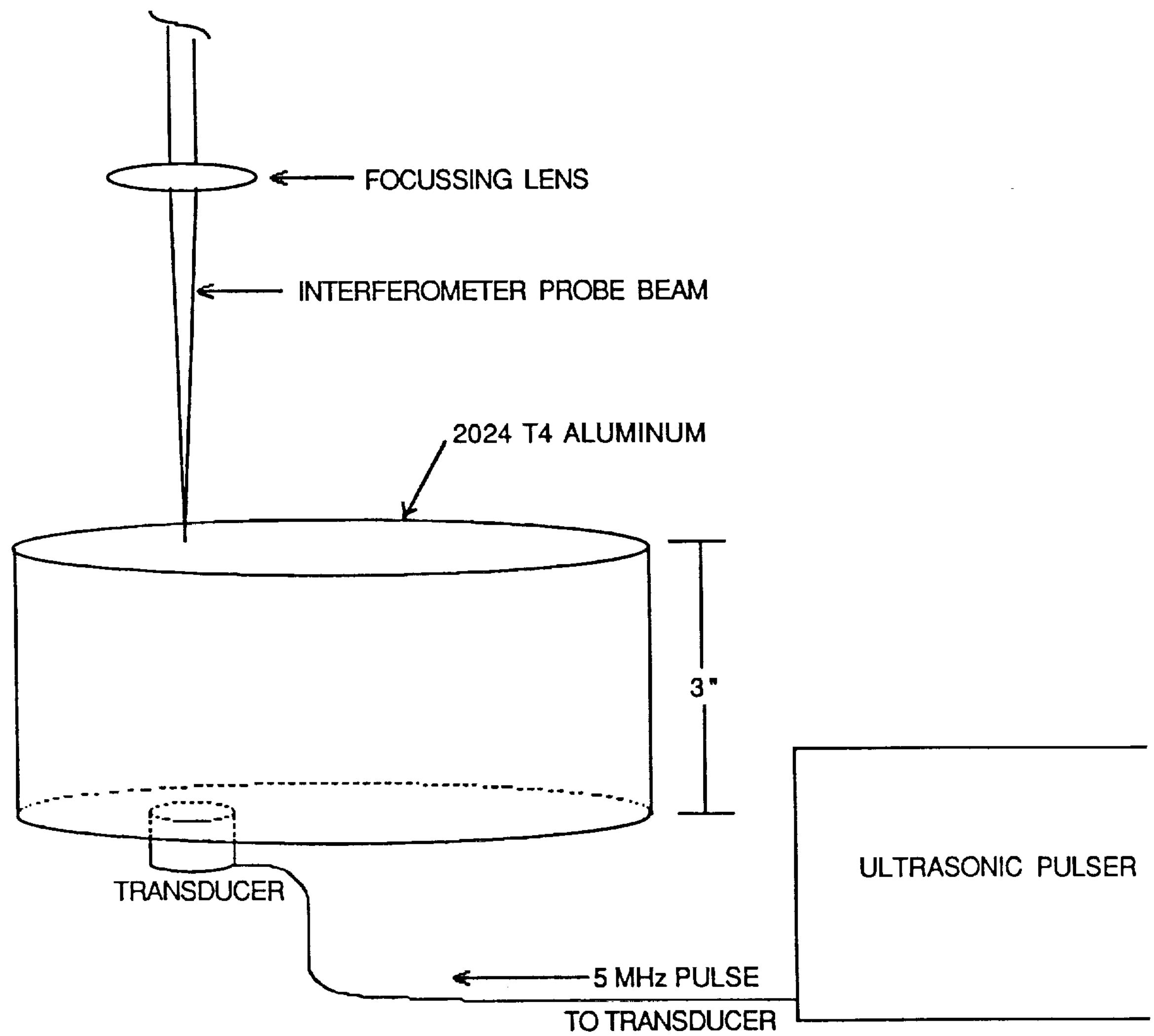
FOCUSSING LENS
INTERFEROMETER PROBE BEAM
2024 T4 ALUMINUM
3"
TRANSDUCER
ULTRASONIC PULSER
5 MHz PULSE
TO TRANSDUCER

AVG. A1

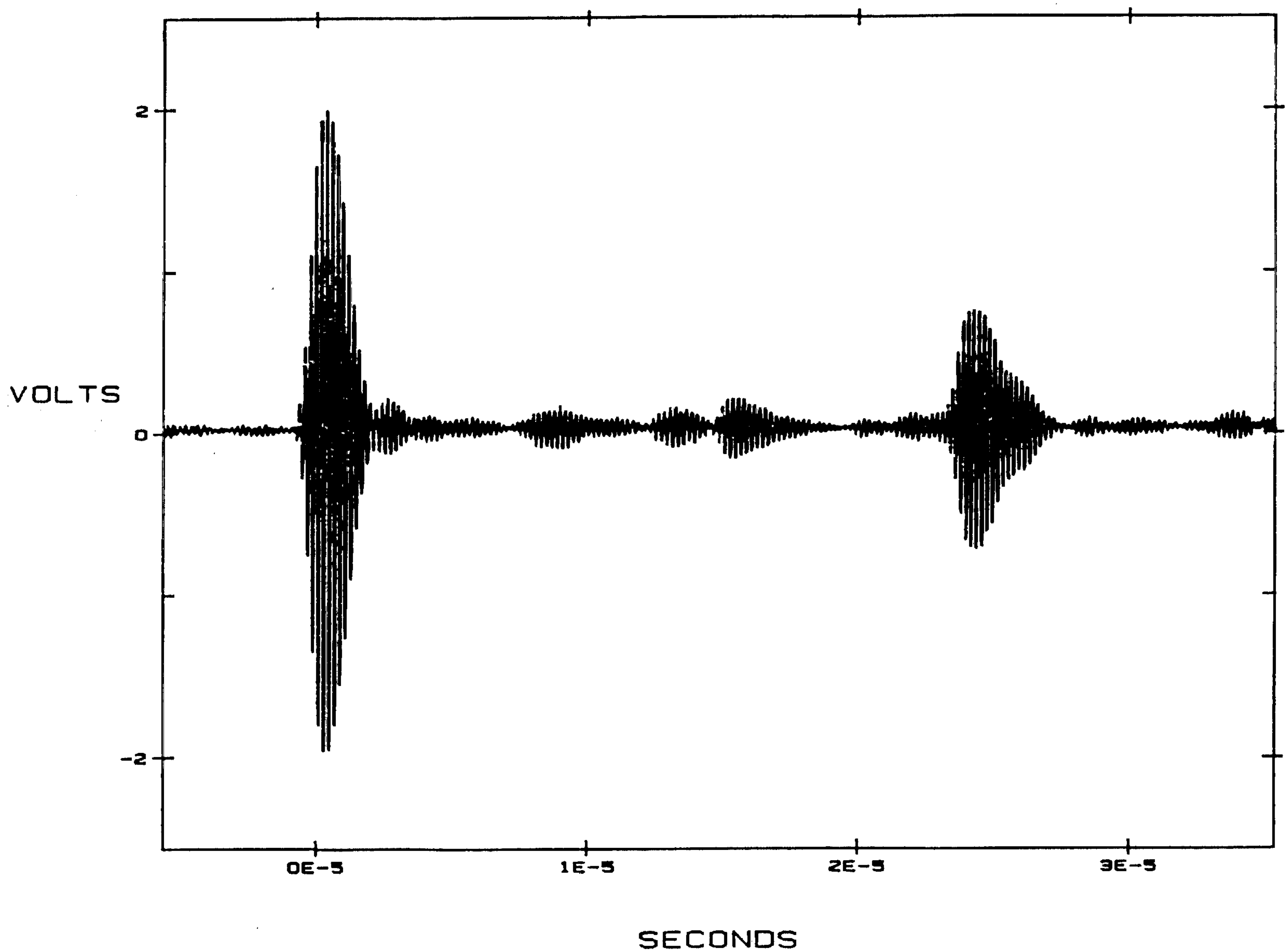

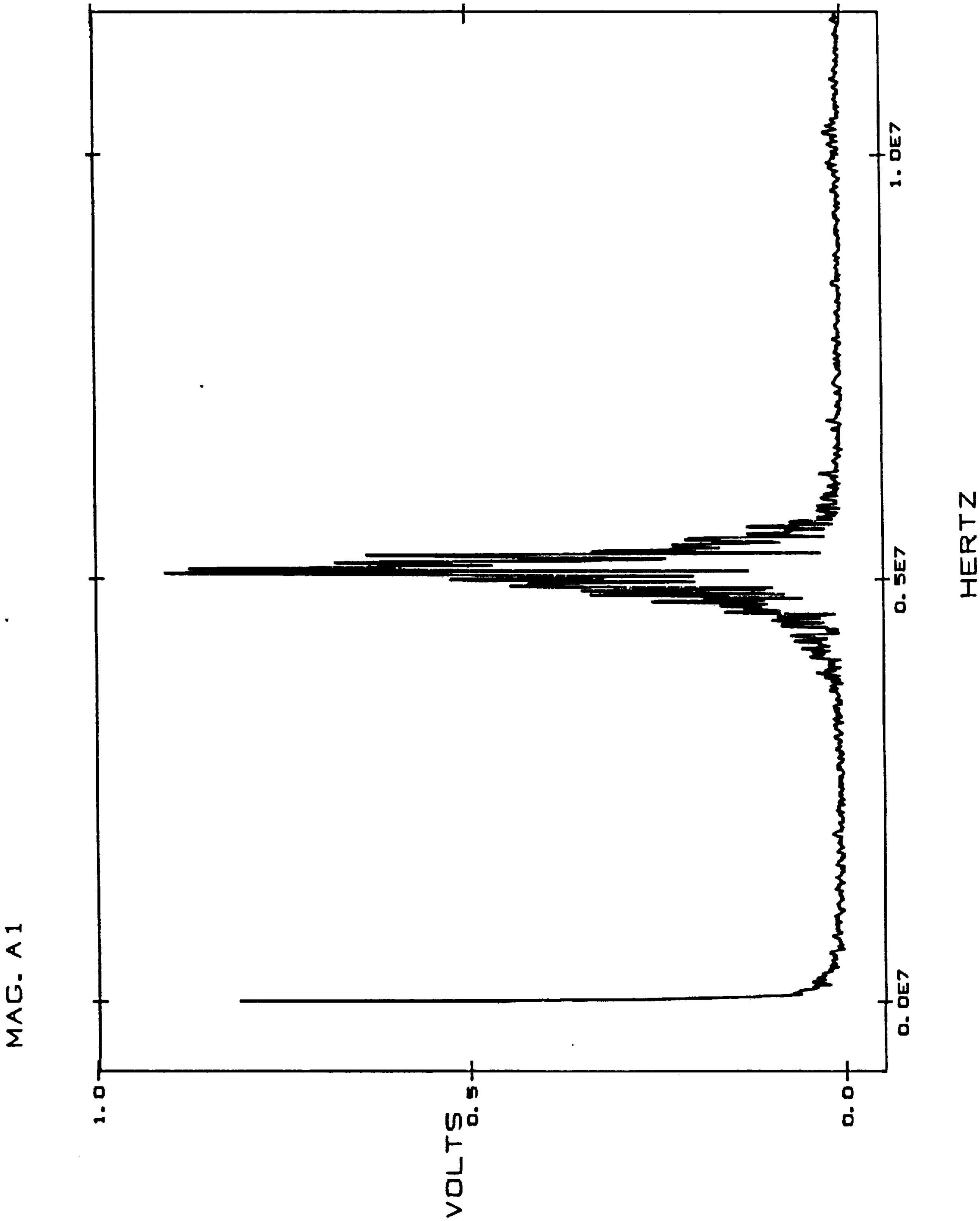
MAG. A1
VOLTS
1.0
0.5
0.0
HERTZ
0.0E7
0.5E7
1.0E7

LASER GENERATION OF ULTRASOUND

KIGRE Nd YAG PULSED LASER

17 mJ PER PULSE

4 ns PULSE LENGTH

3 mm BEAM DIAMETER

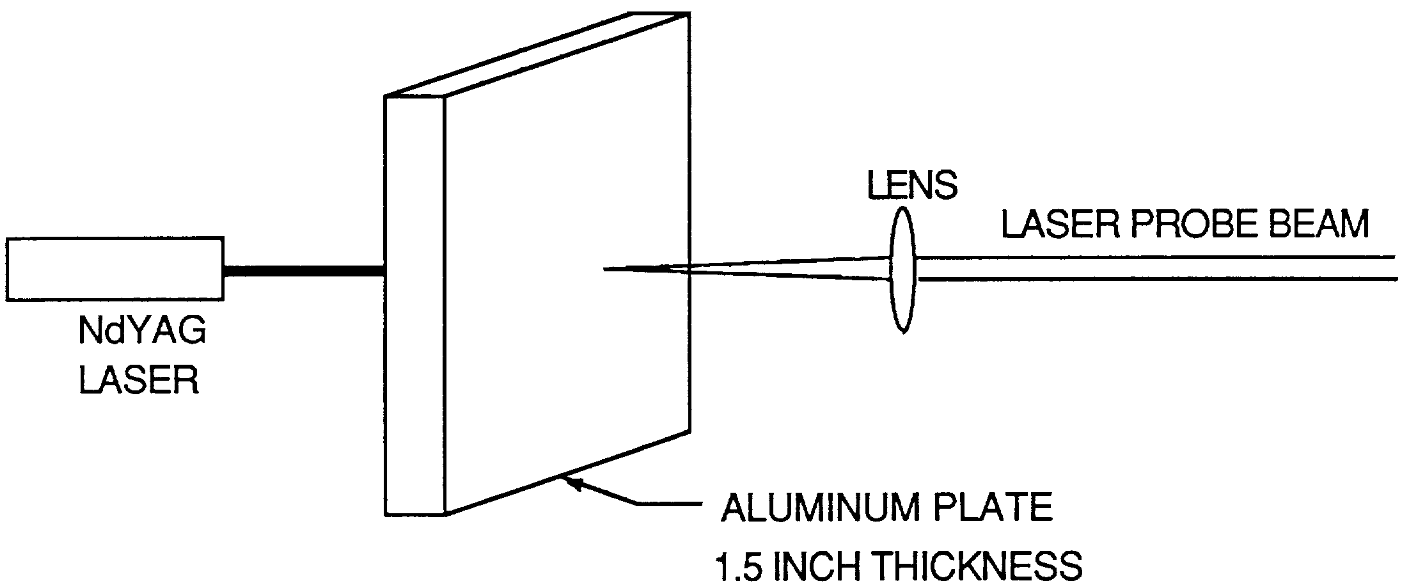

NON-CONTACT GENERATION AND DETECTION OF

ULTRASOUND IN AN ALUMINUM BLOCK

Theoretical Surface Displacement For Laser Generated Ultrasound In A 1.5 in Al Block On Epicenter

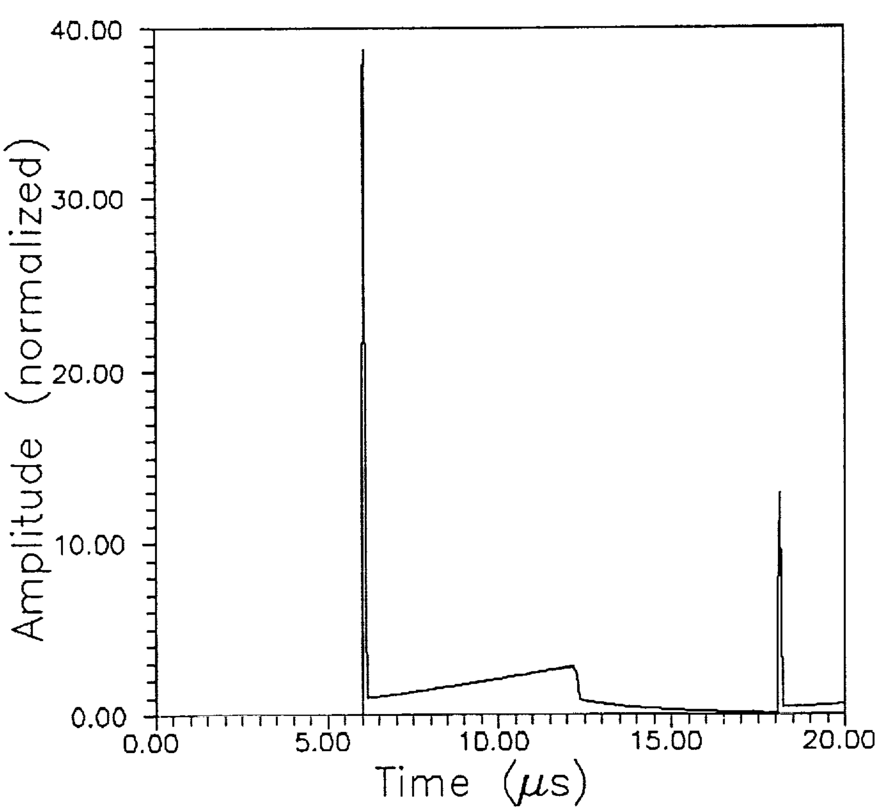

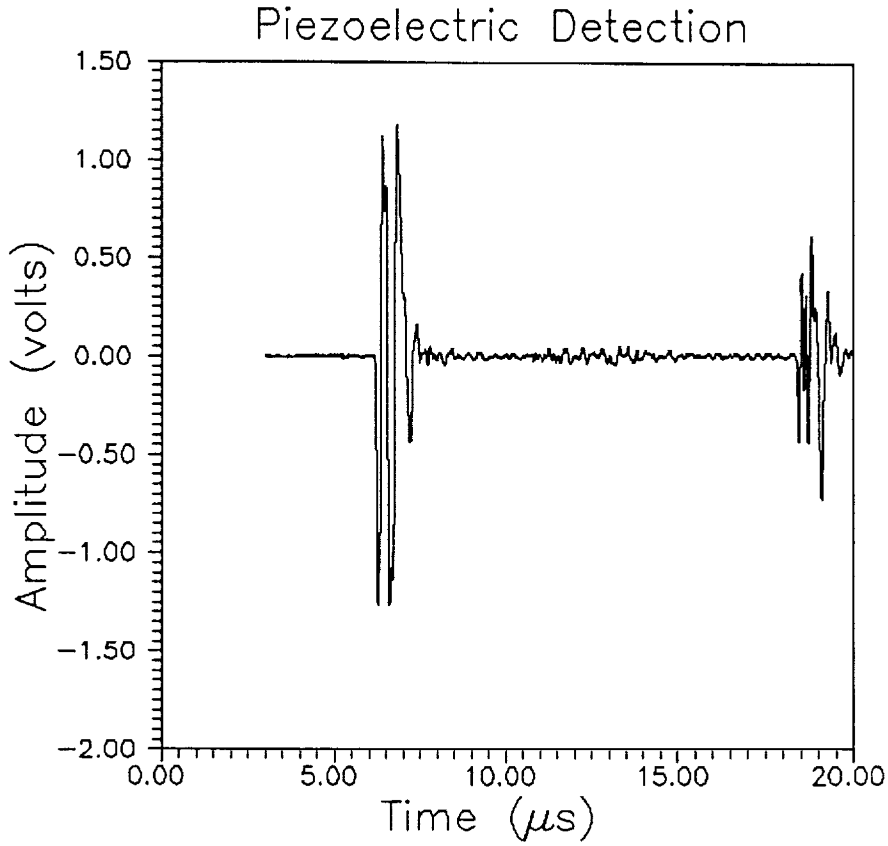

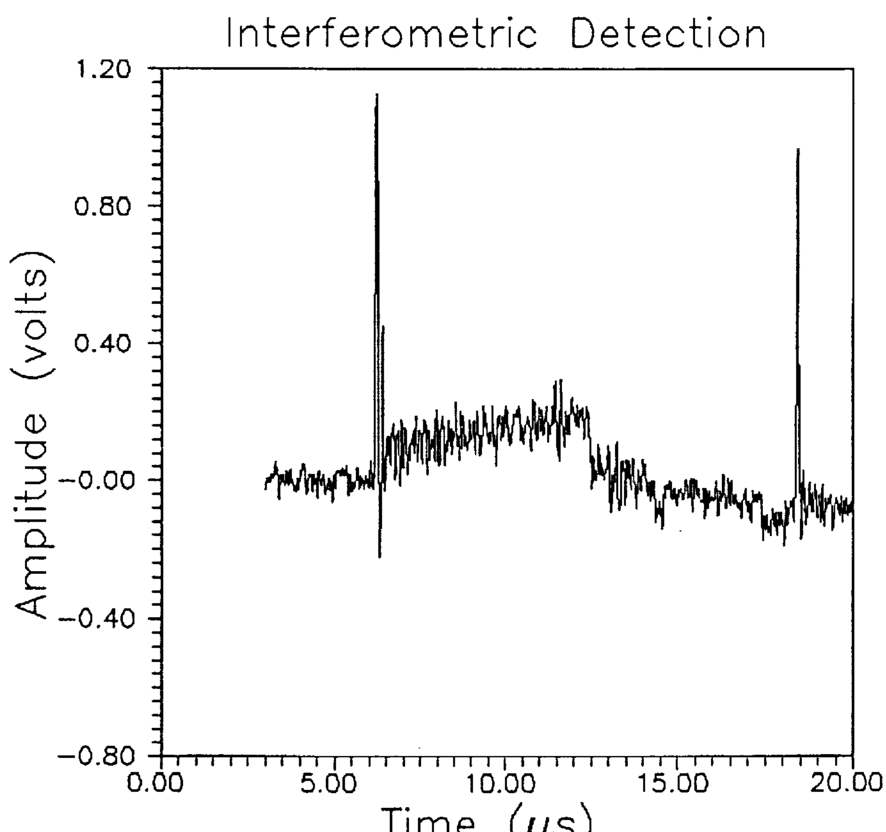

Laser Generated Ultrasound (Al Block-On Epicenter)

Theoretical Surface Displacement For Laser Generated Ultrasound In A 1.5 in Al Block 7/8 in Off Epicenter

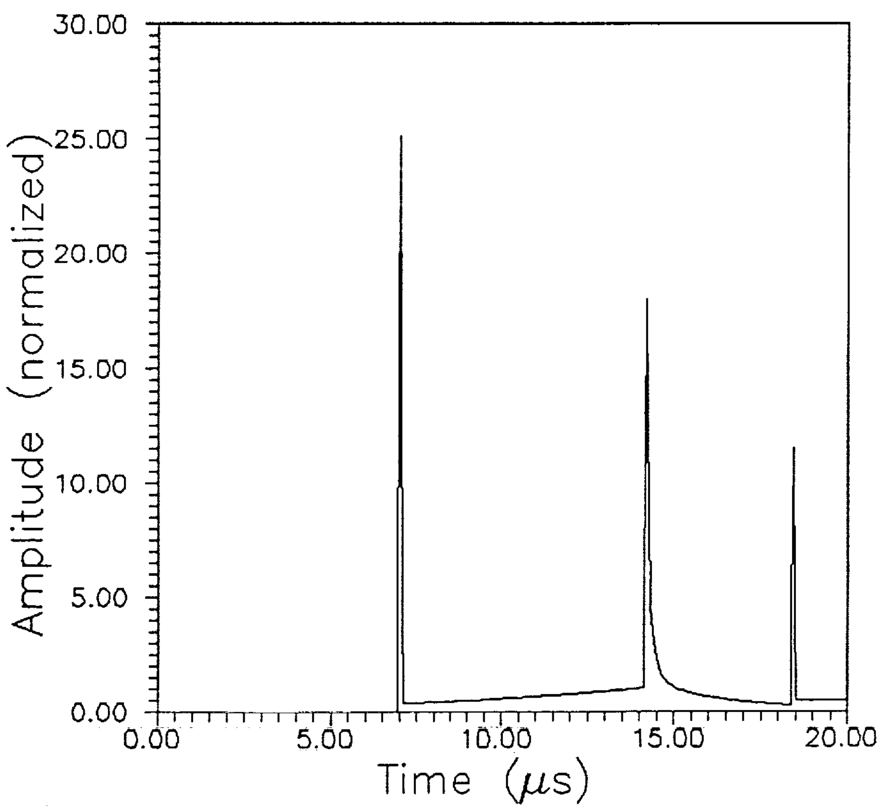

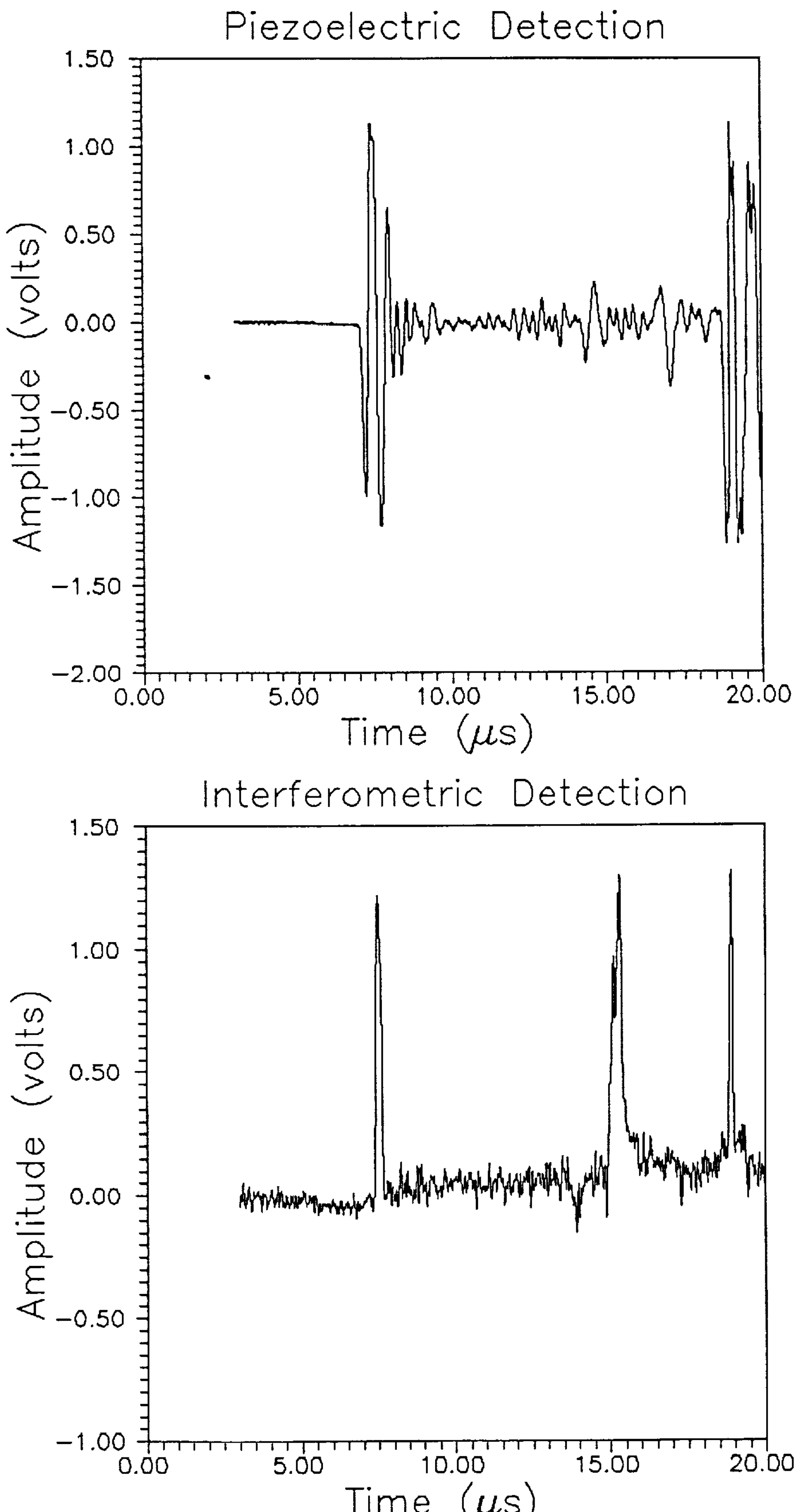

Laser Generated Ultrasound (Al Block-Off Epicenter)

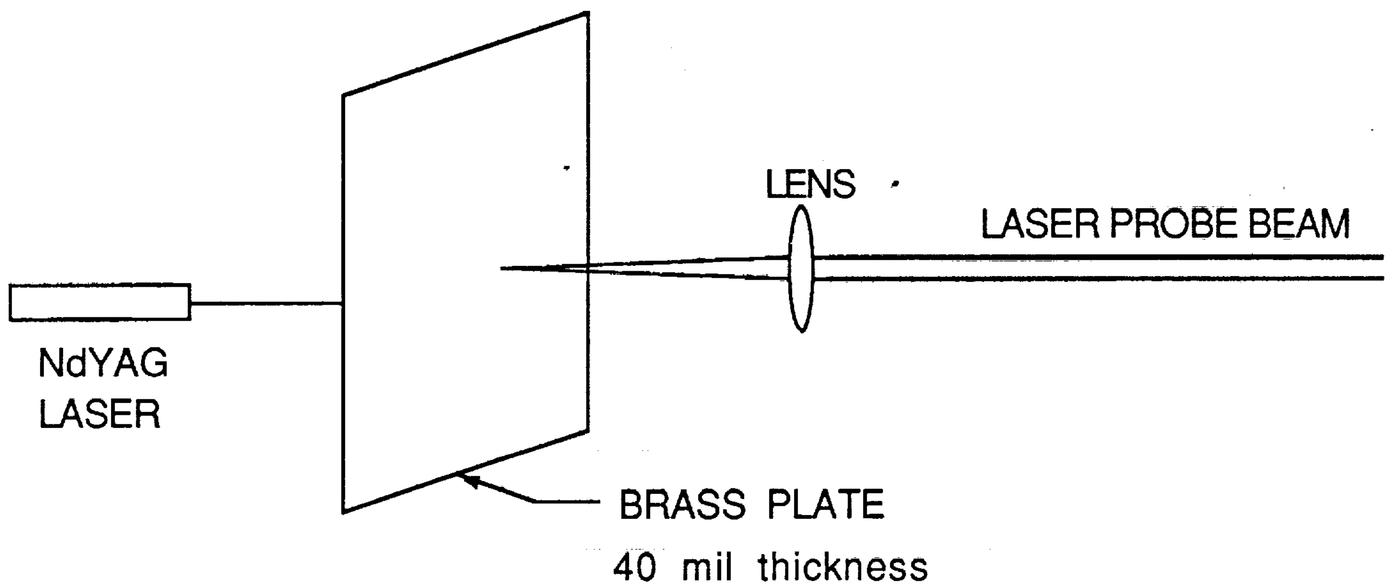

NON-CONTACT GENERATION AND DETECTION

OF ULTRASOUND IN A BRASS PLATE

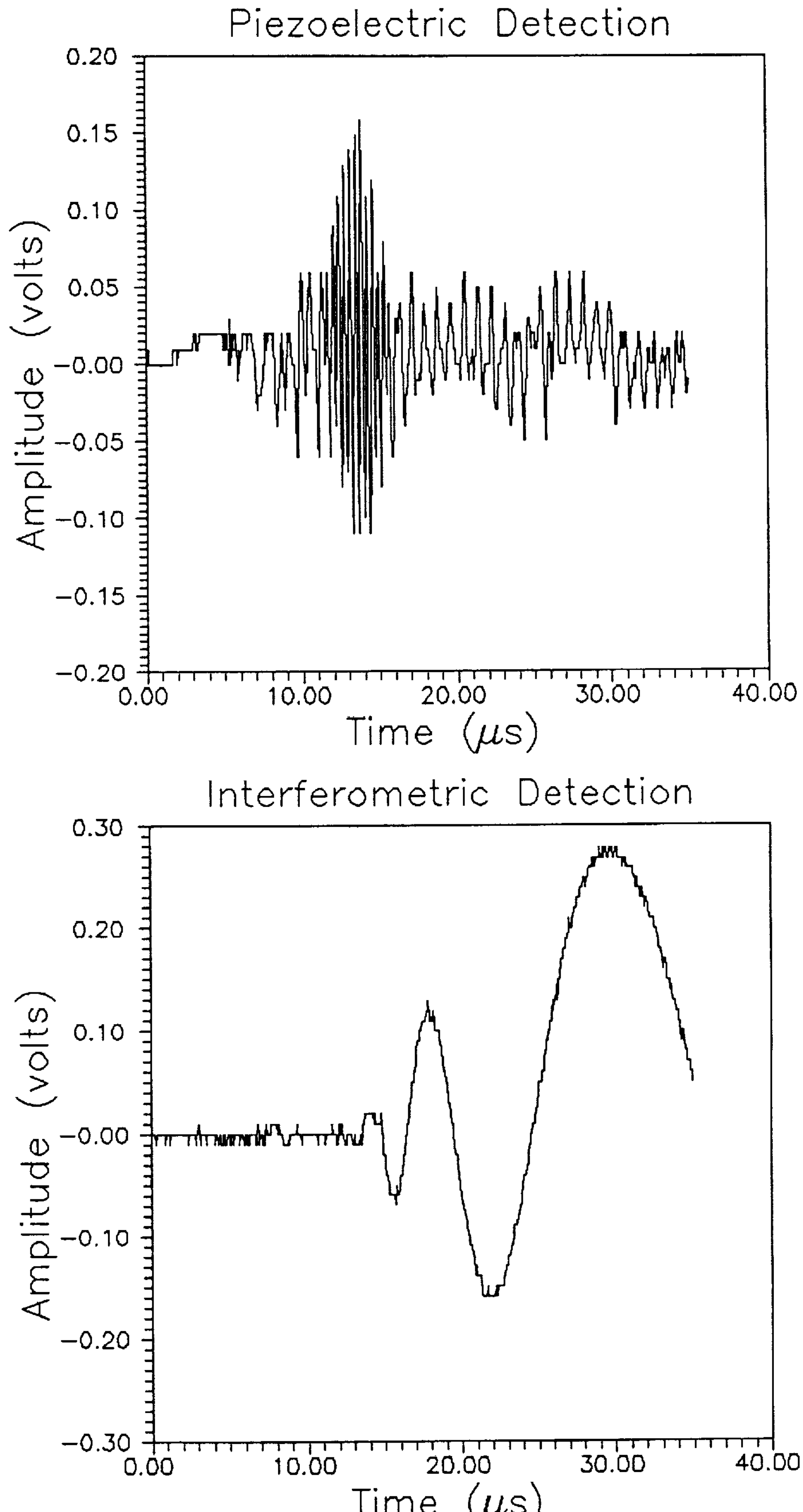

Laser Generated Ultrasound (Brass Plate)

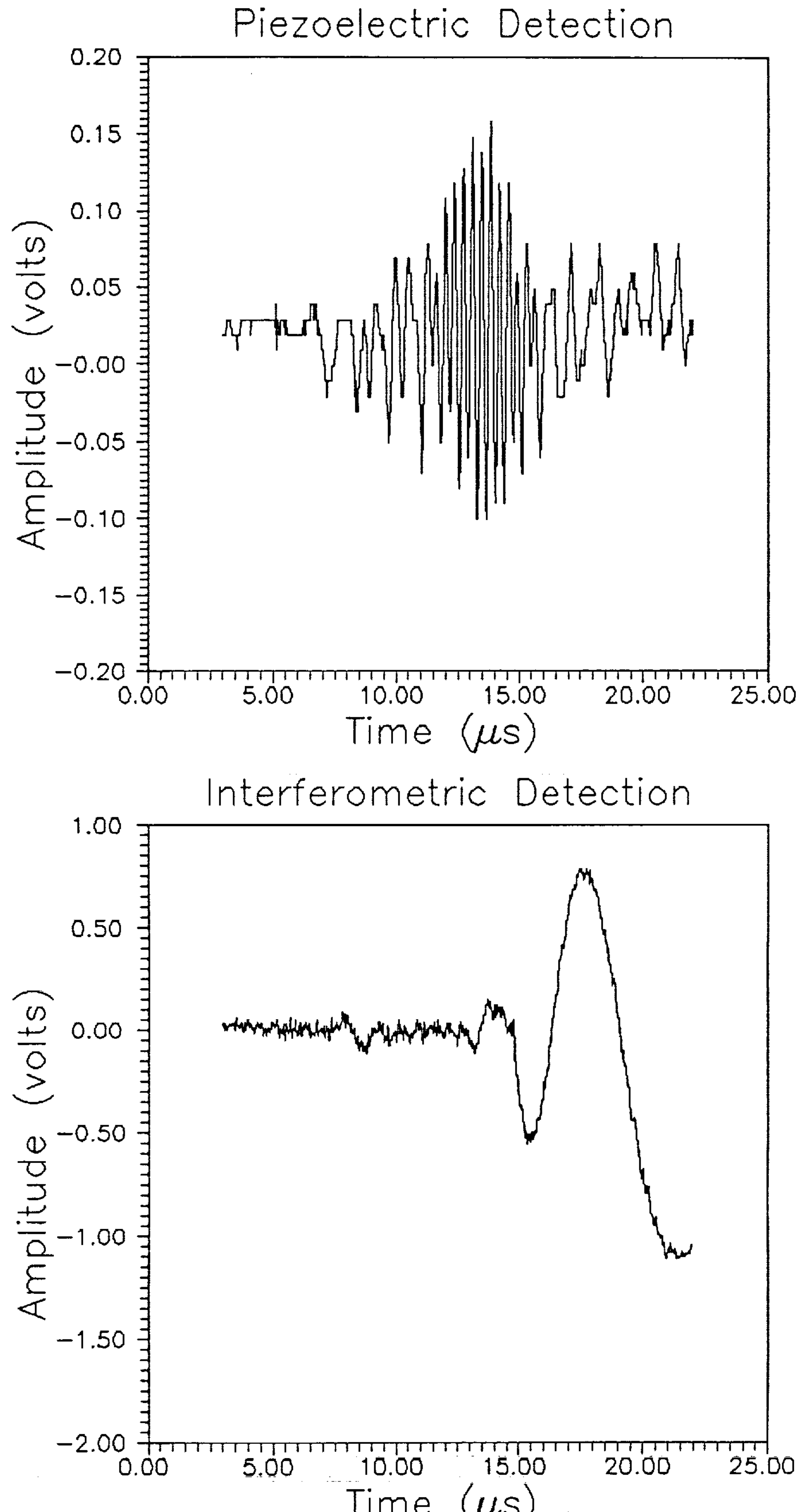

Laser Generated Ultrasound (Brass Plate)

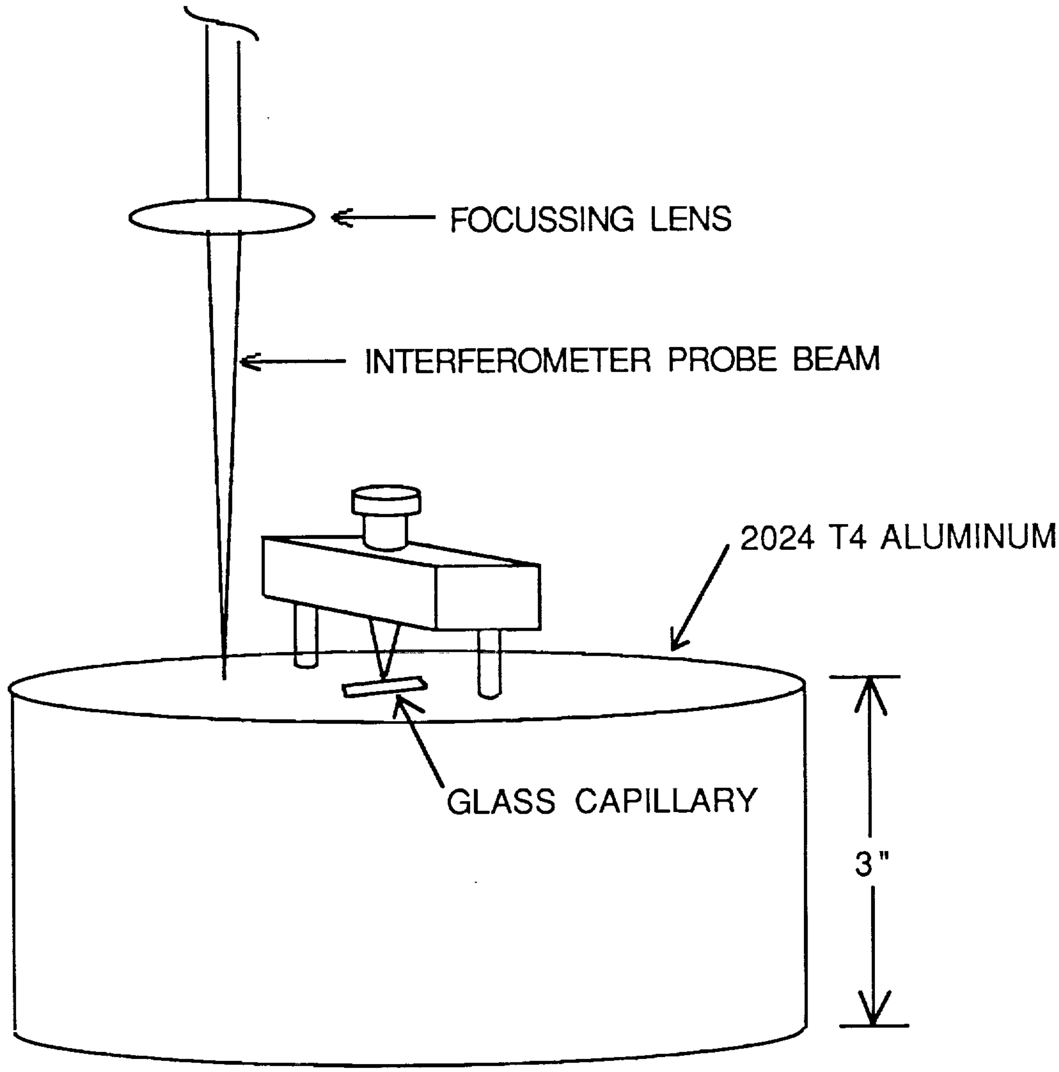
FOCUSSING LENS
INTERFEROMETER PROBE BEAM
2024 T4 ALUMINUM
GLASS CAPILLARY
3"

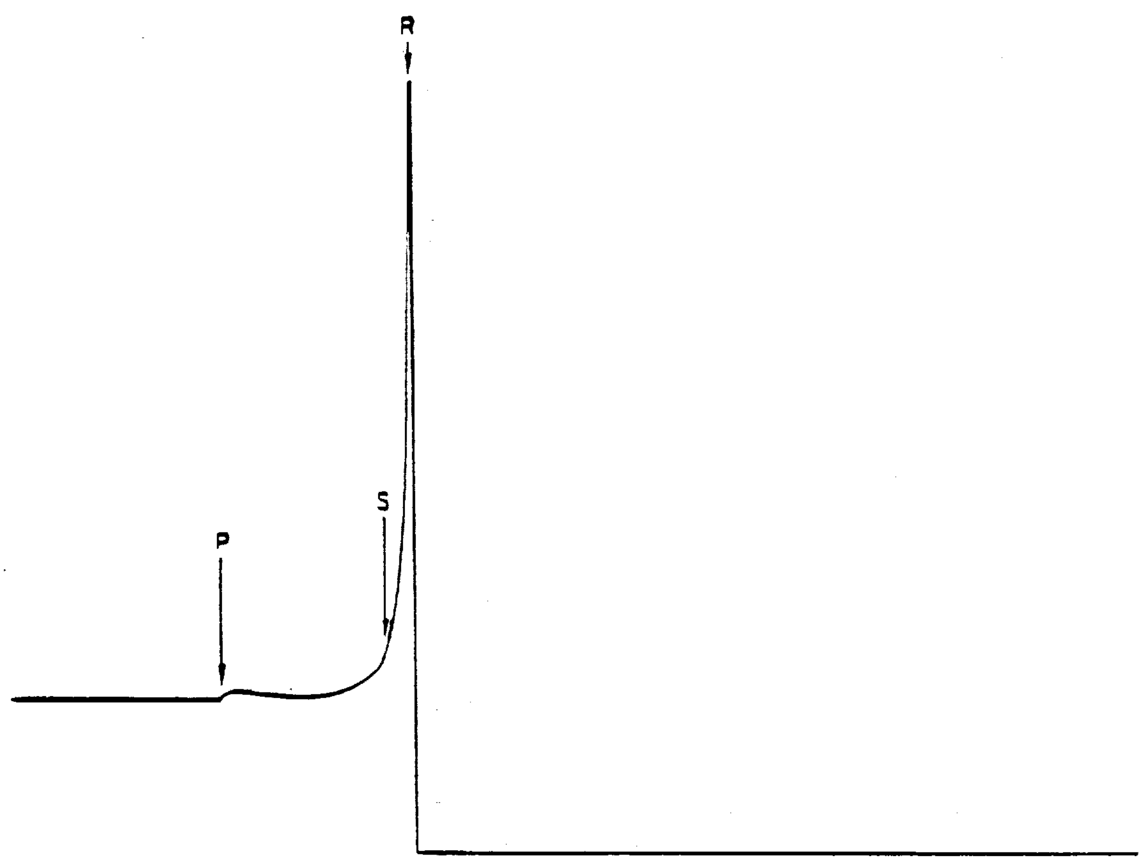

Figure 2. THEORETICAL RECORD OF A STEP-LOADING POINT SOURCE STRIKING AN INFINITE HALF-SPACE

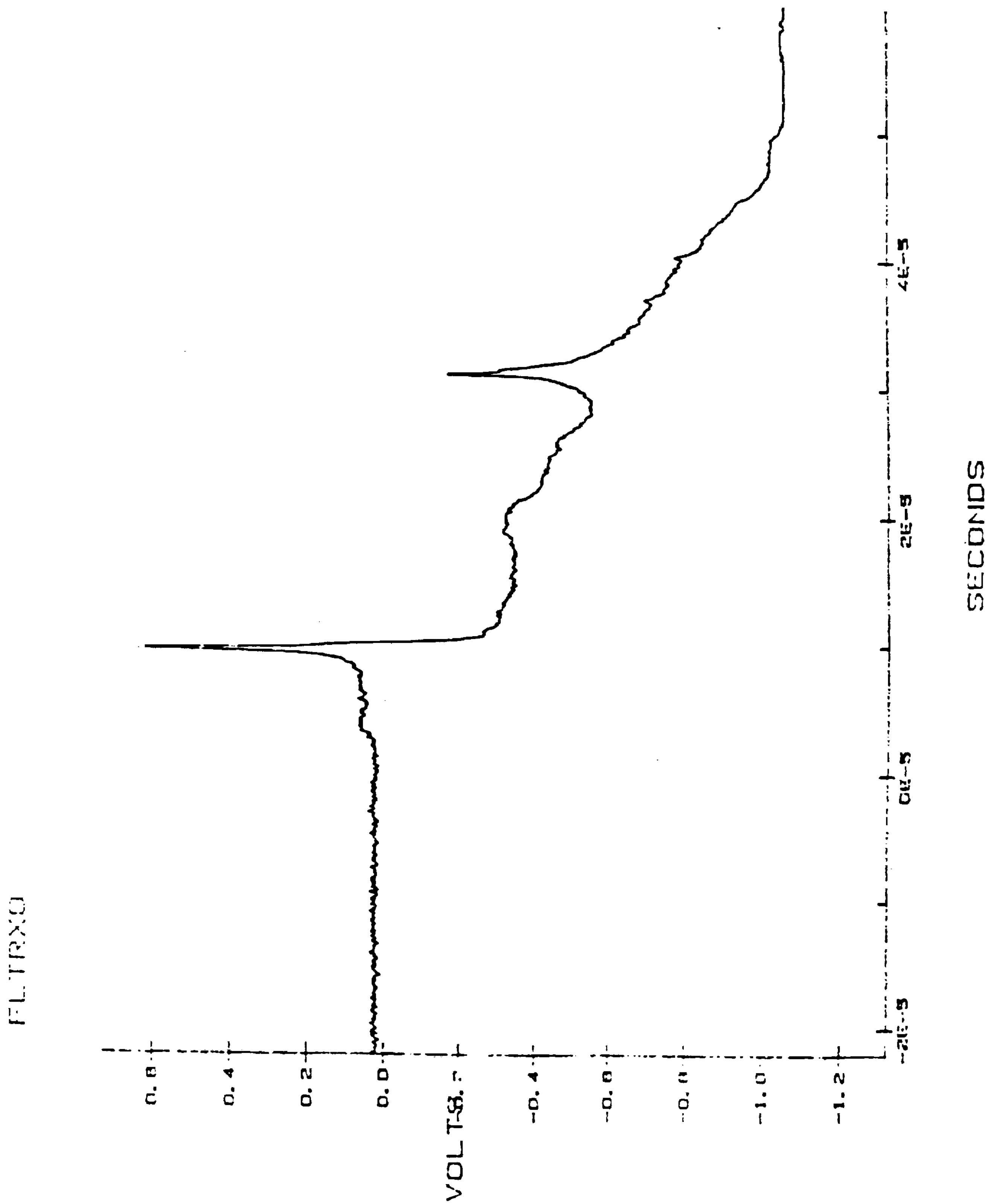
FLTRXO
VOLTS
SECONDS

DIMENSIONS OF SAMPLES USED IN LASER ACOUSTO-ULTRASONIC TESTS

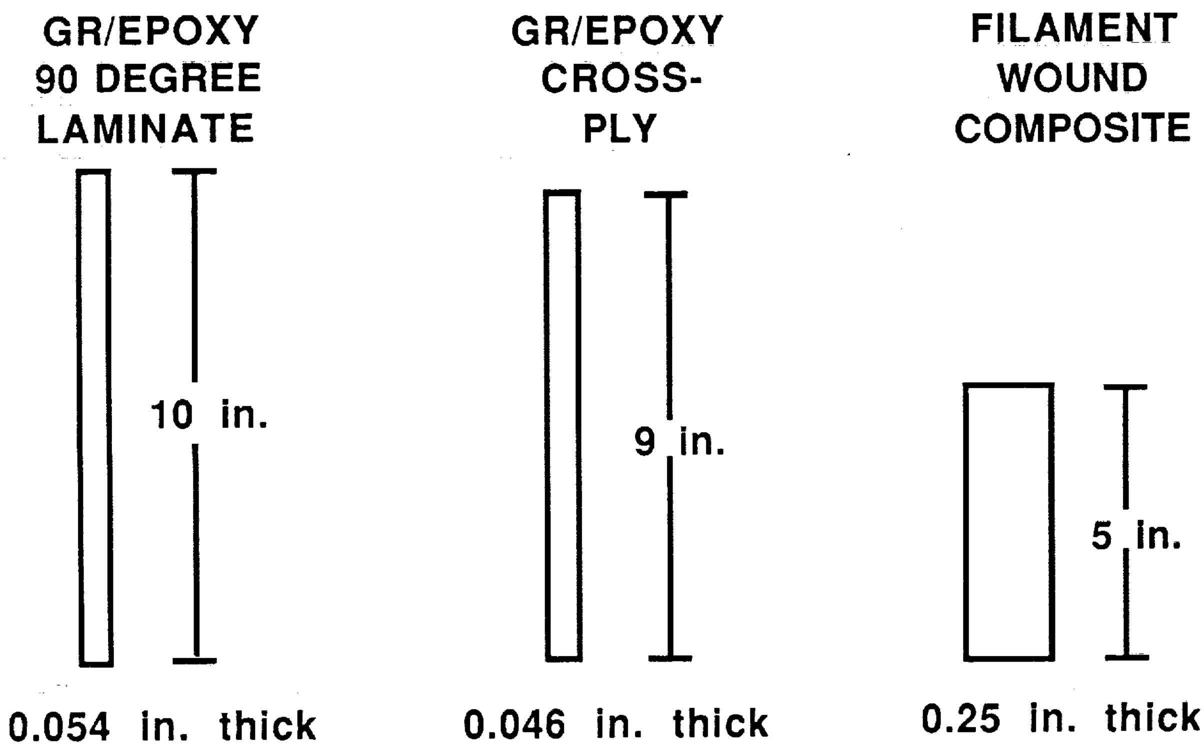

(ALL SPECIMENS 0.5 INCHES WIDE)

*3M SILVER POLYESTER FILM TAPE WAS USED AT DETECTION SITES TO INCREASE REFLECTIVITY

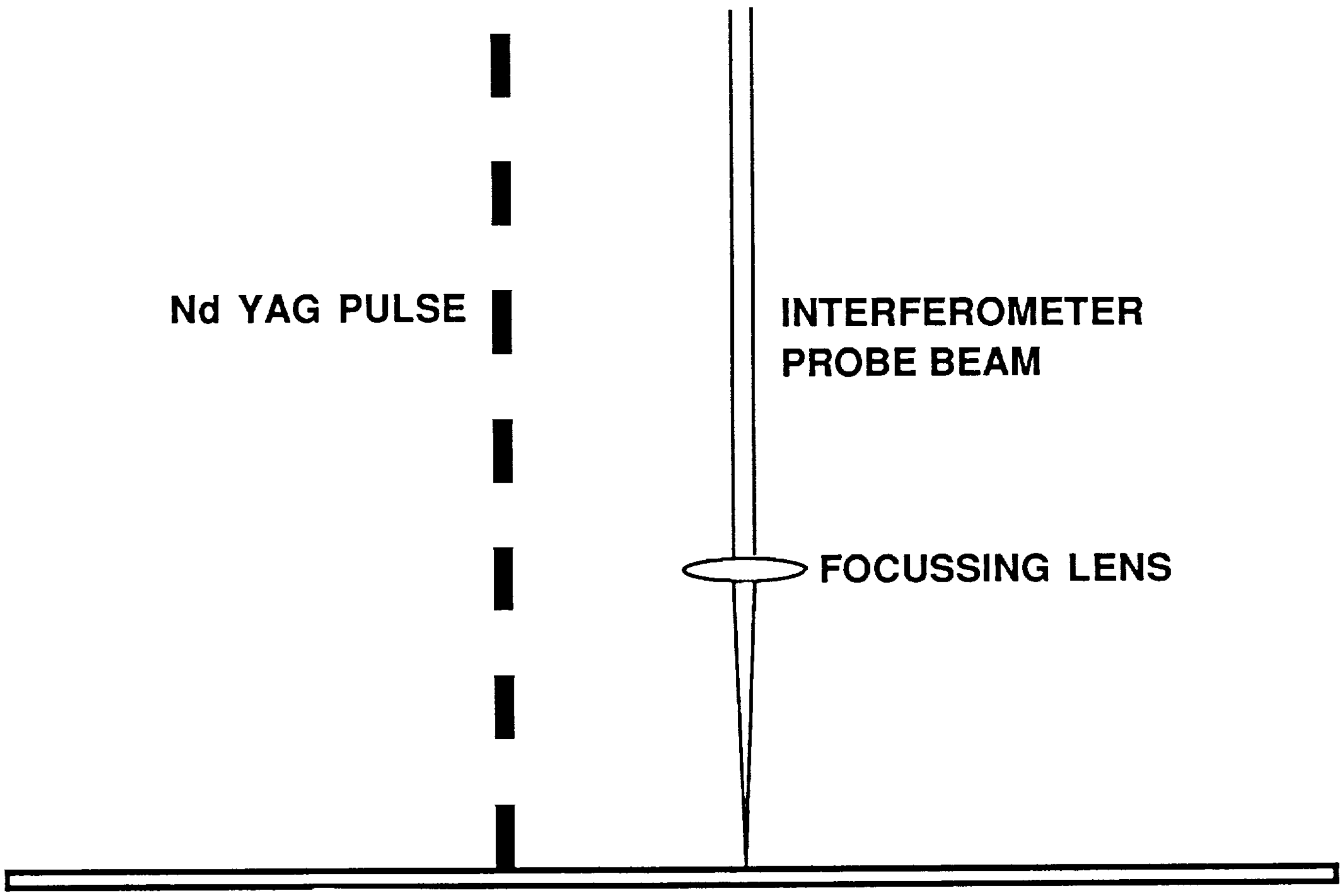

LASER ACOUSTO-ULTRASONICS

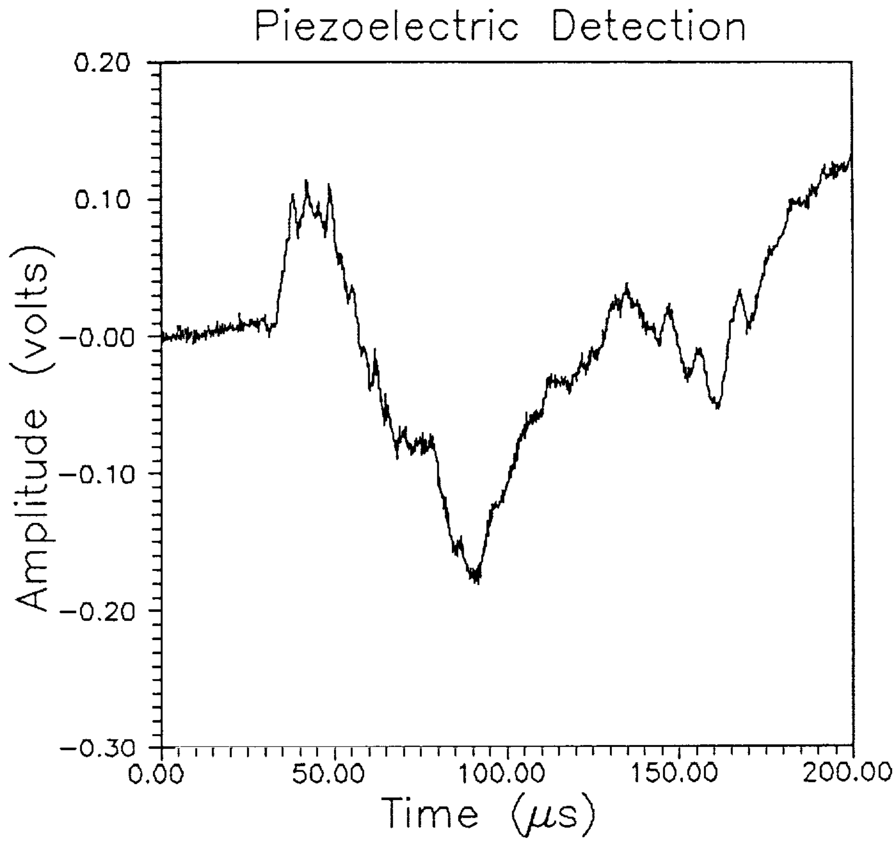

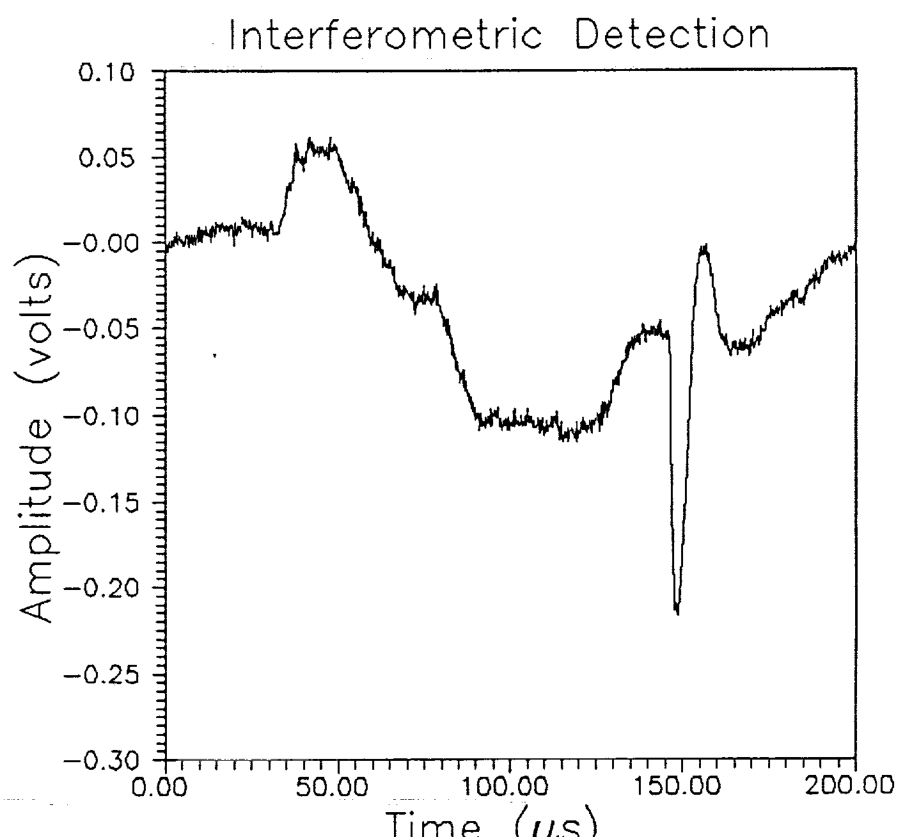

Laser Generation (Filament Wound Composite)

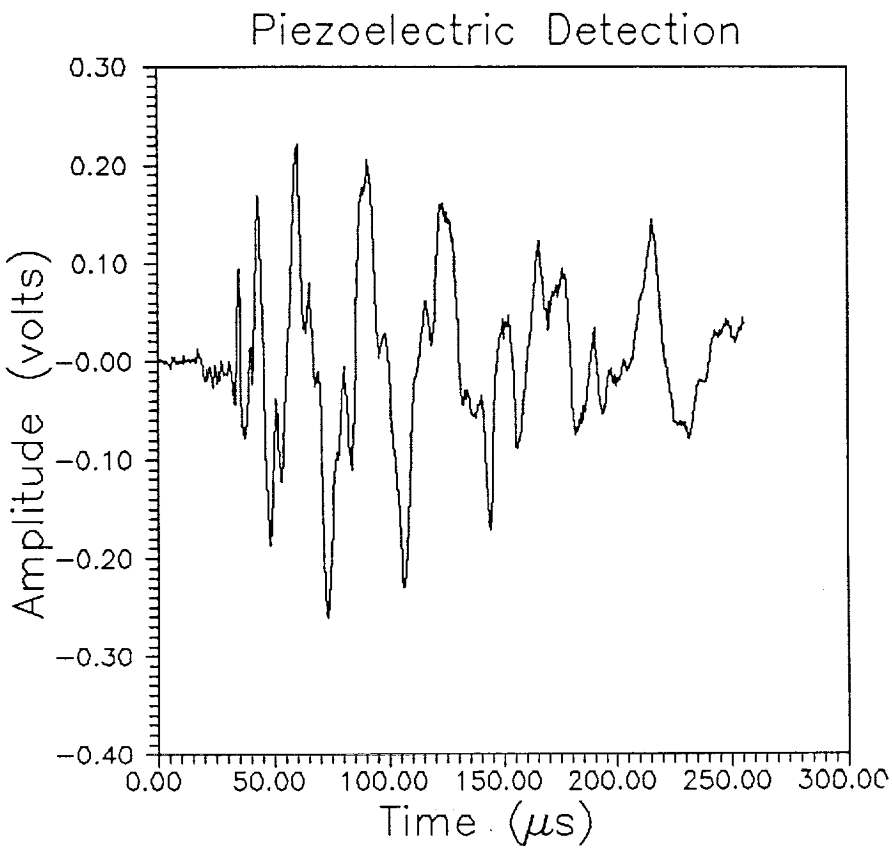

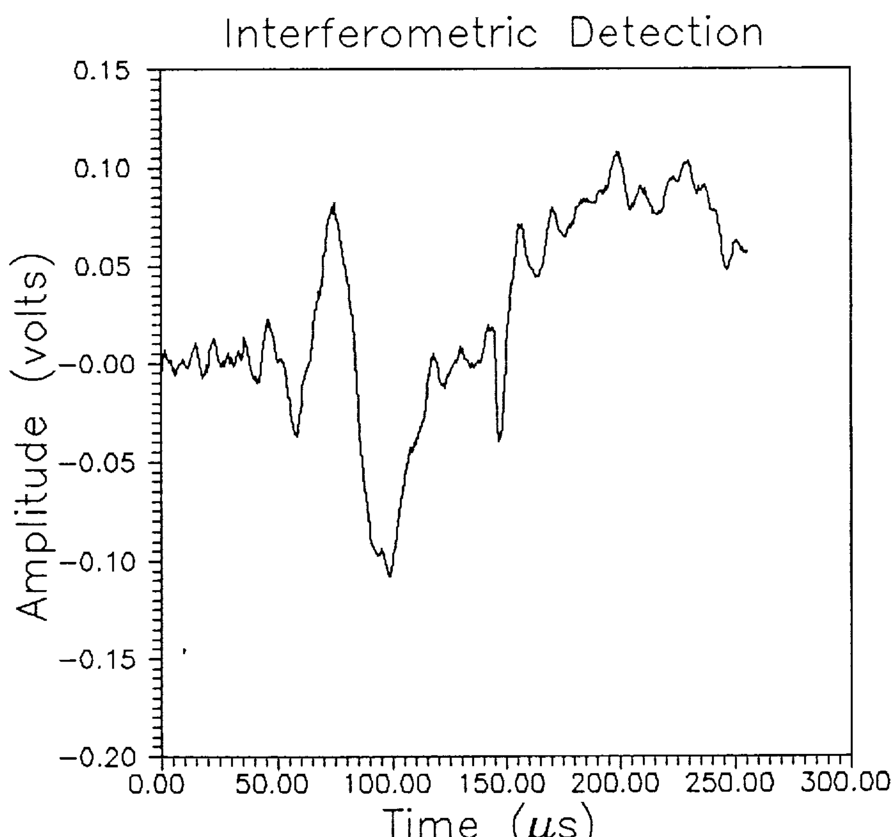

Laser Generation (Gr/Epoxy 90 Degree Laminate)

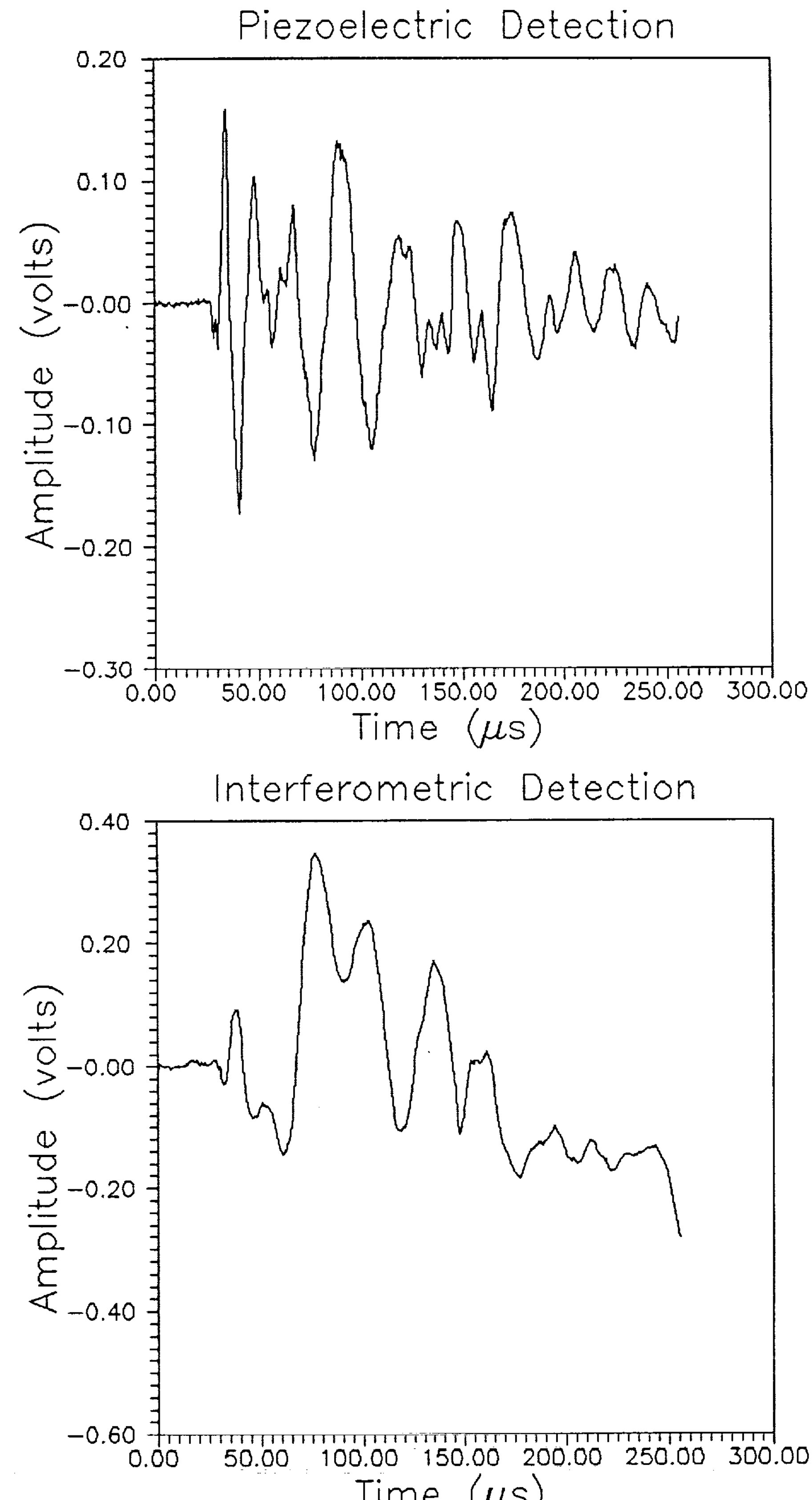

Laser Generation (Gr/Epoxy Cross-Ply)

SUMMARY

LASER ACOUSTO-ULTRASONICS COMPLEMENTS STANDARD PIEZOELECTRIC ACOUSTO-ULTRASONICS AND OFFERS NON-CONTACT NONDESTRUCTIVE EVALUATION.

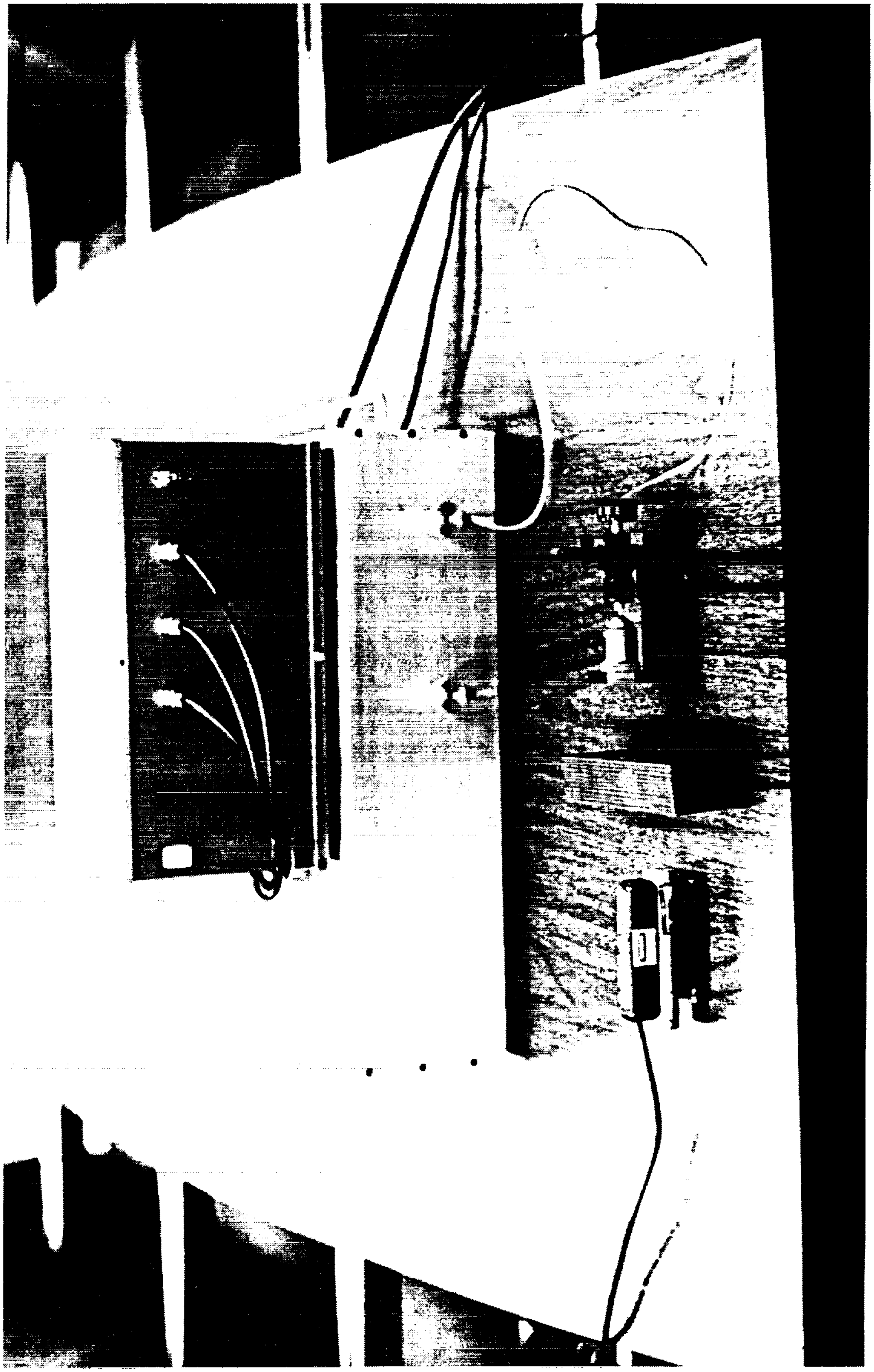

ORIGINAL PAGE
BLACK AND WHITE PHOTOGRAPH

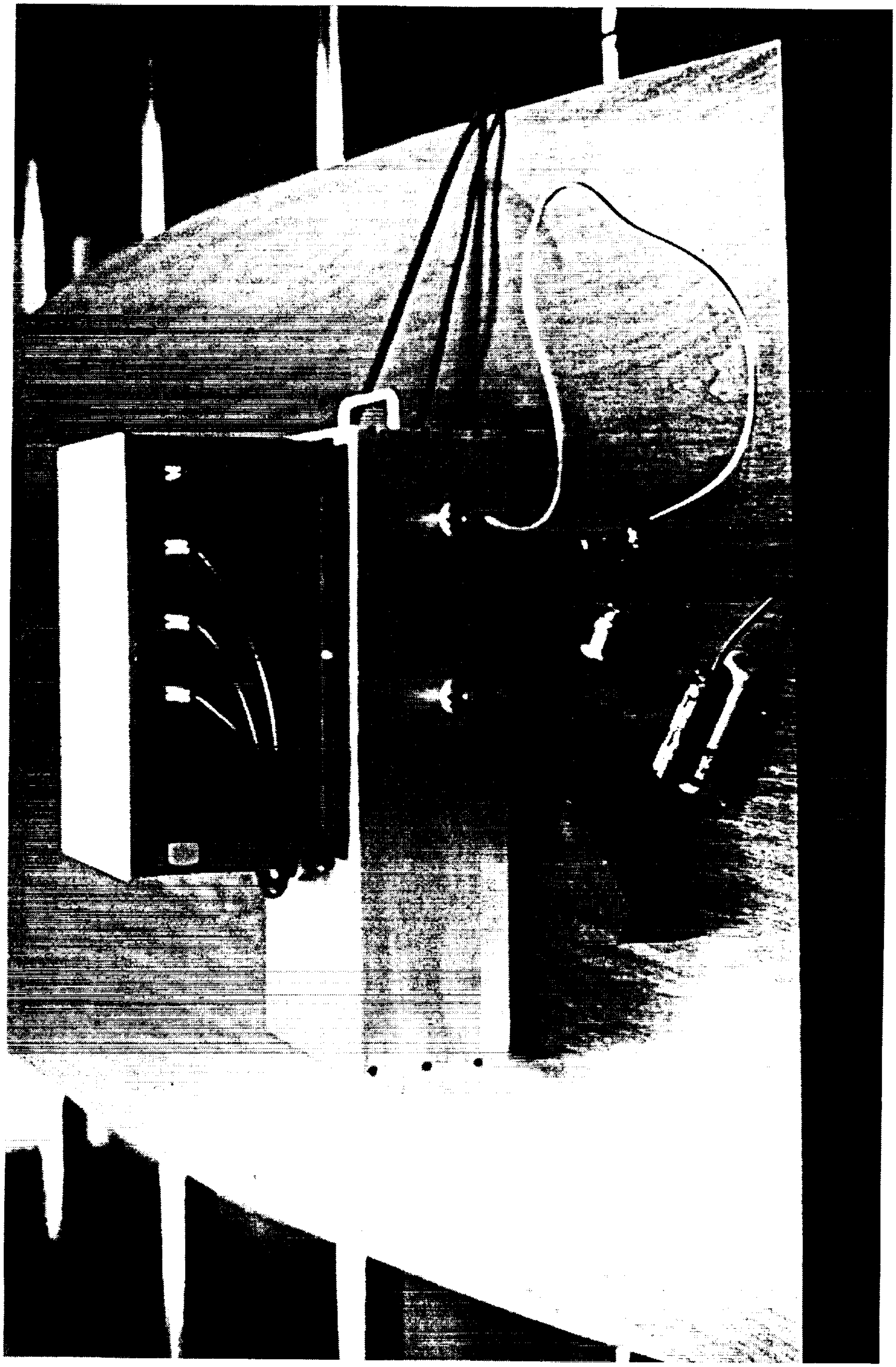

ORIGINAL PAGE
BLACK AND WHITE PHOTOGRAPH

ORIGINAL PAGE IS
OF POOR QUALITY

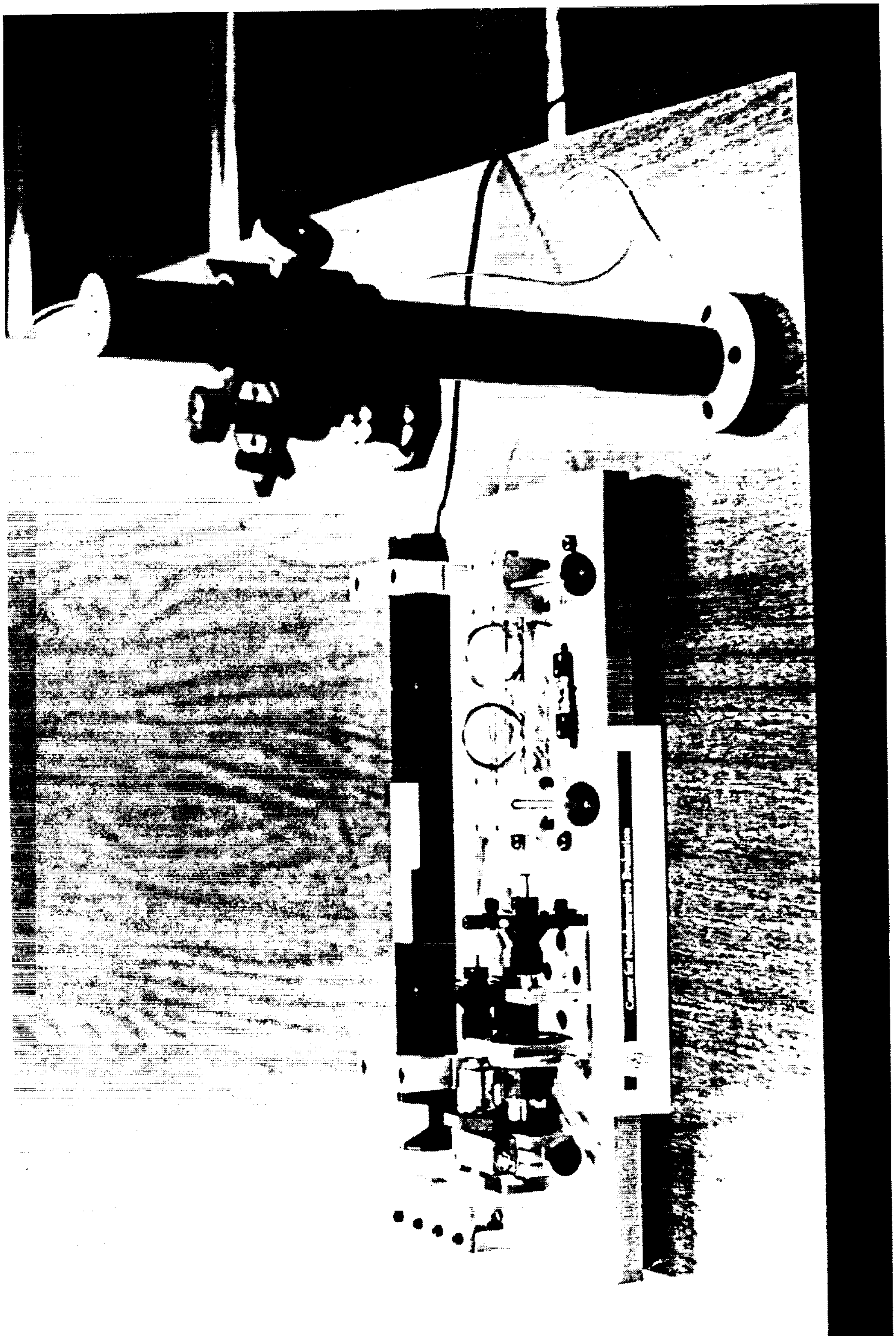

N91-18194

IMAGE CORRELATION NONDESTRUCTIVE EVALUATION OF IMPACT DAMAGE IN A GLASS FIBER COMPOSITE

S.S. Russell

Introduction to Digital Image Correlation
- Image Acquisition
- Speckle Generation
- Bilinear Interpolation
- Displacement and Strain Fields

Damage in Fiberous Composites
- Whitney and Neusimer Model
- Strains as an Indicator
- Failure Criteria as an Evaluation Tool

Damaged Coupons--Cross-Ply Scotchply Gl-Ep Laminate
- Inclusion
- Slit Fibers
- Impact Damage
  - Residual Strength
  - Failure Criteria Maximum Values

Conclusions

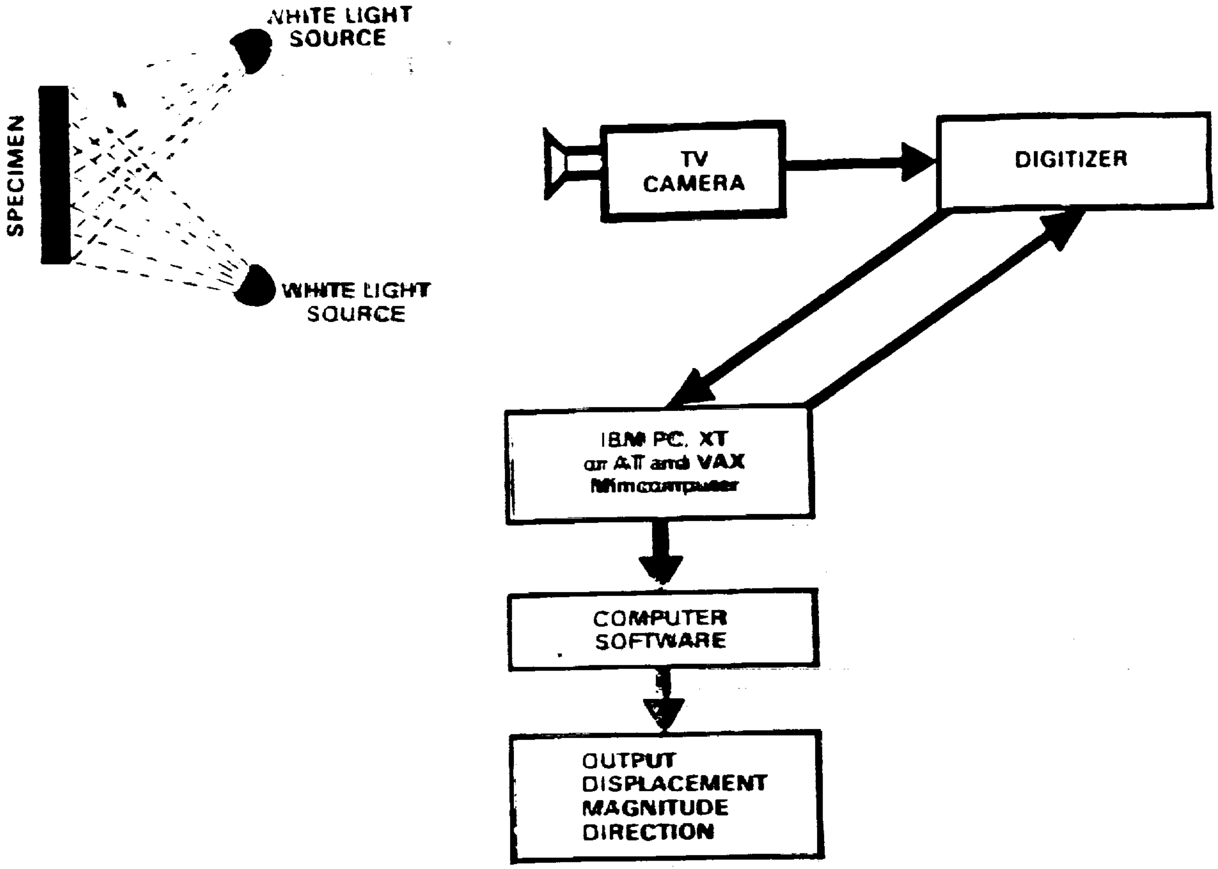

FIGURE 1. EXPERIMENTAL CONFIGURATION FOR IMAGE ACQUISITION AND IMAGE STORAGE.

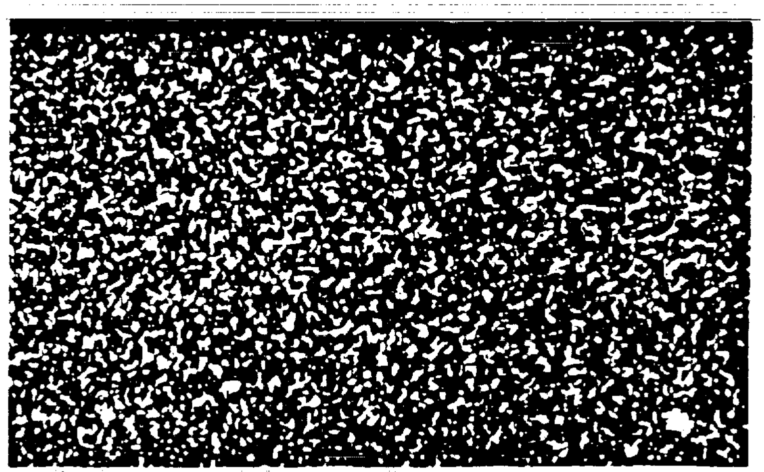

FIGURE 2. TYPICAL RANDOM SPECKLE PATTERN ON SURFACE OF SPECIMENS.

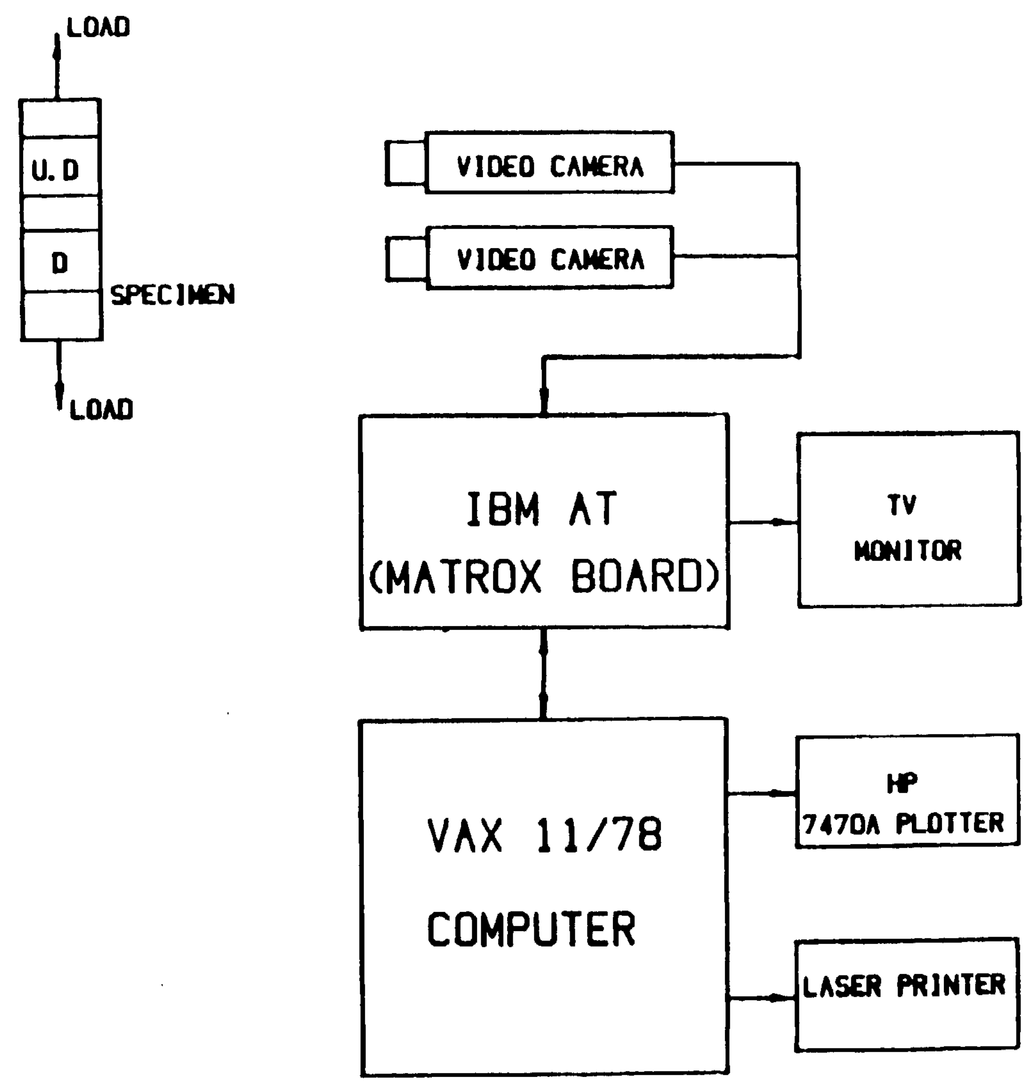

Fig. 4.5 Image processing set-up

C-2

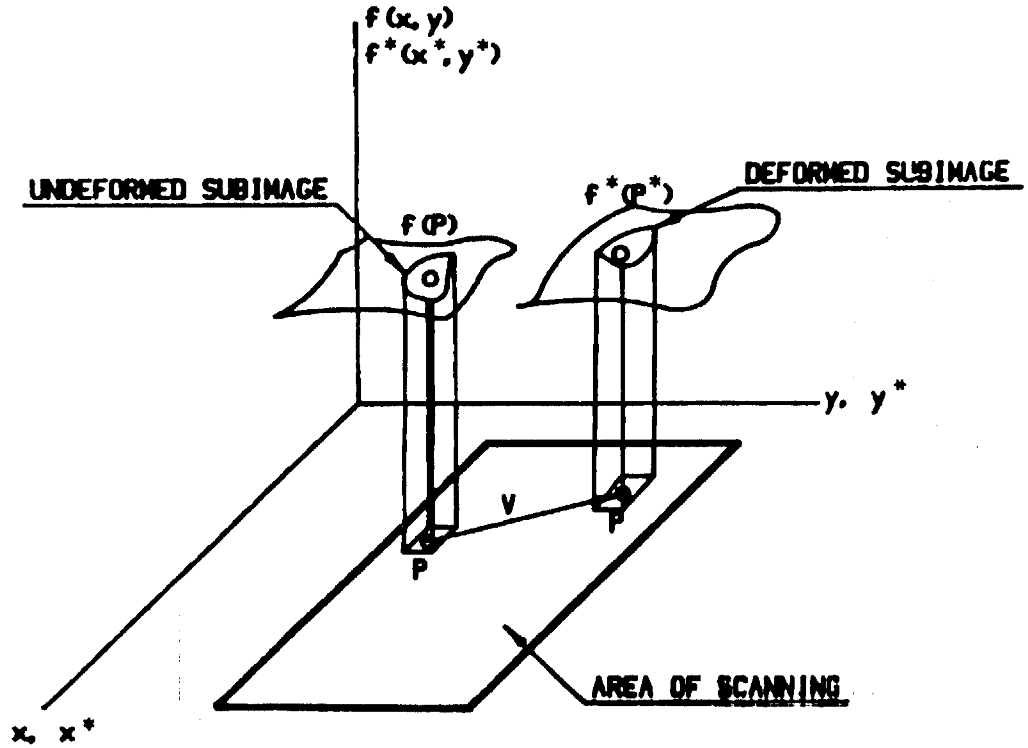

Fig. 2.3 Local motion and Distortion of a subset image

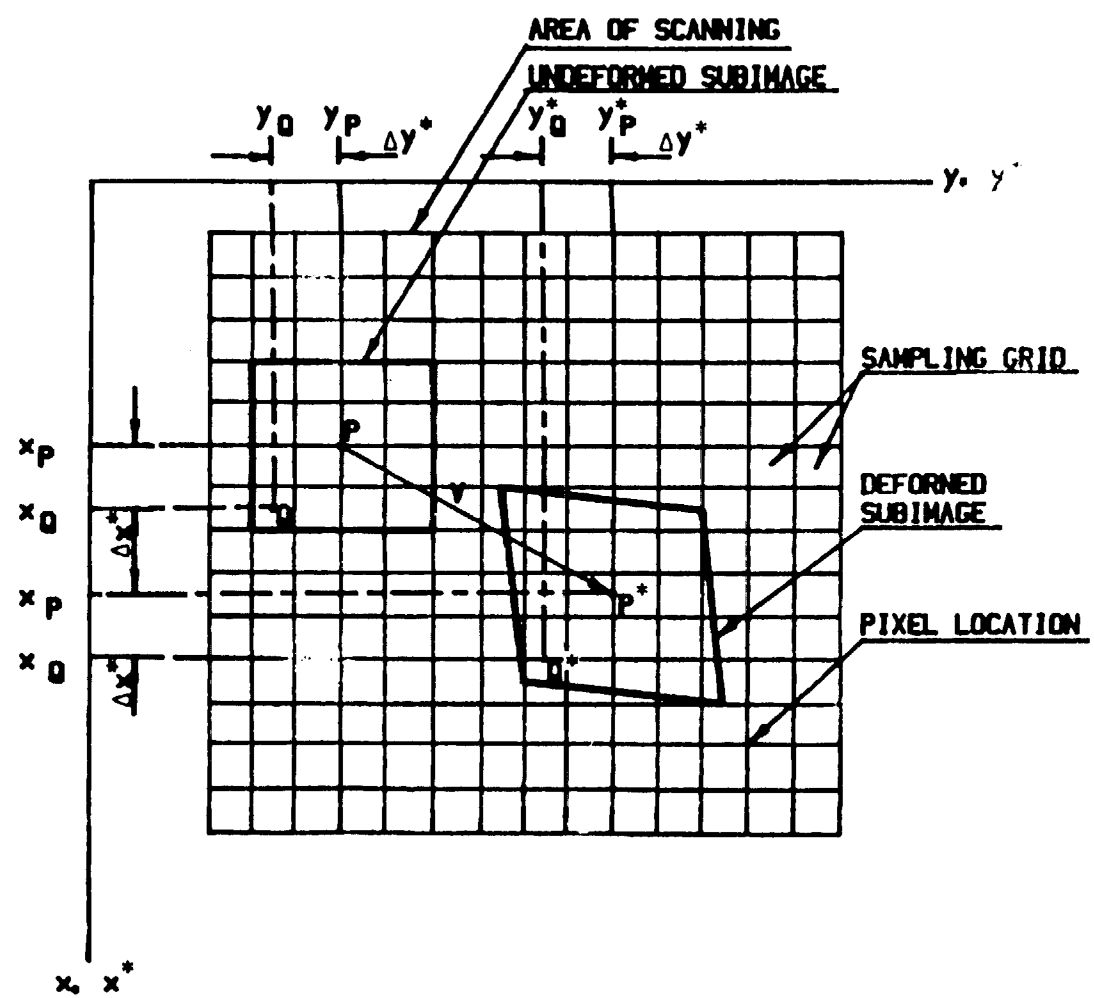

Fig. 2.4 Deformation of a subimage in a sampling grid

Bilinear Interpolation

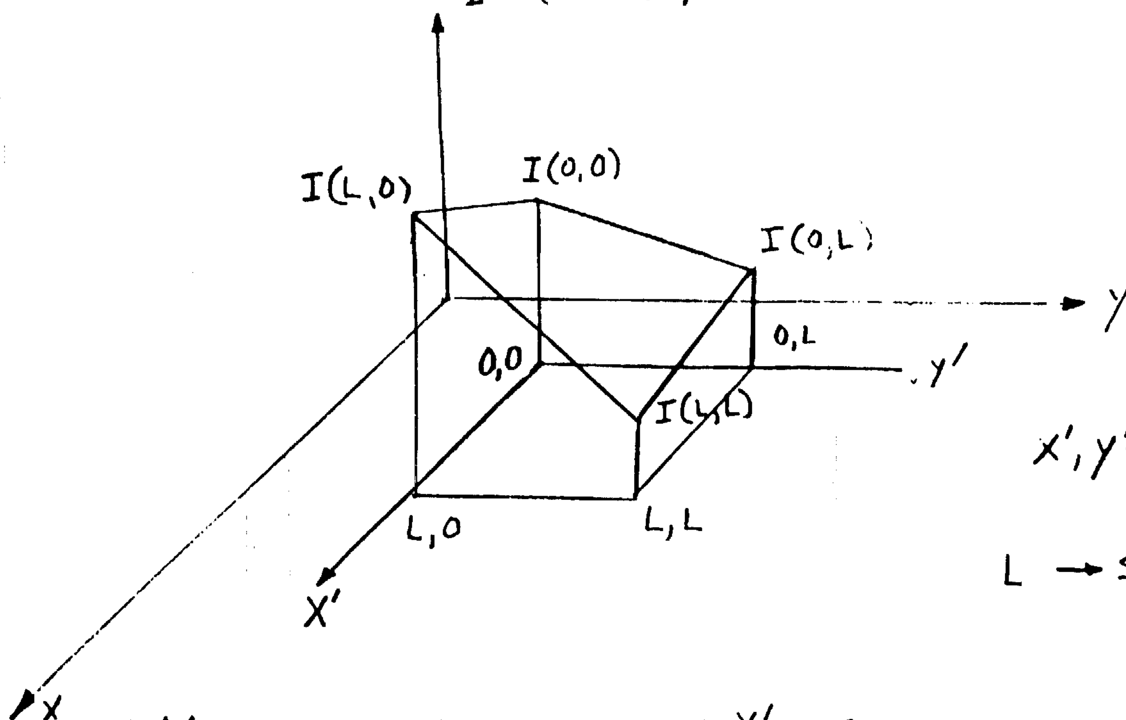

$x', y' \rightarrow$ local co-ordinates

$L \rightarrow$ Subset size

$$I(x',y') = I(0,0) + [I(L,0) - I(0,0)]\frac{x'}{L} + [I(0,L) - I(0,0)]\frac{y'}{L} + [I(L,L) + I(0,0) - I(L,0) - I(0,L)]\, x'y'/L^2$$

$$C\left(u, v, \frac{\partial u}{\partial x}, \frac{\partial u}{\partial y}, \frac{\partial v}{\partial x}, \frac{\partial v}{\partial y}\right) = \frac{\int_{\Delta M^*} f(x,y)\, f^*(x+\xi, y+\eta)\, dA}{\left[\int_{\Delta M} [f(x,y)]^2 dA \int_{\Delta M^*} [f^*(x+\xi, y+\eta)]^2 dA\right]^{1/2}} \quad (2.13)$$

$$\xi = u + \frac{\partial u}{\partial x} \Delta x + \frac{\partial u}{\partial y} \Delta y$$

$$\eta = v + \frac{\partial v}{\partial x} \Delta x + \frac{\partial v}{\partial y} \Delta y$$

(pixels)

$$\epsilon_{xx} = \frac{\partial u}{\partial x} = \frac{u(200,100) - u(160,100)}{40 \text{ (pixels)}}$$

$$\epsilon_{yy} = \frac{\partial v}{\partial y} = \frac{\Delta v}{\Delta y}$$

etc.

Use Strains as Indicator of Damage
Use Control Load

Concept: Measure strains, generate Tsai-Hill failure map

$$F_I = A\,\varepsilon_1^{\,2} + B\,\varepsilon_2^{\,2} + C\,\varepsilon_1\,\varepsilon_2 + D\,\gamma_{12}^{\,2}$$

where

$$A = \frac{Q_{11}^{\,2}}{X^2} + \frac{Q_{12}^{\,2}}{Y^2} - \frac{Q_{11}\,Q_{12}}{X\;Y}$$

$$B = \frac{Q_{12}^{\,2}}{X^2} + \frac{Q_{22}^{\,2}}{Y^2} - \frac{Q_{11}\,Q_{22}}{X\;Y}$$

$$C = \frac{2\,Q_{11}Q_{12}}{X^2} + \frac{2\,Q_{12}Q_{22}}{Y^2} - \frac{Q_{11}\,Q_{22} + Q_{12}^2}{X\;Y}$$

$$D = \frac{Q_{66}^{\,2}}{S^2}$$

$$Q_{11} = \frac{E_1}{1 - \nu_{12}\,\nu_{21}}$$

$$Q_{12} = \frac{\nu_{12}\,E_2}{1 - \nu_{12}\,\nu_{21}}$$

$$Q_{22} = \frac{E_2}{1 - \nu_{12}\,\nu_{21}}$$

$$Q_{66} = G_{12}$$

SUPPORTING RESEARCH

- Whitney and Nuismer model
  JCM, Vol. 8, July 1974

"failure occurs when the average stress over some distance, a_0, equals the unnotched laminate strength."

Hole

$$\sigma_N = \sigma_0 \left[\frac{2(1-\xi_2)}{2 - \xi_2^2 - \xi_2^4} \right]$$

where

$$\xi_2 = \frac{R}{R + a_0}$$

a_0 is material parameter
$a_0 \sim 0.15$ for 1002 Gl-Ep Scotchply

Notch

$$K_q = \sigma_0 \sqrt{\pi a_0 \xi_4}$$

where

$$\xi_4 = \frac{C}{2C + a_0}$$

C is 1/2 notch length

1 ~ 256 pixels ⟶ 40 pixels ~ 0.156 in
in.

So critical distance is appropriate.
However, damage is generally complex stress-strain state!

Test Case: Cross-Ply Gl-Epoxy Scotchply Coupons

Damage: Inclusion
Slit Fibers
Impact Damage

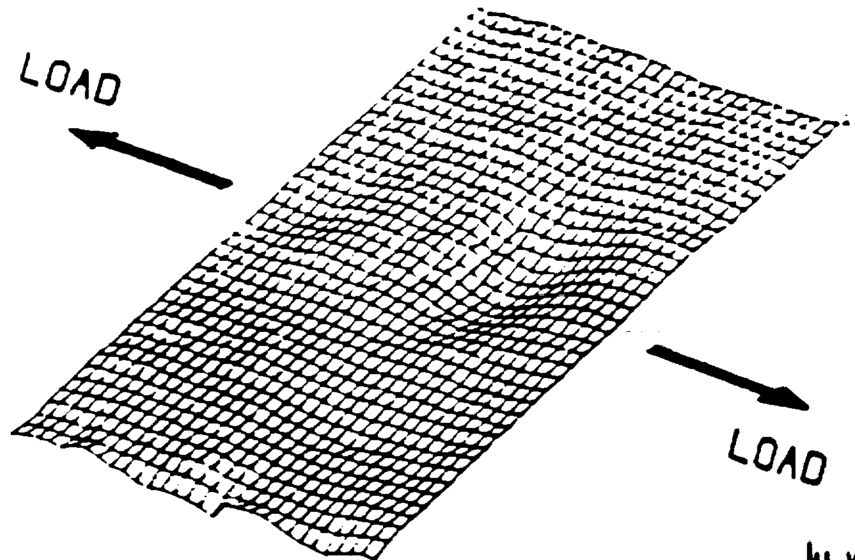

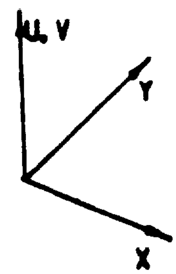

(a) Axial Displacement u

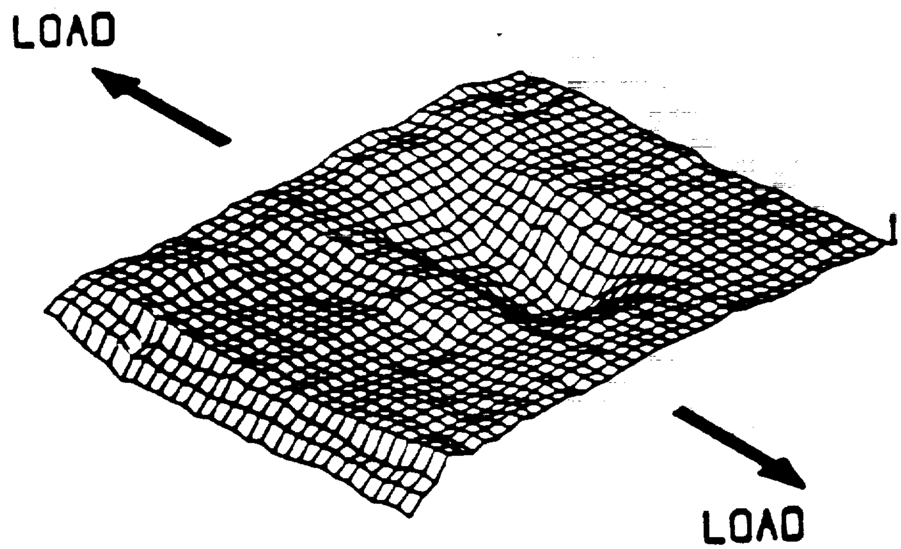

(b) Transverse Displacement v

FIGURE 6. DISPLACEMENTS FOR MYLAR INCLUSION.

$[0, 90_4, 0]^\circ$ $\epsilon_x = 0.33\%$

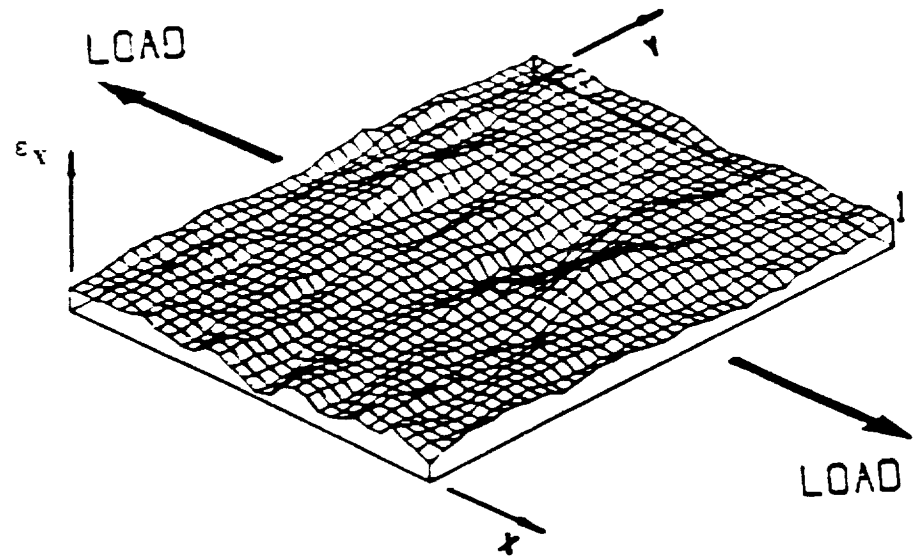

(a) Axial Strain ε_x

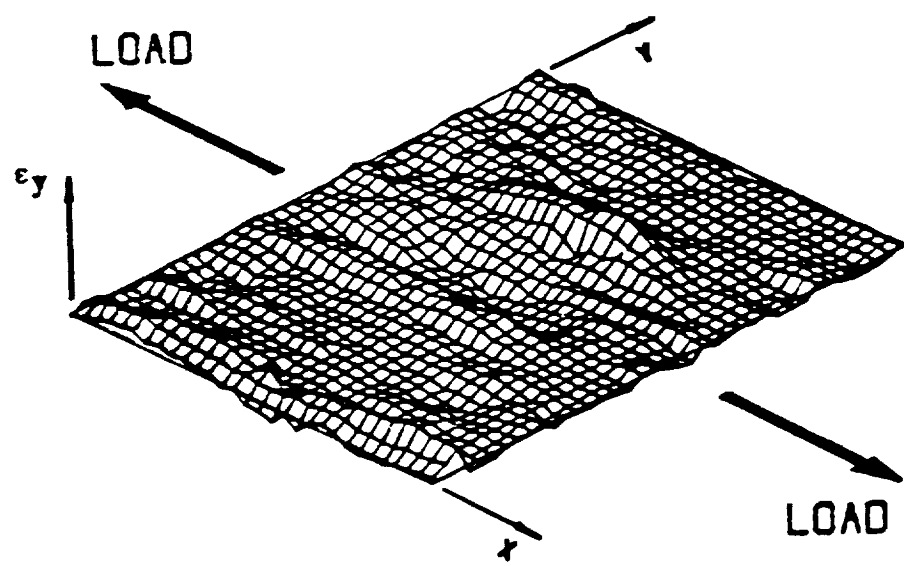

(b) Transverse Strain ε_y

FIGURE 7. STRAINS FOR MYLAR INCLUSION.

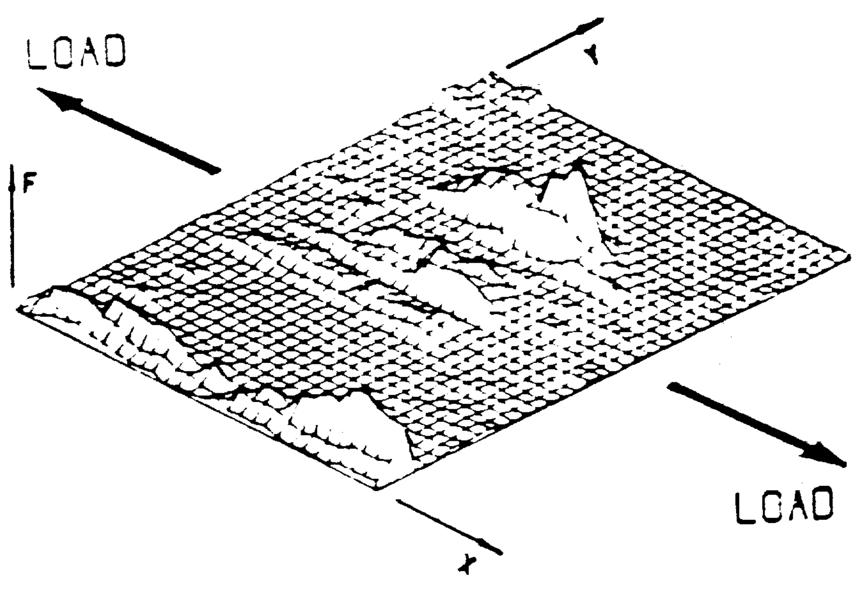

FIGURE 8. FAILURE FUNCTION (F) FOR MYLAR INCLUSION.

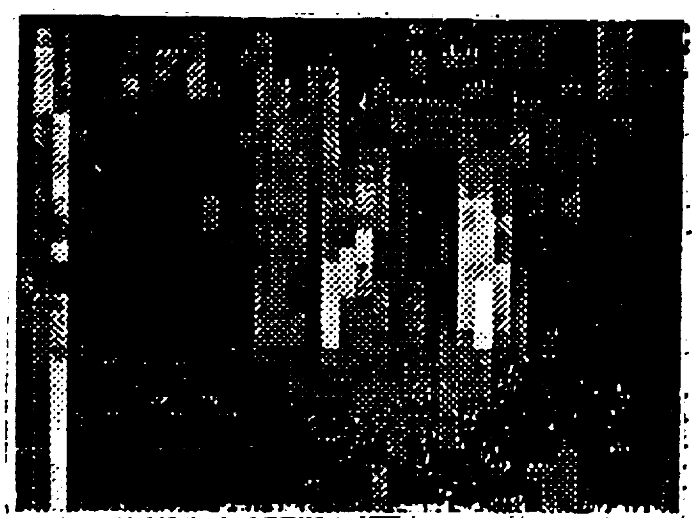

E 9. GREY LEVEL FAILURE FUNCTION (F) FOR MYLAR INCLUSI
BLACK TO WHITE SIGNIFIES INCREASING VALUES OF F.

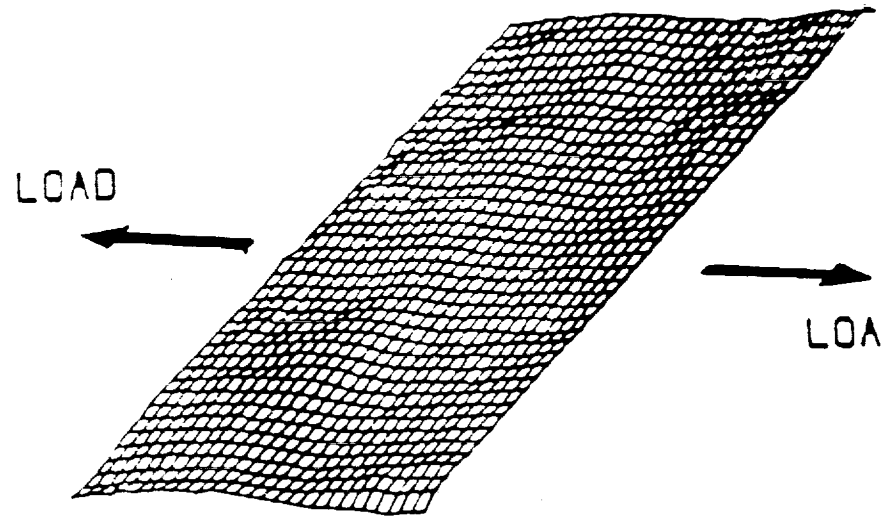

(a) Axial Displacement u

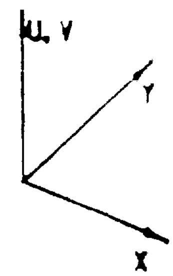

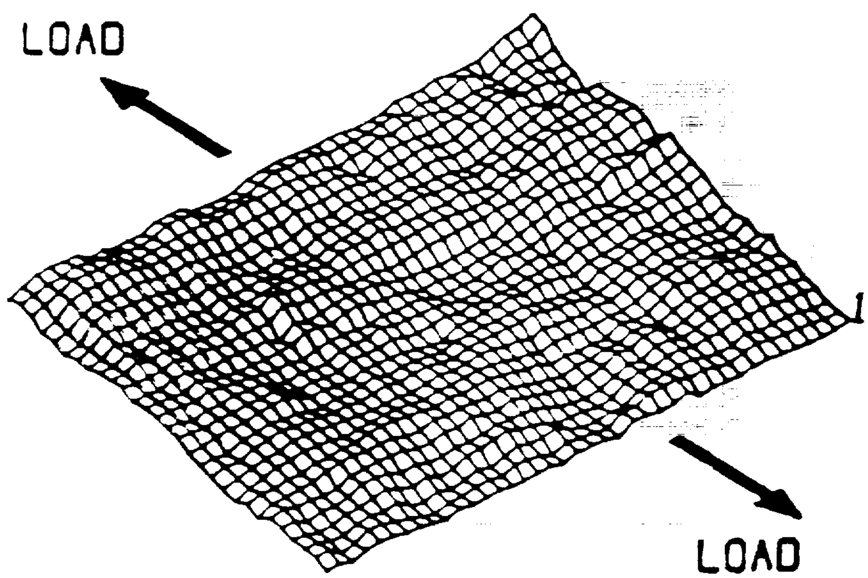

(b) Transverse Displacement v

FIGURE 11. DISPLACEMENTS AWAY FROM THE INCLUSION.

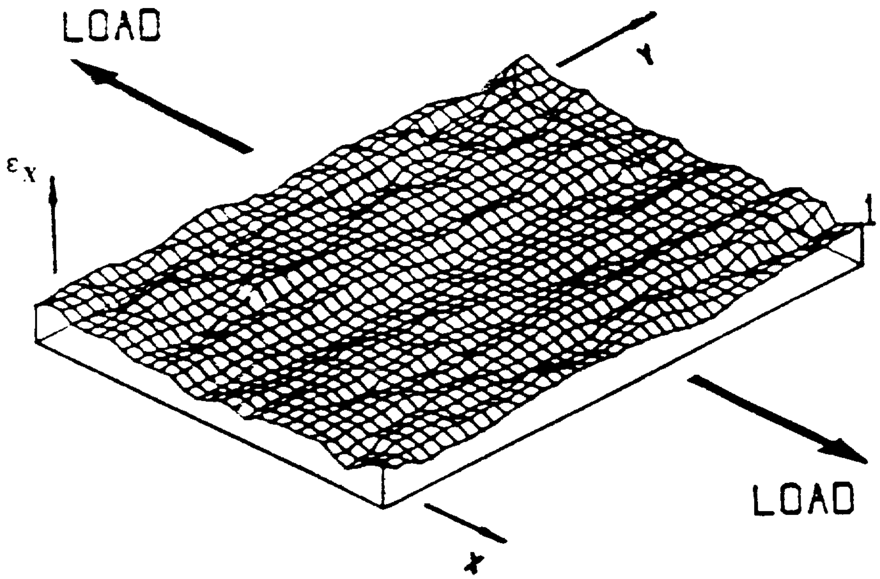

(a) Axial Strain ε_x

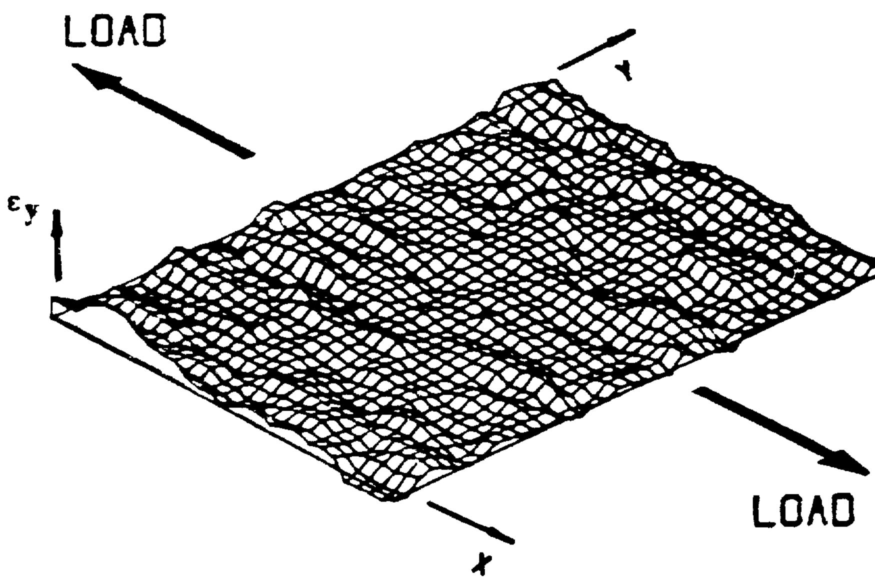

(b) Transverse Strain ε_y

FIGURE 12. STRAINS AWAY FROM THE INCLUSION.

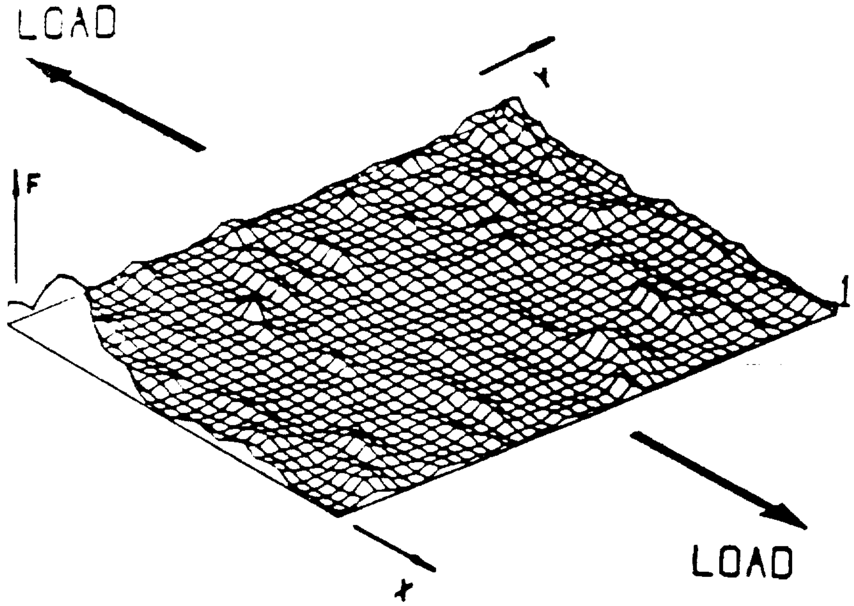

FIGURE 13. FAILURE FUNCTION (F) FIELDS AWAY FROM THE INCLUSION.

FIGURE 14. GREY SCALED FAILURE FUNCTION FIELD AWAY FROM THE INCLUSION.

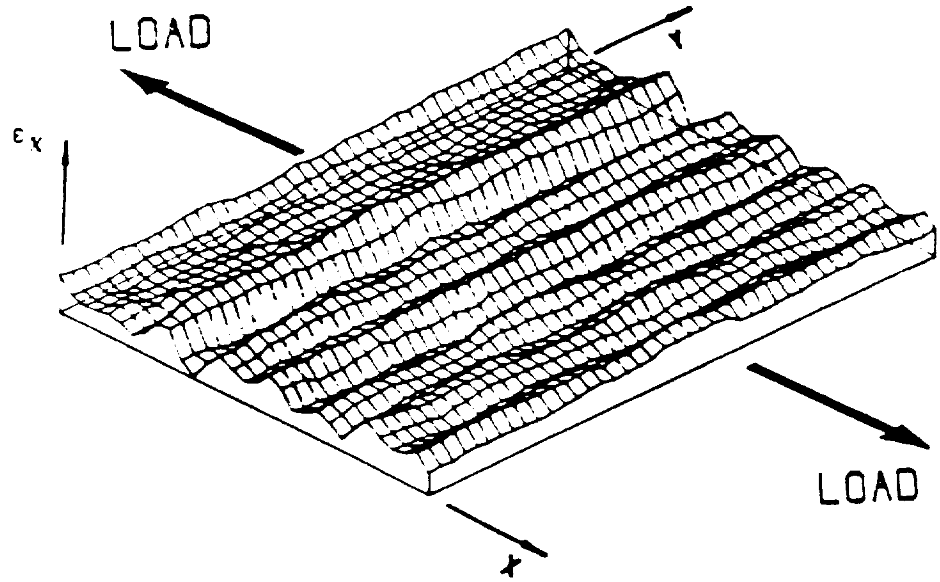

(a) Axial Strain ε_x

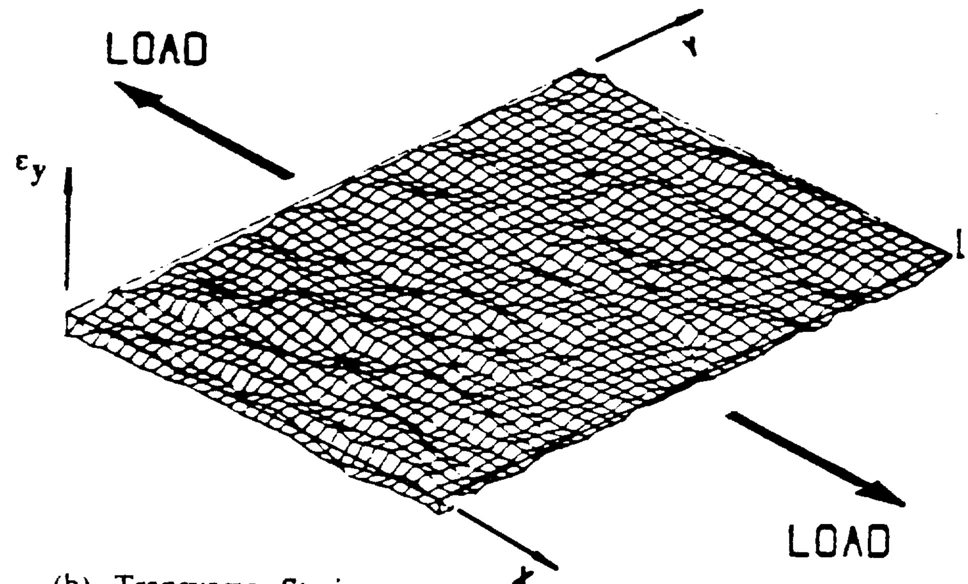

(b) Transverse Strain ε_y

FIGURE 16. STRAINS FOR SPECIMEN WITH SLIT THROUGH BACK 0° PLY.

$\epsilon_x = 0.4\%$ $[0_2\ 90_3\ 0_2]$

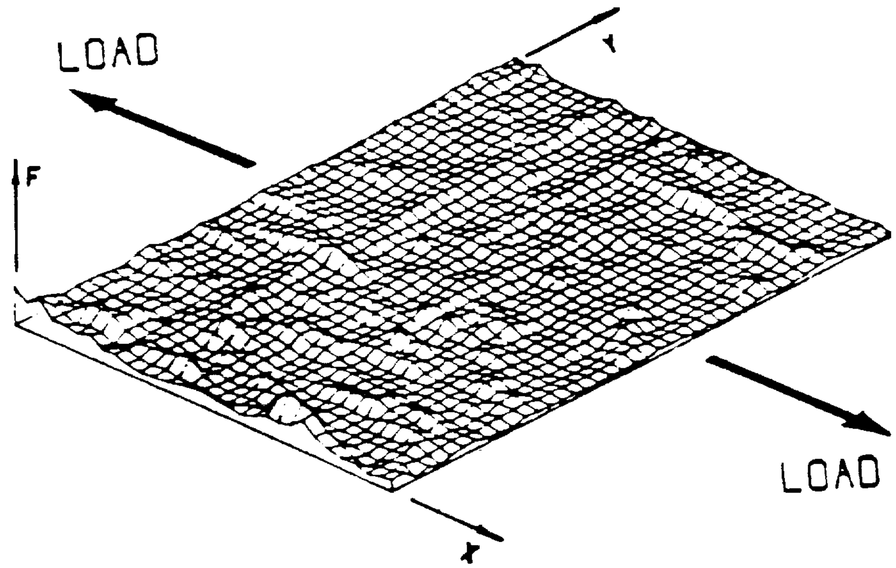

FIGURE 17. FAILURE FUNCTION (F) FOR SPECIMEN WITH SLIT THROUGH BACK 0° PLY.

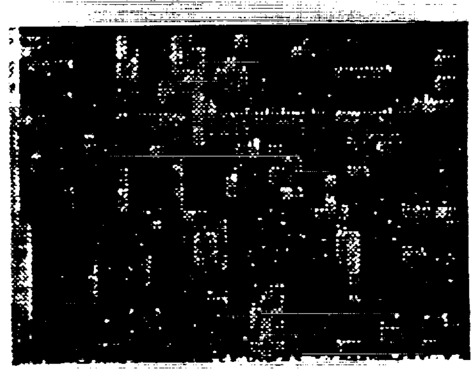

FIGURE 18. GREY LEVEL PRESENTATION OF FAILURE FUNCTION FOR SPECIMEN WITH SLIT THROUGH BACK 0° PLY.

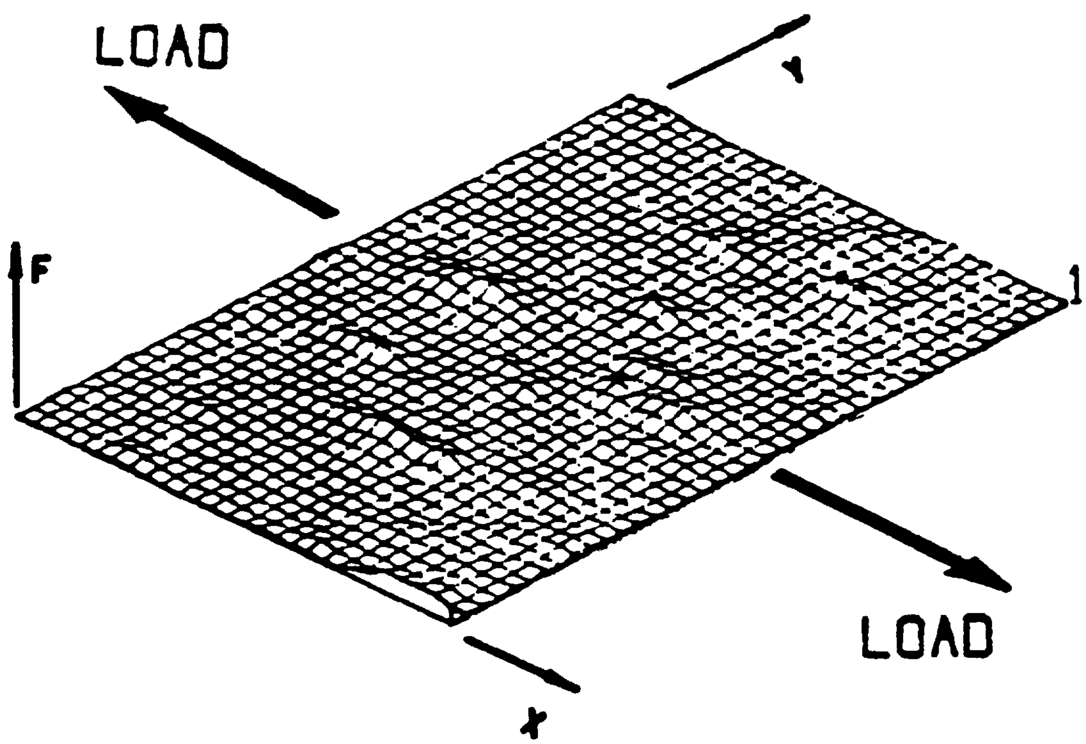

FIGURE 21. FAILURE FUNCTION (F) AT IMPACT DAMAGED ZONE.

$[0°, 90°_3, 0°]$

$\epsilon_x = .26\%$

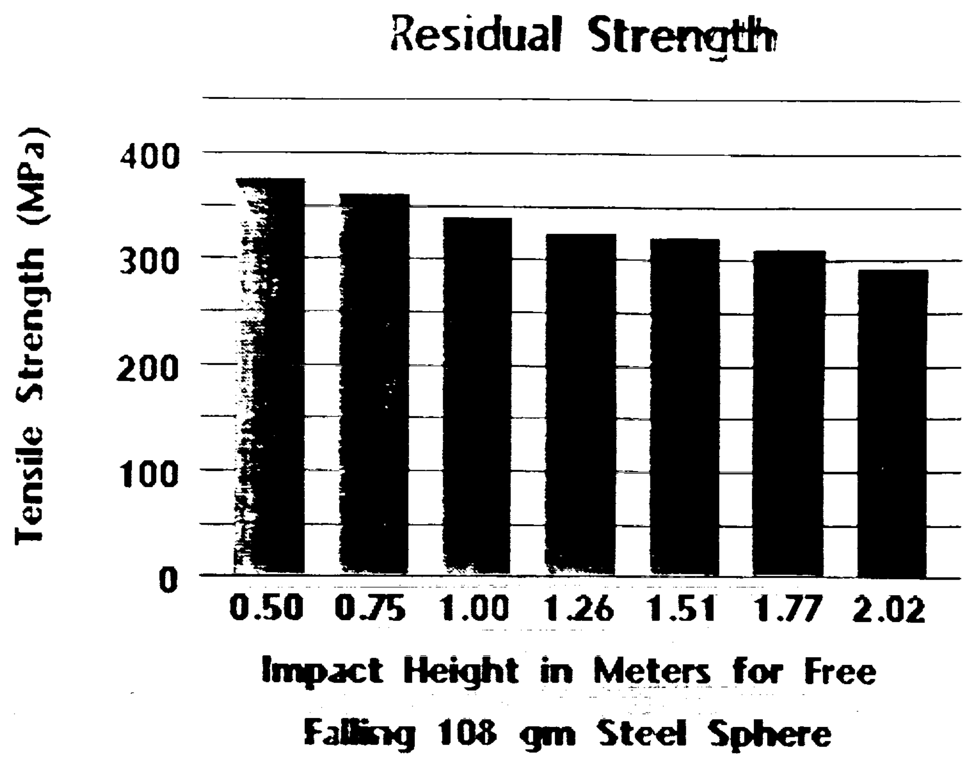

FIGURE 22. STRENGTH OF IMPACTED [0°, 90°$_3$, 0°] SPECIMENS

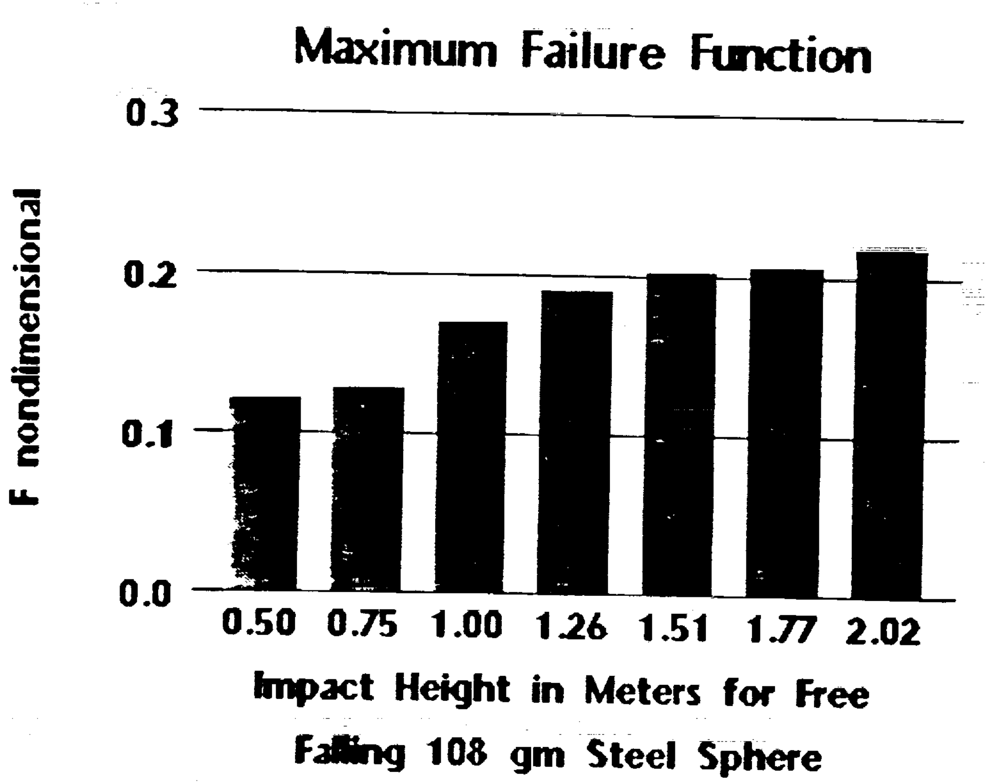

FIGURE 23. MAXIMUM FAILURE FUNCTION (F) FOR IMPACTED [0°, 90°$_3$, 0°] SPECIMENS.

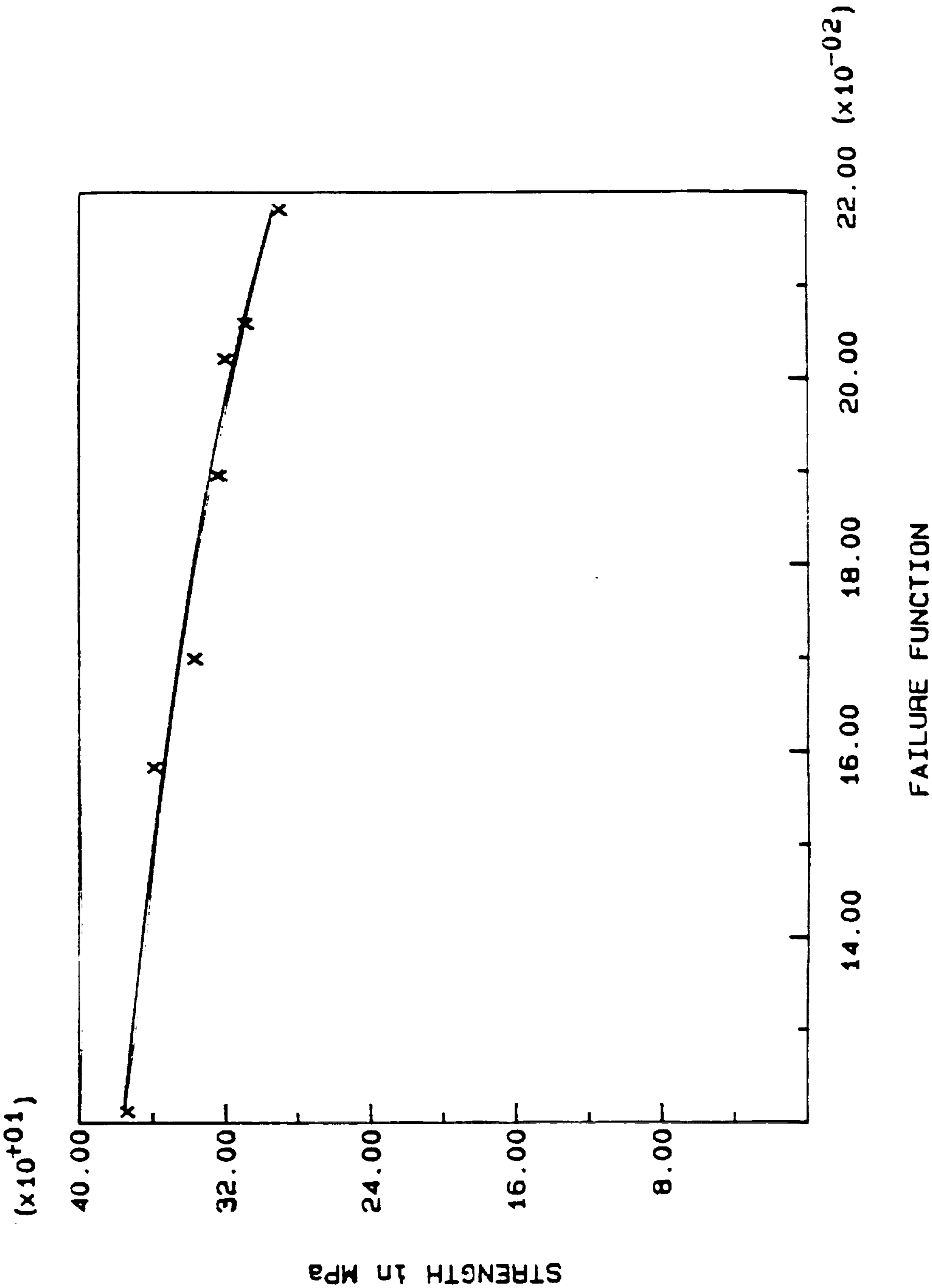

STRENGTH in MPa
(x10^+01)
40.00
32.00
24.00
16.00
8.00
FAILURE FUNCTION
14.00
16.00
18.00
20.00
22.00
(x10^-02)

CONCLUSIONS

- IMAGE CORRELATION ACCURACY--0.03%
- STRAINS CAN BE PROCESSED THROUGH TSAI-HILL FAILURE CRITERIA TO QUANTIFY DAMAGE
- STATISTICAL DATA BASE MUST BE GENERATED TO EVALUATE CERTAINTY OF DAMAGE ESTIMATE
- SIZE EFFECTS NEED CONSIDERATION
- BETTER NUMERICAL TECHNIQUES NEEDED FOR PREVIOUS TWO GOALS

N91-18195

EDDY-CURRENT INSPECTION OF SHUTTLE HEAT EXCHANGER TUBE WELDS*

C. V. Dodd†, G. W. Scott‡ and L. D. Chitwood†

ABSTRACT

The Space Shuttle Main Engine is inspected during manufacture, after each test firing, and as part of refurbishment between missions. The LOX heat exchanger has four tubing welds in locations that are difficult to reach and inspect. The most difficult to access is located approximately 30.6 in. (0.78 m) from the inlet, through tubing 0.190 in. (4.83 mm) ID, past a 90 degree, 0.69 in. (18 mm) radius bend, and approximately halfway around a loop 16.5 in. (42 cm) diameter. We designed a multiple property test using computer-aided engineering software written, at ORNL earlier, that modeled the tube and probe and enabled simulation of instrument response in the inspection environment. Design parameters were optimized for a single-winding, single-layer "pancake" coil. The necessary sensitivity to small defects can be achieved within the limits imposed by material variations. The probe contains an array of eight coils. Four coils each are mounted 90 degrees apart on the equators of two plastic spheres joined at their poles by a straight section. The two four-coil arrays are offset 45 degrees, so that as the probe passes through the tube, one coil covers each 45 degree segment of the wall circumference. Lift-off up to 0.008 in. (0.2 mm) is electronically compensated by corrections developed in the design, so there is no requirement to maintain intimate contact between the probe and the tube wall.

Experimental multifrequency measurements performed on tubing weld specimens supplied by Rockwell Rocketdyne Division indicated the presence of ferrite in the welds, which likely accounts for anomalous results observed in single-frequency eddy-current tests. In addition, there was a weld pedestal that ranged up to 0.004 in. (0.10-mm) in the tube samples tested. This pedestal tended to produce signals that were in a direction opposite to that of the defect signals.

The system response to multiple discrete frequencies was simulated by computing the response to each independently and combining the results. The presence of ferrite in the welds suggested the use of pulse excitation to reduce sensitivity to variations in permeability. Final system tests demonstrated that a 0.005 in. (0.13 mm) deep defect could be detected with the array probe, using the three-frequency eddy-current instrument driving the multiplexer coils. A 0.003 in. (0.08 mm) deep defect and a 0.006 in. (0.15 mm)

---

* Research Sponsored by NASA

† Oak Ridge National Laboratory, operated by Martin Marietta Energy Systems Inc., under contract DE-AC05-84OR21400 with the U.S. Department of Energy

‡ Martin Marietta Michoud, New Orleans.

deep defect at the welds were detected in the split tube samples. A single coil was driven by the impedance analyzer at three and then six frequencies. The signal to noise ratio was best at the six-frequency test, which indicates that the pulse test, with its higher frequency content, will be superior to the three-frequency test. However, the pulsed measurements were not made due to time constraints.

INTRODUCTION

Background

The present method for manufacturing inspection the of welds in heat exchanger tubing and combustion chamber injection posts in the Space Shuttle Main Engine (SSME) uses single-frequency eddy currents. There were difficulties with signal interpretation and probe clearances through accesses when using this method. Eddy-current tests have not been applied to the inservice inspection of these components.

The Oak Ridge National Laboratory has expertise in multiple-frequency and pulse excited eddy-current inspection technology.[1,2] The incentive for use of multiple-frequency techniques is the need to achieve accurate detection and sizing of weld flaws while rejecting or discriminating against the effects of variations in other properties, such as tubing wall thickness or probe liftoff. Single-frequency systems respond to several different property variations, and in many cases cannot distinguish the anomalous test indications from flaws, causing false positives.

Pulse Eddy-current (PEC) technology effectively examines the part with many frequencies.[3,4] Measurements of the pulse shape required for analyses, however, can be accomplished with simpler, more reliable, and less expensive instrumentation than that required for multiple discrete frequencies. If the pulses are large enough, they saturate any permeability changes in the material and reduce their effect on the test. Nevertheless, PEC was a later development because the analysis leading to signal processing algorithms was more difficult.

Problem

A representation of the heat exchanger along with the three welds that were proposed for technique development are shown in Figure 1. The welds are listed below:

(1) the LOX heat exchanger Primary Tube-Bifurcation Joint Transition (RS008812 -#3 in Figure 1);

(2) the LOX Heat Exchanger Secondary Tube-Bifurcation Joint (so-called "Baby Pants") welds (RS008812 -#1 and #2 in Figure 1); and

(3) the Main Combustion Chamber Injection Posts which are straight tubes in the same size range with similar welds.

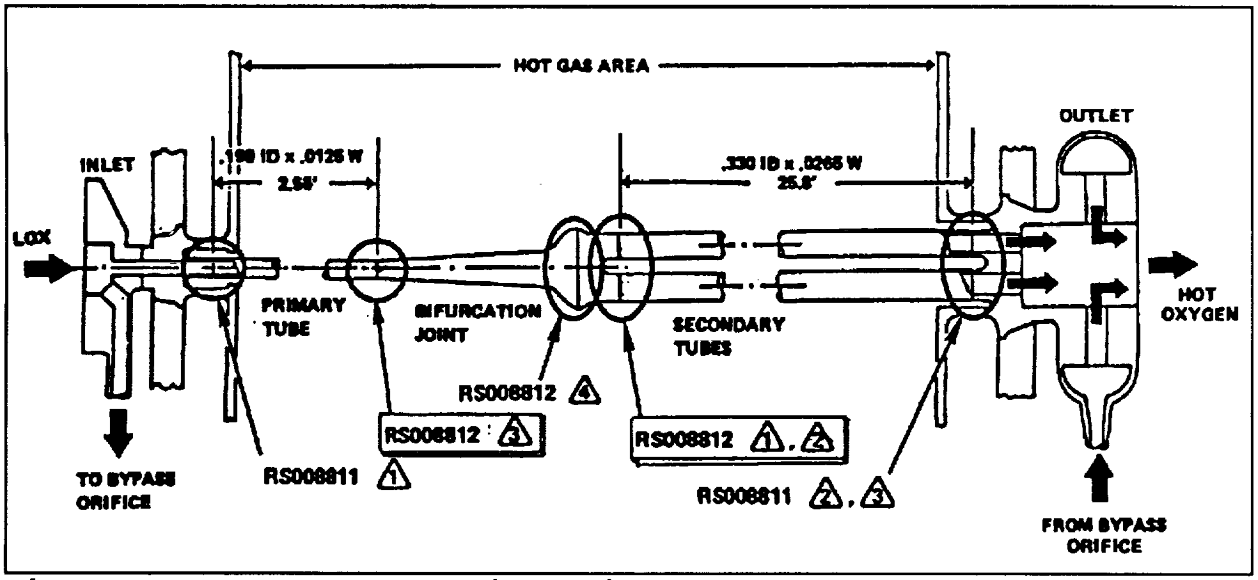

Figure 1 Space Shuttle Main Engine Heat Exchanger Tube Assembly

The second weld from the inlet (RS008812 -#3 in Figure 1) was judged the most difficult and was selected for demonstration. Weld #3 joins the 0.190 in. ID x 0.0125 in. wall inlet tubing to the expansion tubing. It is located approximately 30 in. downstream of the inlet flange, but the probe must negotiate a sharp (0.69 in. radius) bend to reach the weld. Alternate access is from the outlet port, but from that direction, the probe must traverse approximately 26 ft. of 0.330 in. ID tubing wound into a cylindrical coil approximately 16 in. diameter.

The target flaw for detection is 0.003-in.-deep x 0.075-in.-long. Depth is measured in the radial direction; length is measured circumferentially. Flaws of this general shape may result from lack of penetration in the original weld or cracks induced by forming or low cycle fatigue during service.

Capability is desired for manufacturing inspection, inservice inspection following ground test engine firing, and inspection during refurbishment between shuttle flights.

Objective

This goal of this project was to develop the system necessary to demonstrate in the laboratory that an eddy-current system can inspect the tubes and welds described above, screening for the existence of flaws equal in size to, or larger than, the target flaw. The laboratory system was to include the probe necessary to traverse the tubing, the electronics to drive (i.e., electrically excite) the probe and receive and process signals from it, a data display, data recording and playback devices, and microprocessor software or firmware necessary to operate the system.

APPROACH

Eddy-Current Database Review and Preliminary Estimates

ORNL has an extensive library of software that accomplishes for eddy-current testing what is now commonly called "computer aided engineering" (CAE). This software allows the insertion of various parameter values for a complete test environment, including a simulated specimen, probe coil, and instrument. These parameters can be systematically varied to produce an optimized coil design and a set of optimized system operating parameters (e.g., operating frequencies) for a specified range of specimen properties.

From the results of years of simulations for many system designs, a large database has been developed. This database provides a ready reference for the rapid estimation of new problems and a checkpoint for new results as they are computed. Approximate curves and "rules of thumb" have been developed. These indicated that, for defect detection in this size tubing and with these conductivity values, a coil mean radius of about 0.025 in. and an operating frequency of 1.5 MHz were suitable. With these parameters, a defect about 20% of the wall thickness should be detectable.

Probe Configuration

Rocketdyne previously developed a fluid pumping system, freon filled, capable of propelling a string of spherical beads to pull a cable through the finished heat exchanger. Therefore, we looked at bead shaped carriers for the probe coils that could be adapted for use with the existing freon drive system. However, for the demonstration system, a rigid dumbbell shaped carrier (two spheres connected by a straight section) was connected to a stiff cable that could be pushed by hand through the inlet entry tube. Figure 2 shows the probe form inside the bend in the tube. The coils are molded to the spherical shape of the probe form and mounted in the recesses provided.

The freon pumping system offers limited restraint against torques and appropriate connections can prevent continuous rotation of the beaded inspection probe. To accomplish inspection of the entire weld circumference, probe coils were mounted on two successive beads in a string with an angular offset to create a circular array, so that when the complete string has passed the weld, the entire circumference will have been inspected. The probe contains an array of eight coils. Four coils each are mounted 90 degrees apart on the equators of the two spheres, in patterns which are offset 45 degrees. The diameter of the spheres was chosen to allow passage around the curve in the tubing and through the weld sections of the tube. The shape of the probe allows the probe to pass the small 90 degree entry bend without flexing the straight section.

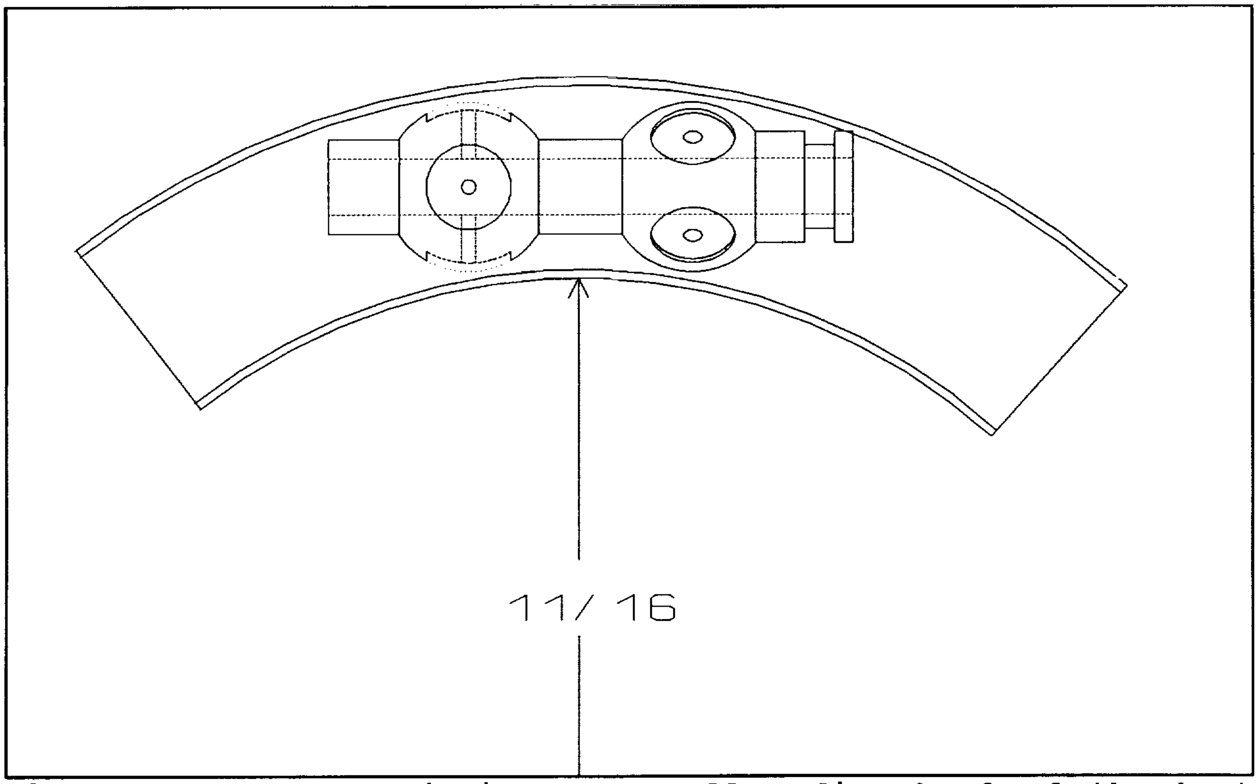

Figure 2 Probe form inside the small radius bend of the heat exchanger tube

Coil Design

Dimensions and electrical parameters for individual probe coils were estimated from reference data derived from the results of previous computer simulations, as described above. However, because of the introduction of variables not considered in the preliminary estimate, confirmatory simulation by computer was considered to be a prudent precaution. Although the coils in the holder have spherical contours, the approximation of a flat pancake coil was the best available. The curvature of the coil will add some liftoff to parts of the coil. The effect of this curvature can be approximated by making the liftoff for the flat coil case equal to that of the curved coil, measured at the mean radius of the curved coil.

System Options and Configuration

Probes using coil arrays similar to that described above have previously been used with single-channel instrumentation by including a multiplexer to switch connections to the instrument in a programmed sequence. Sufficient switching speed can be achieved to compensate for continuous probe motion while ensuring adequate surface coverage. Single-channel instrumentation is significantly less costly and awkward to operate than multichannel.

Three instrument packages were considered for evaluation and laboratory demonstration:

(1) A Hewlett-Packard Model 4192A Low Frequency Impedance Analyzer, controlled through a General Purpose Interface Bus (GPIB, IEEE-488 standard) by an existing laboratory computer (IBM System-9000 or PC AT);

(2) A modular multifrequency eddy-current instrument with phase-sensing capability, designed and built by ORNL, controlled by GPIB with the laboratory computer; and

(3) A pulse-excited eddy-current instrument of initially unspecified configuration.

RESULTS AND DISCUSSION

Functional System Design, Modeling, and Simulation

A modeling program initially written and used for flat plates was modified to accommodate the design of a so-called "pancake" coil, which is a low profile cylindrical coil with its axis normal to the surface against which it is used. The probe design incorporates these coils with their axes coincident with radii of the spherical beads, placing the major plane tangent to the sphere and approximately parallel to a tangent of the inside tube wall.

Early results from the simulations (which included full instrument response and data processing) indicated that a pulse instrument would be superior to the multifrequency instrument for this application. The multifrequency instrument and the pulsed instrument both give similar responses and collect data that contain similar information with the following exception. The multiple frequency inspection was more affected by the permeability variations observed in the weld region. In cases where the tube wall material has a large permeability value, the electromagnetic wave generated by the probe will not penetrate the material. Thus, the outer surface of the material cannot be inspected. However, with high power pulses the material can be saturated and inspected in a manner similar to that of normal eddy-current tests. Although the permeability of the weld is not great enough to shield the outer part of the tube, it does cause a variation in the signal which must be compensated for and which increases both the overall noise and the difficulty of the measurement.

Coil Design

Coil design simulations were carried out for the pancake coil. The properties of the test were varied over the ranges shown in Table 1. Instrument readings were computed for a total of 500 different combinations of the properties. A least-squares fit relating the readings to the properties yielded a set of linear coefficients. The fitting coefficients are linear but can be multiplied by nonlinear combinations of the readings. The rms error in the measurement of a particular property for both the fit and instrument drifts was calculated for the entire range of variation of the properties shown in Table 1. The instrument readings were computed at six different frequencies (0.2, 0.5, 1, 2, 5, and 10 MHz), and a pattern of nonlinear readings was fitted to the properties for each combination of frequencies taken three at a time. The frequency and reading combination that gives the least error was chosen. This error varies as the coil size (mean radius) is varied. The results of the error calculations for the pancake coil are shown in Table 2.

Table 1 Range of property variations for the NASA heat exchanger problem.

Defect depth	0 - 6 mils
Wall thickness	13 - 17 mils
Resistivity micro-ohm cm	70 - 90
Lift-off	0 - 8 mils

It appears that the optimum mean coil radius is 0.0325 in. and that the minimum error remains 0.0006 in. between 0.030 and 0.035 in. mean radius. Typical inner and outer radii would be 0.8 and 1.2 times this value. The variation in the material will generally limit the detectability to a defect depth equal to about 5 to 10% of the tube wall thickness. By increasing the mean radius slightly, to 0.035 in., a larger gauge wire can be used which will further ease the fabrication problems and give better coverage with no sacrifice in sensitivity. With such a coil size, an array of eight coils spaced at 45 degree angular offsets will ensure sufficient coverage to prevent any circumferentially oriented defects from escaping detection.

Table 2 Defect measurement error (in.) due to the property variations.

Coil Mean Radius	Defect Size Error
0.020	0.00088
0.025	0.00076
0.030	0.00062
0.0325	0.00062
0.035	0.00062
0.040	0.00092

Although our discussion has centered on the detection of defects, any of the other property variations, such as liftoff (and therefore tube inner diameter), wall thickness, conductivity, and permeability can also be determined. These properties can be computed from the same readings that the defect sizes are, but using a different set of coefficients. Other properties can be discriminated against, such as the variations caused by tube supports. The only requirement is that the property variations be present in an adequate number in the calculated or experimental readings. We can then determine these properties to the degree of accuracy that we know their input data values.

Instrument Selection

Initial experimental work was done with the HP Impedance Analyzer, using a single coil mounted on a holder. The impedance analyzer was stepped from frequency to frequency using signals from a computer transmitted over the IEEE-488 bus. Although the instrument is rather slow (making only about one reading per second), it is adequate for the low-speed test design readings. A bridge circuit with a differential amplifier was added so that the difference between a reference coil in air and the test coil on the sample could be measured.

Three of the weld samples from Rocketdyne were split so that the liftoff could be varied. The samples were placed in a mechanical positioner that was also controlled over the bus. The samples were scanned at 0.005 in. intervals and the liftoff was varied from 0.0 to 0.008 in. in 0.002 in. increments. About 50 points were taken in the free tube and in the weld reading from each of the six samples. A "shaped" defect value was used for the 0.003 and 0.006 in. defects that were in two of the samples. The "shaped" value was equal to the defect depth when the coil was directly over the defect and decreased as the coil moved away from the defect. This decrease matched the natural response of this type of coil to this type of defect, and is similar to the defect shapes shown in Figure 3.

Measurements were made at frequencies of 200 KHz, 500 KHz, 1 MHz, 2 MHz, 3 MHz, and 4 MHz. Due to limitations on the frequency response of the bridge amplifier, we used 3 MHz and 4 MHz rather than the computed frequencies of 5 MHz and 10 MHz. Fitting coefficients were obtained for both three and six frequencies using these readings. The best three-frequency fit showed an error of 0.0014 in., while the six-frequency error was 0.0013 in. It should be recognized that, although the experimental readings did include the permeability variation, they did not include nearly as many property variations (particularly the defect variations) as the computed readings. In particular, we should have had defect standards with defects in the heat-affected zone and in the bare tubing, as well as in the center of the weld.

Since only two weld defects were available, these were the only ones used. The samples were difficult to align properly due to the small size of both the coil and the samples. A small error in the axial position of the defect could result in a very poor fit. Several attempts were required before the samples were adequately aligned and good fits were obtained. Figures 3 and 4 illustrate the scans of the defects using a three-frequency fit.

These scans are made at five different liftoff values, and plotted sequentially. Although these defects look rather good in the figures, the noise was also high. Scans were also made using a six-frequency fit, and in general, the six-frequency fit was better and less noisy than the three-frequency fit. This suggests that

Figure 3 Scan of 3 mil deep defect for five lift-off values

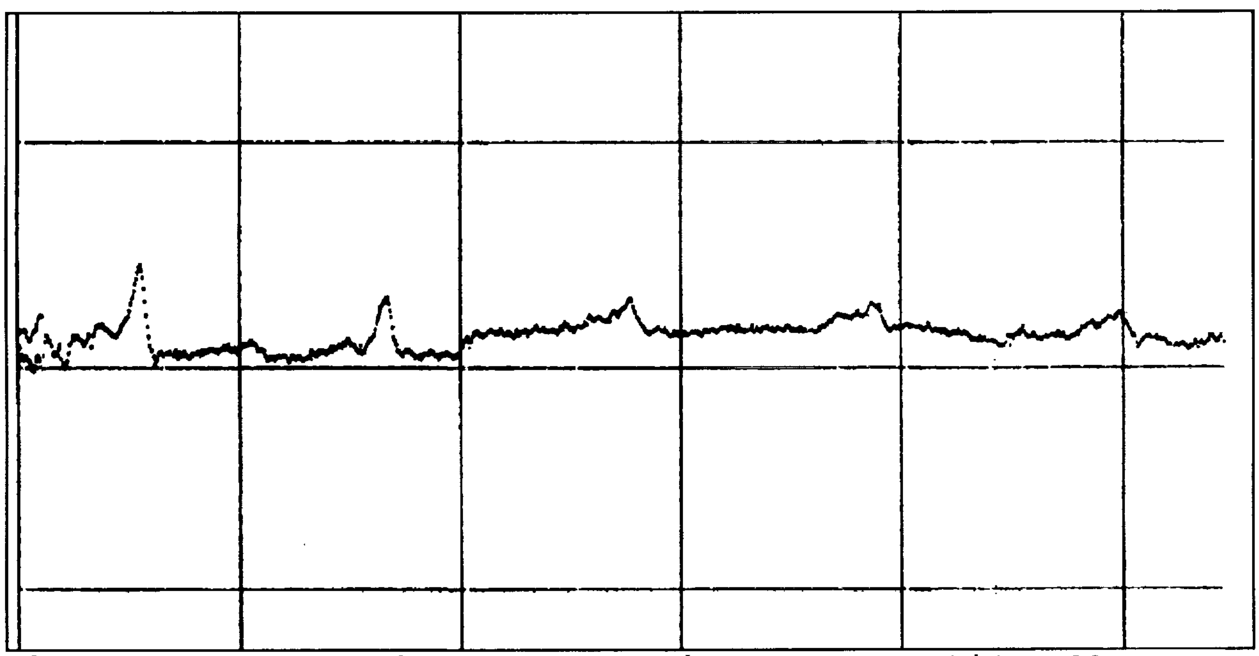

Figure 4 Scan of 6 mil defect for five values of lift-off

the pulse instrument, with its greater frequency content, would give better data.

Neither fit works well for the entire 0.008 in. liftoff range, but scans of the tube samples available showed that none of the tubes would allow more than about 0.004 in. of liftoff. The liftoff of the probe was difficult to set exactly due to the small size of the coils and the irregularity of the samples. The liftoff was quite likely greater than the value assumed for these measurements. Additional fits were run for smaller liftoff ranges and the fits improved as the liftoff range decreased.

The measurements were repeated using the three-frequency instrument, as shown in Figure 5. This instrument consists of three independent oscillators to generate the three frequencies. These frequencies are mixed and then fed to a power amplifier and through a dropping resistor to a coil. The coil signal, which is modified by the interaction with the eddy currents in the conductor, is then fed to three bandpass amplifiers that separate the individual frequencies. The magnitude and phase of each frequency is measured, digitized, and then fed to the controlling computer. Measurements can be made with this instrument about 40 times faster than with the impedance analyzer, and the results, although similar, are not quite as good. This is probably due to a small sample misalignment.

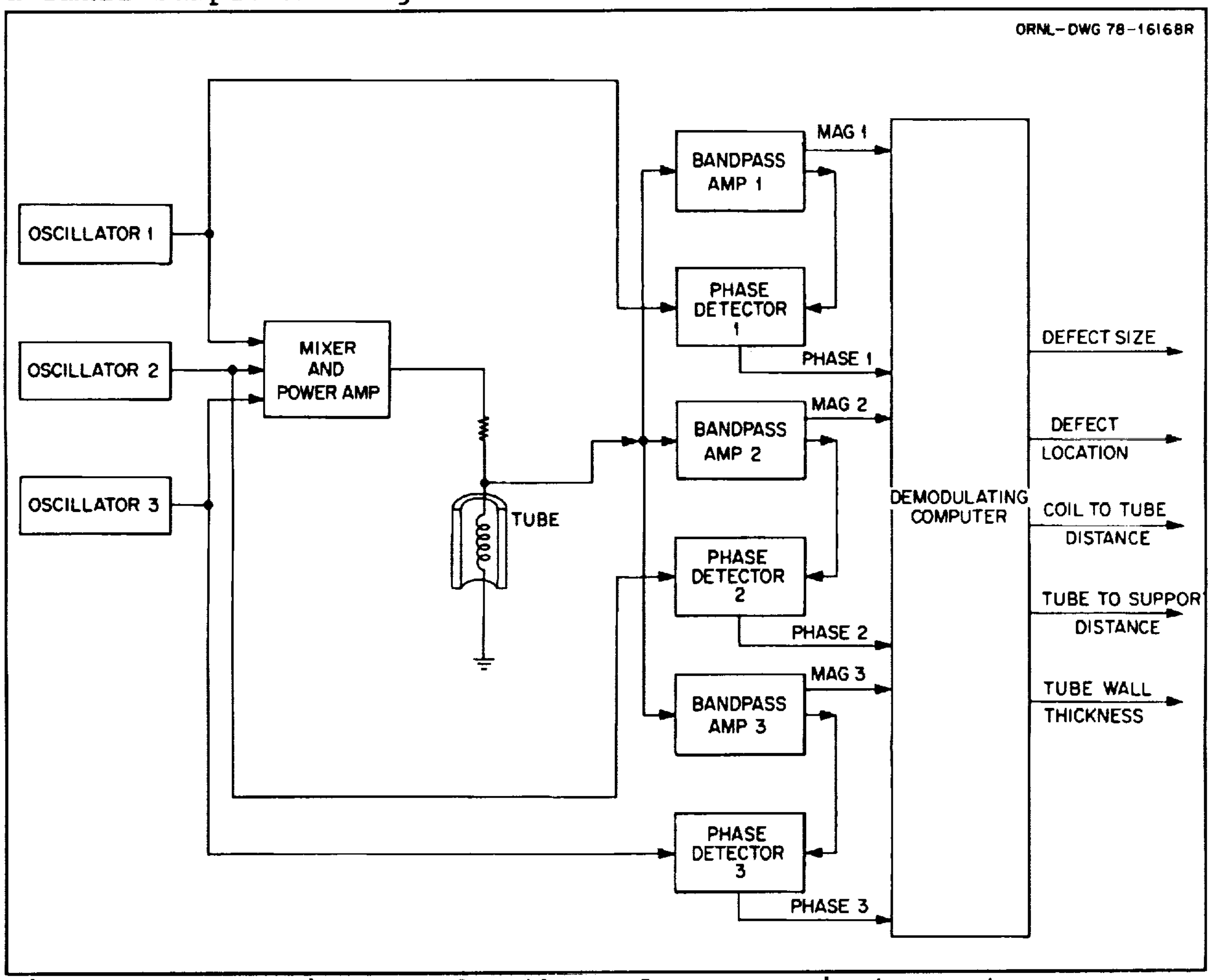

Figure 5 Block diagram of a three frequency instrument

Finally, measurements were made using the array coil. The fitting on the six samples was repeated first using a single coil in the array. The array probe was electrically connected as shown in Figure 6. An unbalanced bridge circuit is formed between the selected coil and the reference coil, and the multiplexer, on signals from the three-frequency instrument, steps from one coil to the next. A program in the microcomputer of the instrument controls the multiplexer module.

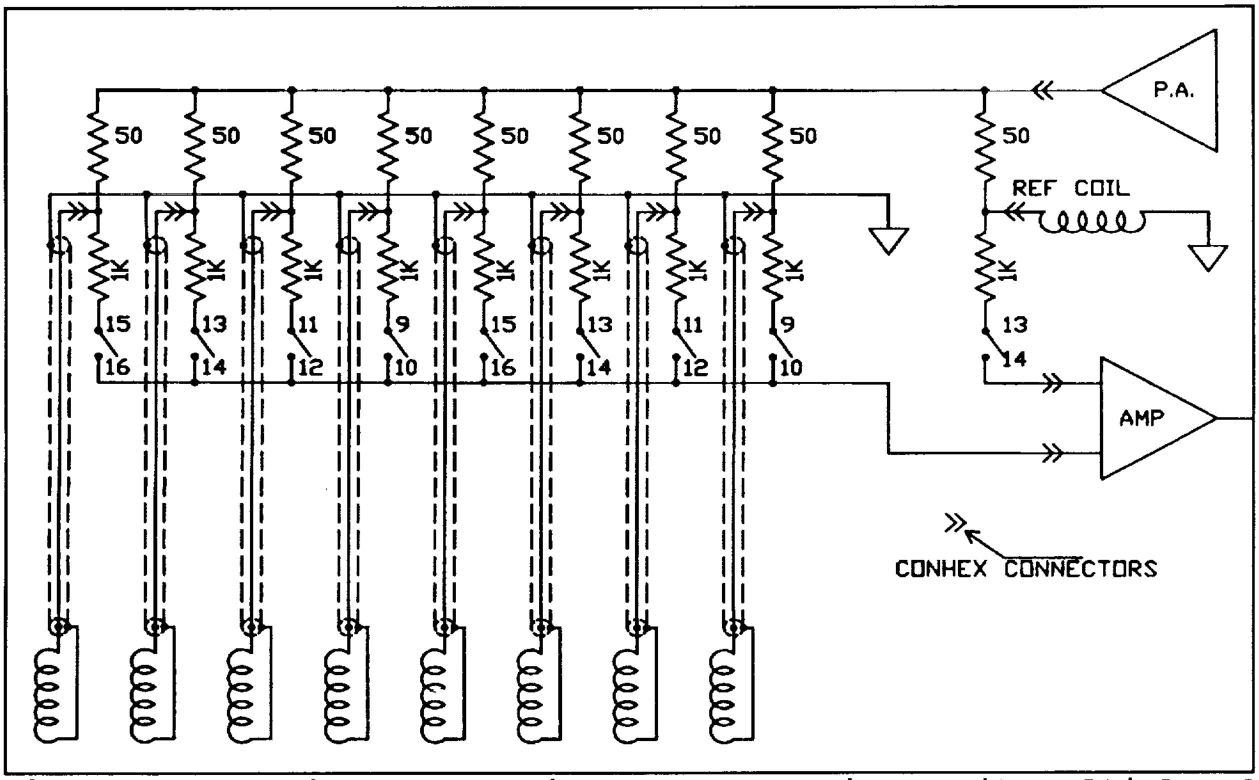

Figure 6 Electrical connections for the eight-coil multiplexed array probe.

The fitting coefficients were calculated for only one coil in the array, and an offset function was calculated from the value of each of the coils in air. This was done because it is very difficult to wind the coils exactly the same, particularly when the coils are this small. The offset is a function of the coil inductance, and is needed to electronically "balance" the bridge with the coil in air. This correction was then applied to each of the coil readings as the multiplexer stepped from coil to coil. This technique saves the time and effort that would be required to run a complete training set on each coil in the array, compute the fitting coefficients, and store a separate set for each coil in the array. A better match would be obtained if a gain correction were also applied. However, to do this requires an additional standard which was not available at the time.

Figure 7 illustrates the scan of an independent tube sample (not one of the standards used to obtain the fitting coefficients). Each trace is from a different coil in the array, and the lowermost coil is the only one positioned to pass over the defects. The first defect is 0.005-in. deep, and the second is 0.007-in. deep. The rising signal at the end of the scan for the upper four coils is from the tube end. The data from these coils are offset by about 0.240 in. from the first four coils (see Figure 2). In plots made on the CRT this offset is corrected so that data from the coils at the same position across the screen represent the same axial location on the tube.

Although the readings from the multiple-frequency instrument were much faster than the impedance analyzer, they are still too slow to allow the weld to be scanned and insure that there is no data skip due to "probe pop." This occurs when the probe hangs on the weld, the cable stretches and then the probe pulls loose. The probe can then move at a rate of 0.5 m/s for a short time, and the examination of a short length of tubing will be skipped. Unfortunately, this is the section where a defect is likely to occur. The maximum data rate for the three-frequency instrument is about 40 readings per second, but about 32,000 readings per second are needed to insure that there are no skips when the tube is inspected at 0.5 m/s. The three-frequency instrument uses an 8080 based microcomputer with an IEEE-488 bus, which has been named the COMP9B computer.[5] Both the 8080 microcomputer and the IEEE-488 bus limit the inspection speed.

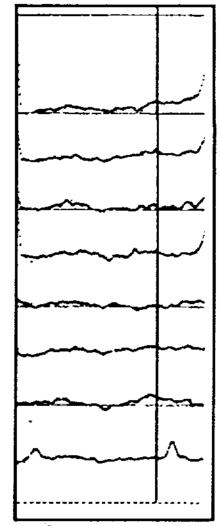

Figure 7 Scan using an array probe.

A block diagram of the pulsed instrument we developed is shown in Figure 8.[4] This instrument generates a pulse that drives a coil. The resulting electromagnetic wave is of sufficient amplitude to saturate any ferromagnetic material near the probe and also generates eddy currents in the sample. This signal can be detected either by a sampling coil or directly using a dropping resistor in series with the primary coil. The signal amplitude as a function of time can be measured, either on the turn-on portion of the signal or the turn-off portion of the signal when a single coil is used. The value of this signal can be offset and amplified at each time interval. This is necessary since the total pulse response may be quite large and the important information may be a small part of the signal. The amplitude of the signal is sampled using a track-and-hold amplifier, digitized, and sent to a computer. This amplitude can be used as a reading to determine the sample properties in a manner similar to that employed for multiple-frequency measurements.

Although the drawing, in the interest of simplicity, includes the components for four channels of data, the instrument actually has eight data channels. The instrument can be set up using signals transmitted over the bus, so that no manual adjustments are necessary. These adjustments include the pulse amplitude, on time and off time, the gain and offset of each amplifier, and the offset of bandpass filter amplifiers (not shown in the block diagram). In addition the time at which each sample is made can be controlled independently.

Since the instrument setup is controlled by a computer program, a large reading pattern can be programmed and then the ones that best fit the sample properties can be selected. In addition, if a new set of properties is encountered as the tube is being scanned, the

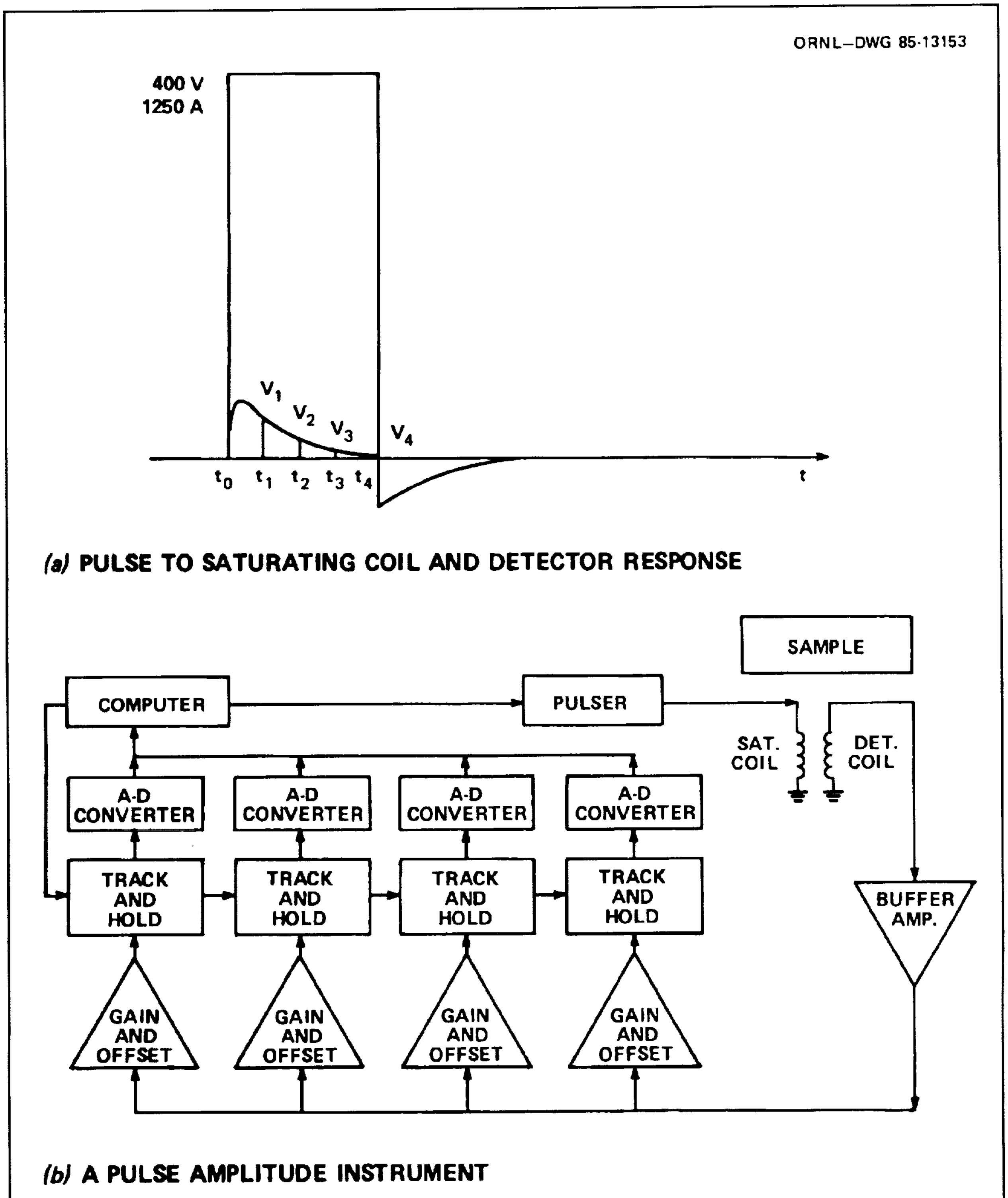

Figure 8 Block diagram of pulsed eddy-current instrument along with a saturating pulse

pulse shape could be changed "on the fly." For example this feature would be needed if a ferromagnetic region were encountered.

The pulse power could be increased to insure saturation, and decreased again to allow probe cooling after the region was passed.

Pulsed Instrument Design

Preliminary design of a pulsed instrument that resides on a PC-AT bus was completed. A block diagram for this instrument is shown in Figure 9. This eddy-current instrument can transfer data at a rate of 400,000 bytes per second, compared to a rate of 1000 bytes per second for the 8080 based COMP9B computer. The pulsed instrument could also pulse one coil at a time and read all the coils in parallel, rather than driving all the coils in parallel and multiplexing the output as the three-frequency instrument does. In addition, less heat would be generated in the probe than would result if all the coils were pulsed every time. The time required for the switching transients to settle out would be eliminated. The analog-to-digital convertors would have to be replaced with faster models, but these are readily available.

The instrument is based on the design of the pulsed instrument described in the previous paragraph, but has been modified to fit on two standard PC-AT bus cards. Bus interface and control circuits were designed using programmable array logic (PAL) chips. These circuits are faster and more compact than comparable discrete logic chips. Tests of the interface chips and some of the pulsed circuit on the bus indicate that some further modification of the circuits will be necessary before an optimum configuration is achievable. However, a transfer of 16 bits of information at a rate of 200 KHz was demonstrated. By using a PC-AT as the controller for the pulsed instrument, we can significantly reduce the cost while increasing access to a large amount of support software. Although the present "test bed" utilizes a 16 bit 80286 microcomputer, a 32 bit 80386 based system should be faster and cost very little more.

CONCLUSIONS

Computerized designs and simulations backed by laboratory tests and demonstrations at ORNL have shown the feasibility of detection of specified flaw properties in tubing welds in the SSME heat exchangers. The flaw signals using a specially designed probe and an existing ORNL multifrequency eddy-current instrument are robust and field interpretable. The probe and flexible cabling can be interfaced to existing drive systems at Rocketdyne to yield a practical working instrument for inspecting tubing welds in the field through existing tube ports with minimal inspection effort. Additional simulations indicate that an even better inspection with greater confidence could be achieved using pulsed eddy-current techniques that have recently been developed at ORNL. This system offers higher speed, lower cost and simpler operation with a computerized instrument now in the design stages.

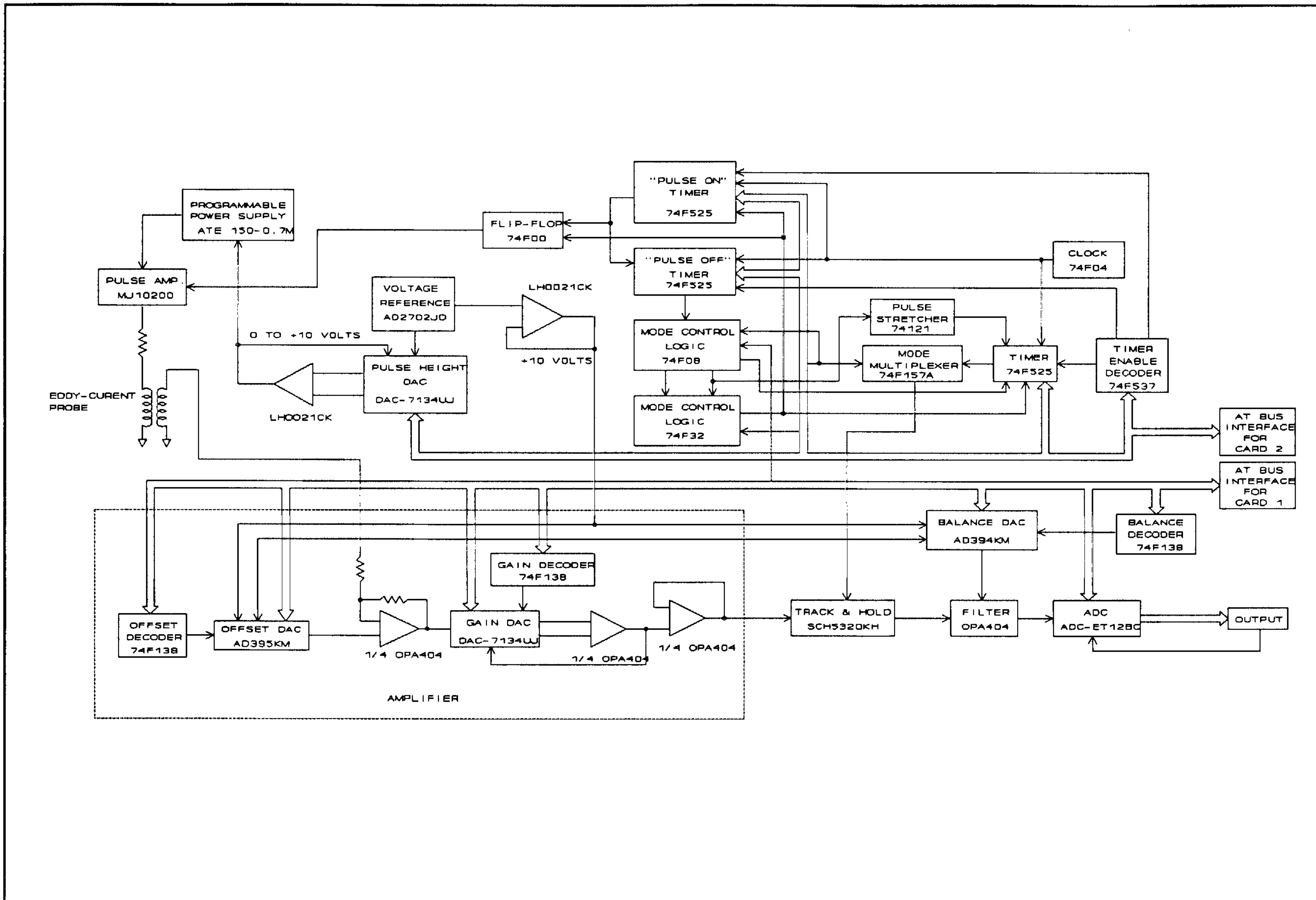

Figure 9 Block diagram of pulsed eddy-current instrument interfaced to a PC-AT bus

ACKNOWLEDGMENTS

The authors would like to acknowledge the assistance of J. R. Pate from Hendrix College in performing the experimental measurements for this report. They further acknowledge the help of J. D. Allen and B. E. Foster in the review of this paper.

REFERENCES

1. C. V. Dodd, G. W. Scott, J. H. Smith, W. E. Deeds, L. D. Chitwood, R. W. McClung, "Development of Multifrequency Eddy-Current Techniques for In-Service Inspection of 2 1/4 Cr-1 Mo Steam Generator Tubing for CRBR," ORNL/TM-8920, February 1984. (Applied Technology)

2. J. H. Smith, C. V. Dodd, and L. D. Chitwood, "Multifrequency Eddy Current Inspection of Seam Weld in Steel Sheath," ORNL/TM-9470, April 1985.

3. C. V. Dodd, D. W. Koerner, W. E. Deeds, and C. A. Pickett "Pulsed Eddy Current Inspection of Thin-Walled Stainless Steel Tubing," ORNL-6408, September 1987.

4. C. V. Dodd and W. E. Deeds, "Eddy-Current Inspection of Ferromagnetic Tubing Using Pulsed Magnetic Saturation," ORNL-6305, July 1986.

5. C. V. Dodd and L. D. Chitwood, "Three-Frequency Eddy-Current Instrument," ORNL/TM-10663, May 1988.

NONDESTRUCTIVE EVALUATION (NDE)
AND
TOTAL QUALITY MANAGEMENT (TQM)
FOR
MISSILE SYSTEMS

NDE FOR AEROSPACE SYMPOSIUM
AUGUST 22-24, 1989
HUNTSVILLE, MARRIOTT

0726-062889-1-3-14

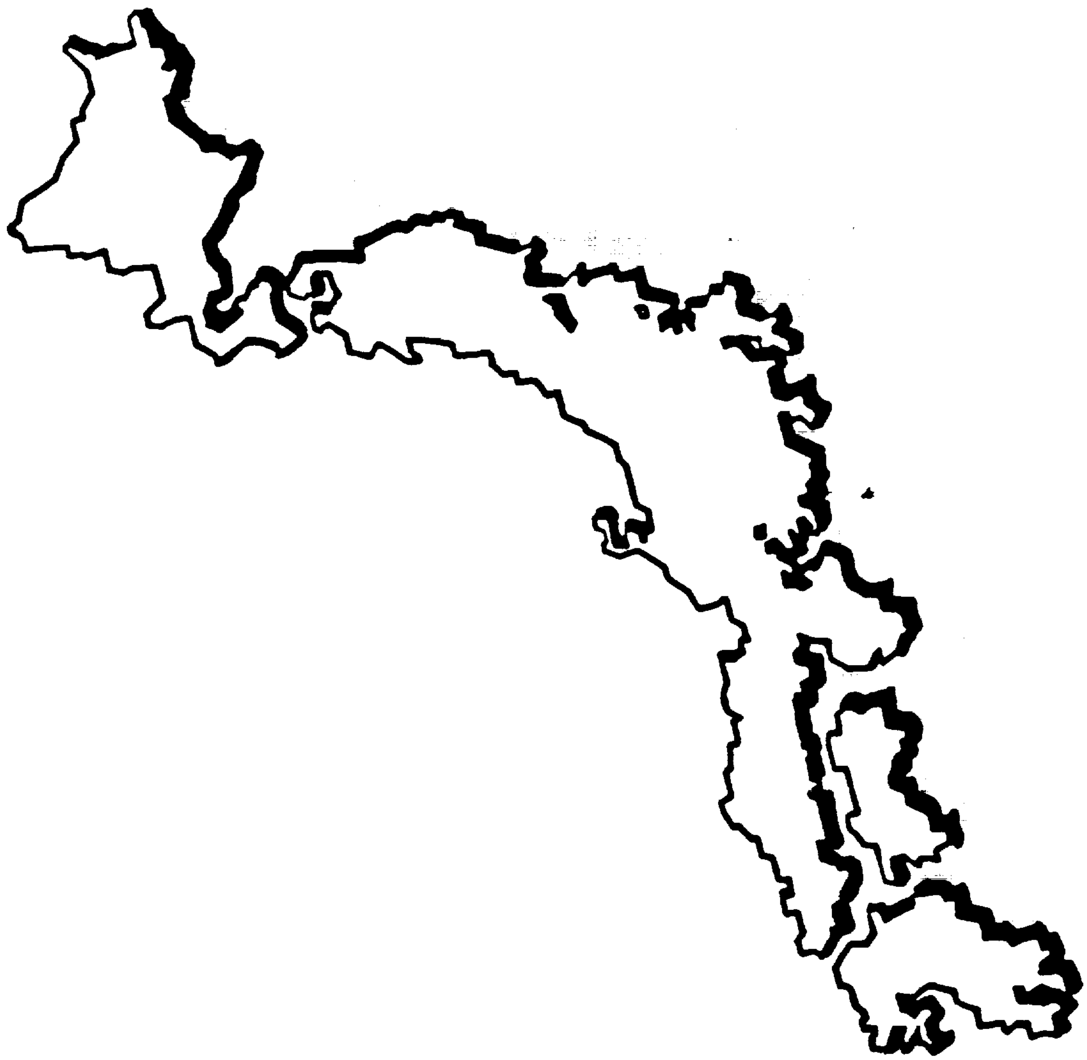

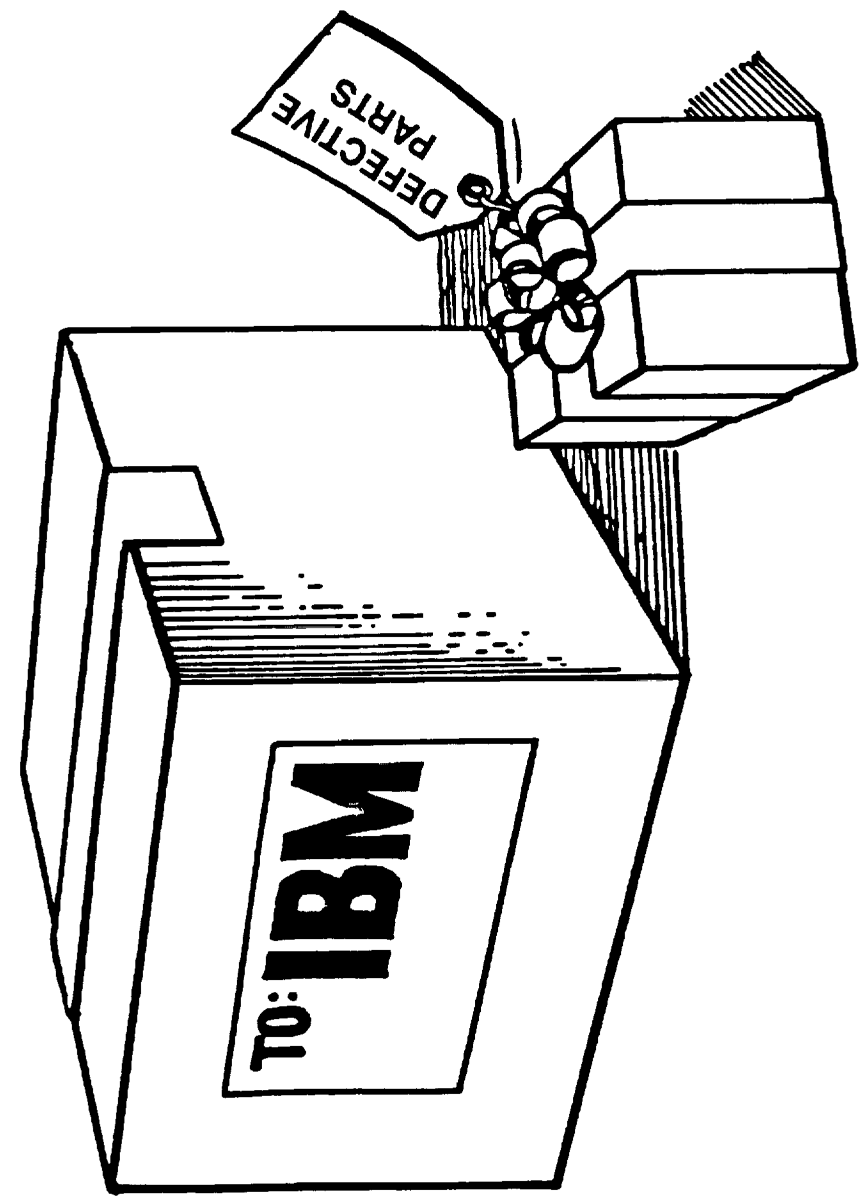
DEFECTIVE
PARTS
TO: IBM

CONSUMER SATISFACTION INDEX (CSI) – CARS

MERCEDES-BENZ	159
TOYOTA	137
JAPANESE CARS OVERALL	115
GERMAN CARS OVERALL	110
FORD	107
CHRYSLER	91
GENERAL MOTORS	81
AMERICAN MOTORS	76

SOURCES:

1. THRIVING ON CHAOS BY TOM PETERS, 1986
2. THE DEMING ROUTE TO QUALITY AND PRODUCTIVITY, W. SCHERKENBACH, 1988

WORLDWIDE PRODUCTION

	1960s	1988
CARS	76%	24%
MACHINE TOOLS	100%	35%
TURNTABLES	90%	1%
COLOR TVs	90% (27 FIRMS)	10% (1 FIRM)

SOURCE : "LOSING THE FUTURE," NEWS SPECIAL
BY SANDY VANOCUR, NOV 1988.

TRADE DEFICITS

(BILLIONS OF DOLLARS)

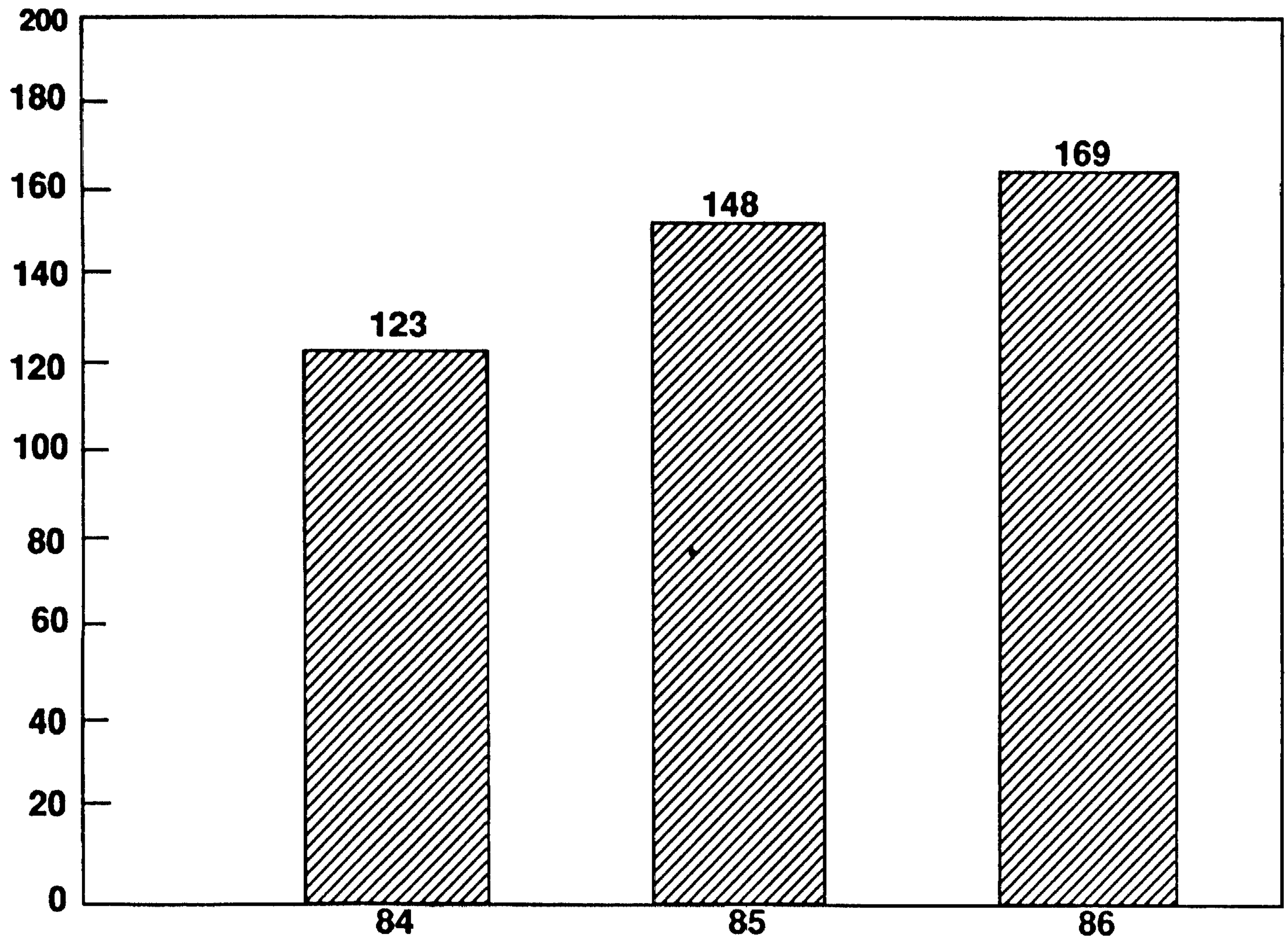

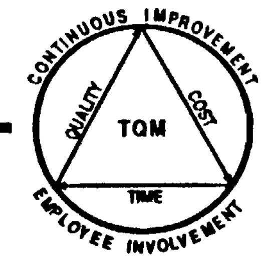

TQM - JAPANESE EMPHASIS

- JAPANESE HAVE BEEN PERFECTING THE TQM PROCESS FOR 40 YEARS (CONTINUOUS PROCESS IMPROVEMENT)

- JAPANESE TQM EMPHASIS IS BASED ON THE PRINCIPLE THAT HIGHER QUALITY RESULTS IN:
  - LOWER COST (LESS SCRAP AND REWORK)
  - SHORTER PRODUCT LEAD TIME (FEWER TEST FAILURES AND PROBLEMS, ALONG WITH HIGHER YIELDS)
  - BETTER PERFORMANCE (HIGHER RELIABILITY)

BOTTOM LINE:

INCREASED CUSTOMER SATISFACTION AND MARKET SHARE

TYPICAL PHASED DEVELOPMENT

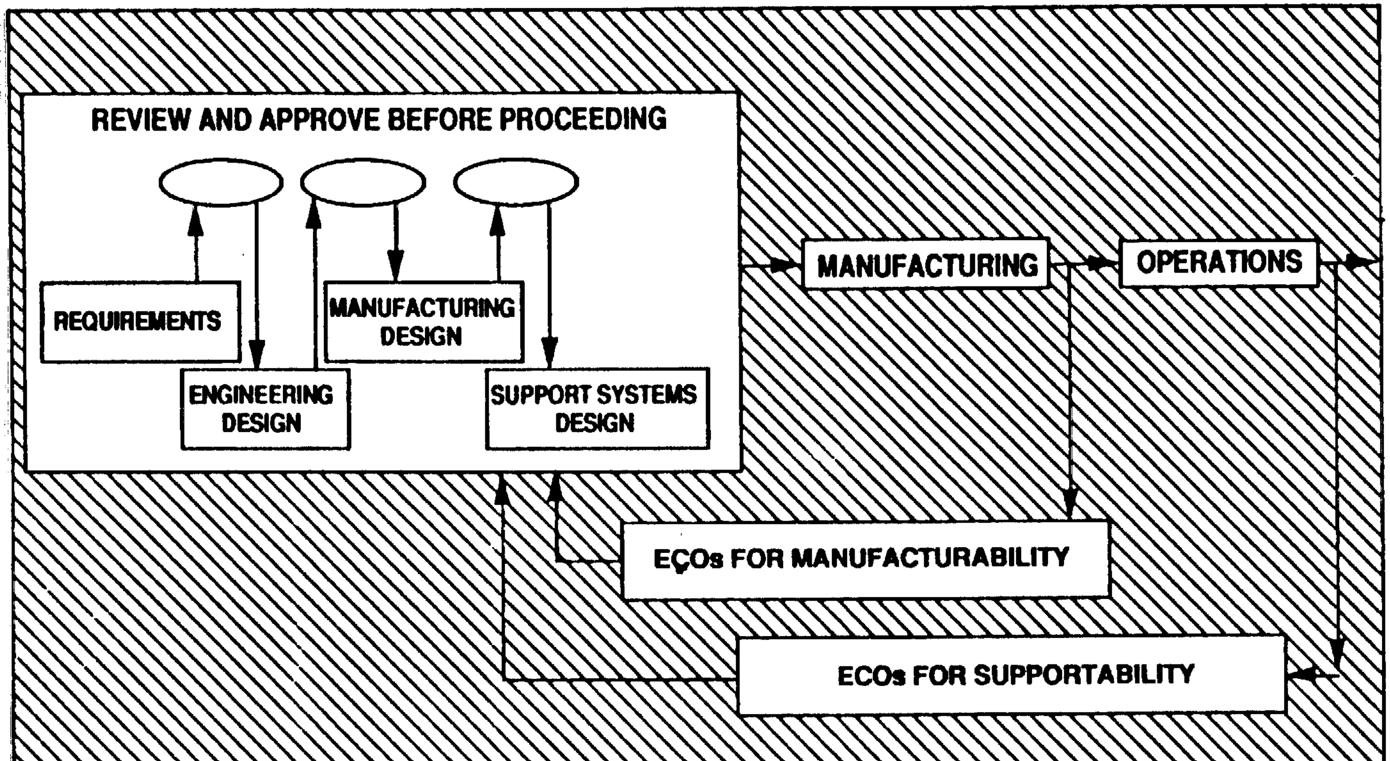

- PASSED FROM GROUP TO GROUP ACCORDING TO SPECIALITY
- LACK OF UNDERSTANDING & INTEREST IN OTHER GROUP'S PROBLEMS
- REDUCED FLEXIBILITY FROM PHASE TO PHASE

CONCURRENT ENGINEERING

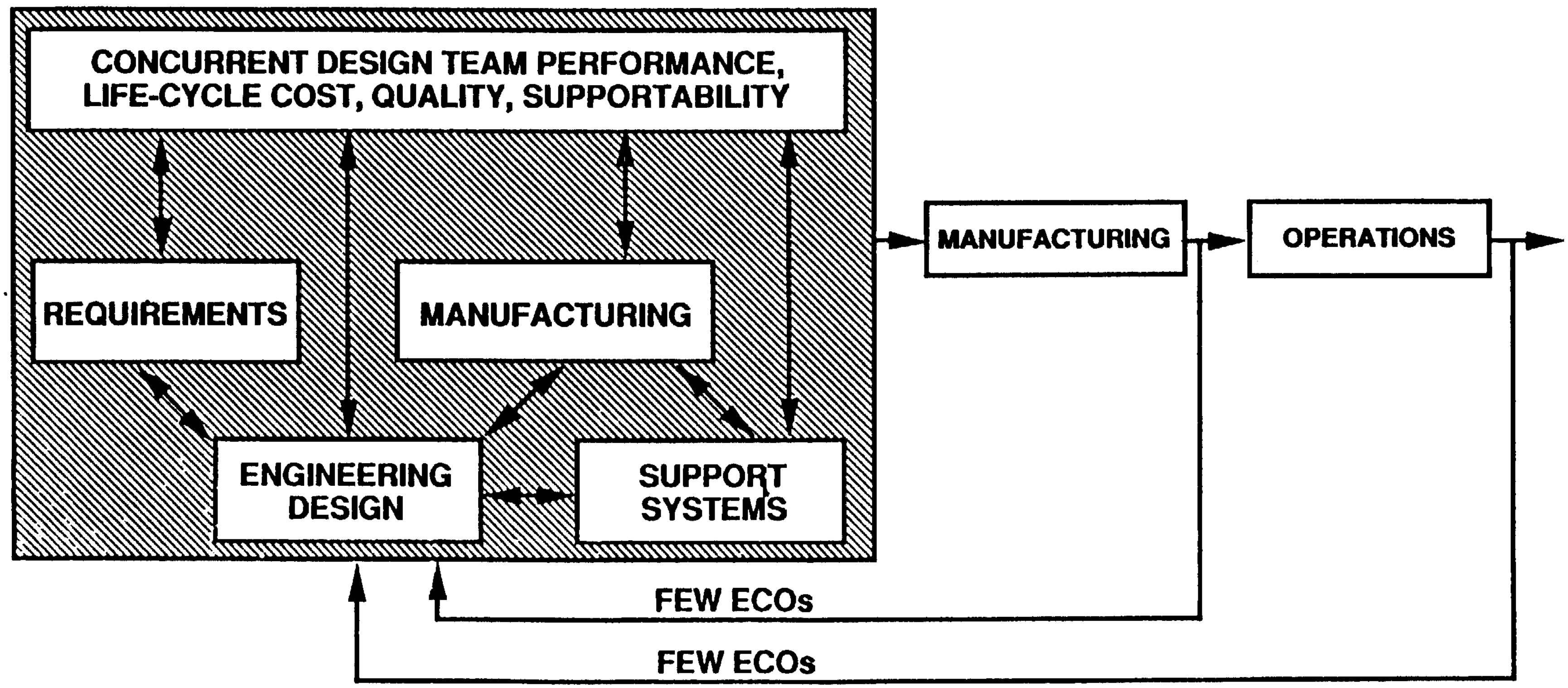

- "DESIGN QUALITY IN VS. INSPECT QUALITY IN"
- "GET IT RIGHT THE FIRST TIME"
- COMPRESSION OF DESIGN & DEVELOPMENT TIME
- LOWEST LIFE-CYCLE COSTS

NUMBER OF ENGINEERING CHANGES OVER PRODUCT LIFE CYCLE

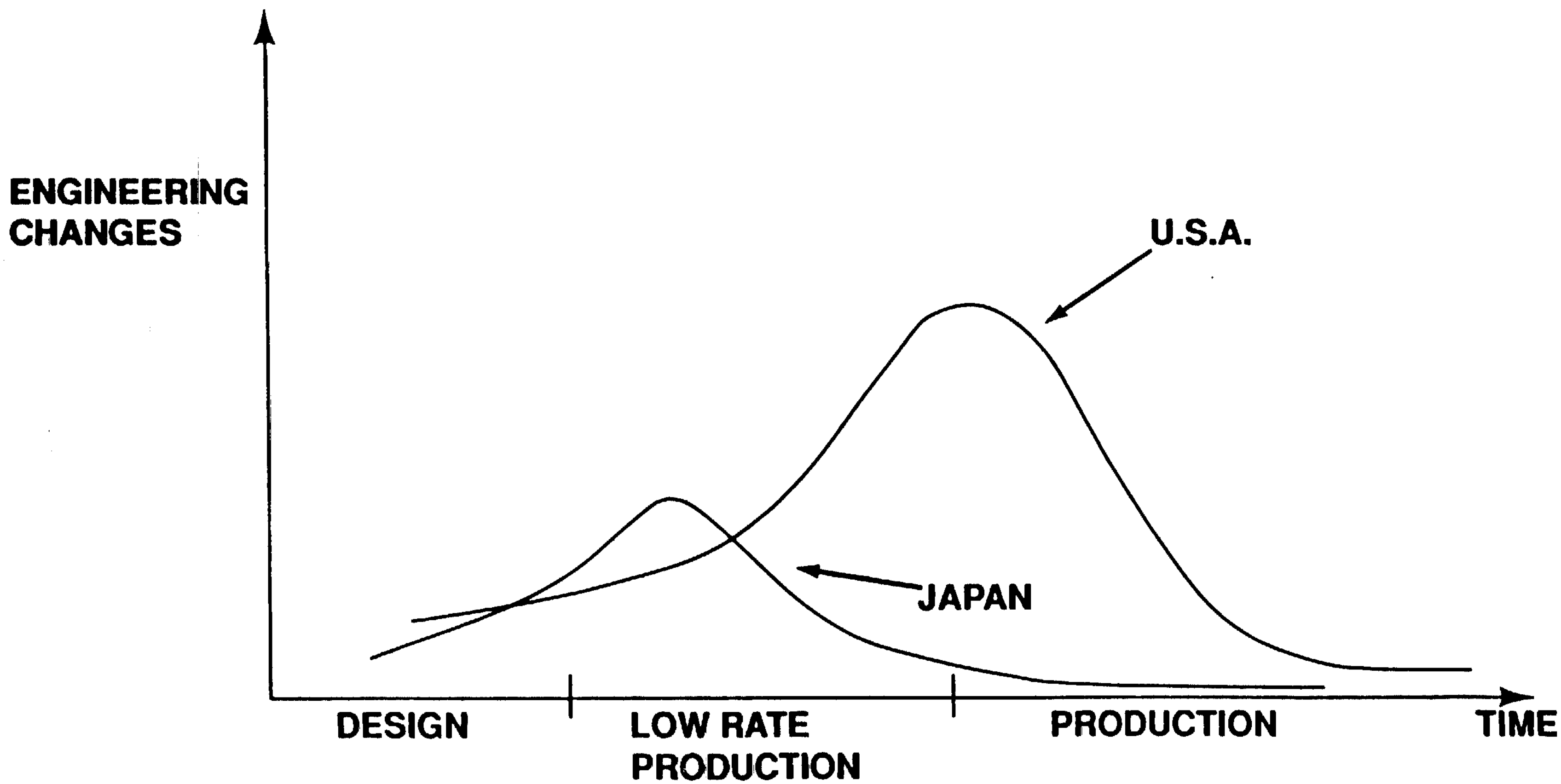

GUIDING PRINCIPLES FOR A TQM PROGRAM

- QUALITY FIRST
- CUSTOMER SATISFACTION
- CONTINUOUS IMPROVEMENT
- MANAGEMENT COMMITMENT
- EMPLOYEE COMMITMENT
- SUPPLIER PARTICIPATION

DR. DEMING : WE MUST HAVE A PROFOUND KNOWLEDGE OF THE PROCESSES - - IN THE USA WE MAKE TOO MANY QUICK FIXES, BASED ON HUNCHES

PROBLEM-SOLVING TOOLS

- PARETO DIAGRAMS
- ISHIKAWA (FISHBONE) DIAGRAMS
- HISTOGRAMS
- CONTROL CHARTS
- SCATTER PLOTS
- PROCESS FLOW DIAGRAMS
- PARAMETER OPTIMIZATION TECHNIQUES
  - TAGUCHI METHODS
  - STATISTICAL DESIGN OF EXPERIMENTS
- CHECK SHEETS
- NEW QUALITATIVE TECHNIQUES

TOTAL QUALITY MANAGEMENT (TQM) - DEFENSE INDUSTRY

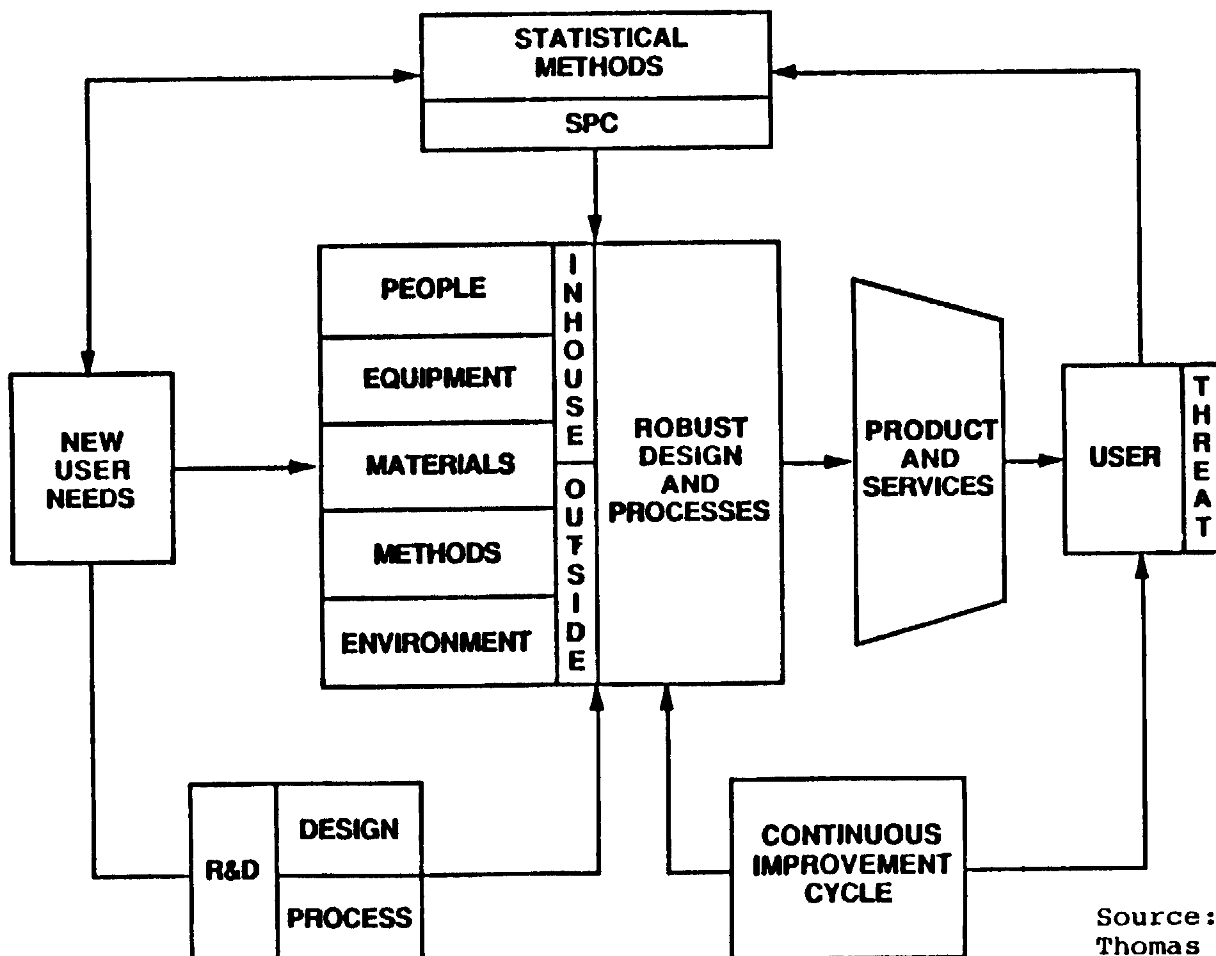

Source:
Thomas R. Stuelpnagel
National Defense, Nov 88

TQM

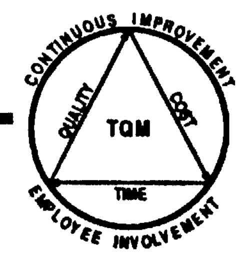

- PARTICIPATIVE SENIOR MANAGEMENT PHILOSOPHY EMPHASIZING QUALITY
- TOTAL LIFE CYCLE DESIGN PHILOSOPHY
- MULTI-LEVEL, CROSS-ORGANIZATIONAL LINKAGES TO OPTIMIZE QUALITY
- CONTINUOUS IMPROVEMENT OF ALL PROCESSES, INVOLVING EVERYONE

PLAN, DESIGN, BUILD AND MAINTAIN QUALITY IN:
"DOING RIGHT THINGS RIGHT THE FIRST TIME"

ORGANIZATION

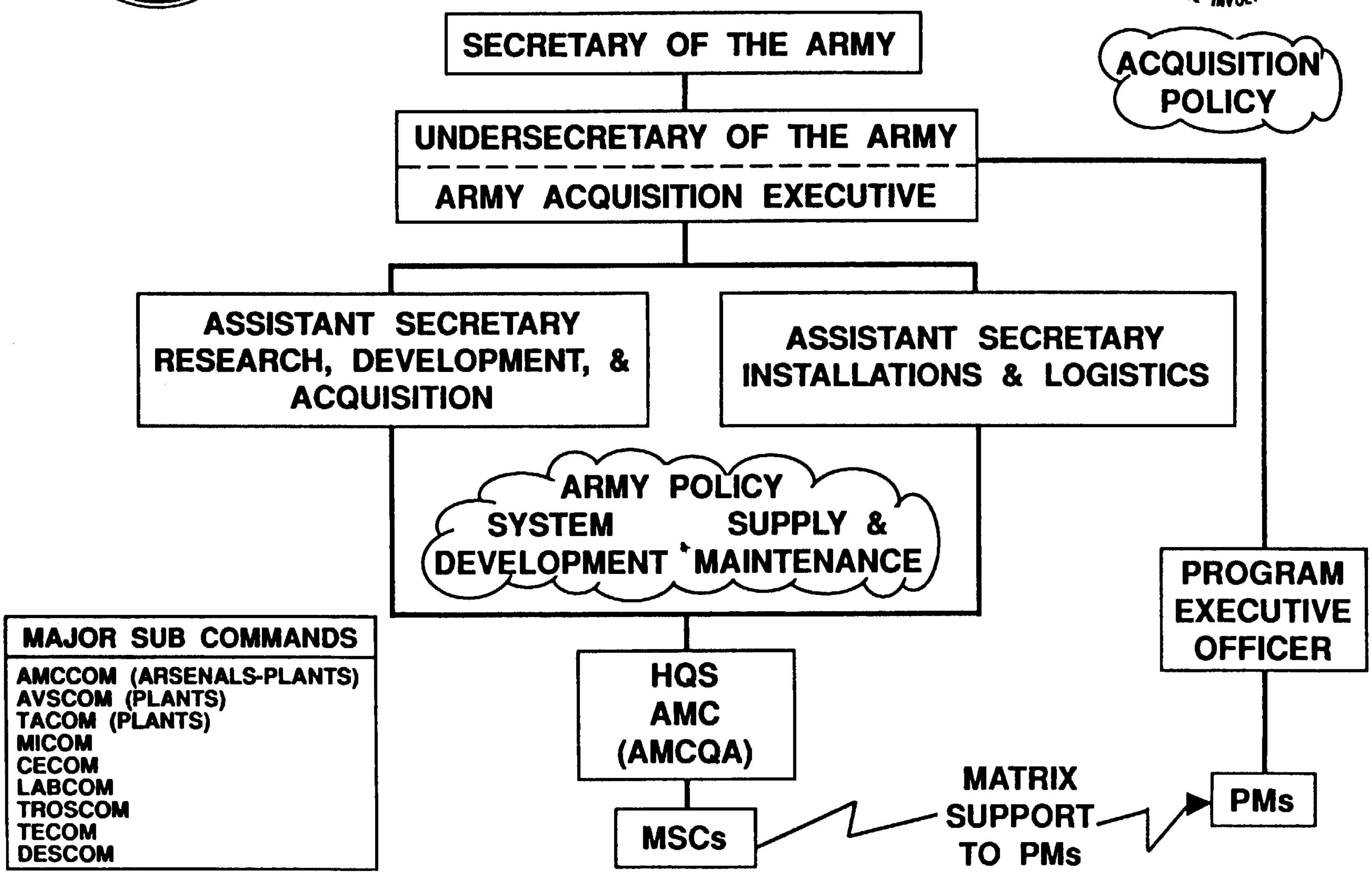

TOTAL QUALITY MANAGEMENT
PAD'S MISSION

- STRATEGY: CONTINUOUS QUALITY IMPROVEMENT PROCESS
- HIGHER LEVELS OF PERFORMANCE IN ALL AREAS OF RESPONSIBILITY
- PROVIDE USER SATISFACTION
- ASSURE MICOM PRODUCTS CONFORM TO CORRECTLY DEFINED TECHNICAL REQUIREMENTS
- ASSURE THAT QUALITY IS EMPHASIZED IN EVERY PHASE OF THE PRODUCT LIFE CYCLE
- INCREASE WAR-FIGHTING CAPABILITY

TOTAL QUALITY MANAGEMENT (TQM)

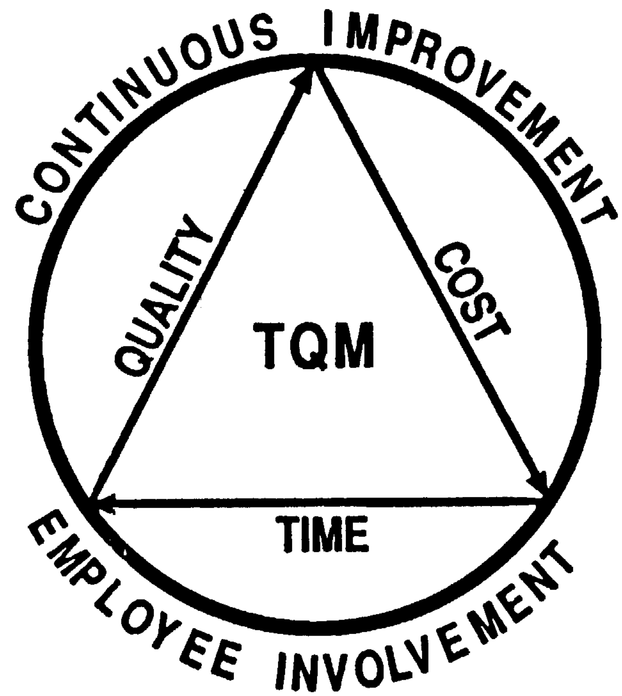

THROUGH NONDESTRUCTIVE EVALUATION (NDE)

NDE A VITAL PART OF TQM

REASONS FOR EMPHASIS:

- RAPIDLY INCREASING COST OF WEAPON SYSTEMS
- TECHNOLOGICAL CHANGES IN STRUCTURES AND PROPULSION SYSTEMS
- DEVELOPMENT OF ADVANCED, LIGHTWEIGHT, HI-STRENGTH MATERIALS
  - SUSCEPTIBLE TO SMALL DEFECTS, MFG FLAWS
  - REQUIRES DEVELOPMENT AND USE OF ADVANCED NDE METHODS
- NDE NECESSITY THROUGH ENTIRE LIFE CYCLE
- QUALITY ASSURANCE ORGANIZATIONS/NDE MUST:
  - PROVIDE DETECTION OF DEGRADED COMPONENTS
  - AND REMOVE BEFORE CATASTROPHIC FAILURE

NDE A MAJOR AMC THRUST AREA

- DESIGNATED BY AMC MANUFACTURING TECHNOLOGY STEERING GROUP MEETING AT AMC HDQTRS 6-7 DEC 88

- OTHER THRUST AREAS THAT REQUIRE USE OF NDE/NDT
  - SURFACE MOUNT SOLDERING TECHNOLOGY (SMT)
  - COMPOSITE MATERIALS PROCESSING
  - ENERGETIC MATERIALS (PROPELLANTS, PYROTECHNICS) MANUFACTURING
  - HEAVY PLATE WELDING
  - ADHESIVE BONDING
  - MACHINING

- GOALS OF THESE NDE THRUSTS AND THIS CONFERENCE ARE:
  - TO PROMOTE COOPERATION MICOM/NASA/INDUSTRY
  - TO GET ADVANCED NDE TECHNOLOGY ON THE FACTORY FLOOR

MATERIALS TECHNOLOGY LABORATORY (MTL) (WATERTOWN, MA)

ARMY CENTER OF EXCELLENCE IN MANUFACTURING NDE

- MANAGE NDE THRUST AREAS
- COORDINATE NDE TECHNOLOGY DEVELOPMENT
  - TECHNOLOGY DEVELOPED IN DOD, INDUSTRY OR ACADEMIA
  - APPLY TO ARMY PROBLEMS
- TEAMWORK:
  - MTL
  - SOUTHWEST RESEARCH INSTITUTE
  - JOHNS HOPKINS LABORATORY
- ACTION AREAS:
  - IDENTIFY R&D AREAS & COORDINATE RESEARCH
  - EVALUATE AND FUND PROJECT PROPOSALS
  - EVALUATE & DEMONSTRATE NEW EQUIPMENT & TECHNOLOGIES
  - SPONSOR SEMINARS & TECHNICAL TRAINING
  - TRANSFER NDE TECHNOLOGY INTO MANUFACTURING

MICOM RESEARCH, DEVELOPMENT AND ENGINEERING CENTER (RDEC)

SYSTEMS ENGINEERING & PRODUCTION DIRECTORATE (SEPD) NDE INITIATIVES

- MANUFACTURING METHODS AND TECHNOLOGY (MM&T)
- MATERIALS TESTING TECHNOLOGY (MTT)
  - AR 700-90, ARMY INDUSTRIAL PREPAREDNESS PROGRAM
  - MICOM REG. 70-32J, MM&T, MTT & MILITARY ADAPTATION OF COMMERCIAL ITEMS
- "MANTEST", MICROCIRCUIT THERMAL SCREENING
  - A MANUAL CHIP SCREENING SYSTEM
  - AVAILABLE FOR DEMONSTRATION
- AUTOMATIC OPTICAL INSPECTION OF PRINTED WIRING BOARDS – FY 89
- LASER DEVICE TO DETECT FLAWS/MICROCRACKING IN OPTICAL FIBERS
  - THROUGH INDUCED STRESS
  - IN PLANNING STAGE

MICOM PRODUCT ASSURANCE DIRECTORATE
NDE/NDT

- RESPONSIBILITY FOR CERTIFICATION OF CRITICAL PROCESSES
  - SOLDERING
  - WELDING
  - NDE/NDT
  - ADHESIVE BONDING

- QUALITY AUDITS
  - NDE/NDT CAPABILITIES, PROCESSES AT CONTRACTOR PLANTS AND ARMY DEPOTS

- SOLDERING TECHNOLOGY & CERTIFICATION CENTER
  - VANZETTI LASER INSPECTION SYSTEM
  - X-RAY INSPECTION SYSTEM
    - PROJECTED OPERATION LATTER PART FY 89
    - CONDUCT NDE STUDIES OF SOLDER JOINTS, PRINTED WIRING BOARDS, SURFACE MOUNT TECHNOLOGY (SMT)
  - SMT STUDY FY 89-90

MICOM PRODUCT ASSURANCE DIRECTORATE NDE/NDT (CONT)

- NDE REQUIREMENTS IN QUALITY ASSURANCE PROVISIONS (QAPs) FOR TECHNICAL DATA PACKAGES (TDPs)

- HANDBOOK FOR NDE/NDT (25 VOLUMES)
  - 20 METHODS
  - PREPARATION OF QAPs FOR TDPs
  - AVAILABLE HERE AT CONFERENCE

- RELATED DISCIPLINES
  - STATISTICAL PROCESS CONTROL (SPC)
  - SPECIAL INSPECTION EQUIPMENT (SIE)
  - ENVIRONMENTAL STRESS SCREENING (ESS)

RAM ENGINEERING AND SYSTEM ASSESSMENT

TQM RELATED ACHIEVEMENTS

RAM TESTING OF STOCKPILE - SHELF LIFE ASSESSMENTS

SYSTEM	INITIAL PREDICTION	CURRENT PREDICTION
REDEYE	3 YRS	23 YRS
HAWK MTR	5 YRS	20 YRS
TOW	5 YRS	20 YRS
SHILLELAGH	5 YRS	22 YRS
DRAGON	5 YRS	16 YRS

- CONFIRMED RELIABILITY
- CONFIRMED SAFETY
- SAVED REPROCUREMENT/REBUILD COSTS

PATRIOT-5 TO 7 YEARS

$2 BILLION COST AVOIDANCE

SYSTEM ASSESSMENT OF FIELDED SYSTEMS

- MLRS PROBLEMS
- ENGINEERING CHANGES
- INCREASED MEANTIME BETWEEN FAILURES OVER 100%

INCREASED COMBAT CAPABILITY

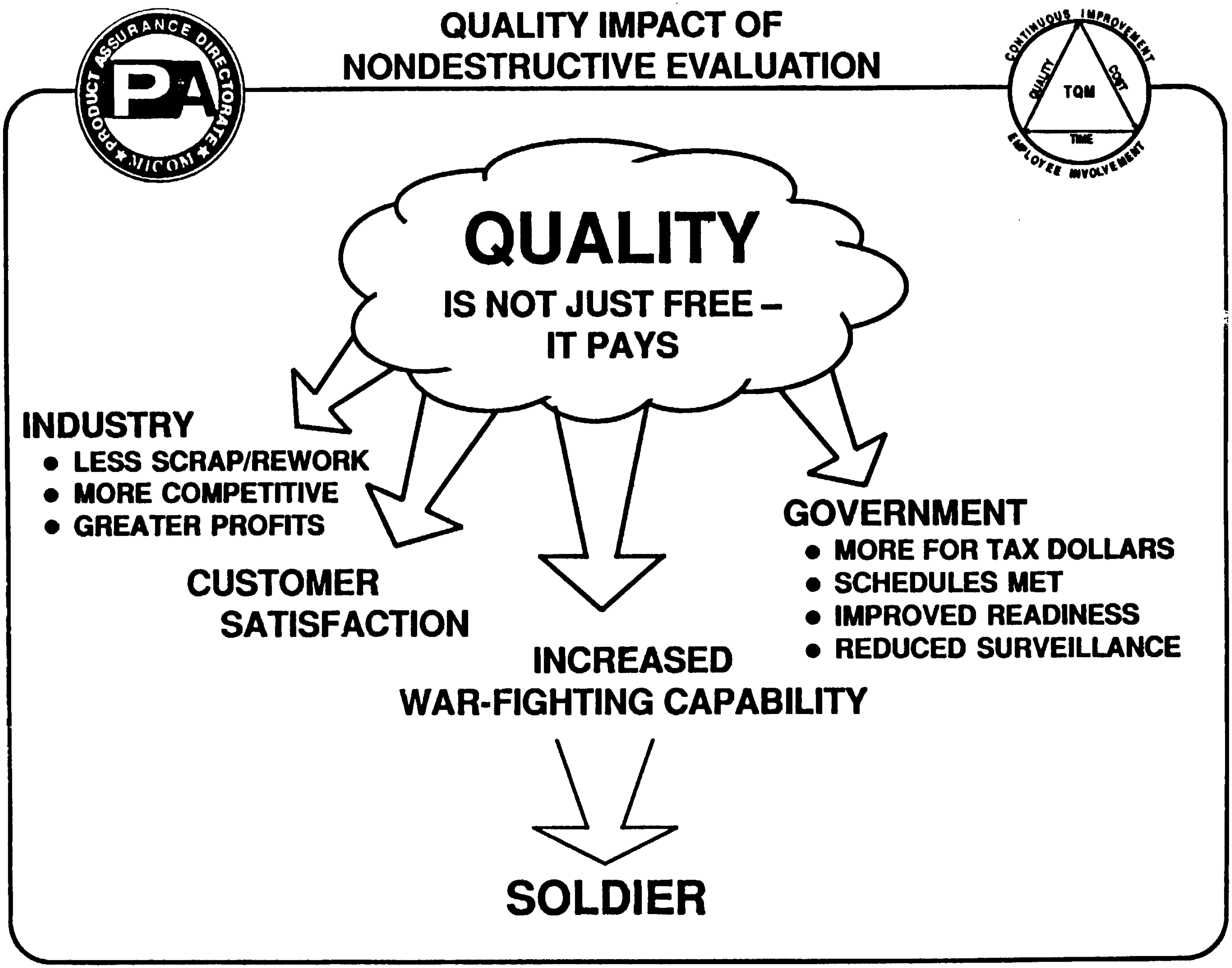

PRODUCT ASSURANCE DIRECTORATE ★ MICOM ★
PA
QUALITY IMPACT OF
NONDESTRUCTIVE EVALUATION
CONTINUOUS IMPROVEMENT
TQM
QUALITY
COST
TIME
EMPLOYEE INVOLVEMENT
QUALITY
IS NOT JUST FREE –
IT PAYS
INDUSTRY
• LESS SCRAP/REWORK
• MORE COMPETITIVE
• GREATER PROFITS
CUSTOMER
SATISFACTION
GOVERNMENT
• MORE FOR TAX DOLLARS
• SCHEDULES MET
• IMPROVED READINESS
• REDUCED SURVEILLANCE
INCREASED
WAR-FIGHTING CAPABILITY
SOLDIER

N91-18196

ACOUSTO-OPTIC SIGNATURE ANALYSIS FOR INSPECTION OF THE ORBITER THERMAL PROTECTION TILE BONDS

J. G. RODRIGUEZ, D. M. TOW, and B. A. BARNA
Idaho National Engineering Laboratory
EG&G Idaho, Inc., P.O. Box 1625
Idaho Falls, ID 83415-2209

INTRODUCTION

The goal of this research is to develop a viable, noncontacting NDE technique for the inspection of orbiter thermal protection system (TPS) tile bonds. Phase II, discussed here, concentrated on developing an empirical understanding of the bonded and unbonded vibration signatures of acreage tiles. Controlled experiments in the laboratory have provided useful information on the dynamic response of TPS tiles. It has been shown that several signatures are common to all the "pedigree" tiles. This degree of consistency in the tile-SIP (strain isolation pad) dynamic response proves that an unbond can be detected for a known tile and establishes the basis for extending the analysis capability to arbitrary tiles for which there are no historical data.

The field tests of the noncontacting laser acoustic sensor system, conducted at Kennedy Space Center (KSC), investigated the vibrational environment of the Orbiter Processing Facility (OPF) and its effect on the measurement and analysis techniques being developed. The data collected showed that for orbiter locations, such as the body flap and elevon, the data analysis scheme, and/or the sensor, will require modification to accommodate the ambient motion. Several methods have been identified for accomplishing this, and a solution is seen as readily achievable. It was established that the tile response was similar to that observed in the laboratory [1]. Of most importance, however, is that the field environment will not affect the physics of the dynamic response that is related to bond condition. All of this information is fundamental to any future design and development of a prototype system.

DEVELOPMENT OF ACOUSTO-OPTIC TECHNIQUES

Phase II has seen important progress in the area of sensor development. There is now a much better understanding of the sensor's capabilities and limitations. The sensor response has been modeled and verified with experiments using a piezo pusher. In addition, a long focal length lens has been incorporated that allows data collection at up to 10 m away [2].

The laser cavity response to light scattered from vibrating surfaces has been successfully modeled. The model has been used to explain several characteristics of the signal that arise when the vibration amplitude exceeds half the light wavelength [2]. If the model's criteria are violated, then nonlinear effects are predicted. These nonlinear effects have been observed. Frequency doubling occurs when the vibration displacement approaches the magnitude of a wavelength of laser light. Signal attenuation and frequency doubling are observed when the "at rest" distance to the sample violates nonlinearity. This understanding will

PRECEDING PAGE BLANK NOT FILMED

result in improved performance with the existing hardware and possibly development of an improved servo scheme that will allow the sensor to accommodate large amplitude vibrations, such as the ambient vibrations encountered in the OPF. The model is presently being used to study improved methods for extracting the vibration signal.

TILE RESPONSE STUDIES

The goal of the tile response studies was to develop an empirical understanding of the bonded and unbonded vibration signatures of acreage tiles covering the underside of the orbiter. Pedigree tiles were used in controlled unbonding experiments to reduce effects due to differences in tile geometry. A limited number of unbond geometries were simulated using a vacuum mounting fixture specially designed for this project. The experimental work clearly shows that bond condition affects tile response in consistent and quantifiable ways.

The vacuum mounting fixture will first be described to facilitate an understanding of experimental methods. Experimental results will then be presented.

Vacuum Chuck

A vacuum chuck for easy simulation of unbonds was developed. (During Phase I, unbonds were simulated by first bonding the tile to an aluminum plate and then slicing through regions of the SIP with a razor blade to mimic unbonds. An easier and more repeatable method of simulating unbonds was needed.) The vacuum chuck is an aluminum plate with a nearly square array of vacuum holes, slightly smaller than the 5 x 5 in. SIP (Figure 1). When a SIP is mounted backwards on a tile, such that the RTV side faces out, the tile can be securely held by placing the RTV-sealed SIP against the face of the chuck and drawing a vacuum. Unbonds are simulated by taping over regions of vacuum holes. Tests were conducted to study the repeatability of tile response with bonds simulated using the vacuum chuck. Tiles were mounted on the vacuum chuck at times separated by a few weeks with little effect on the dynamic response.

Tile Bond Analysis

The central thesis of this work is that bond condition can be determined by studying the vibrational response of a tile excited by acoustical energy. Investigations have centered on identifying response characteristics that reliably predict unbonds. A number of characteristics have emerged as promising candidates for this purpose and will be discussed in this section. The primary focus of the discussions will be on results obtained with the pedigree tiles, using the vacuum chuck to simulate unbonds. Before considering response characteristics of unbonded tiles, a brief description of tile vibrational modes is in order.

The vibrational modes of a TPS tile can be of either the rigid body type or the flexural type. In rigid body modes, vibration results from rocking, piston, or twisting actions of the rigid tile against the spring action of the SIP. Twisting motions will not be considered here because the displacement sensors used for this work detect only motion normal to the tile surface. In the flexural modes the tile bends as it vibrates; tile

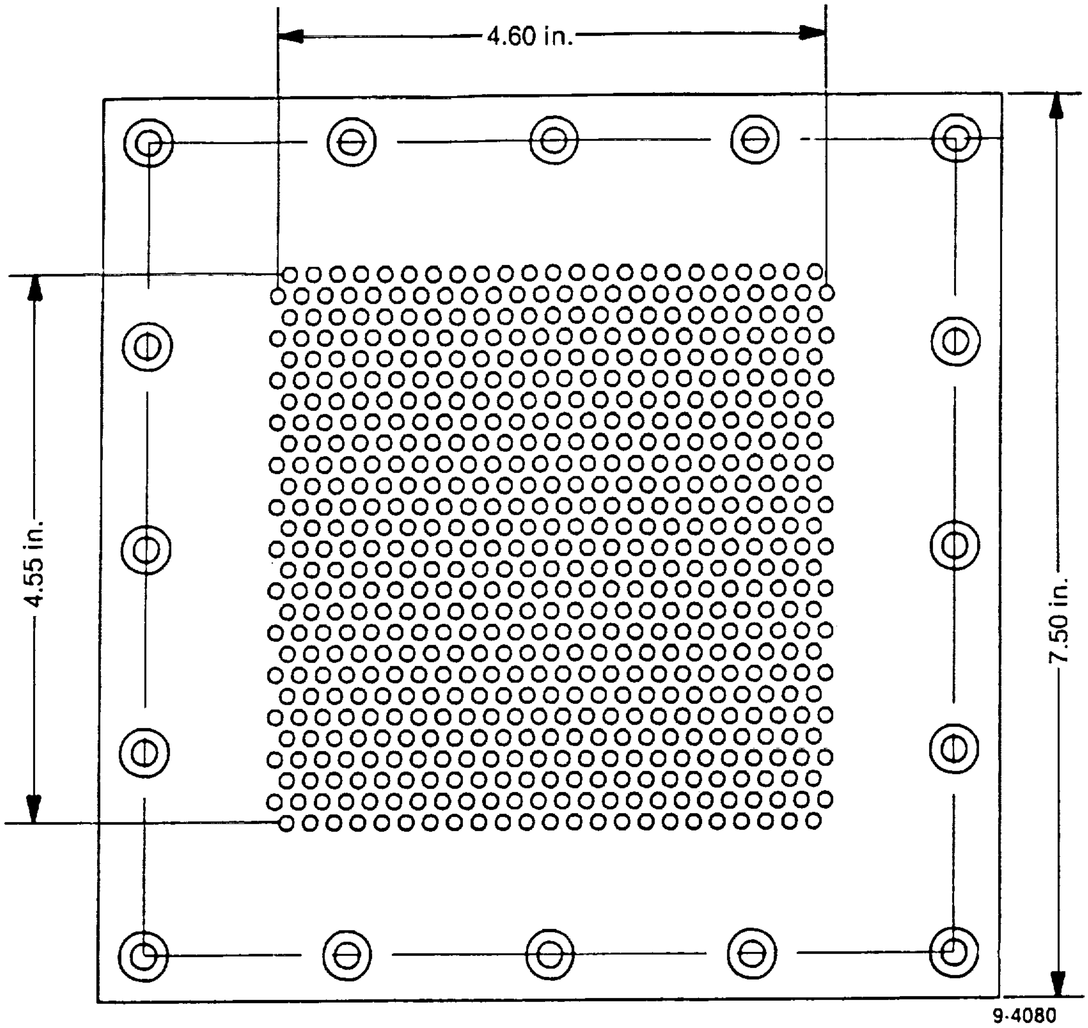

Fig. 1. Vacuum chuck.

stiffness provides most of the spring action. For TPS tiles examined to date, the frequencies of the two types of vibrational modes fortuitously separate into distinct nonoverlapping ranges; the rigid body modes appear below 1400 Hz, while the flexural modes appear above 1600 Hz. This separation aids in the interpretation of some of the phenomena observed in tile vibrational responses.

A number of characteristics have emerged as promising candidates for unbond indicators. They are listed here and explained in the text which follows.

1. Downward frequency shift of rigid body modes.
2. Amplitude of the vibrational response.
3. Elongation of initial oscillations in transient tile response.
4. Asymmetrical response characteristics in unbonded tiles.

Downward Frequency Shift of Rigid Body Modes

In order to quantify the frequency shifts as unbonding progresses, a measure of the center frequency for each unbond condition is needed. Four measures of the center frequency of the rigid body modes were developed and evaluated. All operate on spectra over the rigid body frequency range of 0 to 1400 Hz. Spectra are calculated using fast Fourier transform (FFT) without windowing. The magnitude of the FFT terms is used in two of the center frequency calculation methods; magnitude squared is used in the remaining two.

The methods were evaluated by applying them to data collected during unbonding experiments with three pedigree tiles--9073, 9074, and 9075. The vacuum chuck was used to simulate unbonds. Data were collected from the three tiles under four bond conditions: fully bonded, 25% unbonded, 50% unbonded, and 100% unbonded. The 25% unbond was a 2-1/2-in. square region in the upper right corner of the 5-in. square SIP. The entire top half of the SIP was unbonded in the 50% unbond tests. The 100% unbond data were collected while the tile was lying face-up on the optical table; this is also referred to as a back shop measurement. Filler bar was present for all measurements, except, of course, for the 100% unbond case. Data were collected at three points on each tile, as illustrated in Figure 2: top center, center, and lower center. Results from the three tiles, for the top center point, are summarized in Figure 3.

Center frequency (as defined above) shows promise of being a reliable unbond indicator when the sample point is near an unbond. To use center frequency for unbond determination, the "good" center frequency must be known beforehand. It may be possible to determine this from knowledge of tile geometry. However, it may not be possible if center frequency is very sensitive to minor variations in geometry or to random variations introduced during mounting. If the latter is true, center frequency may still be used for bond analysis, but it would require an empirical determination of the "good" value after mounting. The technique would not then be useful for inspecting initial tile installations but would be used for postflight examinations. Results obtained from the pedigree tiles suggest that "good" center frequencies may be accurately predicted from nominal geometries. More study of center frequency and the factors that affect it is required.

Amplitude of the Vibrational Response

Larger vibrational amplitudes have been found to correlate with unbonds. Figure 4 shows time series data collected from tile 9074. A relationship between amplitude and the presence of an unbond is evident. However, amplitude also depends on the relative locations of the unbond and sample point. The peak-to-peak amplitude is largest when the unbond is across the bottom. When this is the case, the sample point is over the unbond, and the peak-to-peak amplitude is double the amplitude of the fully bonded tile. When the unbond is along the right side, the sample point is also over the unbond, but the increase in amplitude is only 36%. When the sample point is not over the unbond, the increase is less evident or absent.

The amplitude data discussed here were not collected with the point sensor developed for this work. That sensor has some outstanding characteristics, but measuring absolute amplitude is not one of them. The problem stems from the fact that measurements are proportional to the brightness of reflected light, as well as displacement. The reflectivity of

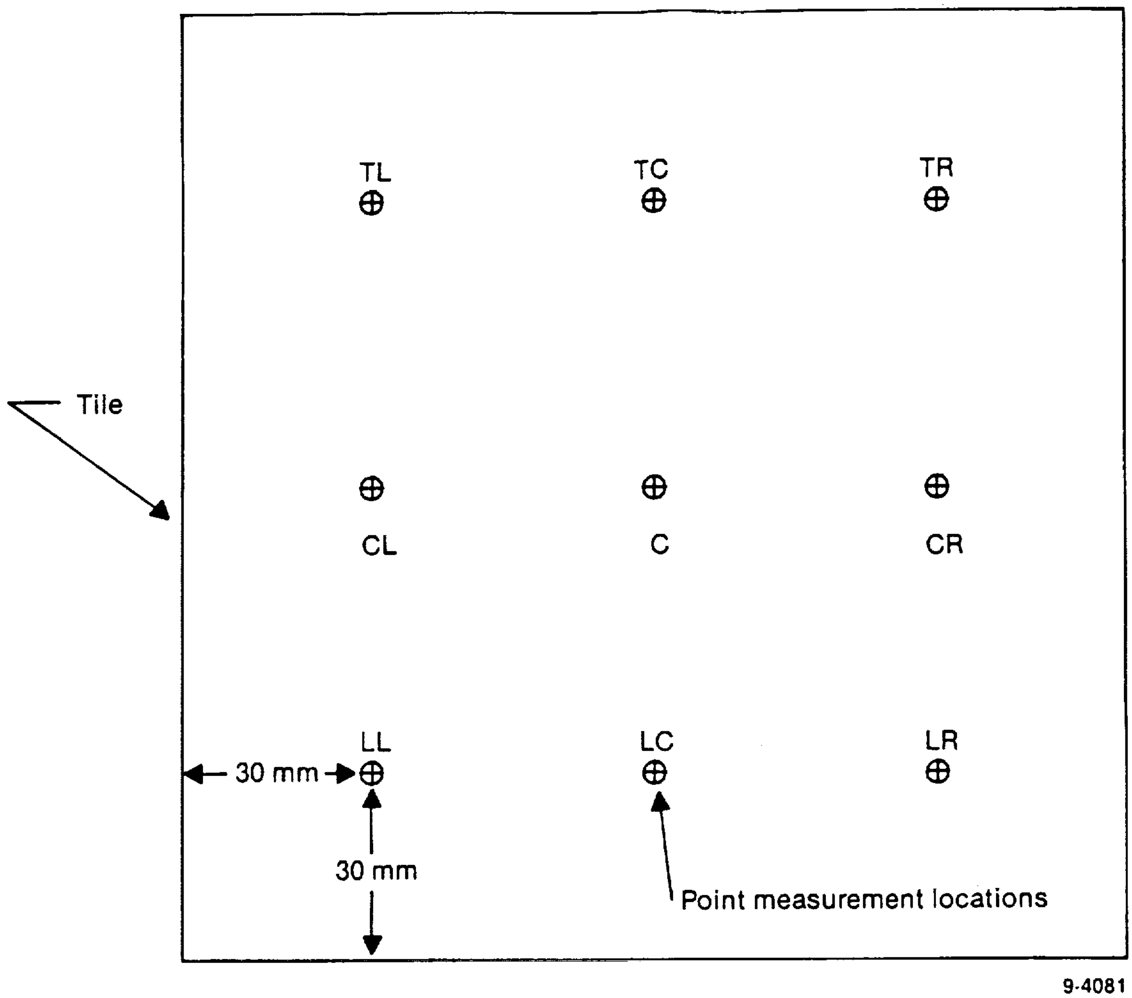

Fig. 2. Vibration measurement points.

tiles varies from point to point, thereby precluding comparison of amplitude data from two different points on a tile. Amplitude data were collected with a laser vibrometer that requires attaching a mirror to the tile. This system is suitable only for laboratory use because of the mirror requirement. The existing sensor could be used on the orbiter if it were possible to calibrate it at each sample point. A fairly simple method of calibration using a dither signal has been proposed. If amplitude is determined to be a necessary measurement for unbond detection, it is felt that an appropriate sensor could be developed with existing technology.

Elongation of Initial Oscillations in Transient Tile Response

The first few milliseconds of tile vibration following excitation exhibit a characteristic that predicts unbonds in the pedigree tiles. This characteristic is the duration of the first few oscillations in the time series data. Figure 5 shows the first 3 ms of time series data for three bond conditions. As unbonding increases, an elongation of the oscillations occurs and the time between zero crossings increases. This phenomenon may be the time domain equivalent of the downward frequency

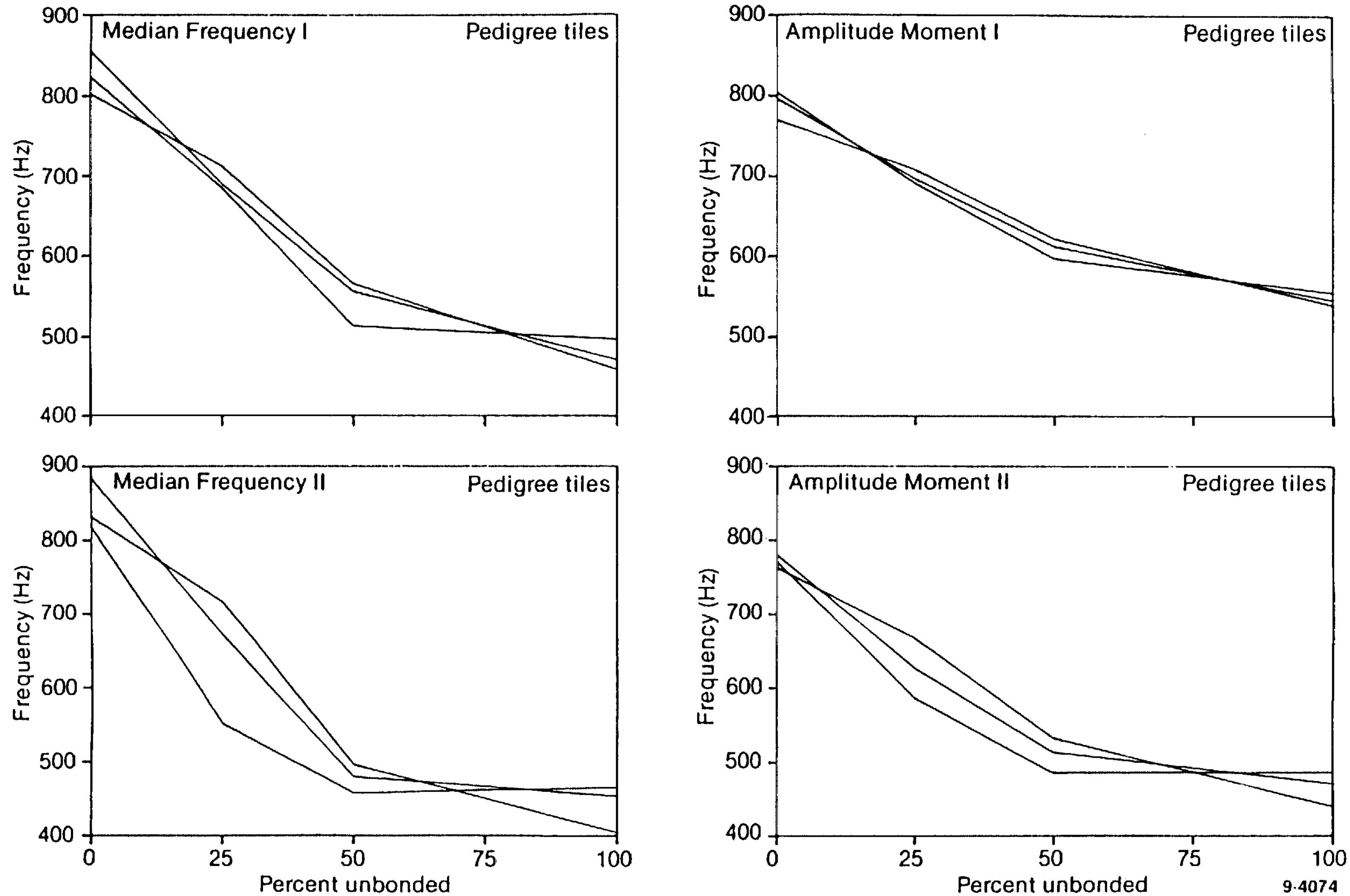

Fig. 3. Calculated center frequency as a function of percent of unbond for the top center point of the three pedigree tiles. The results of four different methods are shown.

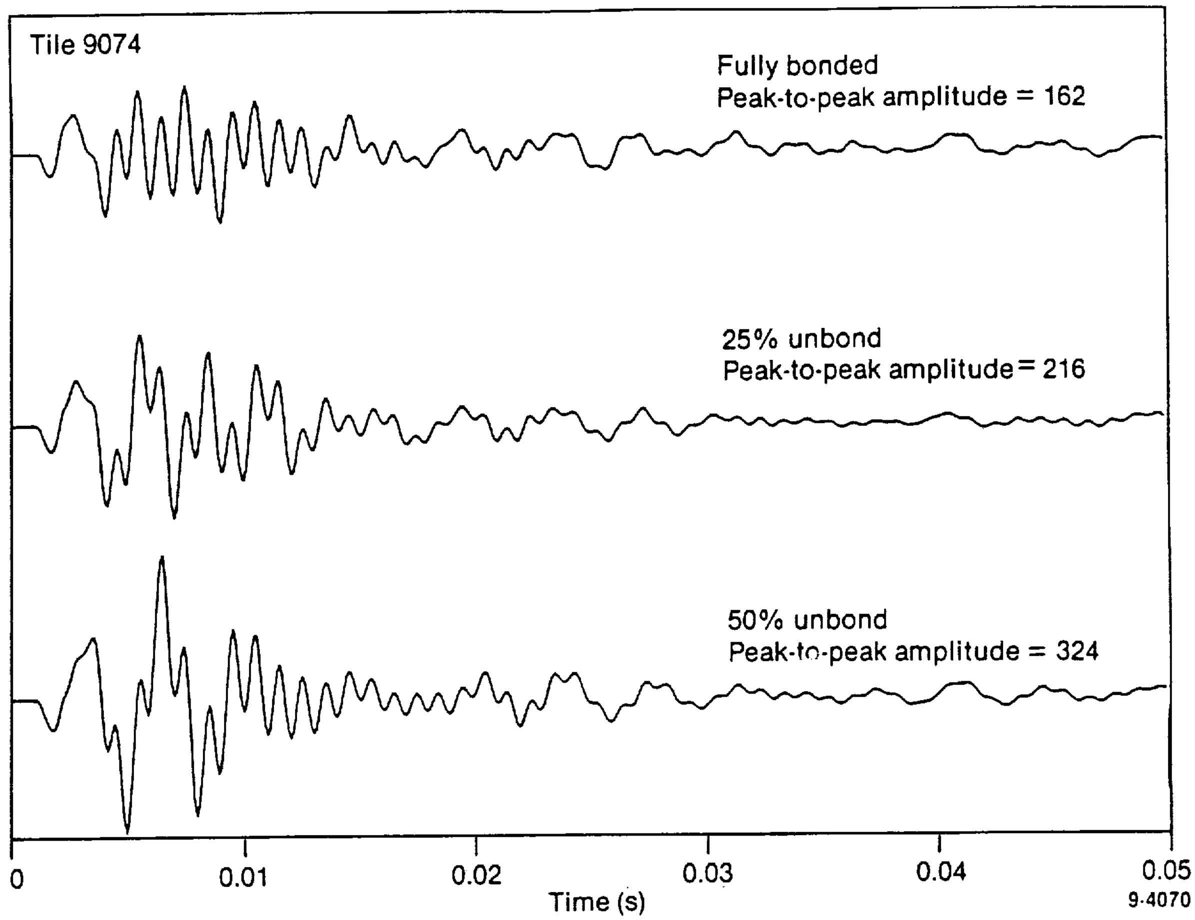

Fig. 4. Effects of unbonds on amplitude.

shifts observed in the rigid body modes. If so, there may be little to gain in studying both phenomena as the bond condition information contained in one may be duplicated in the other. On the other hand, the two may not be that closely related. The time domain phenomenon may provide information about resonance modes not observable in estimated spectra. Spectra estimated using FFT techniques necessarily represent time averages of the frequency content of a signal. The frequency content of a transient process, such as tile dynamic response, changes with time (the process is nonstationary). A time average may not adequately represent the frequency content at a particular time, especially if dominant resonance modes at that time are rapidly decaying. Hence, there is reason to continue consideration of this time domain unbond indicator.

Unbond effects on initial oscillations are affected by the relative locations of the sample point and unbond. Elongation of initial oscillations diminishes as the distance between sample point and unbond increases. Evidence suggests that the relative positions of speaker and unbond may also be significant. This is very similar to the behavior of unbond indicators already discussed. The data from unbonded tiles plotted in Figure 5 were collected at points over the unbonds.

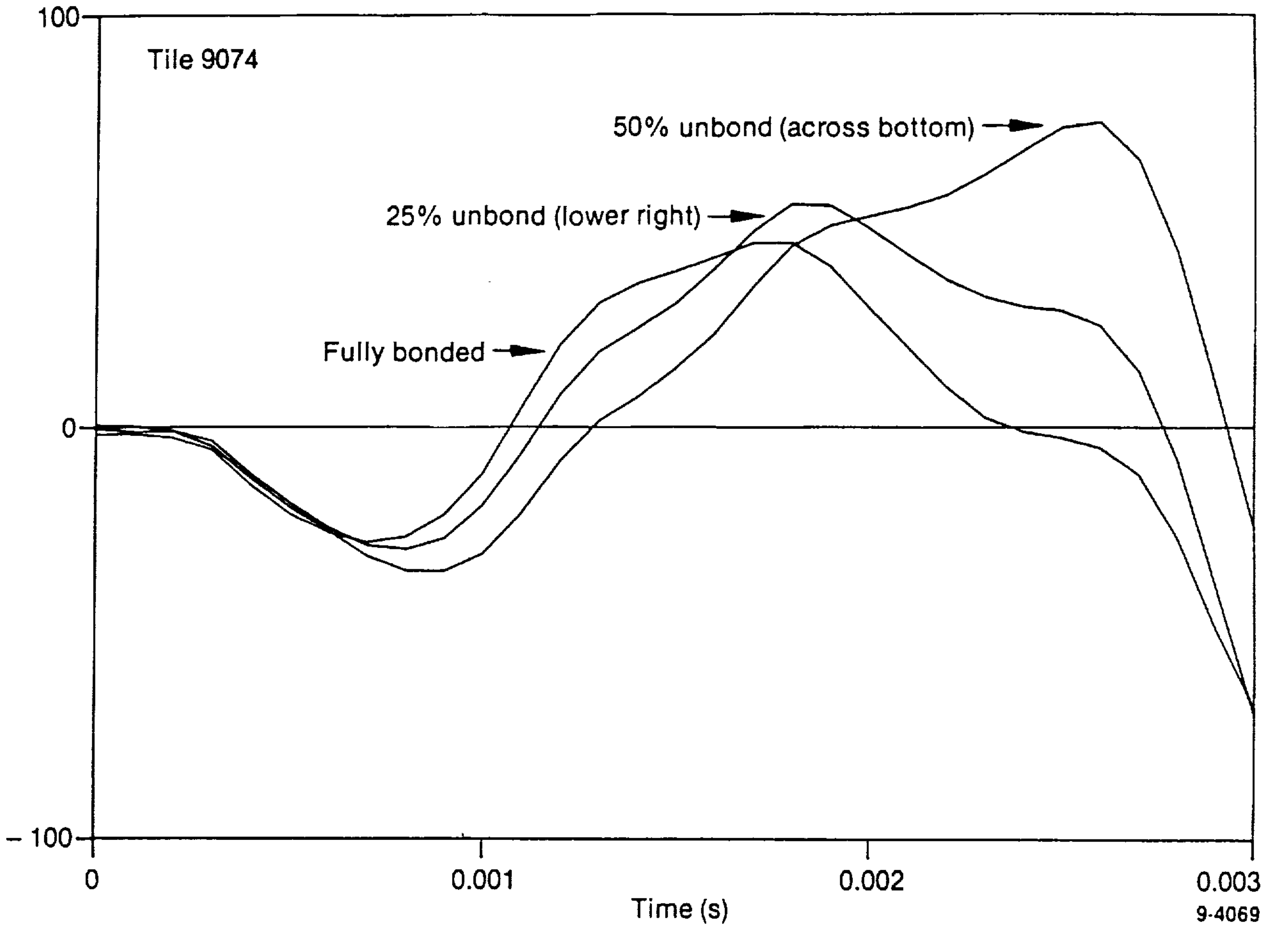

Fig. 5. Effects of the unbond on the initial oscillation.

<u>Asymmetrical Response Characteristics in Unbonded Tiles</u>

The tile response characteristics discussed above exhibit a dependence on the relative locations of the sample point, unbond, and speaker (excitation). This behavior suggests that an asymmetrical response may be useful for identifying unbonds. Asymmetrical behavior of an unbonded tile is illustrated in Figure 6, which shows the response of a bonded tile at two measurement point locations, top left and top right. The speaker position is the same for all plots. It is apparent that the differences in top right and top left spectra are greater when an unbond is present; the spectrum at a given point is apparently more sensitive to changes in speaker location when an unbond is present.

This unbond indicator is particularly attractive since it does not require prior assumptions about "good" tile behavior. It is based on the following two premises:

1. An asymmetrical bond results in asymmetrical tile dynamic response characteristics.

2. Asymmetrical behavior normally observed in bonded tiles is much smaller than asymmetrical behavior due to significant unbonds.

More work is required to verify these two assumptions, as well as devise a method of quantifying spectral asymmetry. Finally, it is clear that this unbond indicator would not detect symmetrical unbonds.

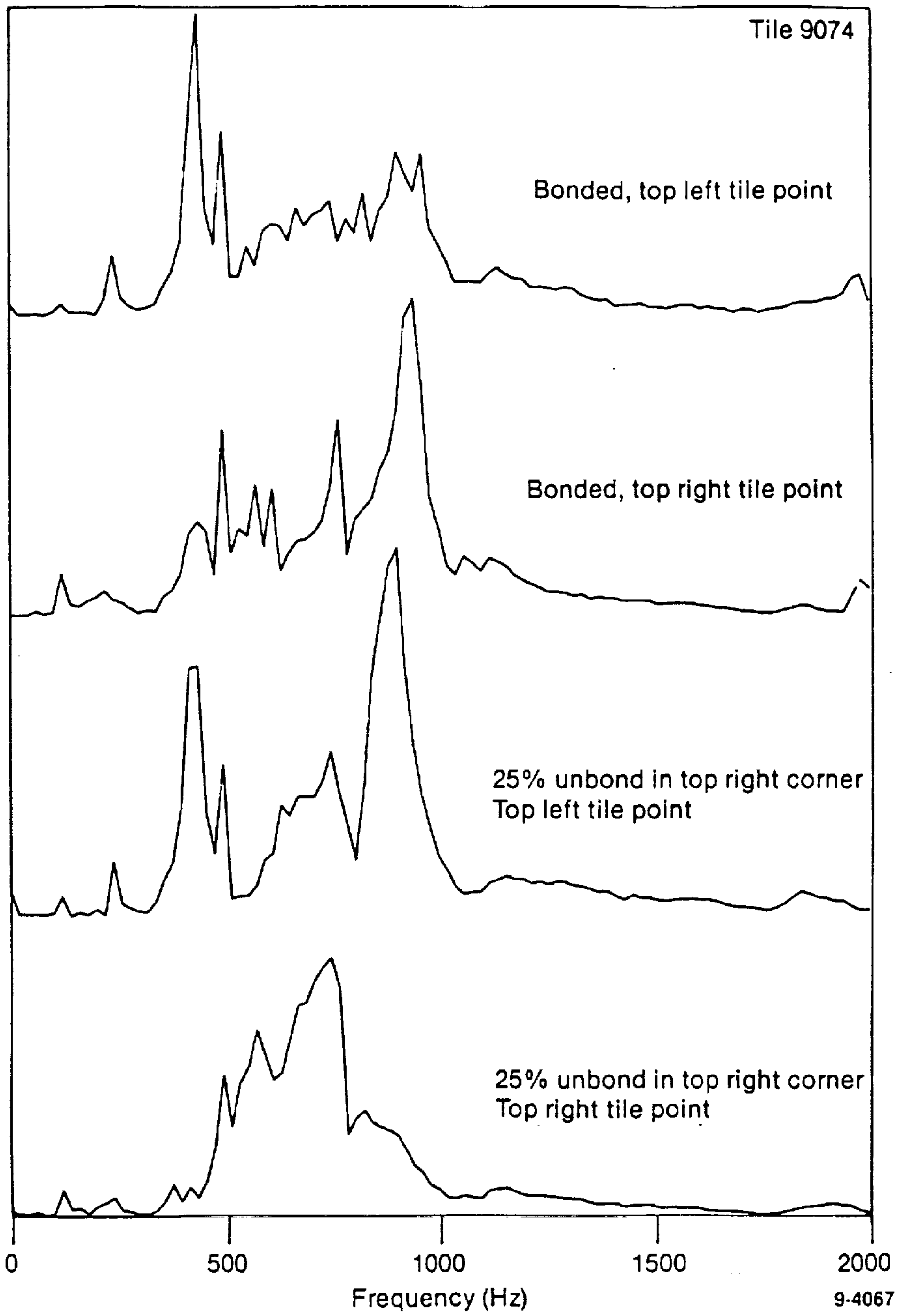

Fig. 6. Effect of sample point location.

FIELD TESTS

The field tests conducted in July of 1988 verified that tile resonances were detectable in the Orbiter Processing Facility environment. The field tests established that the vibration isolation of the sensor system, the long focal length optics, and the excitation methods could function in a field environment. There was no difficulty in obtaining an adequate reflection from the normal tile surfaces, and the pneumatic tires on the cart carrying the laser provided sufficient vibration isolation for the system. However, the measurements, which were made on the Orbiter Columbia, also showed that the sensor response was complicated by ambient motion of the orbiter. While small (~10 μm at 20 Hz), these motions were detected by the sensor and frequently masked the induced excitation. Figure 7 shows TPS data collected near the external tank doors. The data in the two unaveraged data sets in Figure 7a changed phase during our collection period of 50 ms due to the ambient motion. For the 25 averaged data sets shown in Figure 7b, the collection period could be reduced from 50 to 8 ms due to signal cancellation caused by the ambient motion. The motion taking place on the orbiter has reduced the amount of information that the current collection technique can obtain.

Due to the large ambient motion, a fieldable system will require modification of either the sensor or the way the resonance information is extracted with the existing sensor. Details of these options are given below; an evaluation of these approaches is being conducted as part of ongoing work.

There are at least two approaches to overcoming the difficulty caused by the ambient motion of the orbiter. The first is to modify the data analysis so that the sensor nonlinearities do not obscure the desired information. This is possible because the large amplitude ambient vibrations do not change the physics of the bond's effect on the tile's dynamic response; a different measurement technique may be required, but the effect is still there. Some possible modifications are to confine the analysis to the first 5 ms after excitation or to measure peak amplitudes of resonance vibrations induced by a CW tone. The latter technique was actually used during the field test at selected resonances. Figure 8 presents data collected on one of the control surfaces. Here a CW tone was used to excite a tile vibration resonance. The data show that during a "turnaround" point the CW tone can be captured and used for data analysis. The second approach would be to continue sensor development to obtain a sensor that is linear over the required range of vibrations. The approach taken to date has been to use the existing sensor capability, unless and until it is necessary to expend additional resources to acquire a sensor capable of handling large ambient motion. These two approaches are currently being evaluated.

The most significant finding of the field tests is that the response of the tiles on the orbiter is similar to that observed in the laboratory. While it was not possible, or intended, to vary bond conditions on the tiles examined, it was possible to excite resonances and measure their existence with the acousto-optic sensor in a different fashion than the standard data collection method. Quantification of the ambient vibrations of the OPF environment was also significant as their impact can now be incorporated into any future design of analysis techniques and/or sensors.

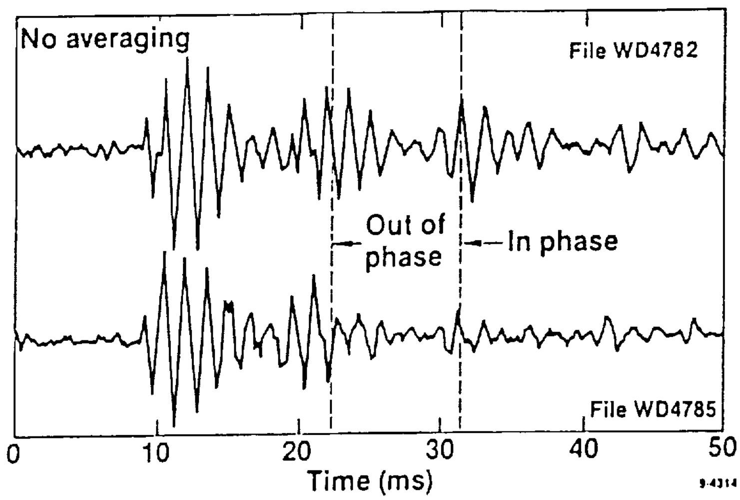

a. Two unaveraged data sets.

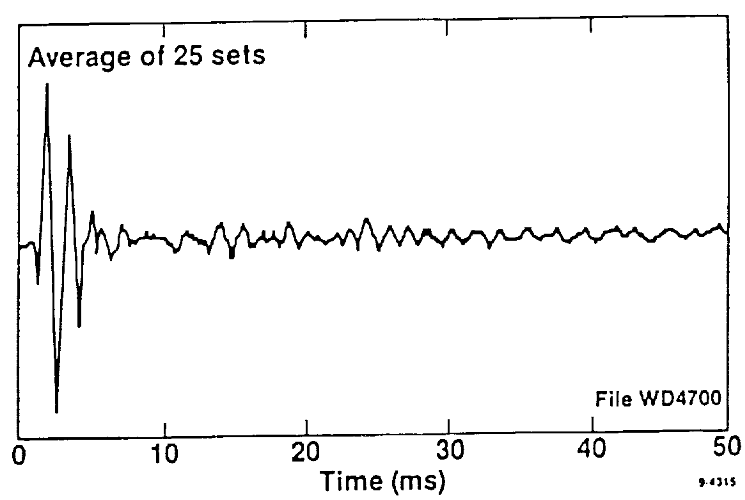

b. Average of 25 data sets.

Fig. 7. KSC field data near external tank door.

EXTERNAL CAVITY

Now that the OPF vibrational environment has been characterized, it is necessary to choose a sensor to operate in this environment. An external cavity has been added to the existing sensor. The cavity consists of a mirror mounted on a piezo pusher and placed in the beam path to the tile. As excessive motion of the tile is sensed, the mirror is moved in an opposite direction to compensate for the motion. The two types of vibrations are separable by filtering since the large amplitude vibrations are generally of lower frequency than the signal of interest. The cavity can compensate for large low-frequency ambient vibrations of less than 100 Hz (Figure 9). The control signal for this cavity variation is derived from the displacement signal output from the laser

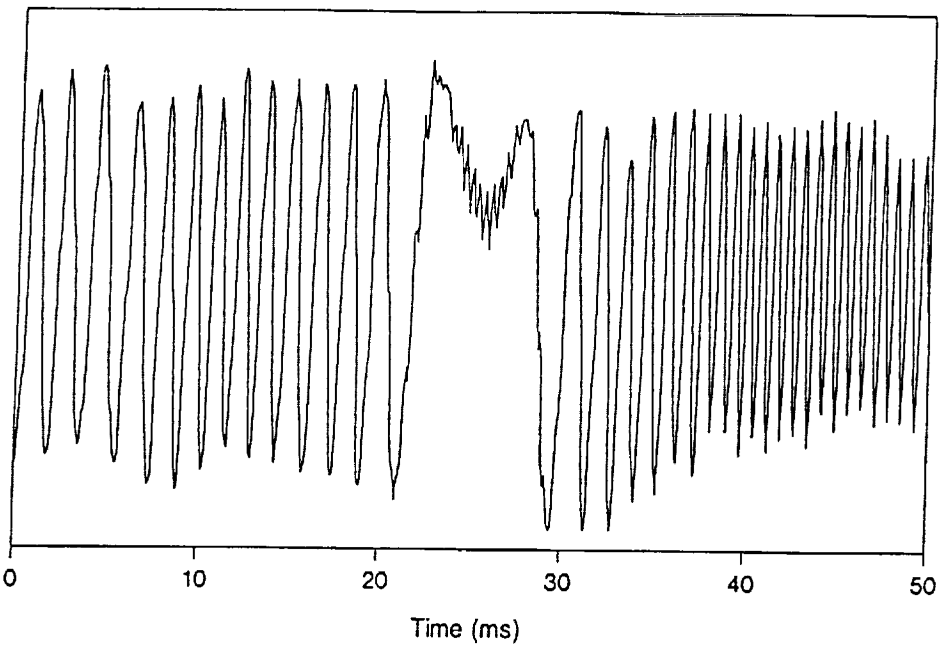

Fig. 8. KSC field data on elevon.

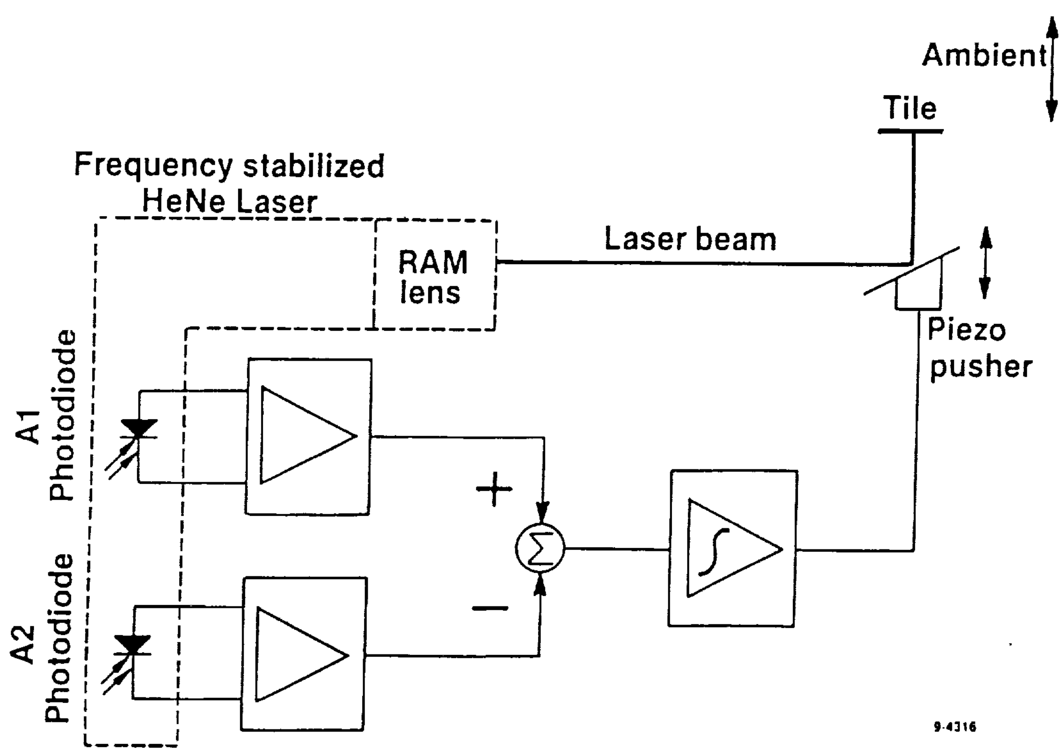

Fig. 9. External cavity block diagram.

sensor. The external cavity has been used to prevent phase inversion of the signal, proving in principle that the approach is capable of improving the fidelity of the signal.

CONCLUSIONS

The past year's work had two basic objectives. The first was to continue development of the sensing technology to the point where preliminary field measurements on the orbiter could be made. This goal was achieved, thanks in large part to the development of the long focal length optics. Valuable information obtained from the field experiments clearly identifies areas where future efforts should be applied.

The second goal was to advance the state of understanding of the physics of tile vibration and vibration measurement to the point where an informed decision could be made on whether or not this approach is viable for field detection of real flaws on the orbiter TPS. This goal was also achieved; concentrating on the pedigree tiles, a number of quantifiable unbond signatures were identified.

The following conclusions summarize the results of Phase II work on this project.

1. Vibration signatures associated with bond flaws are significant, repeatable, and consistent between similar tiles with similar bond flaws. A number of promising bond flaw signatures have been identified. These signatures are quantifiable and consistent among the pedigree tiles. Signatures include frequency and time domain features of the dynamic response, as well as symmetry observations.

2. The measurement techniques developed for this project can work in a field environment. An optical table is not required to make extremely sensitive displacement measurements; the sensor can operate in normal workplace "noise."

3. Modifications to the sensor or to analysis techniques are necessary to accommodate the large ambient motion present in some areas of the orbiter.

The field tests revealed that the ambient vibration of the orbiter is too large for the current sensing method and/or analysis techniques. The current sensor is very good at sensing vibrations with peak-to-peak amplitudes less than 0.5 μm. Motions greater than 13 μm were measured in some areas of the orbiter during the field tests.

ACKNOWLEDGMENT

This work is supported by John F. Kennedy Space Center, NASA, through Department of Energy Contract No. DE-AC07-76ID01570.

REFERENCES

1. B. A. Barna, R. T. Allemeier, and J. G. Rodriguez, "Laser Optic Vibration Sensing for the Inspection of Bonds in the Orbiter Thermal Protection Tiles," Review in Progress in QNDE 7b, edited by D. O. Thompson and D. E. Chimenti (Plenum Press, New York, 1988) p. 1227.

2. B. A. Barna, D. M. Tow, R. T. Allemeier, J. G. Rodriguez, and J. A. Johnson, "Laser Detection of Acoustic Displacement by Destabilizing a Frequency Stabilized Helium Neon Laser," Review in Progress in QNDE 8A, edited by D. O. Thompson and D. E. Chimenti (Plenum Press, New York, 1988) p. 543.

PC-BASED NDE SIGNAL ACQUISITION & ANALYSIS

Tony Mucciardi

Infometrics, Inc.

2nd. Conference on Nondestructive Evaluation for Aerospace Requirements
August 22-24, 1989 Huntsville, AL

ANALOG UT INSPECTION

CRITERIA

- Amplitude Exceeding a Threshold in a Time Gate

- Echo Dynamic Pattern of Indications

PROBLEMS

- Threshold Alarm Alerts Inspector of Indication, but not its Identity

- Inspector's Expertise is Often Not Adequate for Proper Decision

- No Way for Independent Third Party Evaluation without Repeating Entire Inspection & Relying, once more, on Another Inspector's Expertise

DIGITAL UT INSPECTION

- If the Transducer Signal is Digitized & Recorded During the Initial Inspection, Further Analyses can be made -- both by Individuals & by Software Algorithms -- without Repeating the Inspection

- This Archival Capability also Permits the Waveform to be Compared -- Along with its Features -- to Data Recorded in Other Inspections

- Digital Storage of UT RF Waveforms also permits Signal-to-Noise Enhancement Algorithms to be applied to Eliminate, or at least greatly reduce -- Undesirable Signal Contaminants such as Grain Noise, etc.

WHY PCs ?

- FIELD WORTHY - Designed to operate in Office / Work Area w/out Need for Specially Controlled A/C Environment

- SIZE - Portable Versions are quite Rugged & Easy to Transport

- ARCHITECTURE - PC Bus Architecture allows the Integration & Intelligent Control of User-Supplied Boards; mass storage is very cheap

- PRICE - Very Inexpensize

- POWER - With 386-class Machines, PCs have Main Frame Speeds

- PARTS - Readily Available World-Wide

PC-Based Workstation for NDE

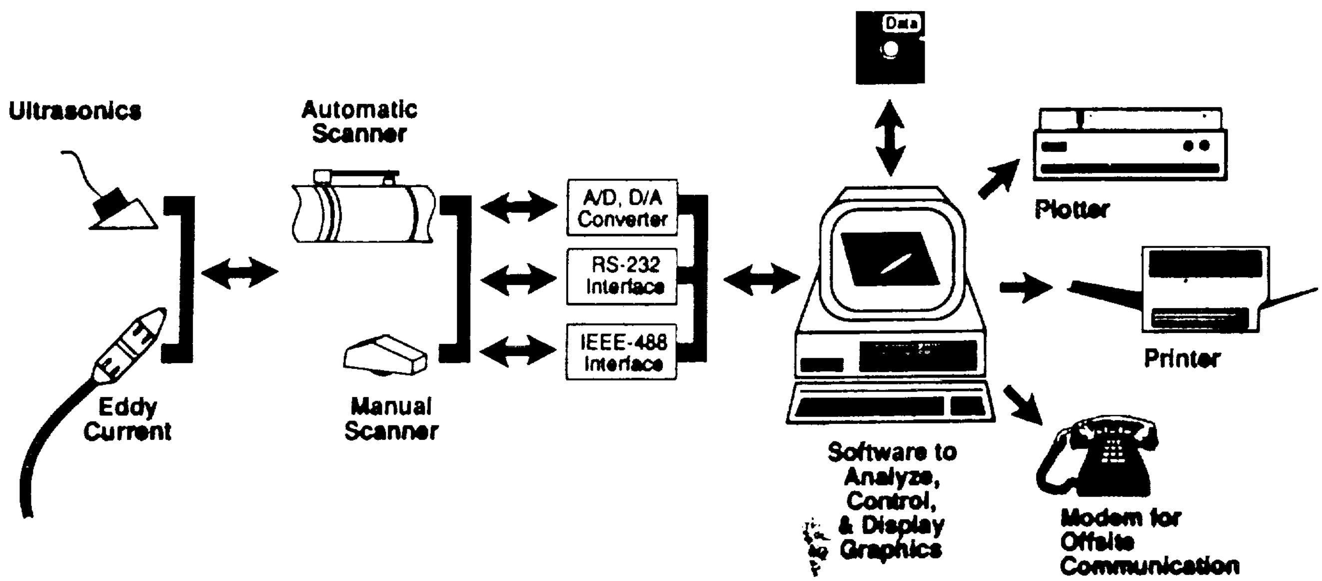

ORIGINAL PAGE IS
OF POOR QUALITY

COMPONENTS OF UT SIGNAL PROCESSING

TRANSDUCER CHARACTERIZATION

- Transducer Evaluation -- time/frequency
- Sound Beam Profiler -- immersion/contact
- Auto Specs + User Specs

DATA ACQUISITION & PROCESSING

- Data Acquisition (multi-channel)
- Clustering
- 3-D Graphics (CAD-like)
- Signal Processing/Filtering (S/N enhance.)
- Lotus 1-2-3 Spreadsheet i'face
- dBase III i'face
- Communications (modem)
- Word Processing/Reporting
- User-Supplied S'ware

FLAW CLASSIFICATION

- Training (auto. Pattern Recognition)
- Analysis

IMAGING

- C- and B-Scans
- 3-D C-scans
- Off-line C-scan Reconstruction
- Image Processing functions

COMPONENTS OF UT SIGNAL PROCESSING

EDDY CURRENT

- Phase Plane analysis
- Multi-Channel
- Multi-Frequency
- Auto. Mixing Algorithm
- Store on Hard Disk for further analyses

SIGNAL QUALIFICATION

- Flaw Detector raised to higher level
- Multiple Gates (inc. overlap)
- Threshold "sense"
- "Analysis" Gate (real-time flaw classif.)
- Alarm menu
- Alarm-disposition menu
- Real-Time S/N Enhancement display

TRANSDUCER EVALUATION TEST

TESTPRO TRANSDUCER EVALUATION TEST
ULTRASONIC TRANSDUCER REPORT
Report_Date: Thu Mar 23 10:59:59 1989
USER PARAMETERS

TRANSDUCER ENTRIES

Serial Number:	144517	**Model/Type:**	Gamma
Manufacturer:	KB Aerotech	**Imersion/Contact:**	Contact
Diameter (in):	0.500	**Focal Length (in):**	n/a
Cntr Freq(Mhz):	2.5	**Date Purchased:**	2-Feb-86

PULSER RECEIVER ENTRIES

Manufacturer:	Infometrics	**Gain:**	10dB
Model/Type:	PCPR-100	**Attenuation:**	40dB
Serial Number:		**Energy:**	175 Volts
Last Calibrate:	May-88	**High Pass Filter:**	50MHz

USER ENTRIES		**OTHER DATA**	
Tester:	Mucciardi	**Cal Block Type:**	Aluminum
Date of Test:	7-Jul-88	**Cable Length:**	1 Meter
Series Number:		**Shoe Type:**	Wedge
Hours of Use:		**Shoe Material:**	Lucite

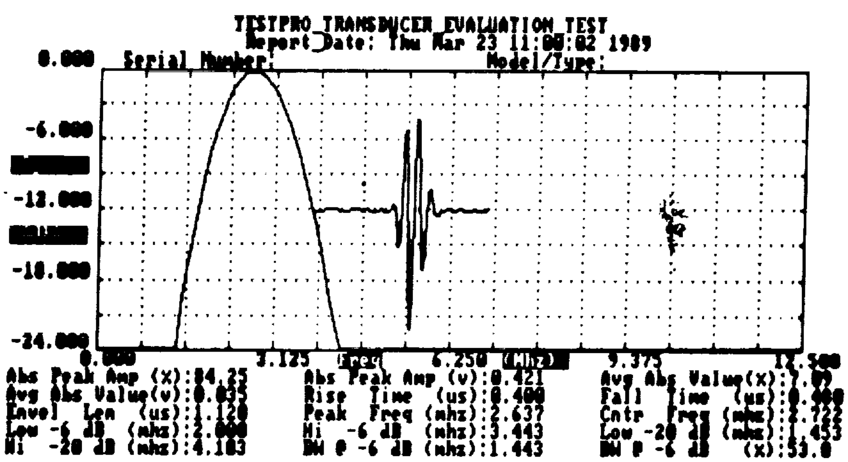

SYSTEM PARAMETERS

Time Delay (us)	:14.080	Hor Res (us/div)	:1.280	Vert Res (v/div)	:0.125
Start Freq (MHz)	:0.000	Hor Res(mhz/div)	:0.7813	Vert Res(db/div)	:3.000
Gate Start (us)	:20.280	Gate Length (us)	:5.120	Gate Length(pts)	:128
Sampl Rate (MHz)	:25.000	Waves Avged(num)	:1	Trigger(Int/Ext)	:Int
FFT Length (pts)	:256	DB Range (dB)	:24.0	Plot in DB (y/n)	:Yes
Pulser Volts (V)	:175	Damping (Ohm)	:634	PW Freq (MHz)	:2.240
Numbr Cycles (1)	:1	Pulser Phase ( )	:-Unipolr	Fixed Atten (dB)	:40
Attenuation (dB)	:30	LPass Filt (MHz)	:9.0		

FEATURES

Abs Peak Amp (%)	:84.25	Abs Peak Amp (v)	:0.421	Avg Abs Value(%)	:7.09
Avg Abs Value(v)	:0.035	Rise Time (us)	:0.400	Fall Time (us)	:0.480
Peak Freq (mhz)	:2.637	Cntr Freq (mhz)	:2.722	Low -6 dB (mhz)	:2.000
Hi -6 dB (mhz)	:3.443	Low -20 dB (mhz)	:1.453	Hi -20 dB (mhz)	:4.103
BW @ -6 dB (mhz)	:1.443	BW @ -6 dB (%)	:53.0	BW @ -20 dB(mhz)	:2.650
BW @ -20 dB (%)	:97.4				

ORIGINAL PAGE IS
OF POOR QUALITY

SPECTRUM COMPARISON

Use Cursors To Move Upper Waveform Up Or Down

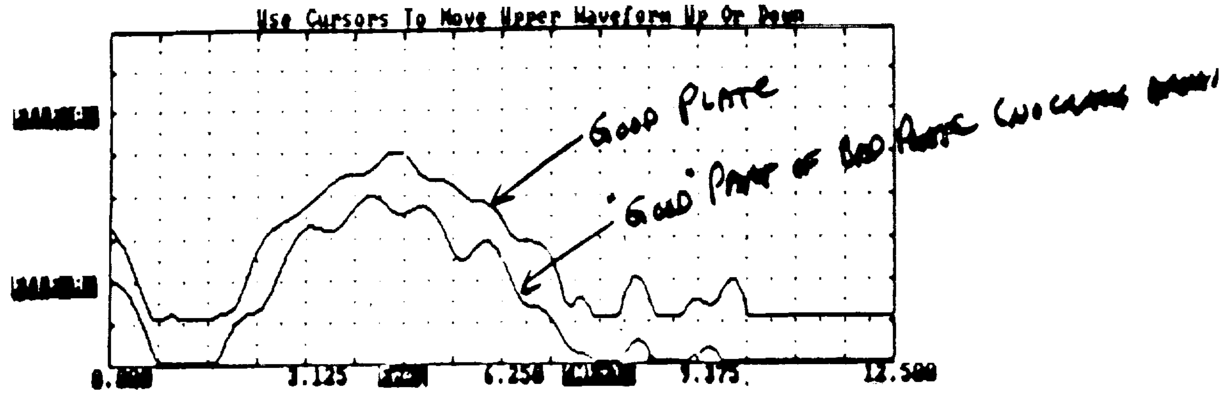

Upper Waveform = Spectrum from record 0 of file C:\TESTPRO\USPOLY01.PD
Lower Waveform = Spectrum from record 1 of file C:\TESTPRO\USPOLY01.PD
Hit P to Print, Escape to Quit

SPECTRUM COMPARISON

Use Cursors To Move Upper Waveform Up Or Down

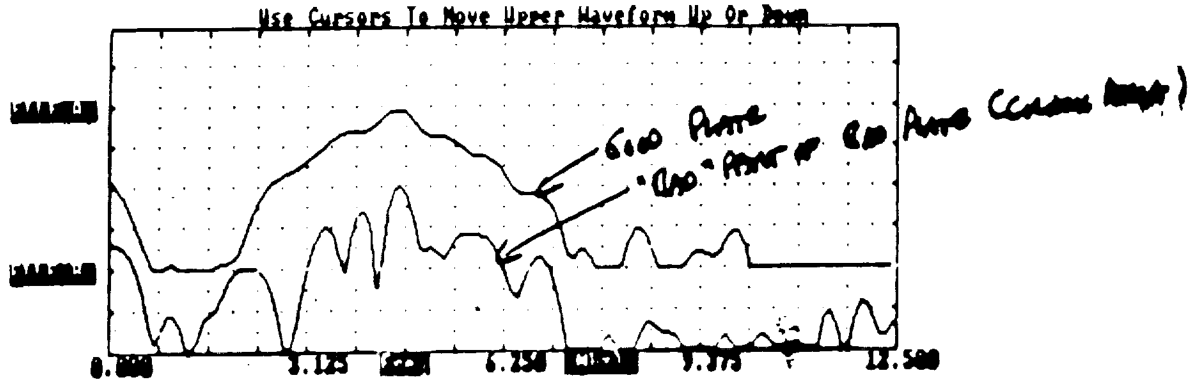

Upper Waveform = Spectrum from record 0 of file C:\TESTPRO\USPOLY01.PD
Lower Waveform = Spectrum from record 2 of file C:\TESTPRO\USPOLY01.PD
Hit P to Print, Escape to Quit

SPECTRUM COMPARISON

Use Cursors To Move Upper Waveform Up Or Down

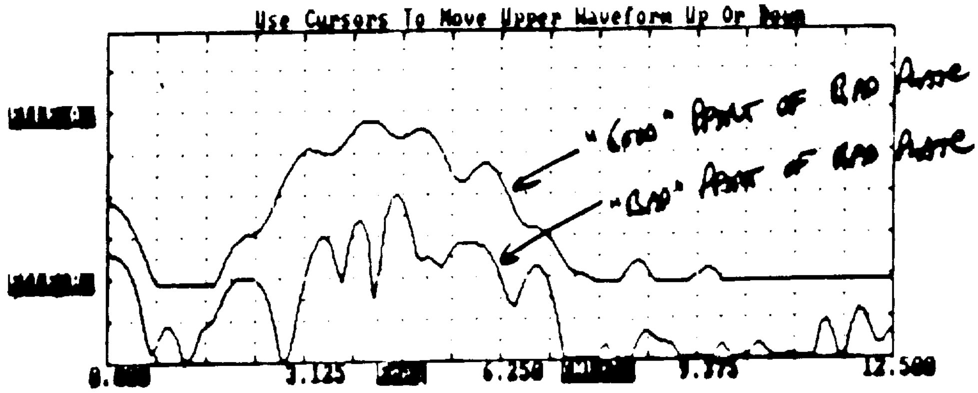

Upper Waveform = Spectrum from record 1 of file C:\TESTPRO\USPOLY01.PD
Lower Waveform = Spectrum from record 2 of file C:\TESTPRO\USPOLY01.PD
Hit P to Print, Escape to Quit

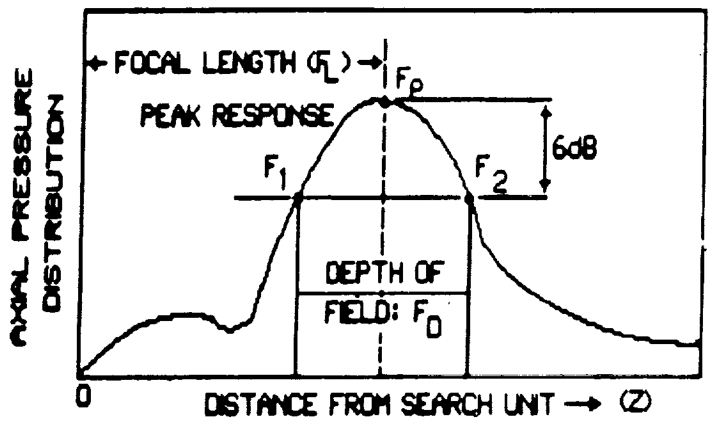

On-Axis Profile Parameters from Focused Search Unit

Fig. 1

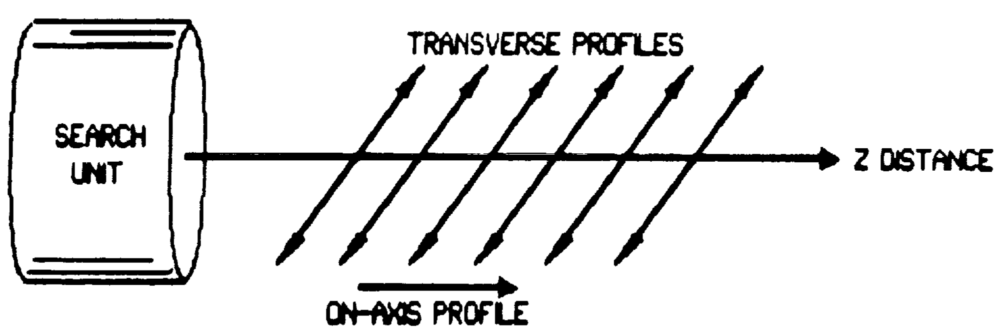

Sound Field Patterns: Transverse Profile

Fig. 2

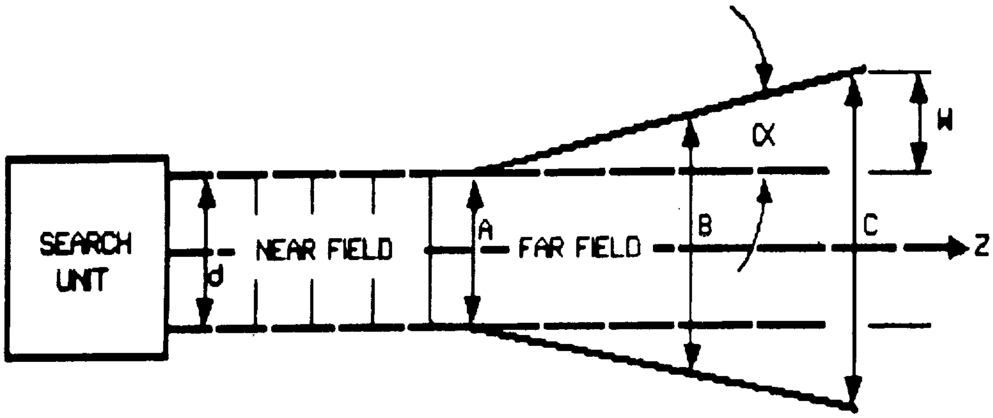

Sound Field Patterns: Beam Spread

Fig. 3

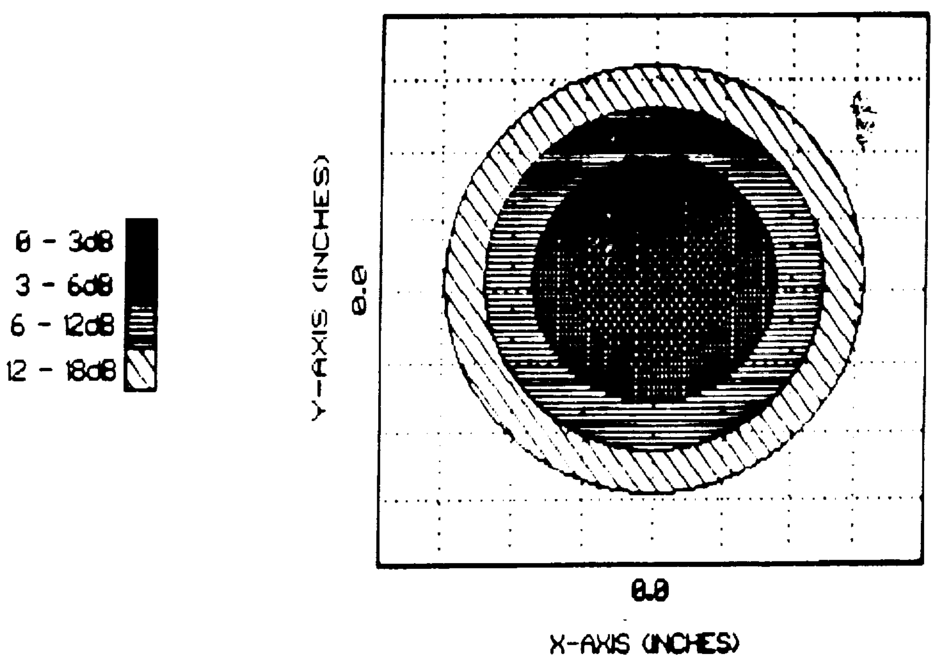

Sound Beam Profile

Fig. 4

Channel Number Is 1

F1 Select Channel
) F2 Create DAC Curve
F3 Display DAC Curve
F4 Save DAC Parameters
F5 Recall DAC Parameters
F6 Select DAC Options
F7 EXIT

Create DAC Curve

Cursor Controls:

→ Move gate right
← Move gate left
↑ Increase gate length
↓ Decrease gate length
↵ Find peak in gate
End Draw DAC curve
Esc Discard DAC and exit

Position transducer at point

Gate Start (μsec): 50.40
Gate Length (μsec): 1.24

Next sequence number: 1

0.93 y: mv/div
1.00 x: μsec/div
44.00 μsec delay
Scan Coord: 1= .000 2= .000 3= .000

Rectify (-) Freeze (+)

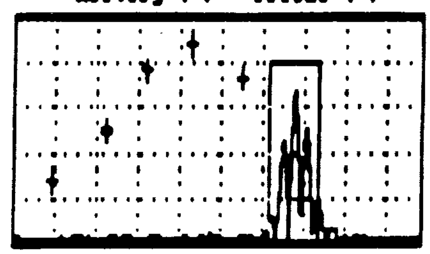

Channel number: 1 DAC Parameter File: test.DAC

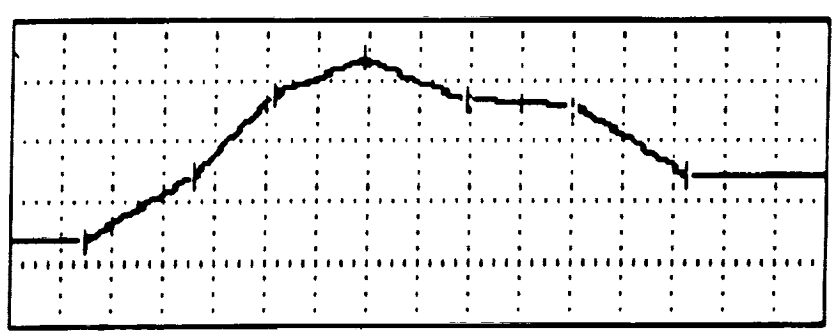

System Parameters

Sample rate (MHz):	25.0
Pulser Atten. (dB):	0
Receiver Gain (dB):	7
Delay (μsec):	44.0
Length (μsec):	10.2
Length (pts):	256

No. of DAC points: 7

Point	[illegible] (μs)	[illegible] (%)
1	44.96	27
2	46.32	48
3	47.32	75
4	48.44	87
5	49.76	73

(More)

PgDn - Next Page ESC - Exit

ORIGINAL PAGE IS
OF POOR QUALITY

TestPro™ DAP ENHANCEMENT (cont'd)...

CLUSTERING (CLS) MODULE

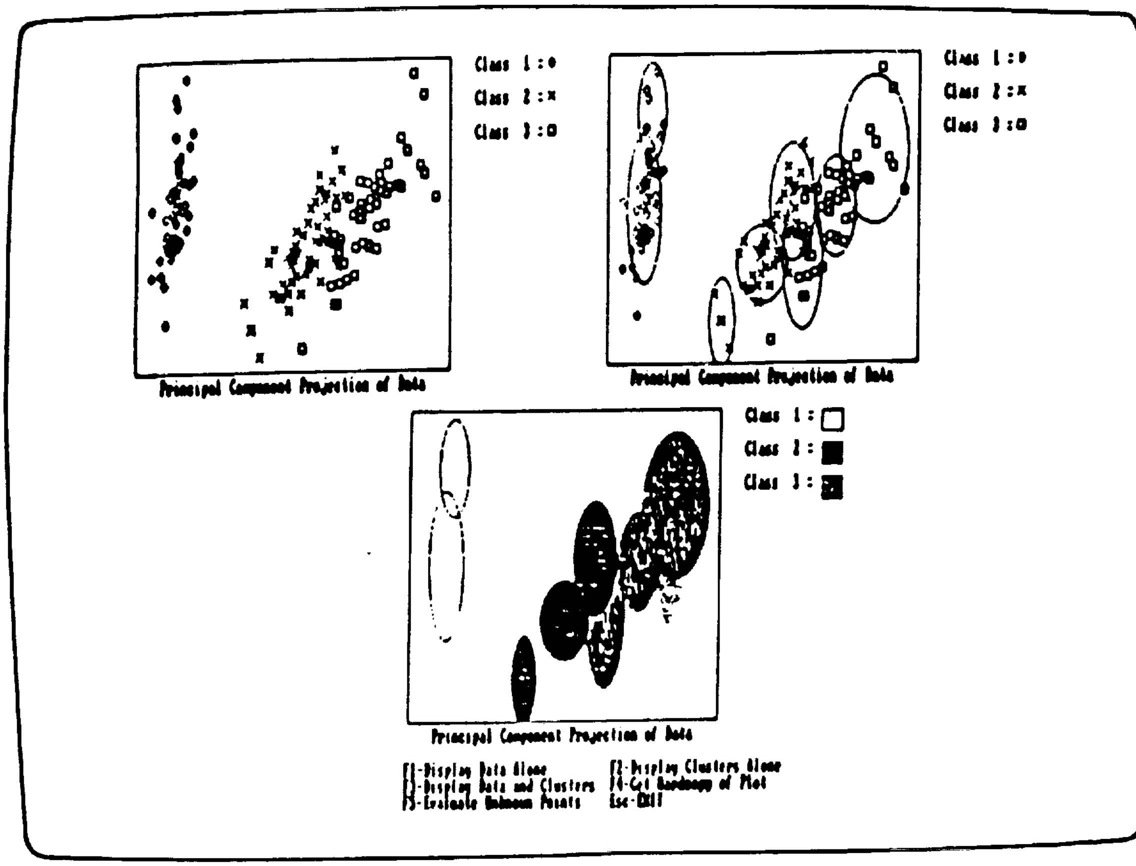

Infometrics

3 - D PLOTTING

WAVEFORM PLOT

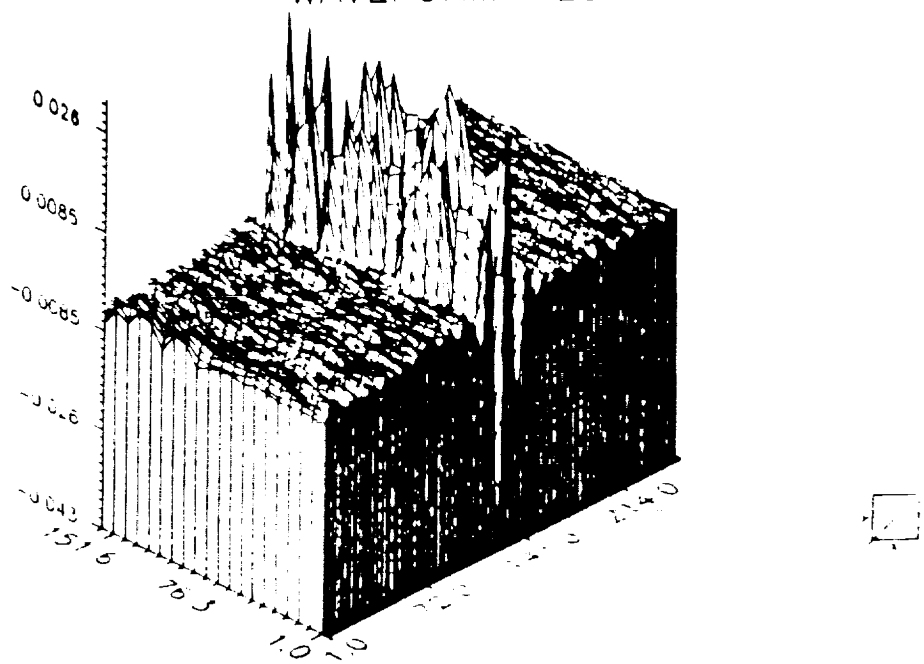

WAVEFORM FEATURE MAP

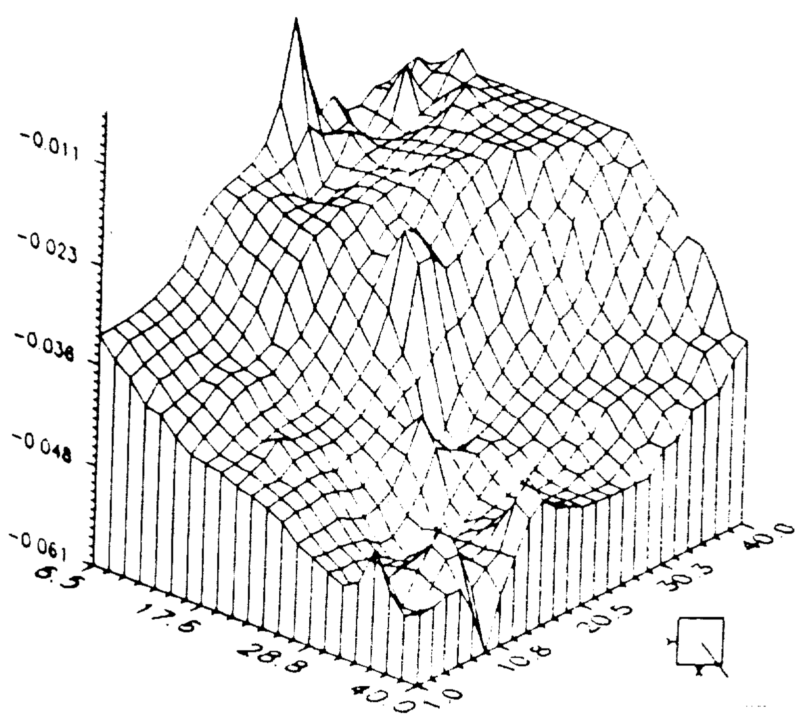

ORIGINAL PAGE IS
OF POOR QUALITY

SIGNAL PROCESSING / FILTERING

Input File: \testpro\WAVUNC.KB1
Output File:

SIGNAL PARAMETERS

Seq. No.: 1
Samp. Rate: 20.00
Gt Strt (pts): 1
Gt Strt (µsec): 66.20
Gt Lng (pts): 256
Gt Lng (µsec): 12.75

ANALYSIS PARAMETERS

Minimum FFT Length: 128
Beg Freq (MHz): .0
End Freq (MHz): 10.0
Log Spectrum: NO
Taper Type: COSINE
Window Type: RECTANGULAR
Filter Type: BAND PASS
Cutoff Freqs: 1.8, 3.0

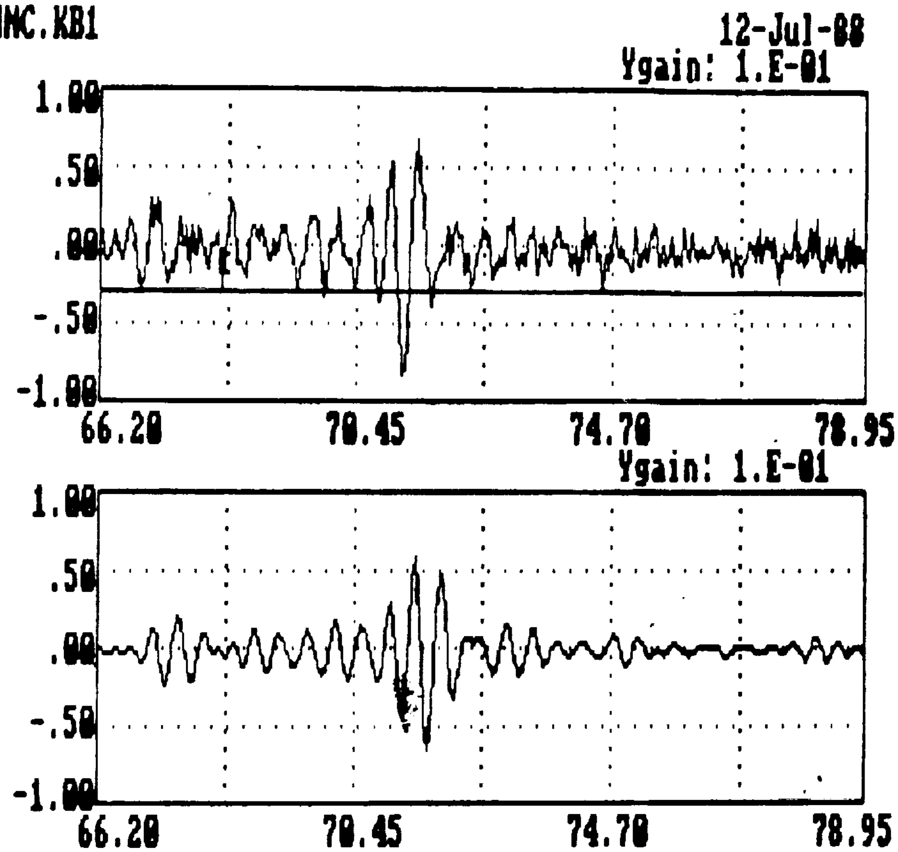

Automated Flaw Classification

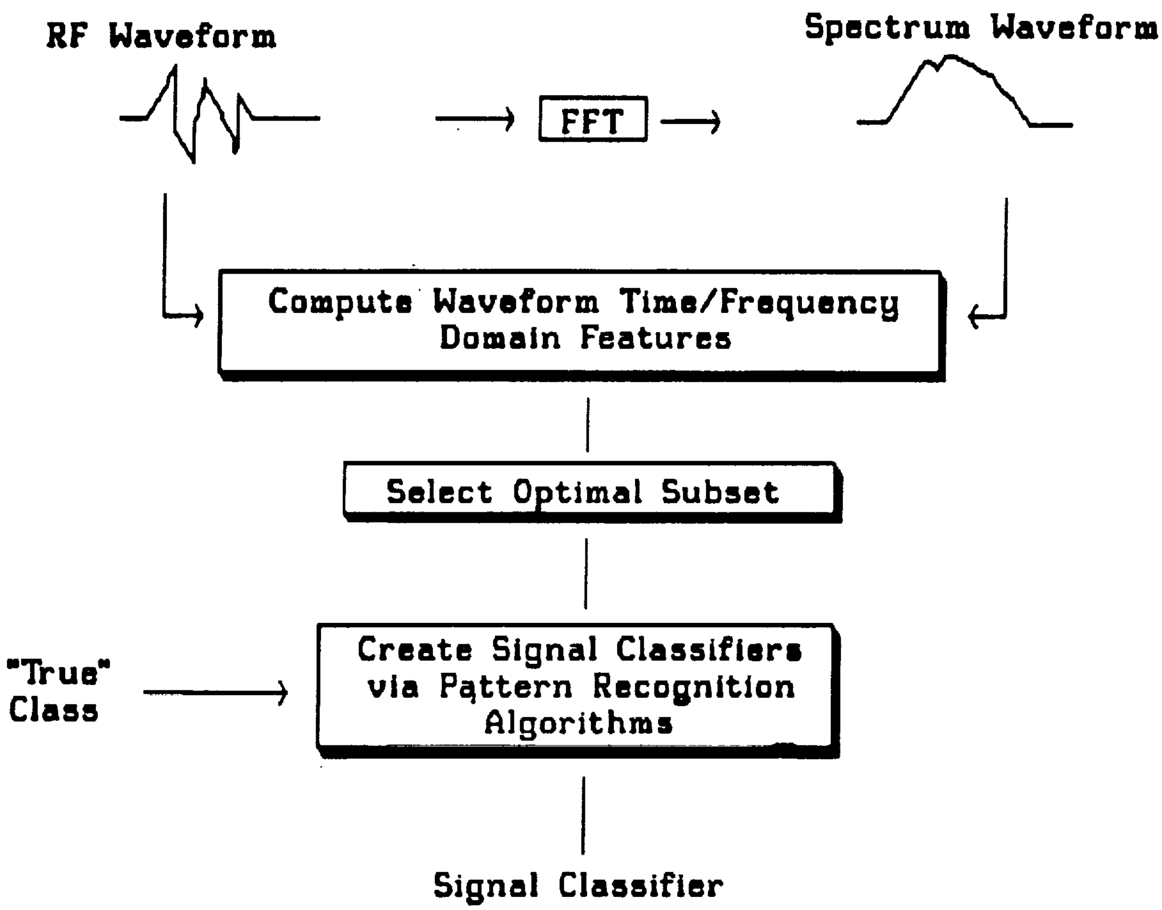

TestPro™ FCE ENHANCEMENT (cont'd)...

ANALYSIS (ANL) MODULE

Number of Classes 3
Optimum Number of Features 4
Waveform ID CAI002
True Class 1

CLASS 1:CRACKS
CLASS 2:COUNTERBORES
CLASS 3:ROOTS

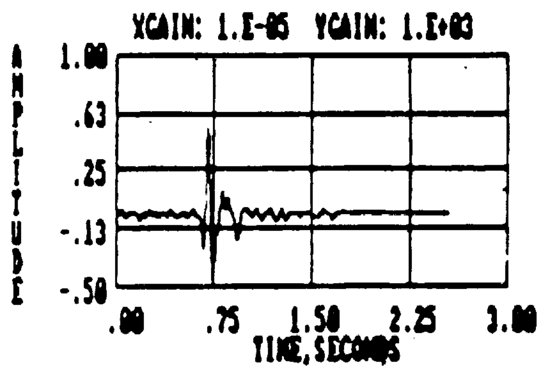

Class Probabilities (%)

CLASSIFIER	CLASS 1	CLASS 2	CLASS 3
SINGLE GAUSS	98.0	1.0	.0
FISHER DISC.	91.0	7.0	1.0
5 PT. NEAR NEIG.	80.0	20.0	.0
7 PT. NEAR NEIG.	85.0	14.0	.0
11 PT. NEAR NEIG.	88.0	11.0	.0

Infometrics

ORIGINAL PAGE IS
OF POOR QUALITY

EXAMPLE OF TWO DIMENSIONAL DISPLAY OF DEFECTS USING TESTPRO

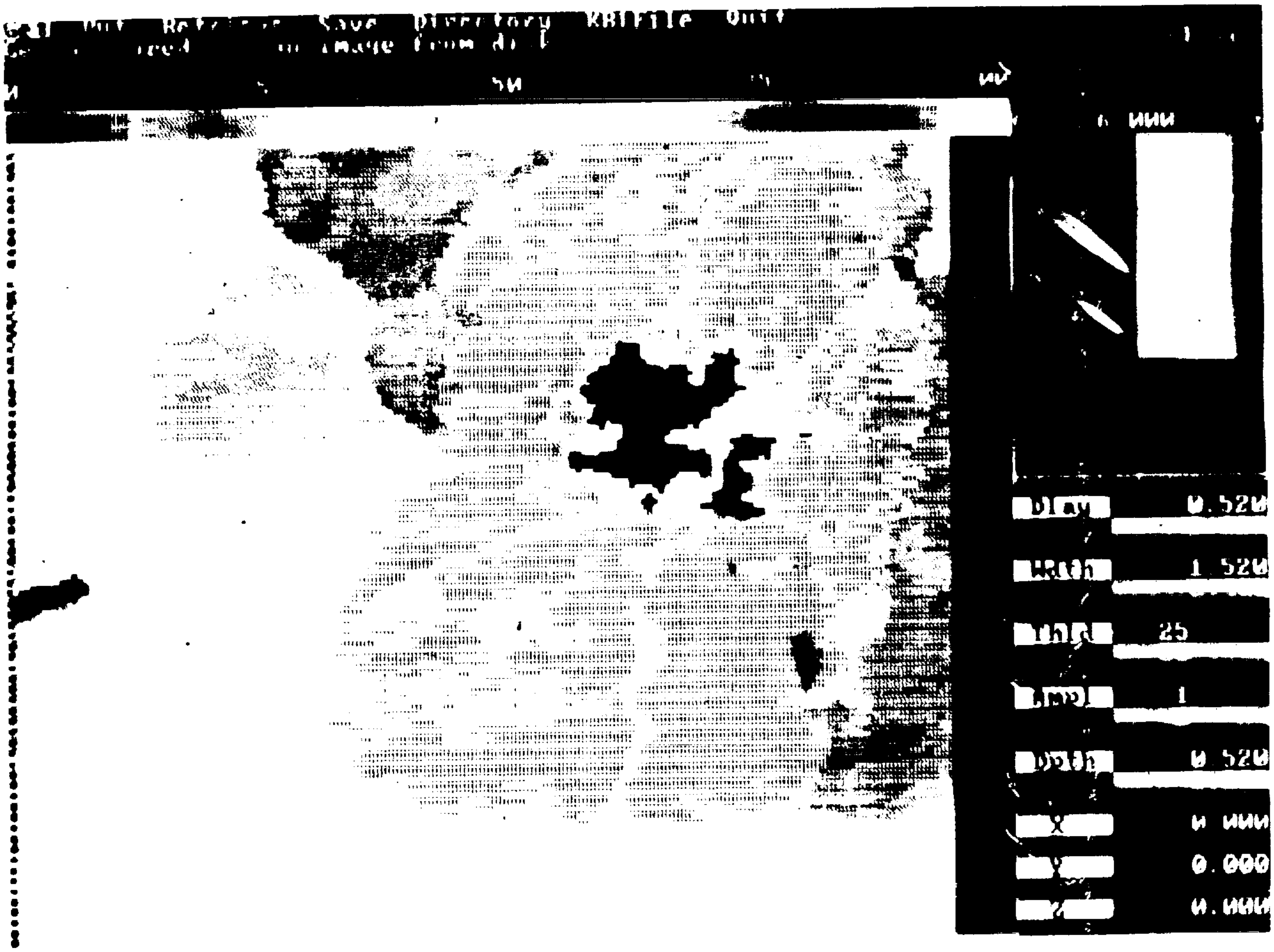

EXAMPLE OF TWO DIMENSIONAL DISPLAY OF DEFECTS USING TESTPRO

C - SCAN.....3 -D VIEWS

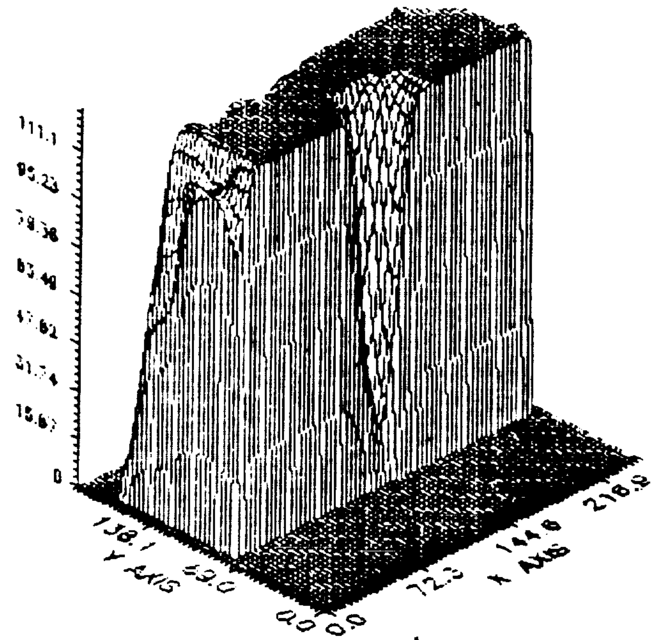

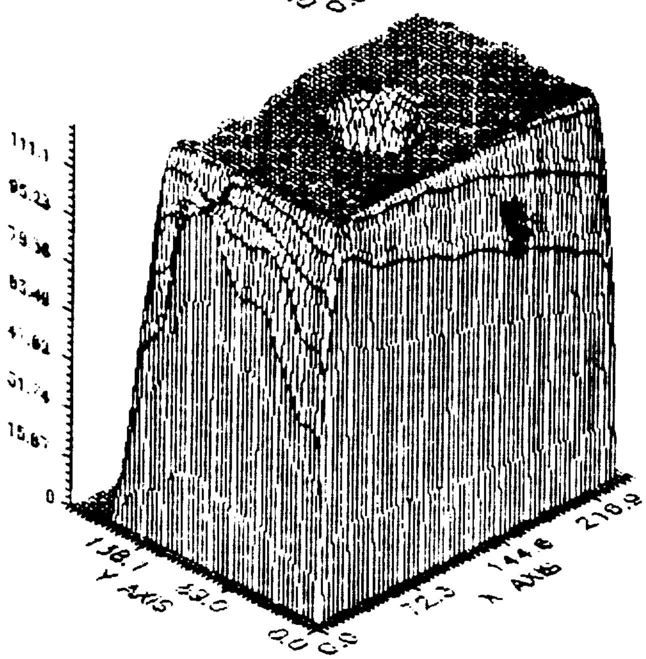

ORIGINAL PAGE IS
OF POOR QUALITY

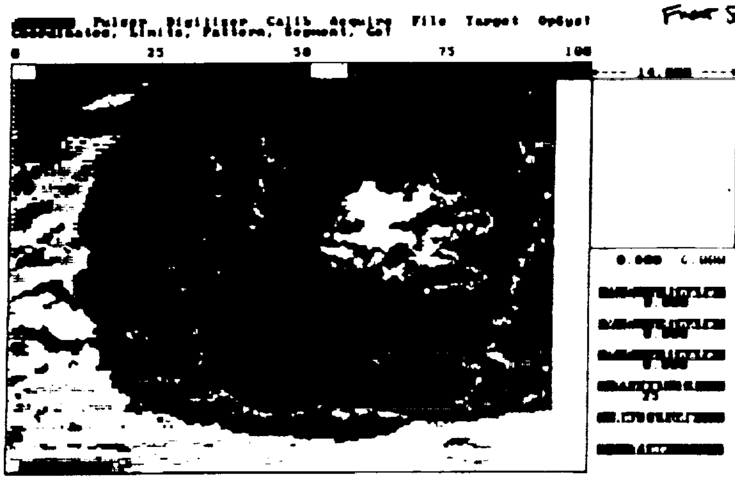

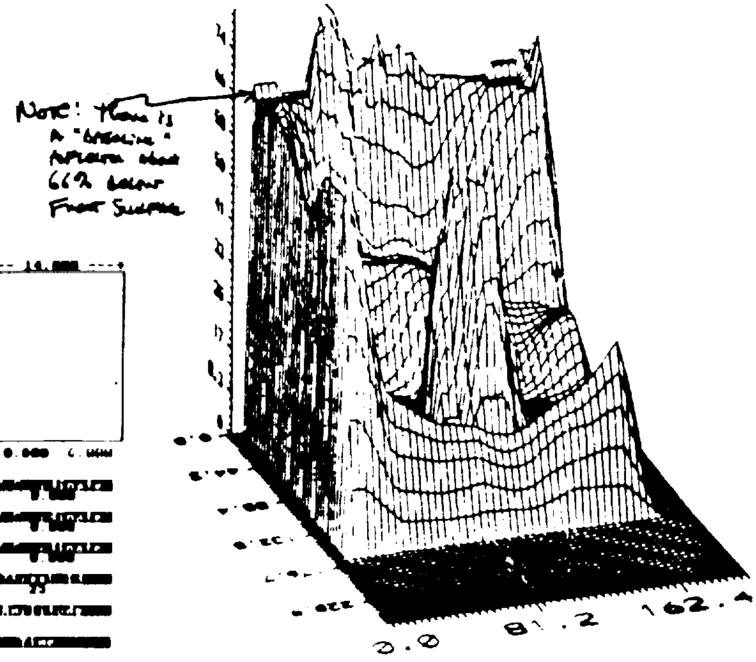

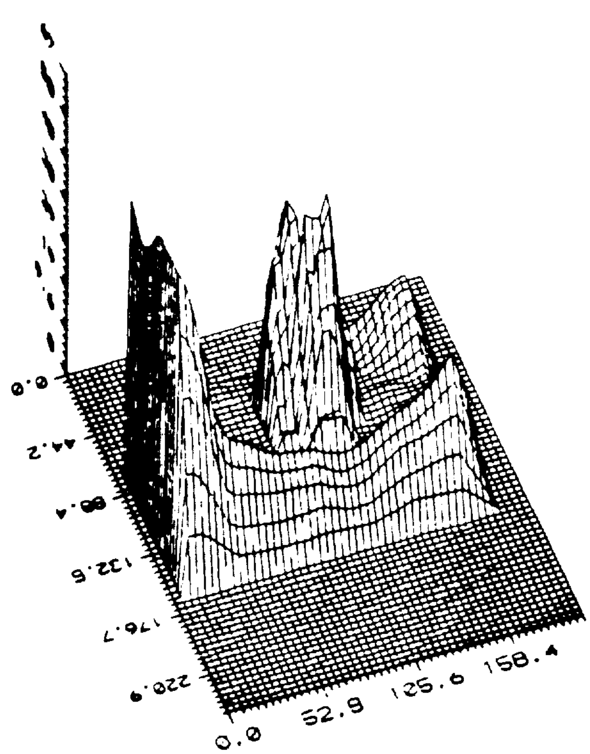

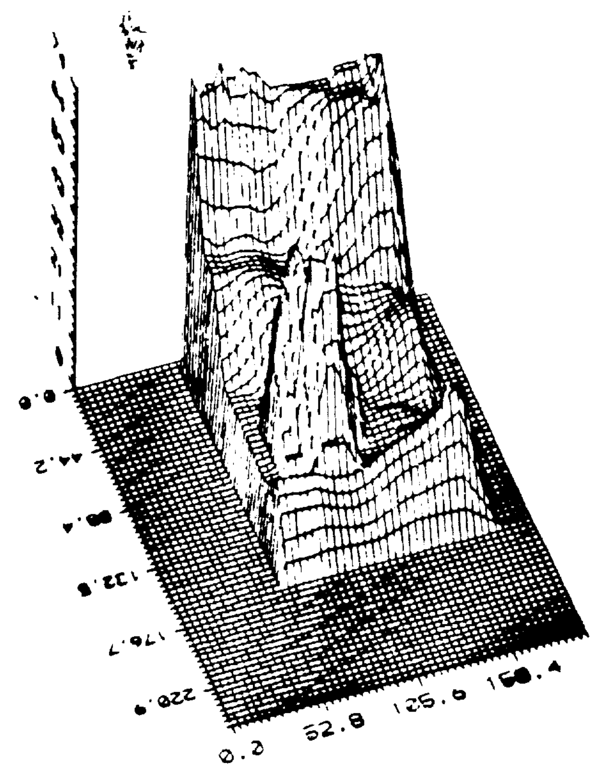

ORIGINAL PAGE IS OF POOR QUALITY

Composite-Impact Damage - Amp.

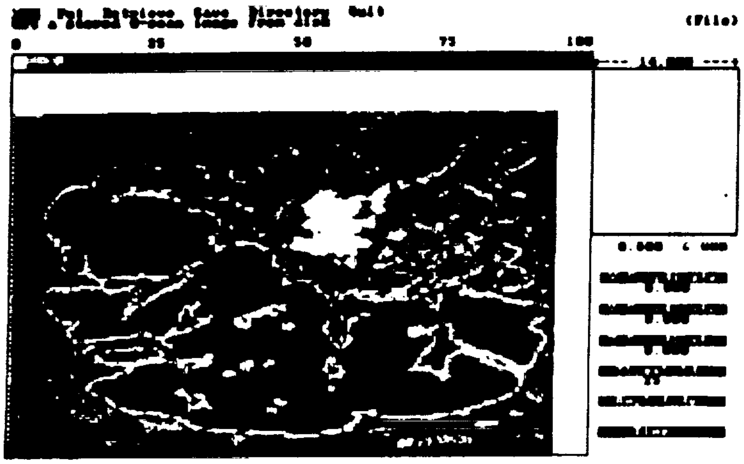

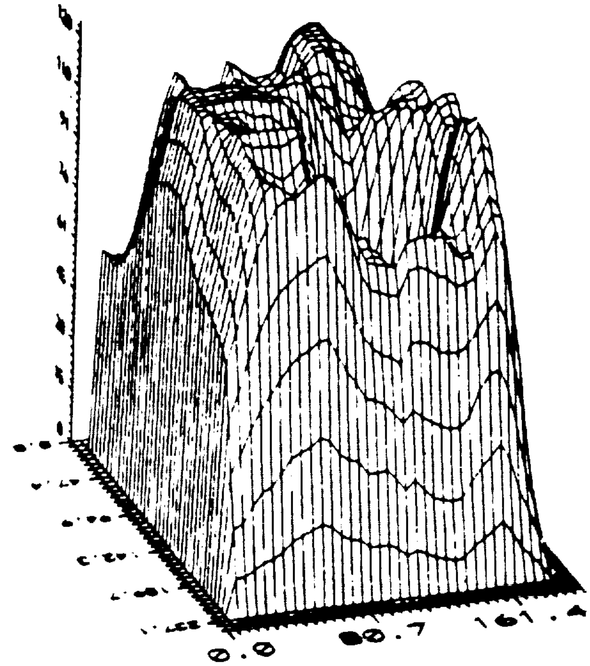

Composite-Impact Damage - Reduced Amp.

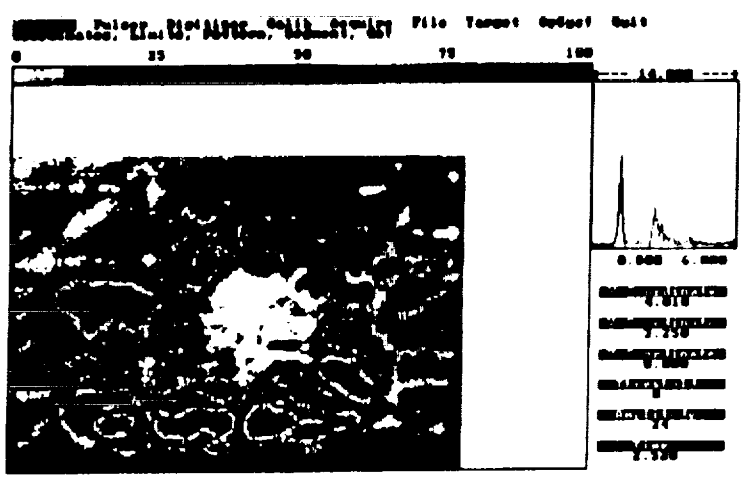

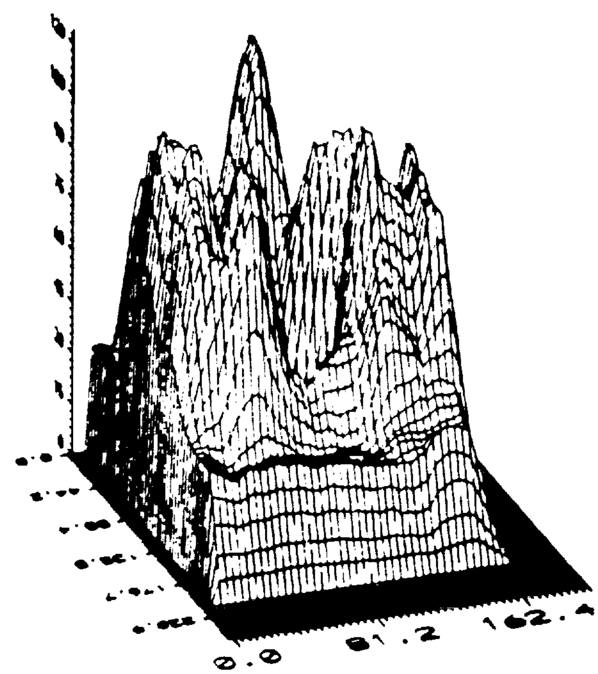

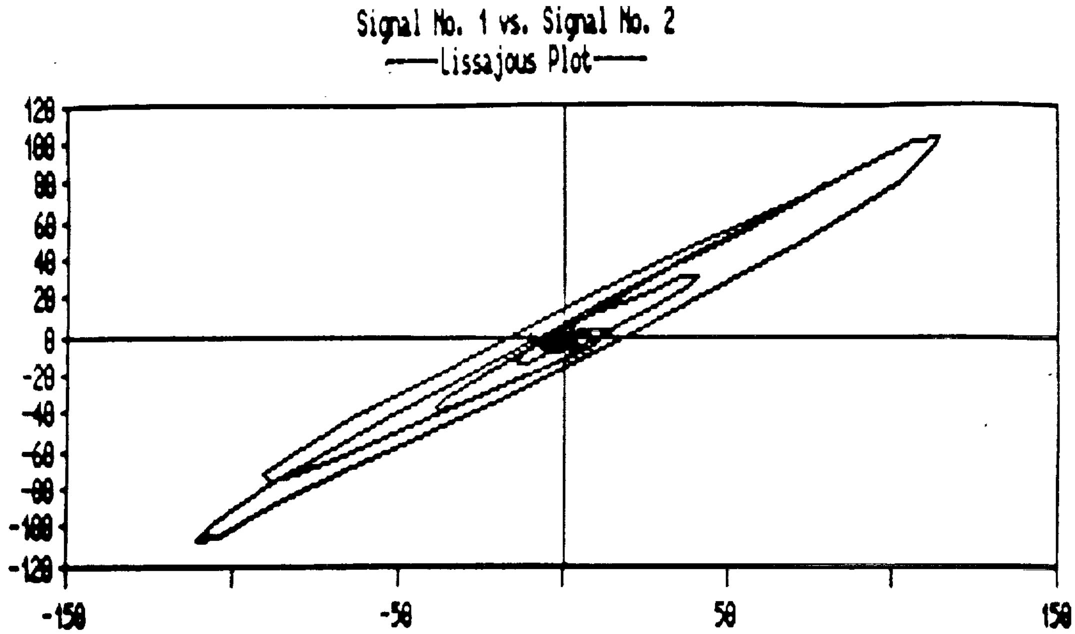

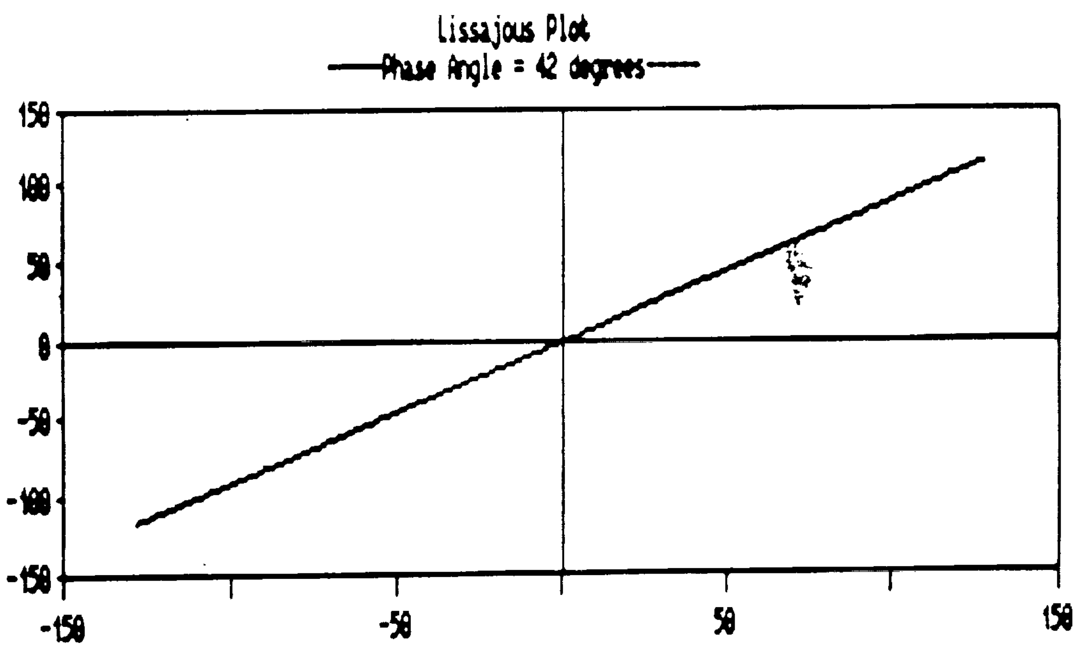

ORIGINAL PAGE IS
OF POOR QUALITY

SUMMARY

- PC-Based Signal Processing is Revolutionizing UT Inspection

- NDE Data are Pieces of Information -- PCs are Information Management Systems

- Changes can be made Relatively Easily because these Instruments are Software-Based

- Main Benefits to User include.....
  - -- Better QC of Field Inspections
  - -- Elimination of 3rd Party Re-Inspections
  - -- Minimize Reliance on Field Personnel as Signal Interpreters

- These Systems Represent the Next Generation of NDE Instruments

N91-18197

ULTRASONIC CORRELATOR VERSUS SIGNAL AVERAGER AS A SIGNAL TO NOISE ENHANCEMENT INSTRUMENT

Doron Kishoni
Senior Research Scientist
Department of Physics, The College of William and Mary
NASA Langley Research Center
Mail Stop 231, Hampton, VA 23662

Benjamin E. Pietsch
Electronics Engineer
Industrial Quality Inc.
19634 Club House Rd., Suite 320
Gaithersburg, MD 20879

ABSTRACT

Ultrasonic inspection of thick and attenuating materials is hampered by the reduced amplitudes of the propagated waves to a degree that the noise is too high to enable meaningful interpretation of the data. In order to overcome the low Signal to Noise (S/N) ratio, a correlation technique has been developed. In this method, a continuous pseudo-random pattern generated digitally is transmitted and detected by piezoelectric transducers. A correlation is performed in the instrument between the received signal and a variable delayed image of the transmitted one. The result is shown to be proportional to the impulse response of the investigated material, analogous to a signal received from a pulsed system, with an improved S/N ratio. The degree of S/N enhancement depends on the sweep rate. This paper describes the correlator, and compares it to the method of enhancing S/N ratio by averaging the signals. The similarities and differences between the two are highlighted and the potential advantage of the correlator system is explained.

INTRODUCTION

Ultrasonic inspection of materials involves generation of elastic waves using a transducer. These waves are transmitted through the media, detected by a receiver and analyzed. In order to retain meaningful interpretation of the data, a sufficient Signal to Noise (S/N) ratio must be obtained. This poses a problem whenever thick and attenuating material is involved. Using high-gain amplifiers to amplify the highly attenuated waves introduces more noise to the system, and events of interest in the signals are often too small to detect. One method of enhancing the S/N ratio is by averaging several of the received signals, using a digitizer that has this capability. The source impulse signals are repeated several times, and the detected signals are digitized and averaged. The temporal resolution of the events in the received signal depends on the impulse width. The pulse maximum repetition rate is limited by the depth of the investigated area. The pulse source should not be repeated until ultrasonic waves of the previous pulse have significantly dissipated. Another limitation is that the pulse amplitude cannot exceed the breakdown voltage of the transducer. These limit the maximum input energy and determine the limit of the signal to noise enhancement by averaging. The following discussion which describes a correlator, is based on a different principle, and can overcome some of the limitations of the averaged pulse system.

THE CORRELATOR

Principle:

A block diagram of the correlator is shown in Figure 1. A pseudo-random digital pattern is repeatedly generated and used to drive a transmitting transducer after proper amplification. The ultrasonic waves which propagate through the inspected material are detected by a receiver transducer. A correlation is performed between the received signal and a reference signal generated by the second pattern generator which is identical in shape to the drive signal, but delayed by a linearly varying amount, governed by the sweep rate. The use of a digitally delayed reference has the advantage of greater accuracy and stability than complicated analog delay lines [ref. 1 for example].

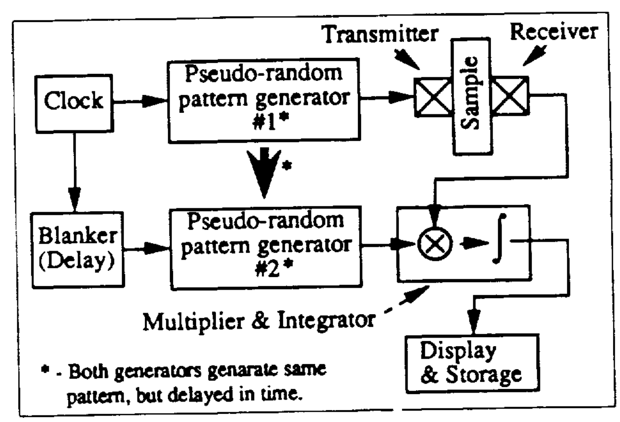

Figure 1. Correlator, schematics.

Theory:

An output $y(t)$ from a linear system can be expressed as the convolution of the system impulse response $h(t)$ with the input $x(t)$ (Figure 2):

$$y(t) = h(t) * x(t) = \int_{-\infty}^{\infty} h(\upsilon)\, x(t-\upsilon)\, d\upsilon \qquad (1)$$

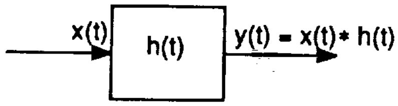

Figure 2. The output as a convolution of the input and the impulse response.

The cross correlation R_{xy} of $x(t)$ and $y(t)$ can be written as:

$$R_{xy}(\tau) = \lim_{T\to\infty} \frac{1}{T}\int_{-T}^{T} x(t)\,y(t+\tau)\,dt \qquad (2)$$

and auto-correlation $R_{xx}(\tau-\upsilon)$ of $x(t)$ as:

$$R_{xx}(\tau-\upsilon) = \lim_{T\to\infty} \frac{1}{T}\int_{-T}^{T} x(t)\,x[t+(\tau-\upsilon)]\,dt \qquad (3)$$

Substituting (1) and (3) into (2) we get:

$$R_{xy}(\tau) = \int_{-\infty}^{\infty} h(\upsilon)\,R_{xx}(\tau-\upsilon)\,d\upsilon \qquad (4)$$

therefore, the cross-correlation of the input and the output is the convolution of the impulse response with the auto-correlation of the input signal:

$$R_{xy} = h * R_{xx} \qquad (5)$$

R_{xx} for white noise is the delta-function, (up to a factor k), therefore,

$$R_{xy}(\tau) = k\,h(\tau) \qquad (6)$$

so that if white noise is injected to the material, the correlation of the input with the detected output $y(t)$ is the impulse response $h(t)$ of the system (Figure 3).

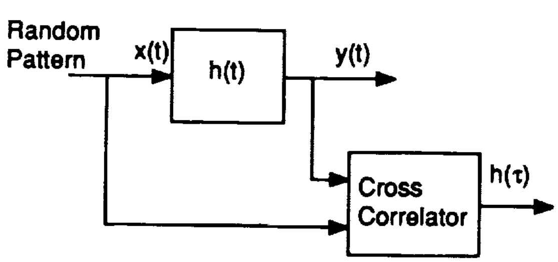

Figure 3. Correlation of random sequenced input with the output yields the impulse response.

In a single-channeled configuration, as applied in the current correlator system, τ is slowly varied according to the sweep rate ($S.R.$), thus, the resultant correlation represents the impulse response transformed to a frequency which is reduced by the inverse of the sweep rate.

The Signal to Noise Ratio Enhancement ($SNRE$) of a system can be defined as:

$$SNRE = \frac{SNR_{output}}{SNR_{input}} \qquad (7)$$

where SNR is the Signal to Noise Ratio. This can be expressed in terms of bandwidth B of the appropriate signals [2-4], where the $SNRE_{power}$ is given by:

$$SNRE_{power} \approx \frac{B_{input}}{B_{output}} \qquad (8)$$

while the $SNRE_{voltage}$ is given by:

$$SNRE_{voltage} \approx \sqrt{\frac{B_{input}}{B_{output}}} \qquad (8a)$$

Both definitions are equivalent in terms of decibels, since the factor is 20 for voltage as opposed to a factor of 10 for power. As the single-channeled correlation transforms the bandwidth to a frequency reduced by the inverse of the sweep rate $S.R.$, the last equation can be written as:

$$SNRE_{voltage} \approx \sqrt{\frac{1}{S.R.}} \qquad (9)$$

which is fixed for any particular sweep rate. A typical value used for sweep rate is 0.1 µsec/sec. The sweep rate is inversely proportional to the acquisition time T_{aq}.

As a comparison, the averaging process for a pulse-system improves the signal to noise ratio by:

$$SNRE_{voltage} \approx \sqrt{n} \qquad (10)$$

where n is number of averages. Again, the acquisition time is linearly proportional to n, thus,

$$SNRE_{voltage} \approx \sqrt{T_{aq}} \qquad (11)$$

Power efficiency comparison:

In a pulse-system with repetition rate of f pulses per second, the total power P into the material can be approximated as:

$$P_p = V_p^2\,t_p\,f_p \qquad (12)$$

where V is the peak voltage of the pulse, and t is its effective duration. (The index p denotes the pulse-system). Typical values are ~300 volts and ~100 nsec duration respectively.

The repetition rate f is limited by the acoustic response in the material. The repetition rate must be low enough to avoid wrap-around of the reflections (Figure 4). The maximum obtained information τ is then not more than the time between the pulses,

$1/f$. The total energy input throughout n averages, w_p, per unit of obtained information, τ_p, can be expressed as:

$$\frac{w_p}{\tau_p} = P_p \frac{T_p}{\tau_p} \geq V_p^2 \, t_p f_p \, n \qquad (13)$$

where T_p is the total acquisition time (of n averages), and P_p is the input power during this time.

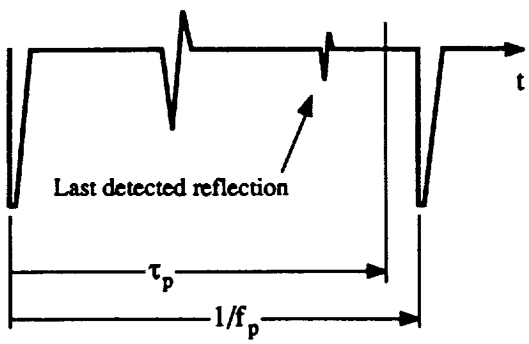

Figure 4. One repetition in a pulse-system that has a repetition rate of f pulses per second, and some possible echoes.

For the correlator system, the input power P is:

$$P_c = \frac{1}{2} V_c^2 \qquad (14)$$

where V is the voltage of the amplified digital random signal, which is on half of the time, on average. (The index c denotes the pulse-system). The acquisition time T is directly related to the duration of the obtained information τ through the sweep rate $S.R.$:

$$\frac{T_c}{\tau_c} = \frac{1}{k\,[S.R.]} \qquad (15)$$

where k is the number of parallel channels that perform the correlation in the correlator. The total energy input, w, per unit of obtained information, τ, would be:

$$\frac{w_c}{\tau_c} = \frac{1}{2} V_c^2 \frac{1}{k\,[S.R.]} \qquad (16)$$

For comparison purposes, if we limit the input power in the correlator system so that both systems input equivalent amounts of power, the ratio of the voltages would have to be:

$$\frac{V_c}{V_p} = \sqrt{2\,t_p f_p} \qquad (17)$$

In such a case, the ratio between the quantities 'total input energy -w, per unit of obtained information -τ' of the two systems would be:

$$\frac{w_p/\tau_p}{w_c/\tau_c} \geq \frac{n}{\left(\frac{1}{k\,[S.R.]}\right)} \qquad (18)$$

which is similar to the ratio between the *SNRE*'s (in term of power) of the systems for a single channel correlator.

EXPERIMENTS

An 11.5 cm thick wood was used as an example of thick highly attenuating material. Two 2.25 MHz half inch transducer were used in a pulse-echo configuration. A single pulse, with the pulse-system configured for maximum safe voltage into the transmitter, resulted in a signal to noise in the received signal which was less than 1, as can be seen in Figure 5.

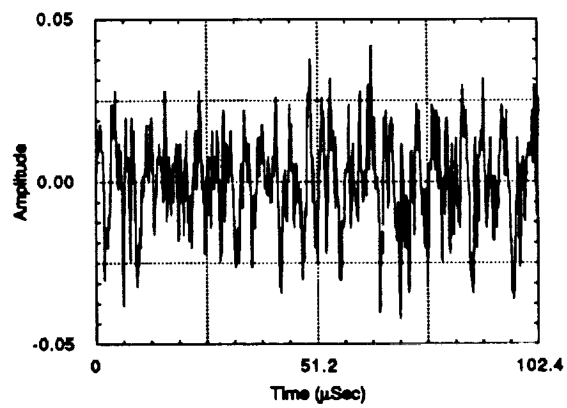

Figure 5. Wood, Single trace obtained with the pulse-system.

Therefore, averaging was required with the pulse-system to be able to detect the signal. A signal obtained after 4096 averages is shown in Figure 6. The excitation is seen on the left side (at relative time 0), and the first arrival through the wood occurs around 57 µsec. Significant noise still exists even in the 4096 averages case, as evident in the time interval 0 to ~57 µsec, before arrival of the first acoustic response of the wood.

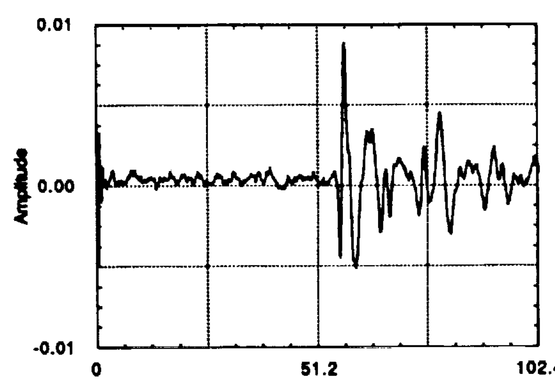

Figure 6. Wood, using the pulse-system, with 4096 averages.

The received signal from a single channel correlator for a sweep rate of 0.1 μsec/sec is shown in Figure 7. The acquisition time was approximately equal to the time required for 4096 averages (hardware dependent of course), although it could be skipped until the expected first acoustic response, thus reduced significantly. The first arrival could be identified again, at ~57 μsec, with a lower noise before first arrival than the noise in the 4096 averages case. (To decrease the noise to the same level, the averaging system required close to 32000 averages). Furthermore, this noise is above the detection frequency of the transducer, thus, further low-pass filtering is possible without deleting actual information.

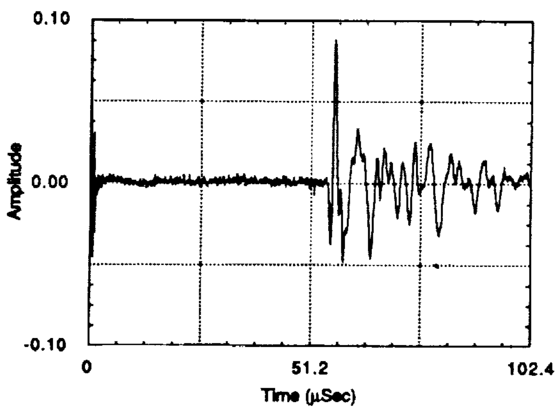

Figure 7. Wood, output from the correlator.

Figure 8 shows the measured signal to noise figures as function of the number of averages in the pulse-system (on a log scale). The noise-level measurements were taken at a region before the expected first arrival, while the signal-level measurements were taken at the region of the first arrival of the acoustic response.

Superimposed on the graph of Figure 8 is the S/N measured from the results of the correlator. The vertical data line on the right represents a single-channel correlator. Increasing values of the input power increased the S/N values as expected. The horizontal coordinate of this data corresponds to an equivalent acquisition time as with the pulse system. A 1024 multiple channel correlator would shorten this time by this factor, thus, shifting this data line to the left, as shown in the left side of the figure.

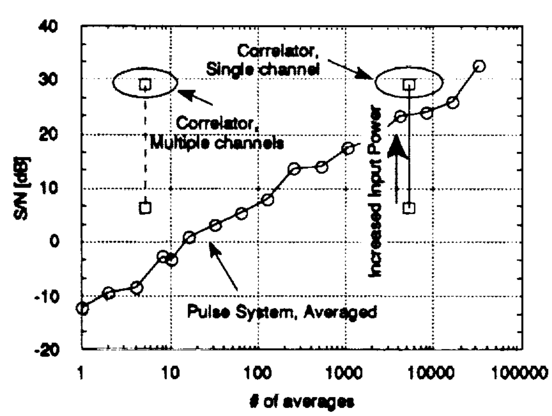

Figure 8. Wood, S/N curve.

A second set of tests were performed measuring ~10 cm thick Teflon. S/N results are shown in Figure 9. Since the attenuation of the material is less than that of the wood sample, the overall S/N figures were better. Yet, the relative behavior of the two systems remain the same. The effect of increasing the number of the channels from a single channel to 1024 channels in a multi-channel correlator is extrapolated in this figure.

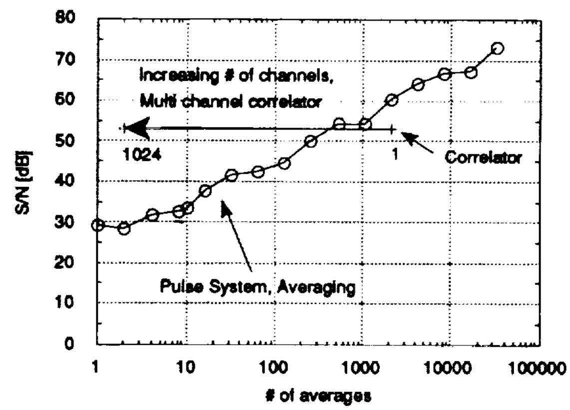

Figure 9. Teflon, S/N curve.

DISCUSSION

Both the correlator system and the averaging pulse-system can enhance the signal to noise ratio, improving it linearly with square root of the acquisition time. The correlator, through its sweep rate *S.R.*, and the averager through the number of averages *n*. The ratio of total input energy per unit of obtained information also have equivalent forms for the two systems.

There are however some important differences between them. While the voltage into the transducer in the pulse-system is limited by the breakdown voltage of the transducer, the correlator system is based on a continuous excitation of the transducer, where the limiting parameter is mainly the maximum power that can be dissipated. The total power can be much higher than in the pulse-system, thus, obtaining stronger signals.

Another major difference is the way the systems collect and enhance the data: A conventional pulse echo averaging system prescribes a fixed minimal time window, according to the thickness of the sample that control the maximum repetition rate. The S/N improves as acquisition time increases (as square root of it). The correlator system, on the other hand, gives prescribed S/N enhancement, according to the chosen sweep rate while the obtained time window increases with the acquisition time. The condition on the correlator corresponding to the maximum repetition rate is the length of the unique pattern in the pseudo-random signal. It should be the inverse of the repetition rate, a condition which is easily obtained.

Furthermore, if the investigated material calls for inspection at a localized suspected region, the correlator system can be configured to skip the early time trace, and start the process of the correlation only at the requested window of time, thus reducing the acquisition time significantly, at any prescribed S/N value. This could not be applied in a conventional pulse echo system, where the minimal time window is fixed.

SUMMARY

The system of choice depends on the relevant problem: The averaging pulse-system is appropriate when the required Signal to Noise Enhancement (*SNRE*) is low and when the full thickness of the material has to be inspected. In this case, fast measurement is possible, where the S/N improves as the averaging continues until adequate signal shows on the screen. The correlator system has the advantage when high *SNRE* is required, particularly when a specific region has to be inspected. The sweep rate will be chosen according to the required *SNRE* and the delay would be set up, and the enhanced trace would almost immediately be obtained. A multi–channel correlator would increase this advantage even more.

REFERENCES

[1] Furgason, E. S., Newhouse, V. L., Bilgutay, N. M. and Cooper, G. R. "Application Of Random Signal Correlation Techniques To Ultrasonic Flaw Detection," Ultrasonics, 13, 1975, pp. 11-17.

[2] Ziemer, R. E. and Tranter, W. H., Principle Of Communication - System Modulation And Noise, Houghton Mifflin Co., Boston, 1976.

[3] Lee, B. B. and Furgason, E. S., "An Evaluation Of Ultrasound NDE Correlation Flaw Detection Systems," IEEE Trans. Sonic Ultrason., vol. SU-29 (6), 1982, pp. 359-369.

[4] Lindgren, E., A., "The Use Of Ultrasonic Correlation Methods For The Investigation Of Phase Transitions In Polytetrafluoroethylene And The Precipitation Hardening Process In 2024 Aluminum Alloy," M.S. Thesis, JHU-CNDE-UCC-1, Johns Hopkins University, 1988.

[5] Kishoni, D., Rosen, M., Berger, H. and Cheng, Y. T., "Signal To Noise Enhancement By An Ultrasonic Cross-Correlator System," IEEE Ultrasonics Symposium, Chicago, Illinois, 1988.

Nondestructive Evaluation of Composite Space Structures

by

B. M. Lempriere
Boeing Aerospace and Electronics

presented to

NDE for Aerospace Requirements
University of Alabama in Huntsville
August 22-24, 1989

Performed under AFAI Contract F04611-88-C-0066
Monitor: Joe Sciabicca

NDE OF COMPOSITE SPACE STRUCTURES

OBJECTIVES:

Identify promising NDI technologies

- In-space inspection of composites structures
- Technology challenges in design, manufacture, and use

Recommend cost-effective technology developments

SPACE SYSTEMS TO BE CONSIDERED

- **Space-Assembled Structures**
- **Deployed Structures**
- **Manned Systems**

NDE OF COMPOSITE SPACE STRUCTURES

APPROACH:

Review existing spacecraft missions and designs

Result:

- No common problems or requirements identified
- Spacecraft are large, complex
- Cannot be shut down, disassembled

Recommendation:

- 3-level monitoring system
- Technologies selected:
  - Acoustic Emission
  - Spectrophotometry
  - Eddy Current
  - Deflectometry
  - Actinometer

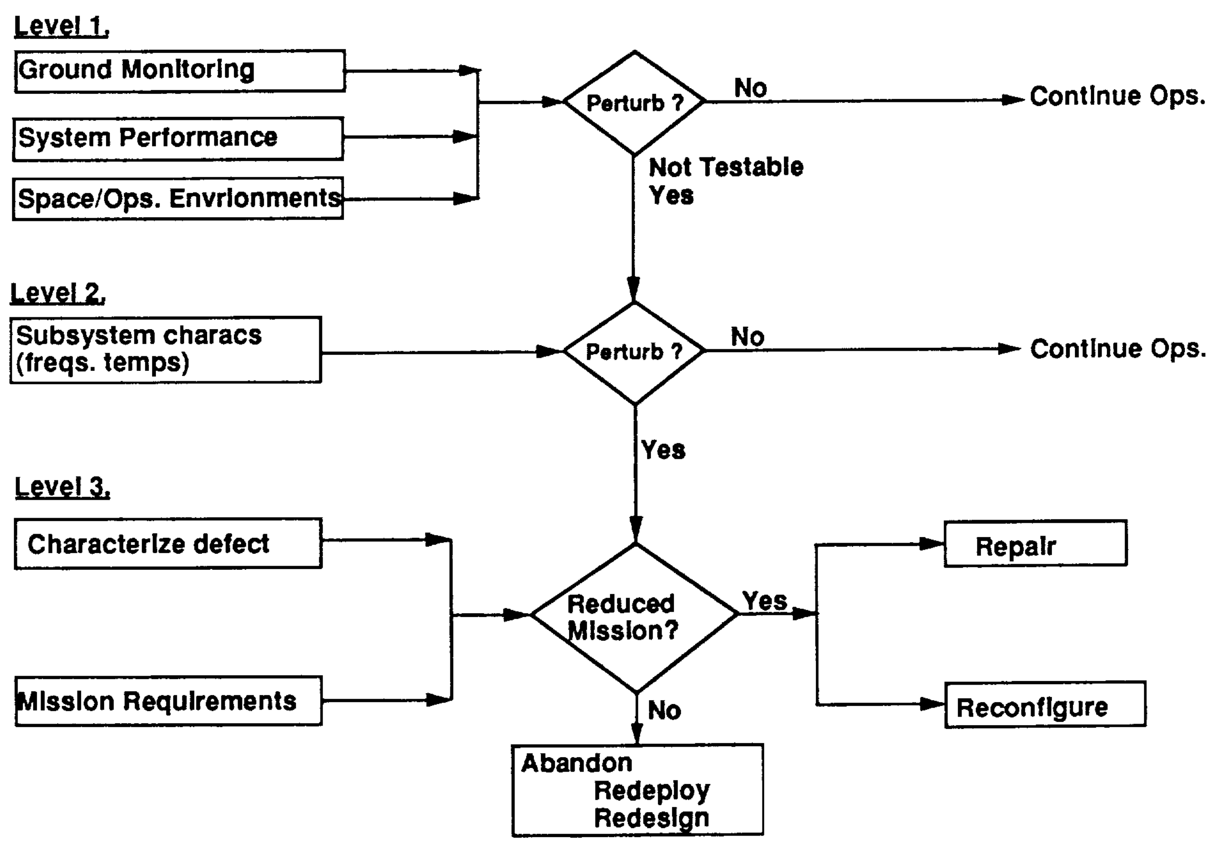

Figure 1. Monitoring Sequence

GEOMETRY MONITORING

Global:
- Interferometers (laser, microwave)
- Extensometers (optical, electrical)
- Goniometers (optical, electrical)

Local:
- Strain gages
- Ultrasonics
- Eddy current
- X-rays/backscatter

DYNAMICS MONITORING

Natural or localized excitation

- o Mode shape, frequency, amplitude
  - Accelerometers
  - Strain gages
  - AE sensors
  - Interferometers

SUBSYTEM LEVEL OF MONITORING

- **Subsystem:**

  Thermal coatings
  Support structure
  Mirror structure
  Pressure vessels
  Smart structure

- **Parameters:**

  Dimensional Precision
  Stiffness
  Strength
  Thermal Control
  Leakage (presure vessels)

CRITICAL COMPONENT LEVEL OF MONITORING

- Critical Components:
  - Truss members
  - Joints
  - Beams and structural support
  - Adhesives

- Parameters:
  - Cracks and Delaminations
  - Stiffness
  - Strain
  - Stress
  - Coating degradation
  - Coefficient of Thermal Expansion (CTE)
  - Surface Damage

NDE of Composite Space Structures

DAMAGE MONITORING

Cracks:

- o UT, CT, EC, resistance wires

Deformation

- o Lasers, UT, etc

Impacts
- o Visual, UT, EC, etc

Residual stress
- o Strain gages

Repairs/maintenance, before and after
- o X-rays, ultrasonics, eddycurrents

Externally-induced damage (hostility, impact, AO)
- o Visual
- o Inference from frequency, stiffness, temperature
- o Thickness measurement

Thermal Coatings
- o Thermometry, spectrometry

Internally-induced damage (fatigue, creep)
- o Inference from frequency, stiffness, temperature

SPACE ENVIRONMENT MONITORING

- Debris/meteorites
  - AE sensors
  - Piezofilm sensors
- Atomic oxygen (AO)
  - Silver actinometer
  - Tapered-element oscillating microbalance
- Solar radiation
  - Protons/electrons: Charge devices (Faraday cup, electrometer)
  - Ultraviolet: Spectrophotometer
  - Gammas/x-rays: Dosimeters
  - Flares: Optical, photocells
  - Trapped particles (Van Allen)
- Cosmic Rays (galactic/solar)
  - Emulsions

OPERATIONAL ENVIRONMENTS

Manoeuvers, internal conditioning

- o Accelerometers
- o Strain gages
- o Temperature/pressure/humidity gages
- o Outgassing/effluents
- o System radiation (power source, output beam)

Table I. LOCAL DAMAGE/DEGRADATIONS WITH PRIORITIES

Damage Type (Alphabetical)			Rank	Priority By Rank	
1	Absorp/Emiss	(AB)	2	1	Aging
2	Aging	(AG)	1	2	Absorp/Emiss
3	Bacteria/Fungi	(BF)	9	3	Contamination
4	Cracks, Delams	(CD)	4	4	Cracks, Delams
5	Contamination	(CO)	3	5	Fatigue
6	Crushing	(CR)	7	6	Major Damage
7	Distortion	(D)	8	7	Crushing
8	Electric Currents	(E)	11	8	Distortion
9	Fatigue	(F)	5	9	Bacteria/Fungi
10	Major Damage	(MD)	6	10	Thinning
11	Residl Stress	(RS)	12	11	Electric Currents
12	Thinning	(TH)	10	12	Residual Stress

Note: Low numbers mean high priority or difficulty

Table II. SIGNIFICANT ENVIRONMENTS AND THEIR IMPORTANCE

	Environment (Alphabetical)		Rank	Priority by Rank	
1	Atomic Oxygen	(AO)	7	1	Maintenance and Repair
2	Hostility	(H)	4	2	Maneuvering
3	Internal Environment	(IE)	8	3	Space Assembly
4	Magnetic Fields	(MF)	11	4	Hostility
5	Maint/Repair	(MR)	1	5	Outgassing/Effluents
6	Maneuvering/Reboost	(MV)	2	6	Space Debris/Meteorites
7	Micro/Artif Gravity	(MG)	12	7	Atomic Oxygen
8	Outgassing/Effluents	(OE)	5	8	Internal Environment
9	Space Assembly	(SA)	3	9	System Energy
10	Sp Debris/Meteorites	(SD)	6	10	Solar Radiation
11	System Energy	(SE)	9	11	Magnetic Fields
12	Space Radiation	(SR)	10	12	Micro/Artif Gravity

NDE of Composite Space Structure

Factors in instrumentation

- Costs of development, installation, operation
- Weight, size, power
- Accompanying software
- Inspection coverage
- Impact of space environment
- Need for human intervention
- Reliability

Table VIII. FACTORS IN MONITORING TECHNIQUES

Alphabetical			By Rank	
General Instruments				
1	Accelerometer	1	Accelerometer	1
2	Aco Emission	3	Eddy Current	2
3	Bacteriology	12	Aco Emission	3
4	Break Wires	4	Break Wires	4
5	Compton Bksctr	16	Deflct/Goniom	5
6	Computed Tomo	17	Fiber Optics	6
7	Deflct/Goniom	5	Strain Gage	7
8	Eddy Current	2	Temperature	8
9	Fiber Optics	6	Visual	9
10	Laser/M'wve Intf	10	Laser/M'wve Intf	10
11	M'wave Refl	14	Spect/Refltry	11
12	Spect/Refltry	11	Bacteriology	12
13	Strain Gage	7	Ultrasonics	13
14	Temperature	8	M'wave Refl	14
15	Thermography	15	Thermography	15
16	Ultrasonics	13	Compton Bksctr	16
17	Visual	9	Computed Tomo	17
18	X-Radiography	18	X-Radiography	18
Specialized Instruments				
1	Actinometer	1	Actinometer	1
2	Calorimeter	3	Hygrometer	2
3	Charge Device	6	Calorimeter	3
4	Debris Flux	7	Dosimeter	4
5	Dosimeter	4	TEOM	5
6	Hygrometer	2	Charge Device	6
7	Gravitometer	8	Debris Flux	7
8	Magnetometer	9	Gravitometer	8
9	TEOM	5	Magnetometer	9

Conclusions

Recommended technologies

- Acoustic emission:
  - Cracking, crushing, fatigue, major damage
  - Hostility, maintenance/repair, maneuvering, outgassing/effluents, space assembly, debris/meteorites
- Spectrophotometry:
  - Absorptivity and emissivity
- Eddy current:
  - Aging, cracks, distortion, damage, thinning
  - Maintenance/repair, maneuvering, space assembly
- Deflectometry
- Actinometry
  - Atomic oxygen

Acousitc Emission

Develop sensors:

- Piezo film
- Integral amplifier, processor
- Packaging/mounting

Evaluate signatures:

- Defects
- Events
- Algorithms

Spectrophotometry

Requirements:

- Spectral resolution
- Angular resolution

Develop:

- Multi-band retractable light source
- Wide-angle retractable detector array
- Spectral analysis microprocessor

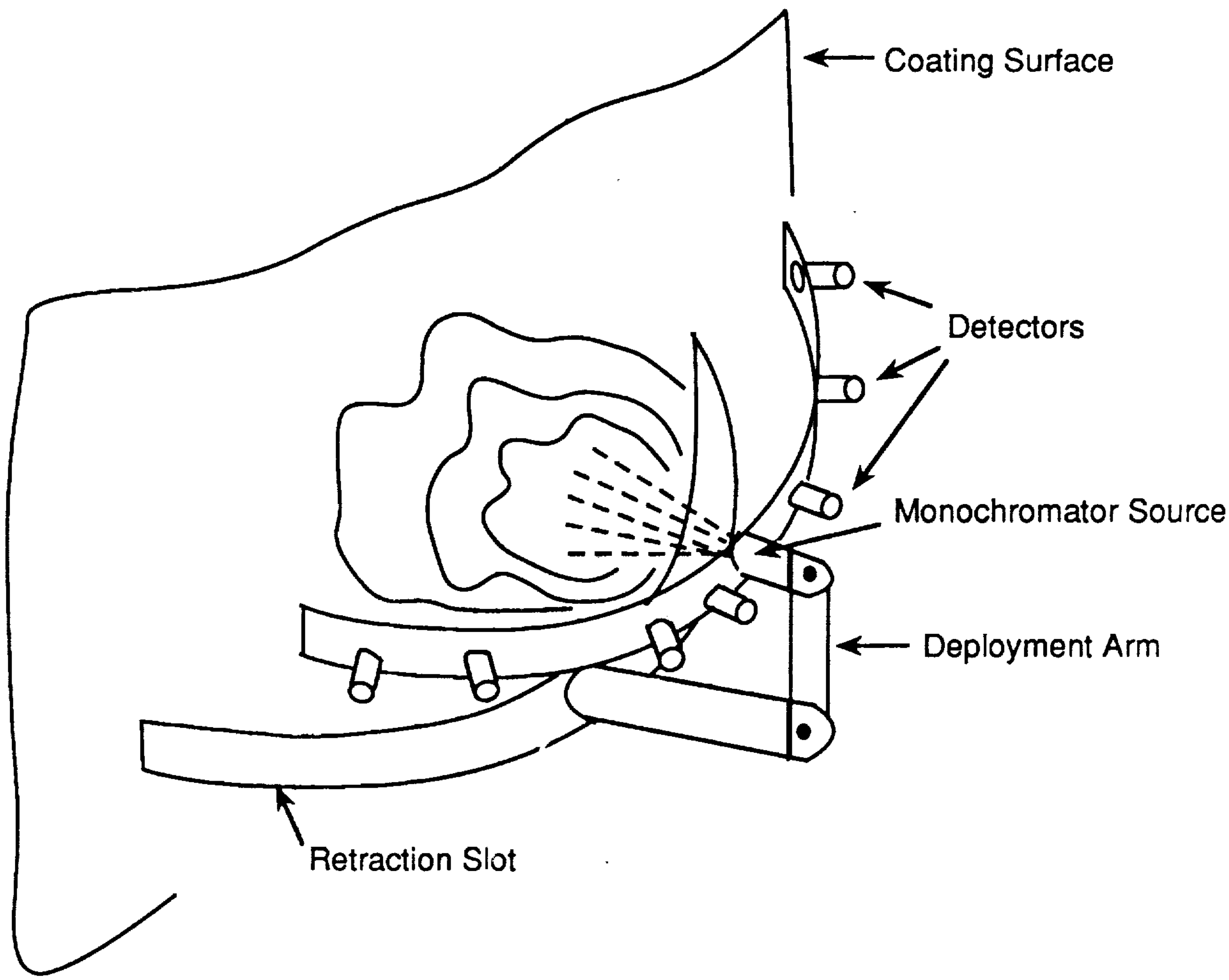

Figure 4. Deployable Spectrophotometer

Eddy Current

Develop:

- Multi-frequency tri-axial probes
- Excitation source, detector
- Correlation algorithms

Calibrate:

- Impedance vs. lift-off
- Impedance vs. conductivity

Deflectometry

Develop

- Mirror system with CCD detectors
- Encoders
- Differential transformers
- Capacitive sensors
- Fiber optic reflectometer

Actinometer

Develop:

- Film with silver strips, dispenser
- Aperture shutter
- Electrical contacts, resistance measurement

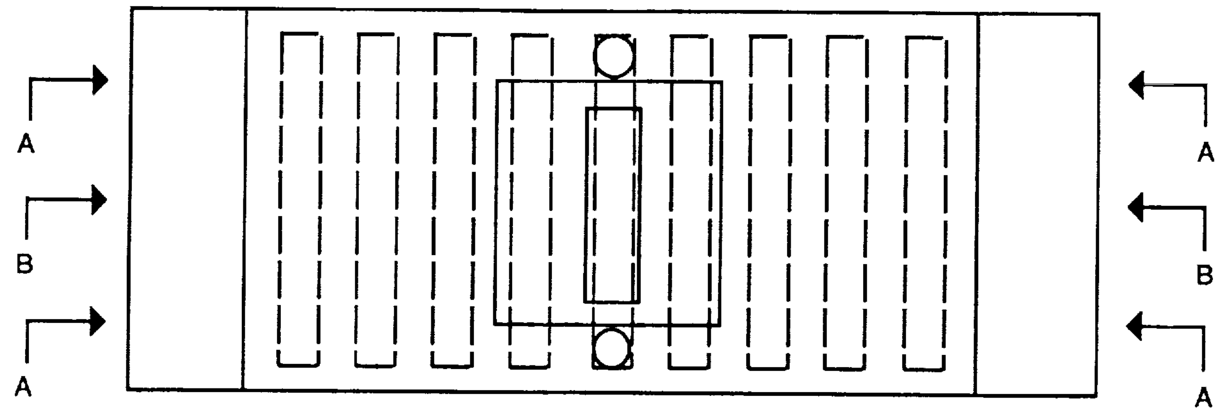

Face View of Aperture

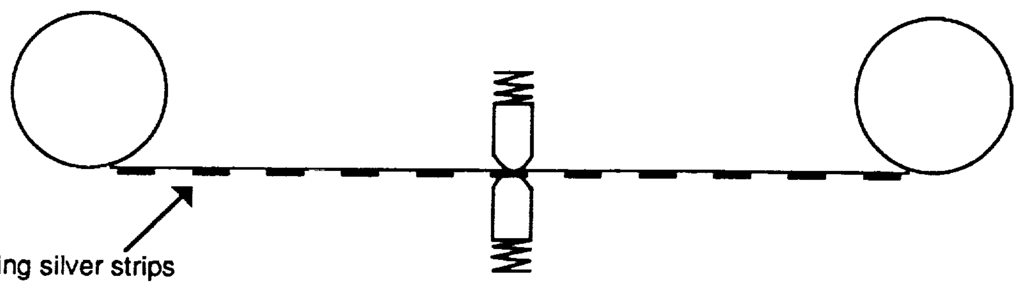

Sections AA: Spring-loaded contacts at both edges of film

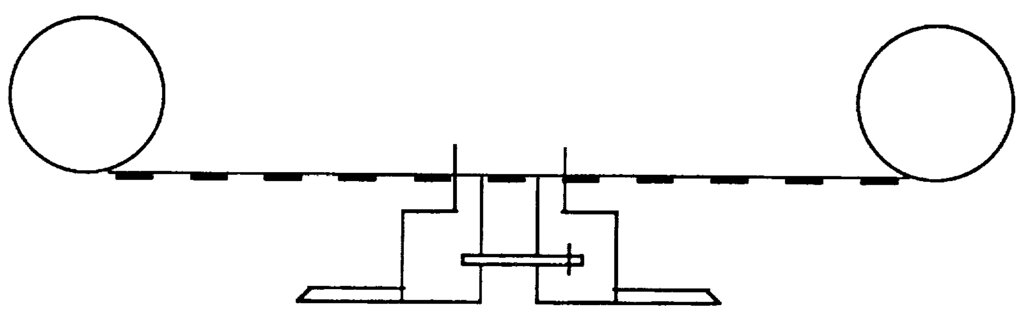

Section BB: Slit Aperture

Figure 3. Multi-use Actinometer

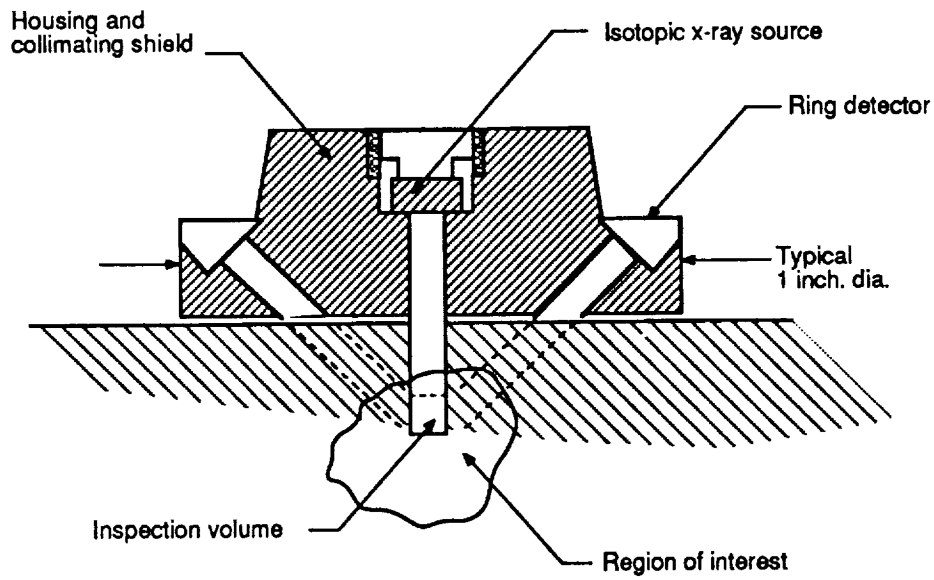

(a) Basic X-Ray Backscatter Gage

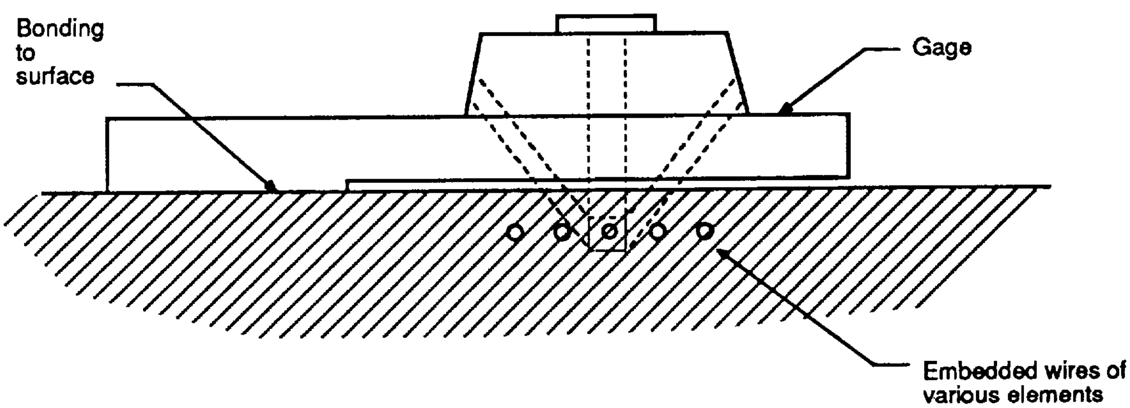

(b) Strain Gage Application

Figure 10. X-Ray Backscatter Gage Concept

Data Handling for SPIP Workstation

by

Richard White, Misa Gage, Brian Lempriere
Boeing Aerospace and Electronics

Presented to

NDE for Aerospace Requirements
University of Alabama in Huntsville
August 22-24, 1989

Performed under

Hercules Contract B-I-7-ER-23321
NASA Contract NAS8-37801

Technical Objective of Solid Propulsion Integrity Program (SPIP) for Nozzles

Boeing Aerospace & Electronics

Improve overall success rate of solid rocket motor nozzles

- Through improved understanding and capabilites

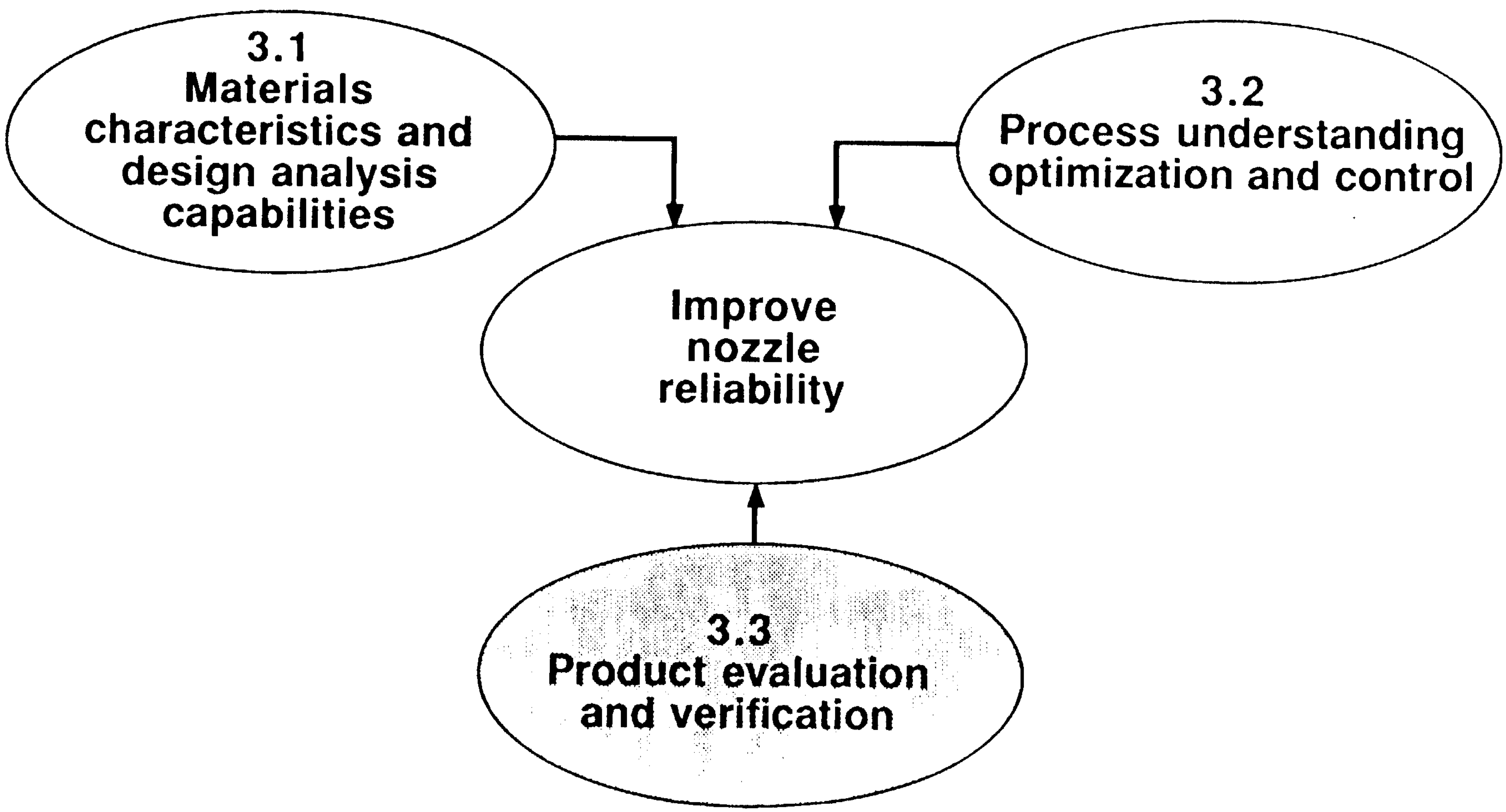

Technical Objective (Continued)

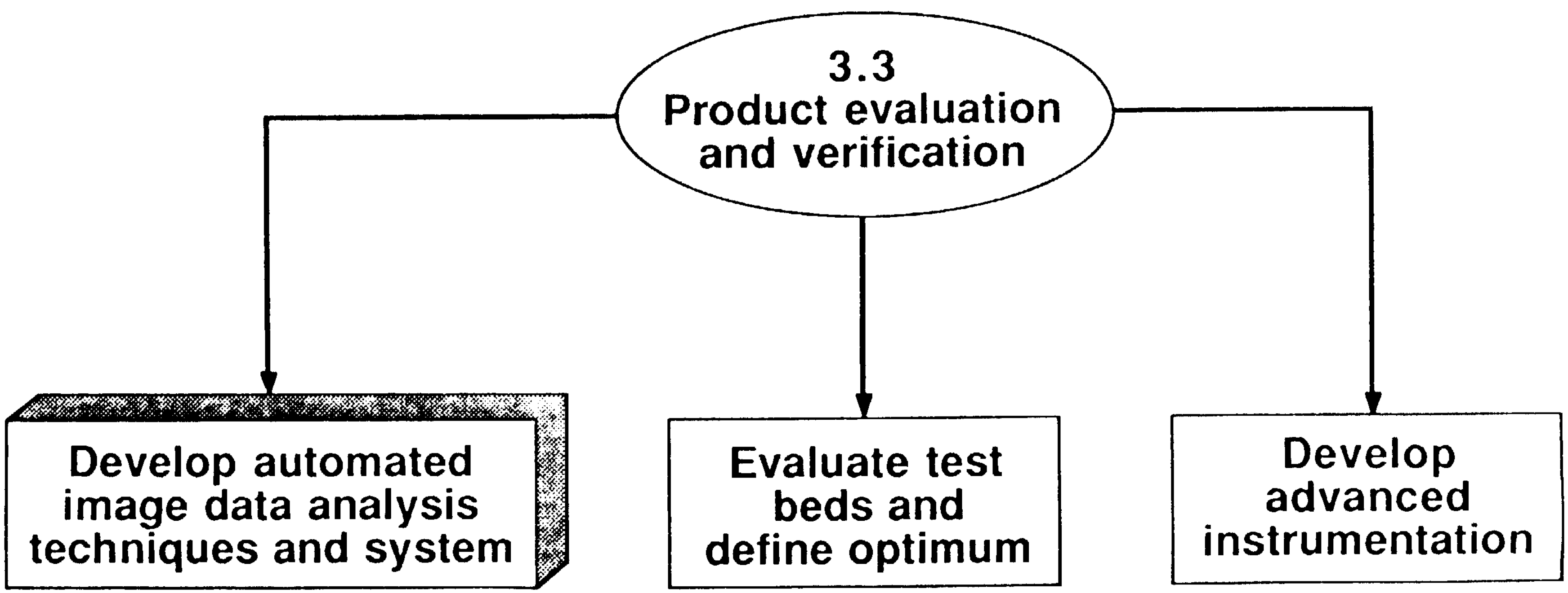

Overall System Uses

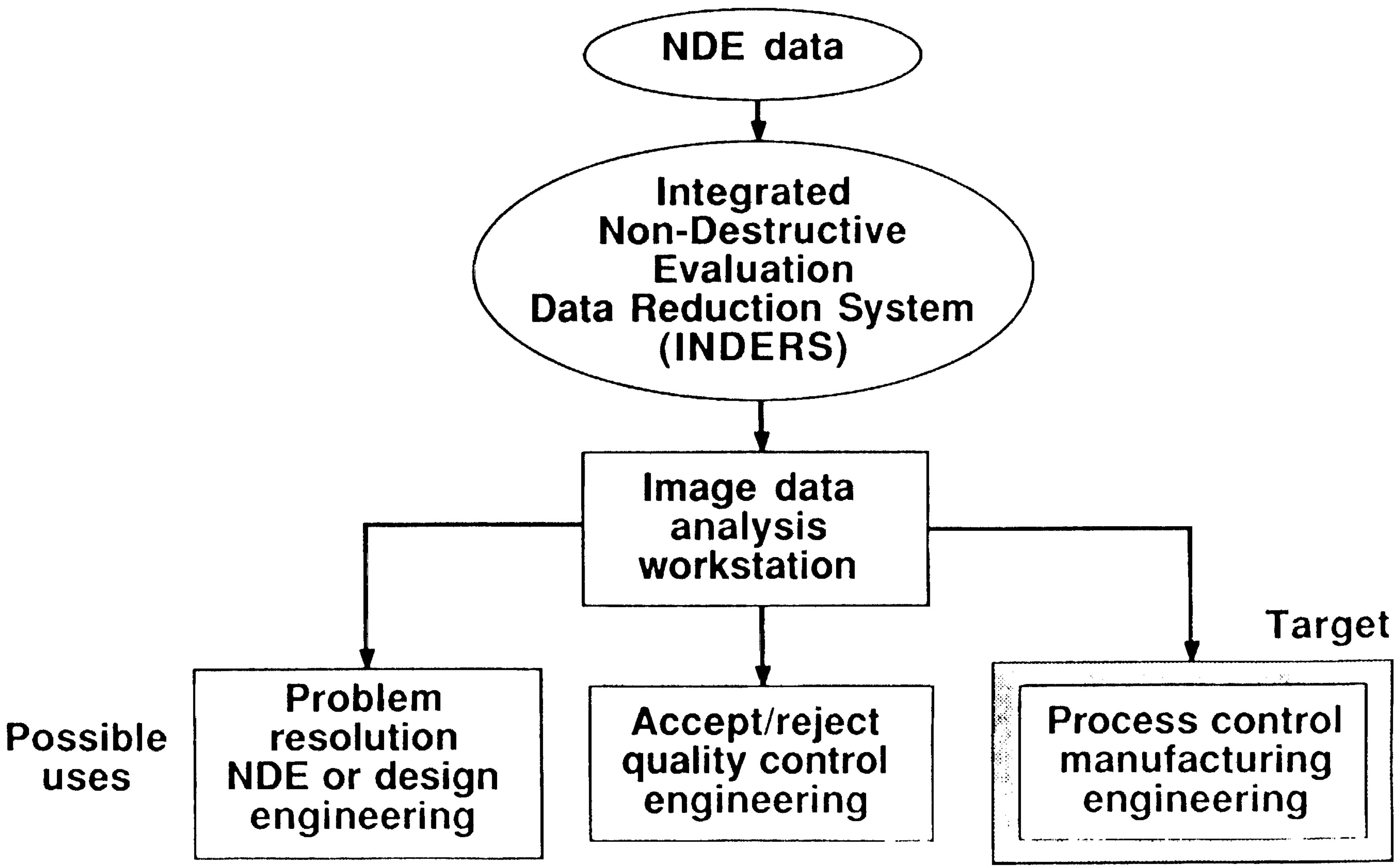

Program Overview

- Provide tools for nozzle manufacturer
  - To review production of NDE data
  - To review process parameters
  - To relate these to the fabrication process
- Review current production and NDE processes
- Select analysis techniques
  - Data display/management
  - Data prioritization
  - Data classification
- Determine hardware and software requirements
- Implement workstation design

Factory Interveiws

- Nozzle manufacturers and users:
  - Aerojet
  - Hercules
  - Hitco
  - Kaiser Pueblo and San Leandro
  - Thiokol
  - UTC/CSD
- What in-process material properties or features need to be monitored? (mostly from production personnel)
- What NDE derived material properties or features are applicable to the production environment? (mostly from NDE technologists)
- What are the requirements for a user interface with the NDE derived material properties or features? (jointly production personnel and NDE technologists)

Inpsection/QC Process

- NDE usually after cure and machining, before bonding
- Present techniques: Tag end test, weight, compression, radiography, alcohol wipe, tap testing
- Advanced techniques: RTR, CT, UT, ET
- Typical floor paper:
  1. Inspect material
  2. Record flow and volume test for each roll
  3. Verify rolls from different batches are not mixed
  4. Verify tape wrap to specs
  5. Verify bagging to specs
  6. Check vacuum and timing
  7. Verify autoclave or hydroclave procedures
  8. Record weight after cure and inspect for wrinkles
  9. Record thicknesses at 0, 90, 180, and 270 degrees
  10. Check machining
  11. Check radiography inspection
  12. Record thicknesses again

Aerospace
Systems
Technologies

PRO Types of Data

Boeing Aerospace & Electronics

- Time
- Temperature
- Pressure
- Chemistry
- Dimensions
- Weight
- Volume
- Photo
- Photo-micrographs
- Certifications
- Inspectors Name/Number
- Operators Name/Number
- ETC.

Inspection Considerations

- Based on customer requirements
- Sometimes drive design
- MRB is largest user
- Presently no NDE until after machining

Aerospace Systems Technologies

Inspection Recommendations

Boeing Aerospace & Electronics

- Catch defect as early as possible
- Report near-tolerance conditions
  (Presently only pass/no pass)
- Provide NDE data before and after cure
- Provide comparison of pre to post fire
- CAD may be helpful in data analysis
- Computerize routing order/inspection data
- CT workstation critiques received
  Reduce CT scan data

Aerospace Systems Technologies

Cause & Effect

Boeing Aerospace & Electronics

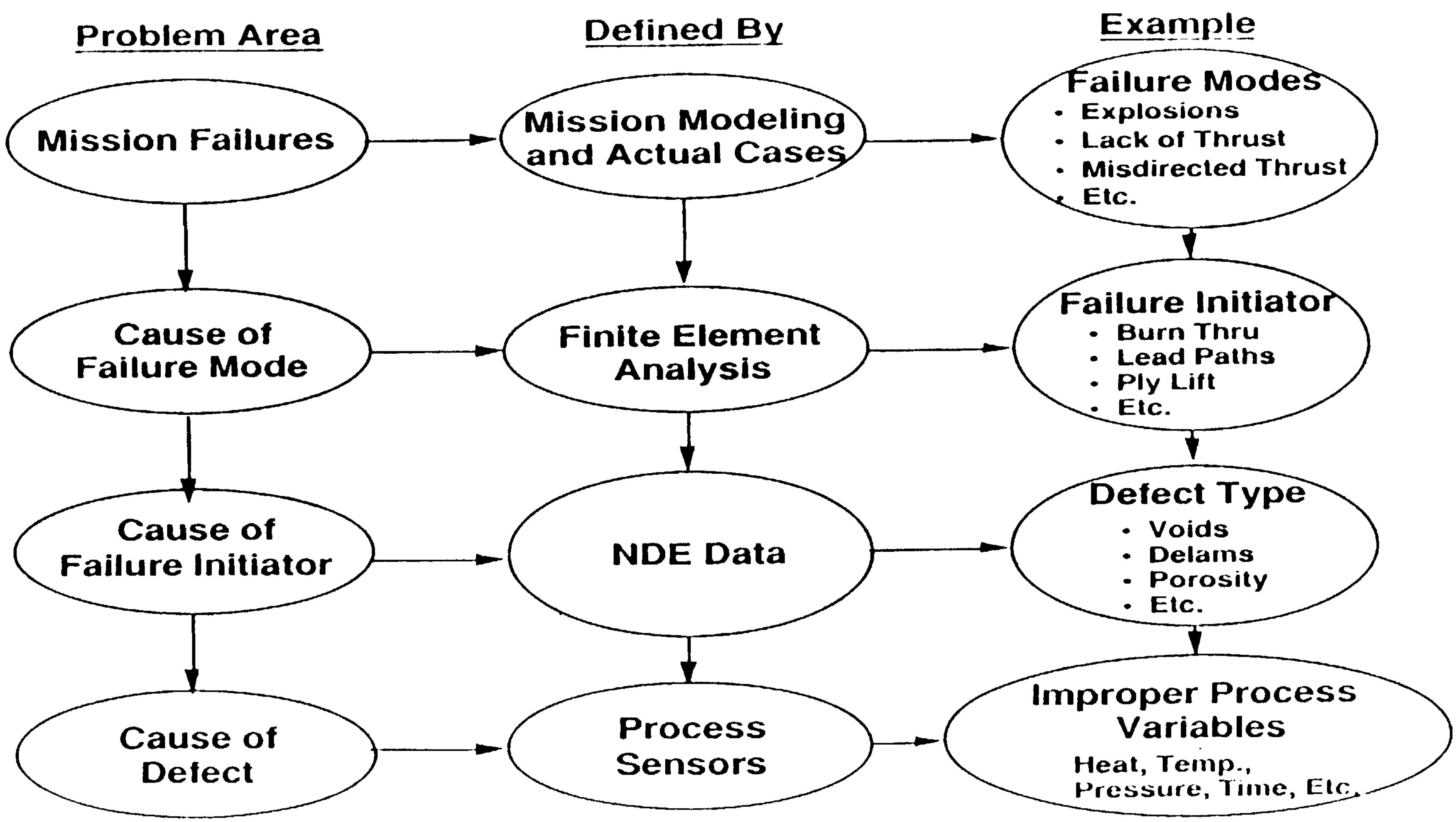

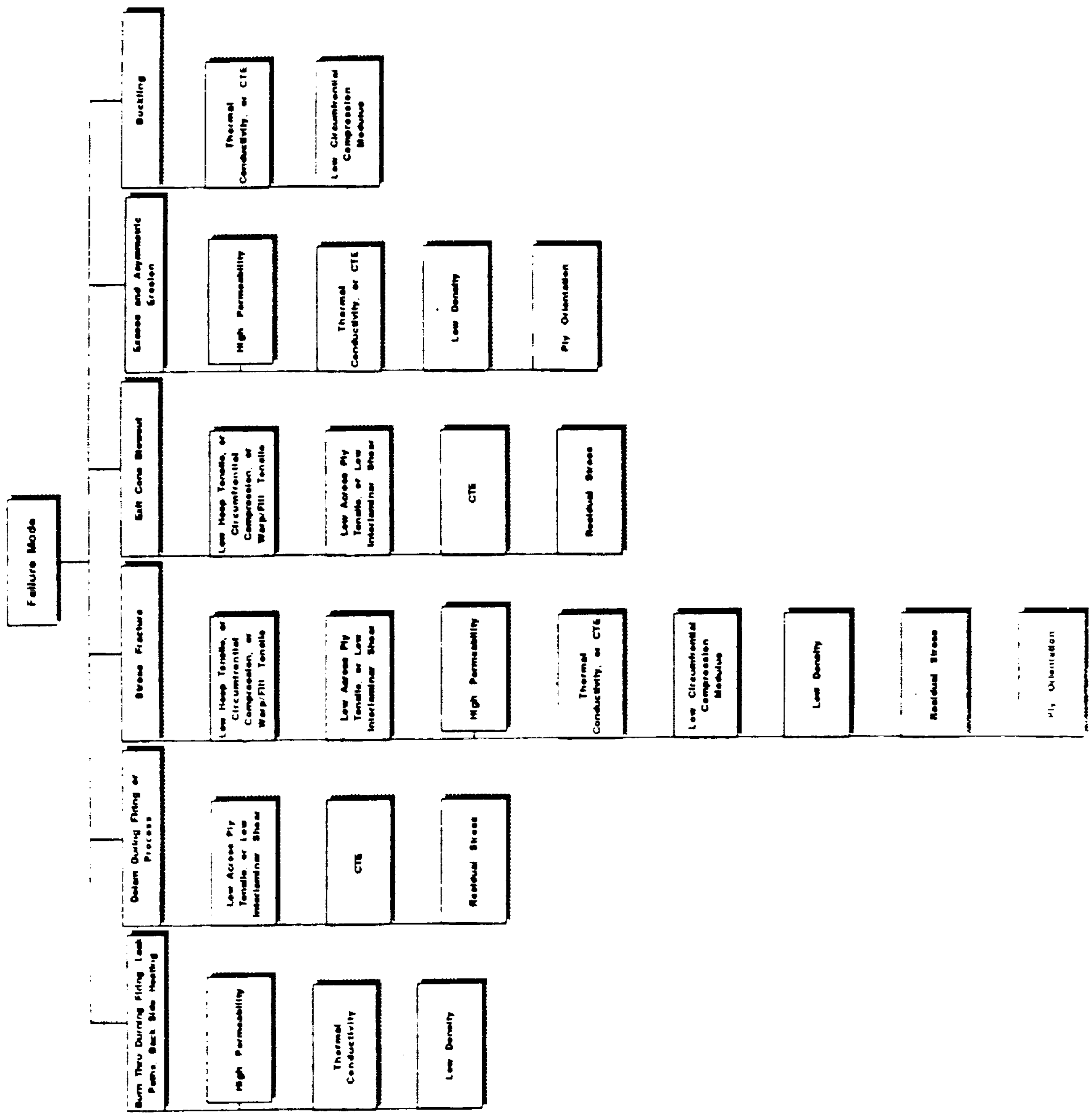
Failure Mode
Burn Thru During Firing Leak Paths Back Side Heating
High Permeability
Thermal Conductivity
Low Density
Delam During Firing or Process
Low Across Ply Tensile or Low Interlaminar Shear
CTE
Residual Stress
Stress Fracture
Low Hoop Tensile, or Circumferential Compression, or Warp/Fill Tensile
Low Across Ply Tensile, or Low Interlaminar Shear
High Permeability
Thermal Conductivity, or CTE
Low Circumferential Compression Modulus
Low Density
Residual Stress
Ply Orientation
Exit Cone Blowout
Low Hoop Tensile, or Circumferential Compression, or Warp/Fill Tensile
Low Across Ply Tensile, or Low Interlaminar Shear
CTE
Residual Stress
Excess and Asymmetric Erosion
High Permeability
Thermal Conductivity, or CTE
Low Density
Ply Orientation
Buckling
Thermal Conductivity, or CTE
Low Circumferential Compression Modulus

SPIP Workstation

Interfaces

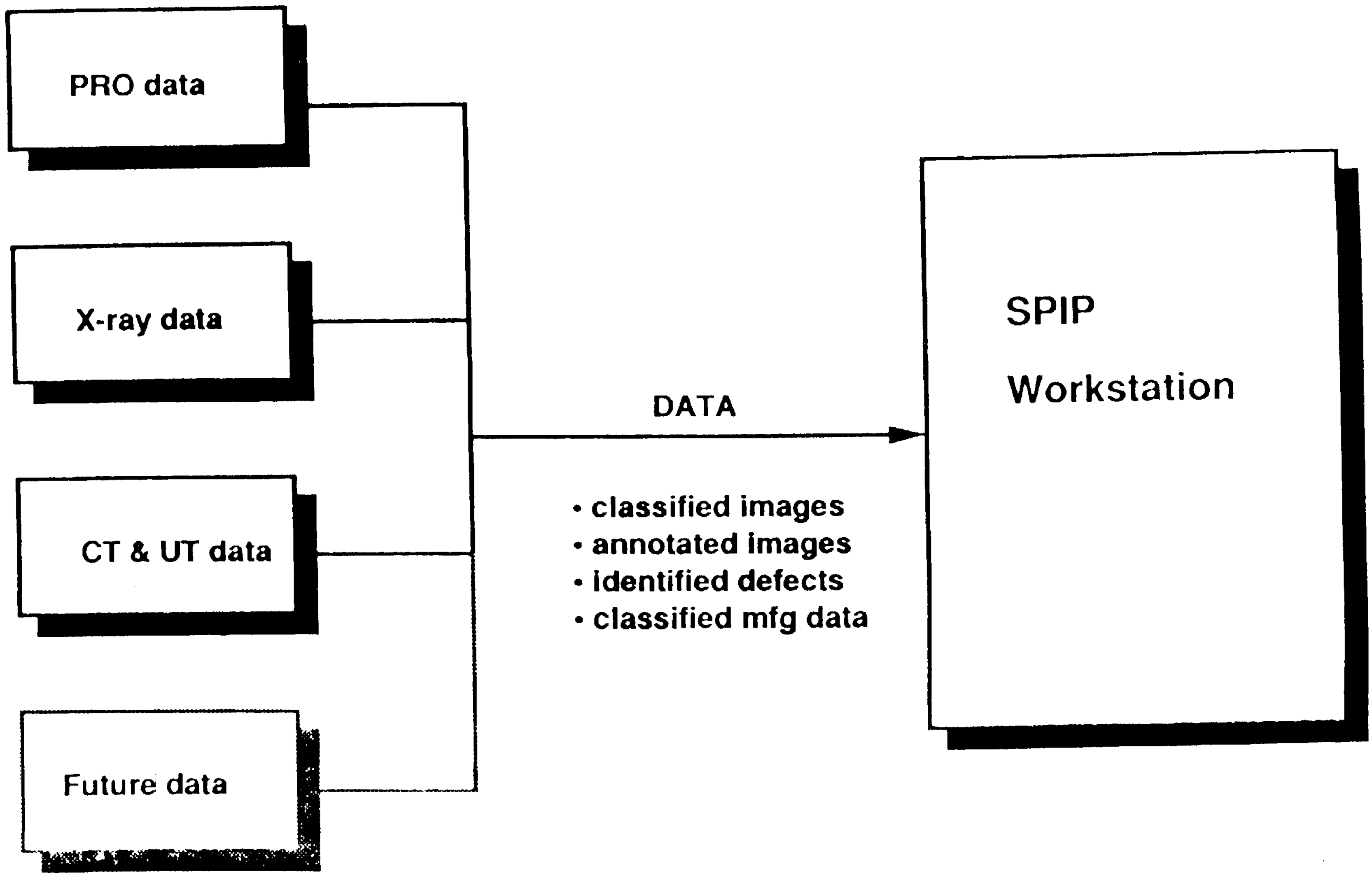

ORIGINAL PAGE IS
OF POOR QUALITY

Aerospace
Systems
Technologies

SPIP Workstation Use

Boeing Aerospace & Electronics

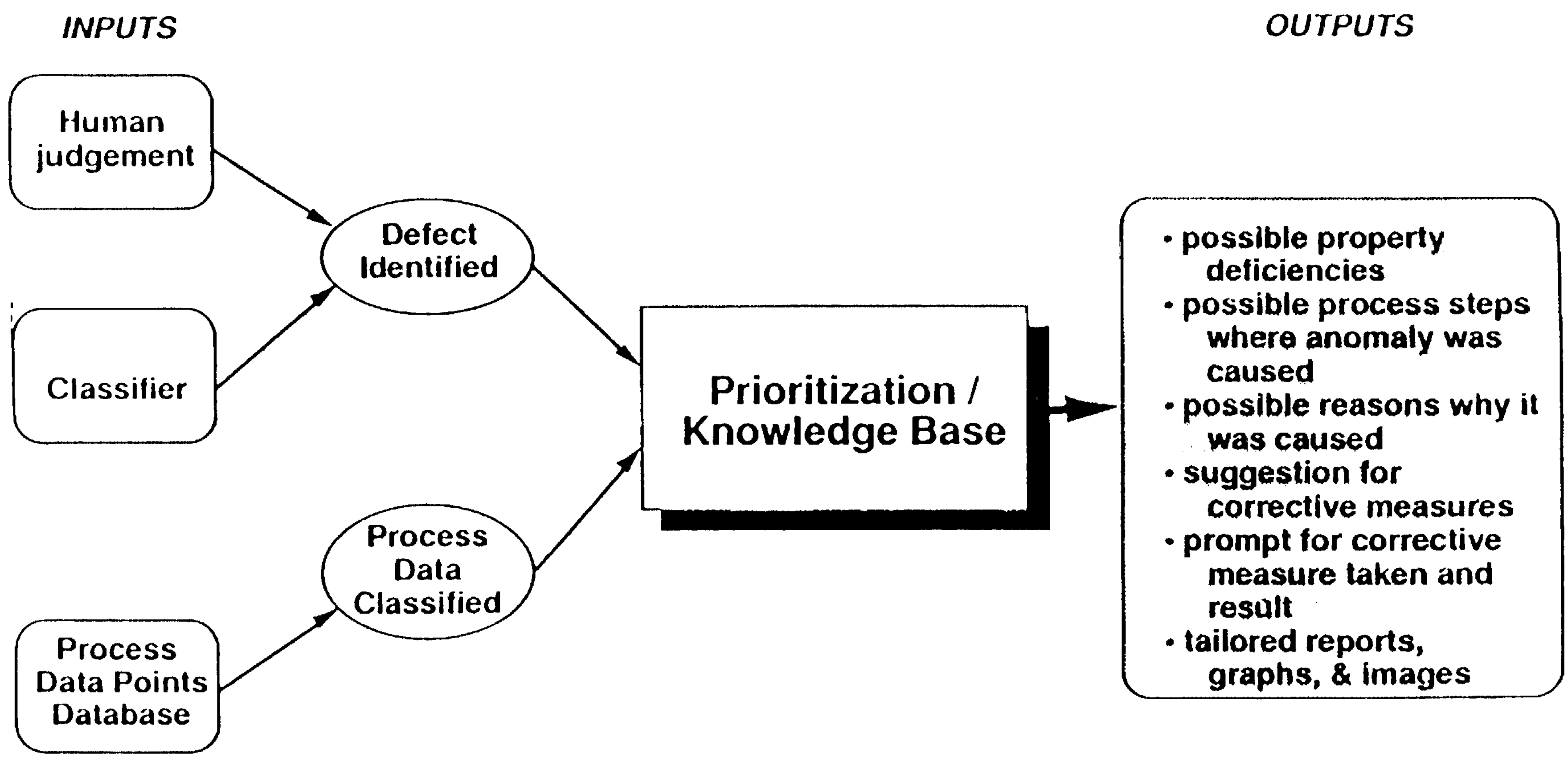

Aerospace Systems Technologies

Quality of Data

Boeing Aerospace & Electronics

	Qualitative	Statistical	Quantitative	Physical
Distinguishing features	Human judgement	Relative to nominal or average	Values independent of equipment	Expressed in engineering units
Examples:				
Radiography	Radiograph density	Low density indications (LDIs)	CT image (Hounsfield units)	Density in kg/m3
Ultrasonics	Amplitude	Gated low amplitude indications	Attenuation and wavespeeds (corrected for test factors)	Interlaminar shear strength (PSI)

← Worse Better →

The Need for Multimodality

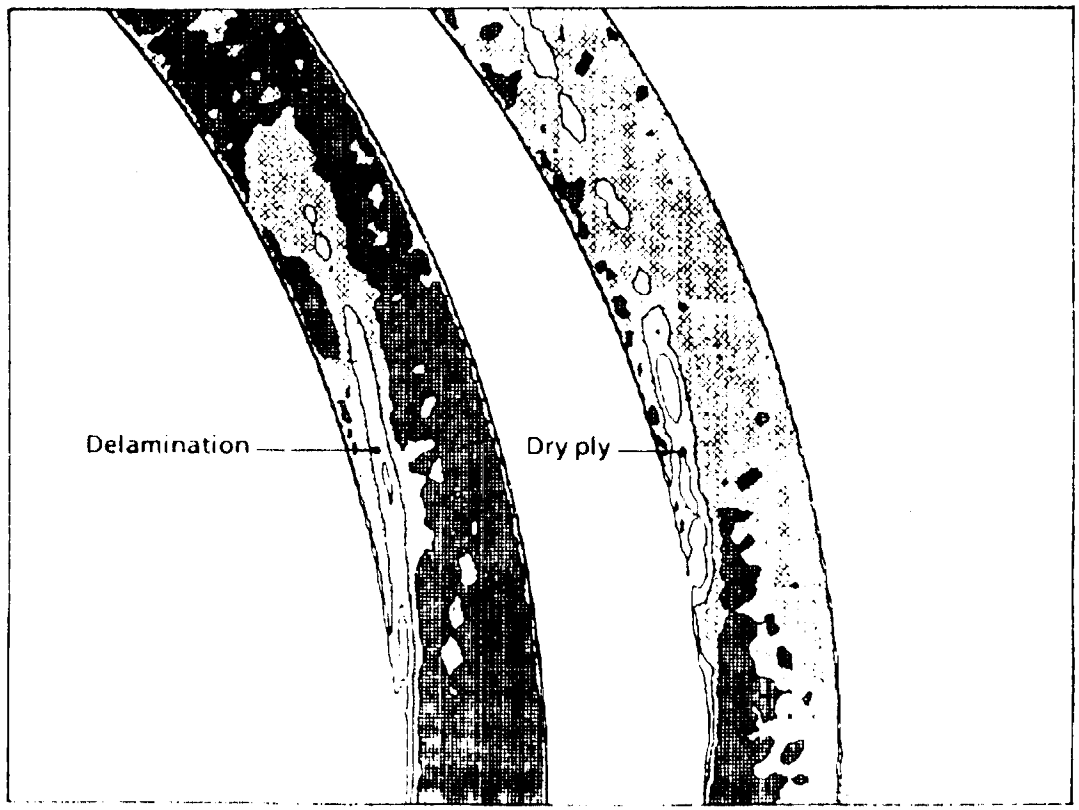

CT images alone may not contain sufficient information to distinguish between an acceptable dry ply and an unacceptable delamination.

ORIGINAL PAGE IS OF POOR QUALITY

Multi-Modal Defect Characterization

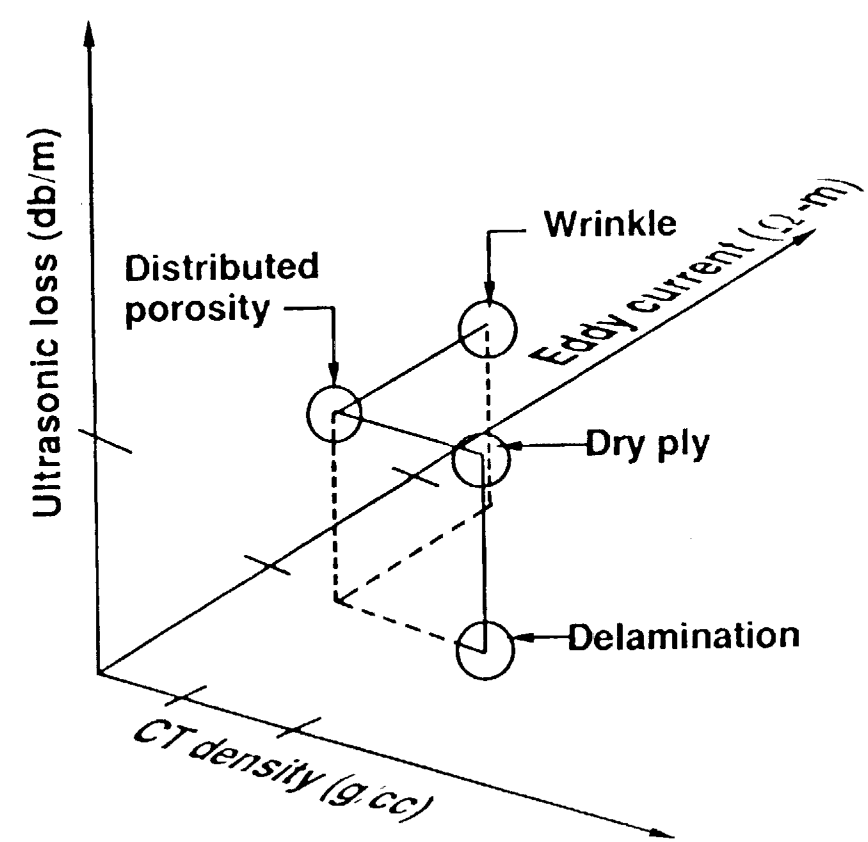

Data Transfer

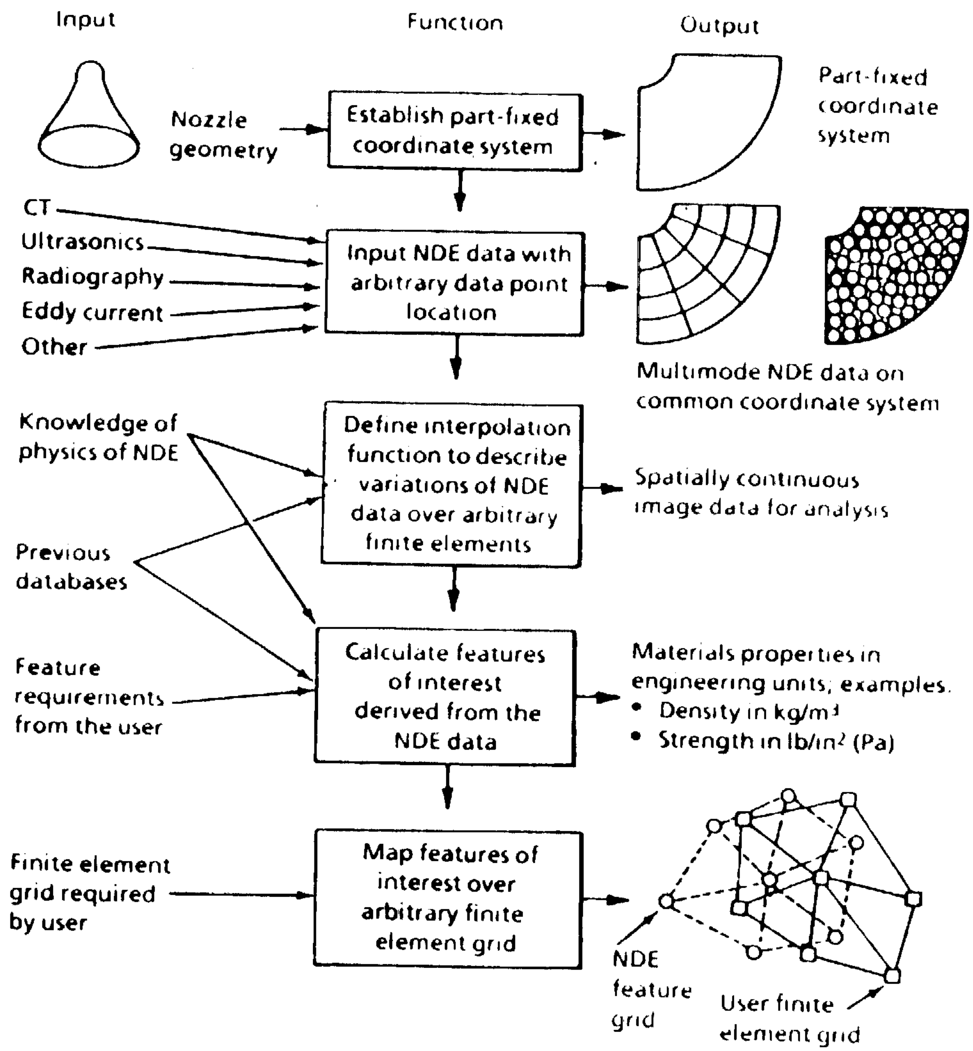

The Boeing INDERS approach to managing NDE data is both systematic and flexible

ORIGINAL PAGE IS OF POOR QUALITY

Data Display

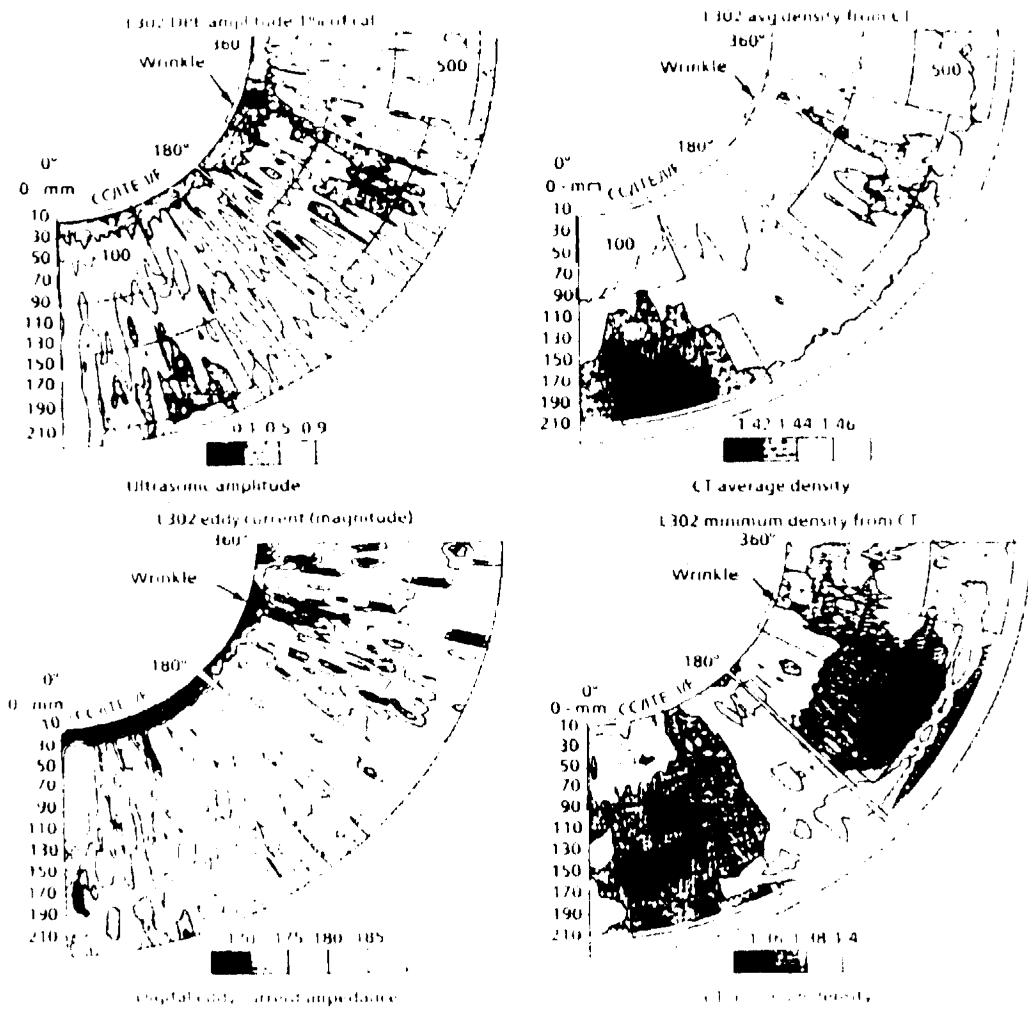

The Boeing approach to NDE feature mapping demonstrates the ability to superimpose multiple features on a common surface (IUS nozzle in this case) with outputs in engineering units

Aerospace
Systems
Technologies

SPIP Workstation

HW/SW Current Options

Boeing Aerospace & Electronics

1	**Dupont - Sun Workstation**	• INDERS hosted on Dupont • Add Sun WS for SPIP • Image Enhancement & Data Handling • Proven technology
2	**Stand-alone Workstation**	• End-item inspection data • INDERS may be on WS • Low cost
3	**NDE and Mfg Workstations Co-located**	• High speed bus between systems for images • Cost out INDERS WS also • X-ray digitizing developed in-house
4	**NDE and MFG Workstations Separated**	• NDE and Mfg in separate locations • Local area network comm. • X-ray digitizing developed in-house

ORIGINAL PAGE IS
OF POOR QUALITY

SPIP Workstation Layout #1

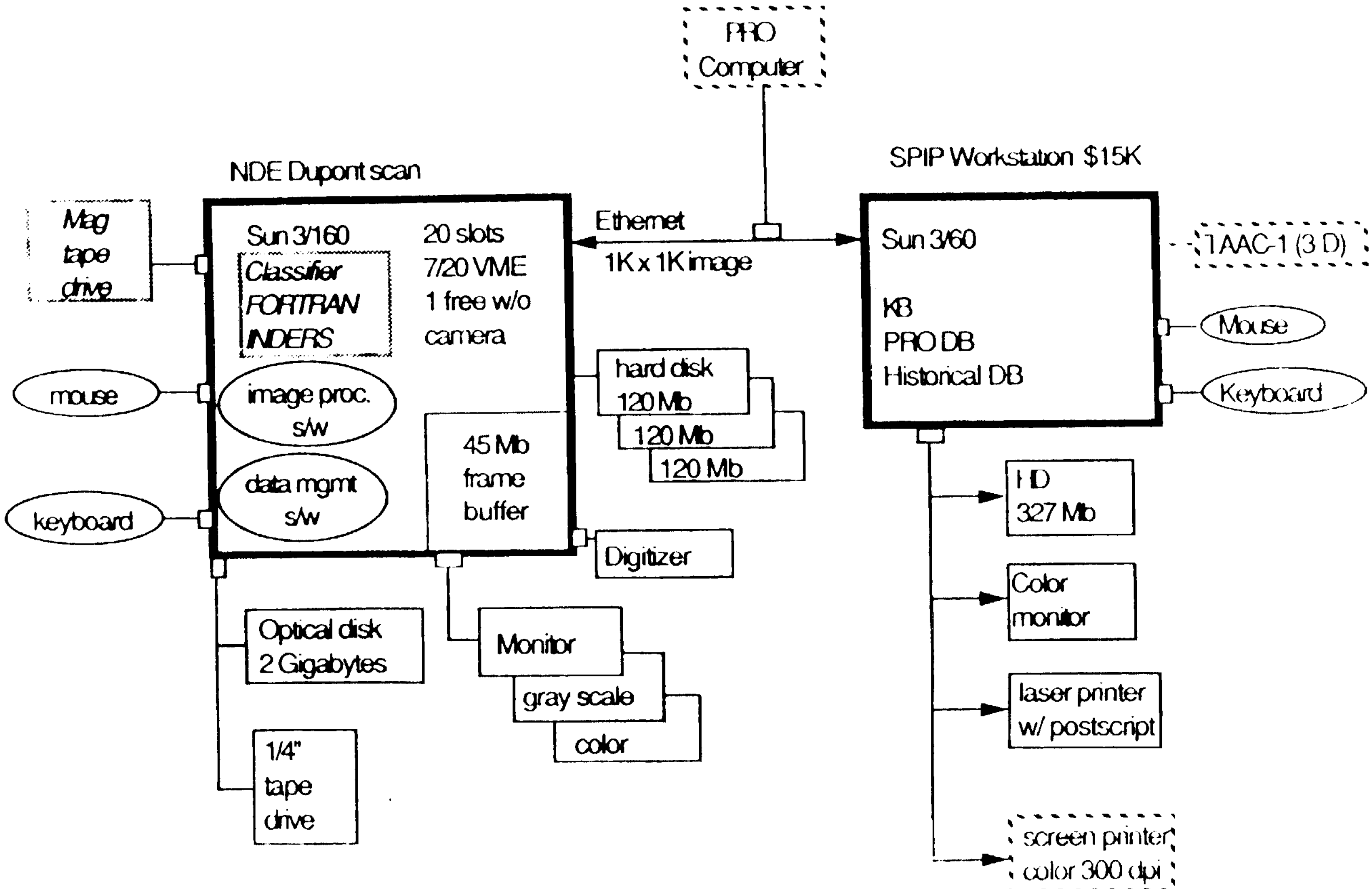

ROM $300 - 400K

ORIGINAL PAGE IS
OF POOR QUALITY

Required Software Packages for Workstation

1. Man Machine Interface/Data Display
   - 3-D color graphics
   - Text display
   - Mac style menu interface
   - 3-D manipulation of objects (rotation, translation, magnify, etc)
   - Image enchancement
   - Data base techniques

2. Data Management
   - Spreadsheet type relational database
   - INDERS formatted data files
   - Graphics display files
   - Archival, retrieval, logging
   - Interface to computertized production data

3. Classifying Images
   - Groups anomalies for display and analysis via statistical methods
     - Normal
     - Questionable
     - Anomalous

4. Knowledge Based Analsyis and Prioritization Based on Production Contraints
   - Knowledge base-expert system
   - Dynamic - add, delete
   - Trend analysis
   - Autocorrelation
   - Blob analysis
   - Pattern recognition
   - Edge following
   - Region growth

NDE DATA APPLICATION

PRESENTED AT

SECOND CONFERENCE ON NONDESTRUCTIVE EVALUATION FOR AEROSPACE REQUIREMENTS

PRESENTED BY

JOSEPH H. HILDRETH
ASTRONAUTICS LABORATORY
EDWARDS AFB, CA

CONTENTS

INTRODUCTION

NDE DATA USED SUBJECTIVELY TO DETERMINE ACCEPTABILITY

- RADIOGRAPHY
- ULTRASONICS

NEWER TECHNOLOGY ALLOWS COLLECTION OF QUANTITATIVE DATA

- COMPUTED TOMOGRAPHY

HISTORICALLY, ANALYSIS PERFORMED ON AS-DESIGNED PART WITH MODIFICATIONS

OBJECTIVE OF NDE DRIVEN ANALYSIS

PERFORM COMPUTERIZED ASSESSMENT OF ACCEPTABILITY ON AS-BUILT PART

MOVE THE ACCEPT\REJECT DECISION PROCESS FROM SUBJECTIVE METHODS TO OBJECTIVE METHODS

NDE DRIVEN ANALYSIS METHODOLOGY

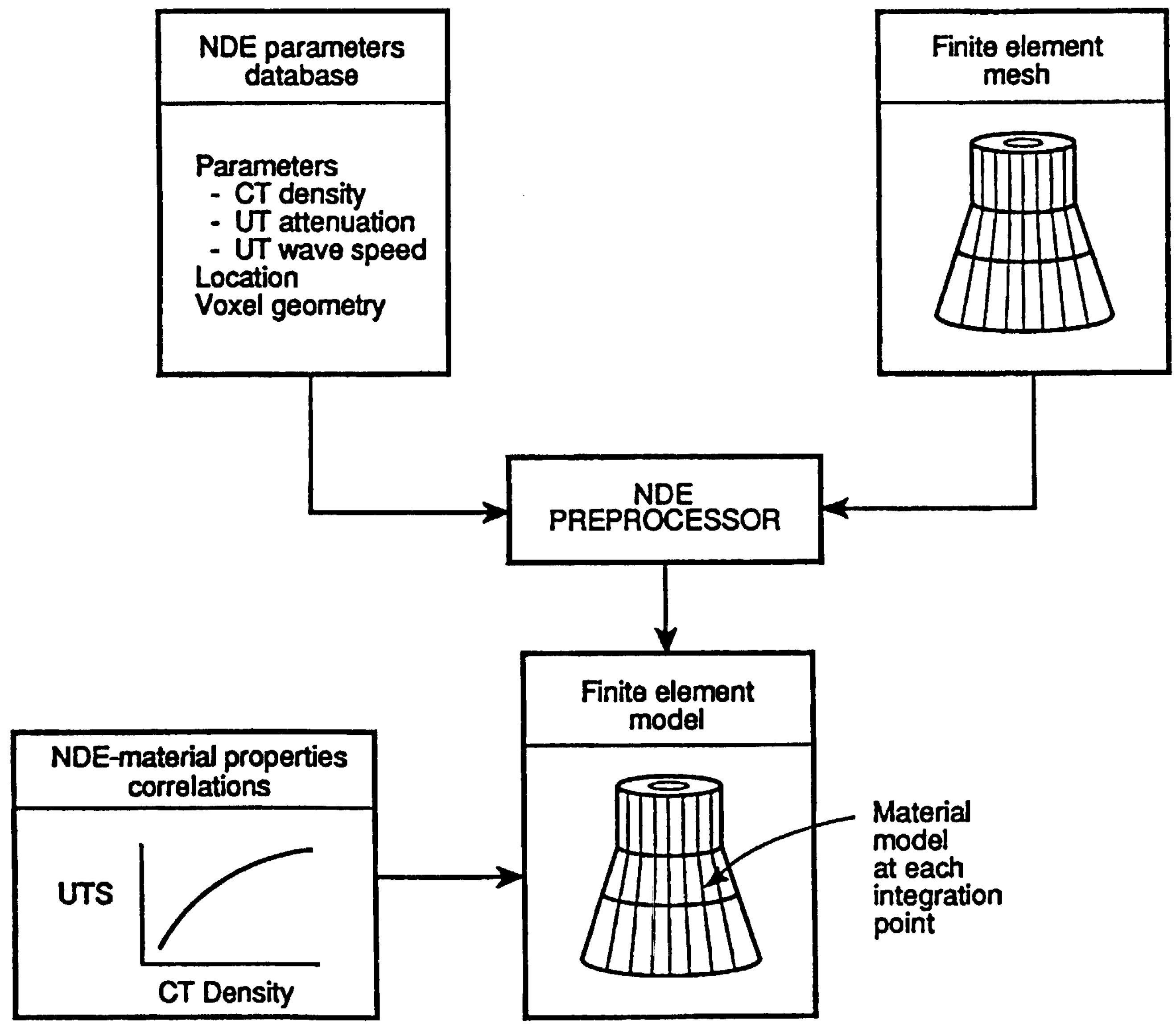

FINITE ELEMENT MESH OF CYLINDER

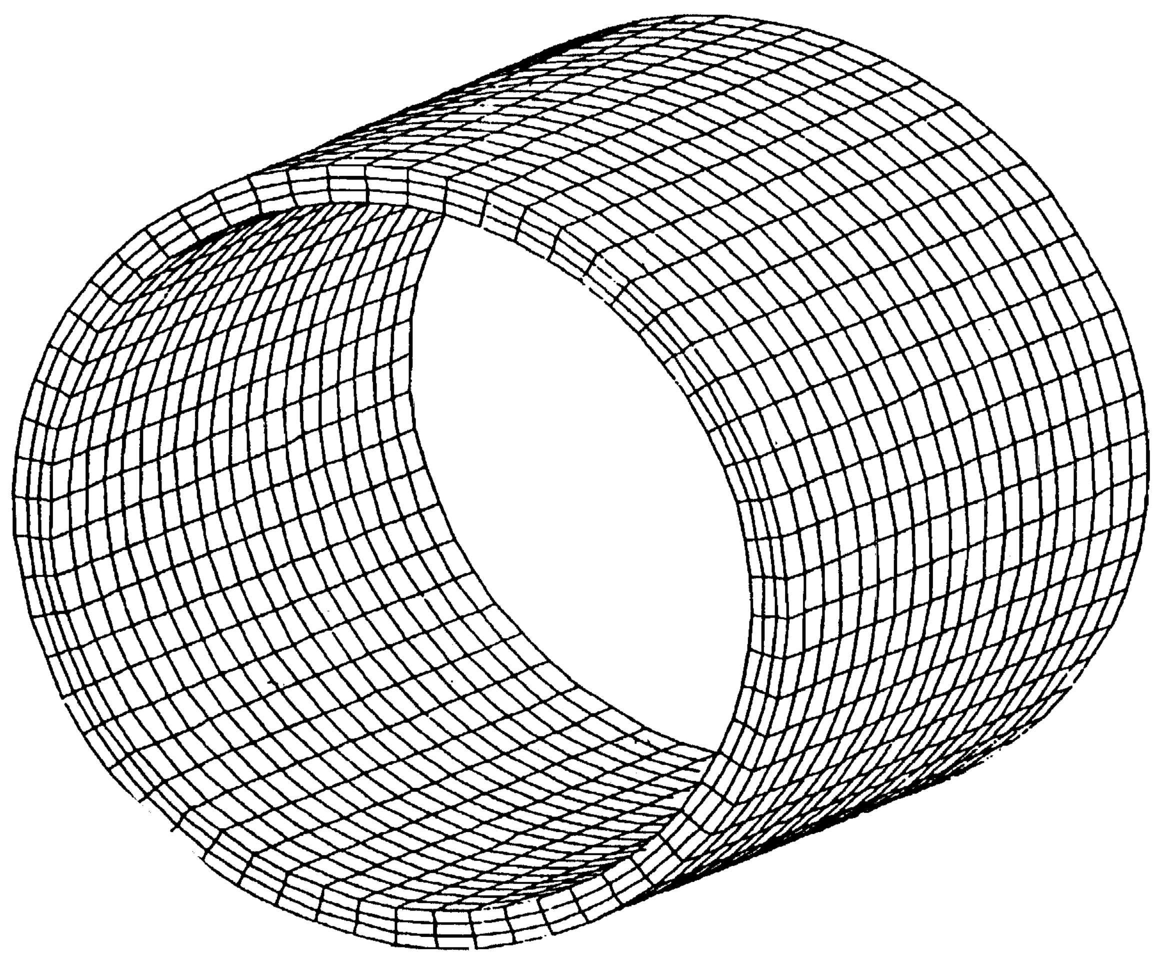

STIFFNESS MATRIX FOR FINITE ELEMENT

$$K = \int_{vol} B^T \; C \; B \; dv$$

SINGLE FINITE ELEMENT

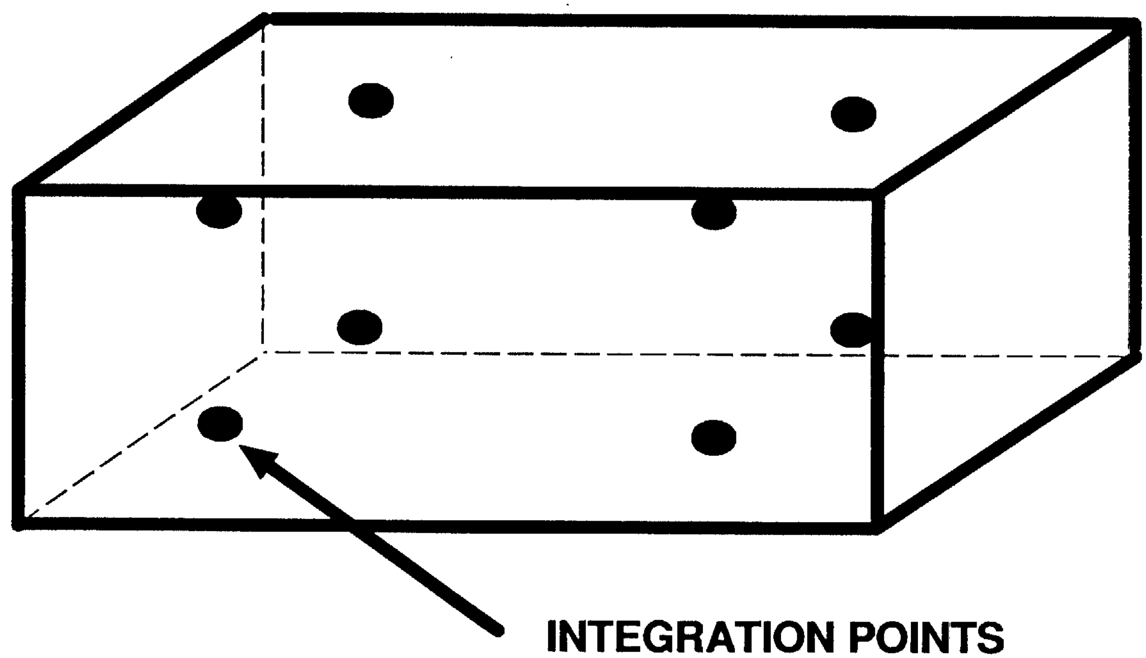

WRINKLED CYLINDER SPECIMEN GEOMETRY

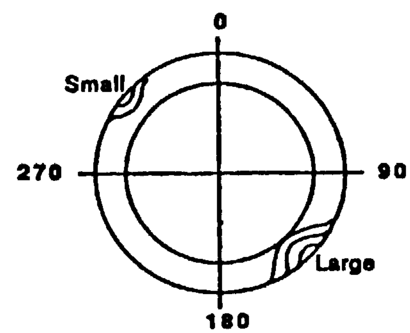

107-1 WRINKLE

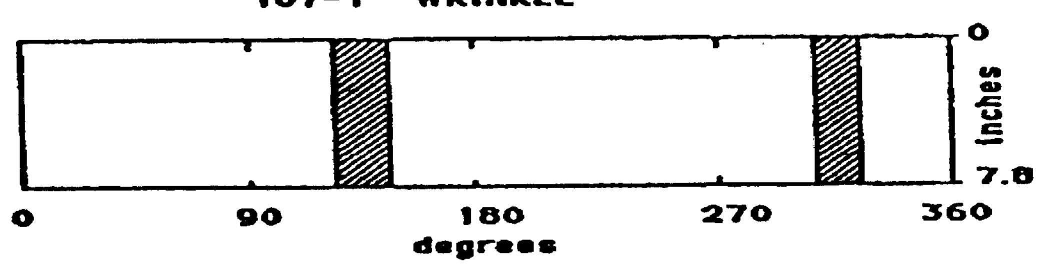

TAPERED AMPLITUDE
WRINKLE CYLINDER

Anomaly:	Wrinkle/wave (2)
Generated by:	Dimpled and machined
Size:	0.1-0.35 Amplitude x 0.8 length 0.0-0.25 Amplitude x 0.8 length
Location (approximate):	135° and 315°

CT Inspection Geometry

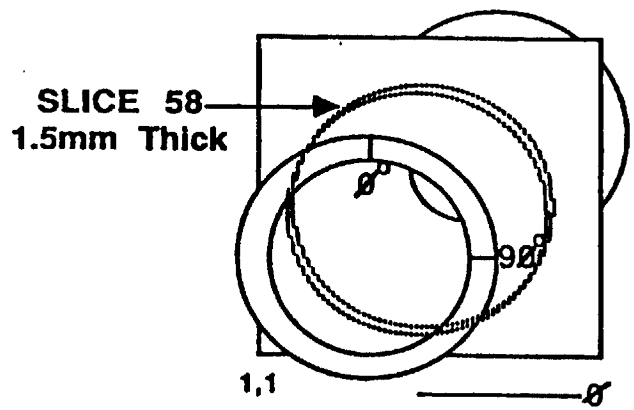

UT Inspection Geometry

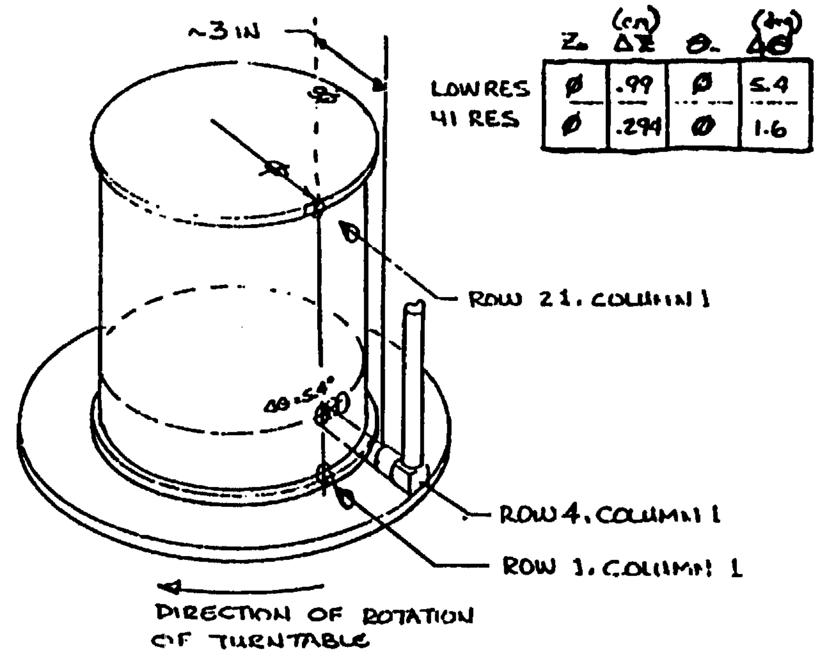

IMAGES OF NDE DATA

CT DENSITY (G/CC)

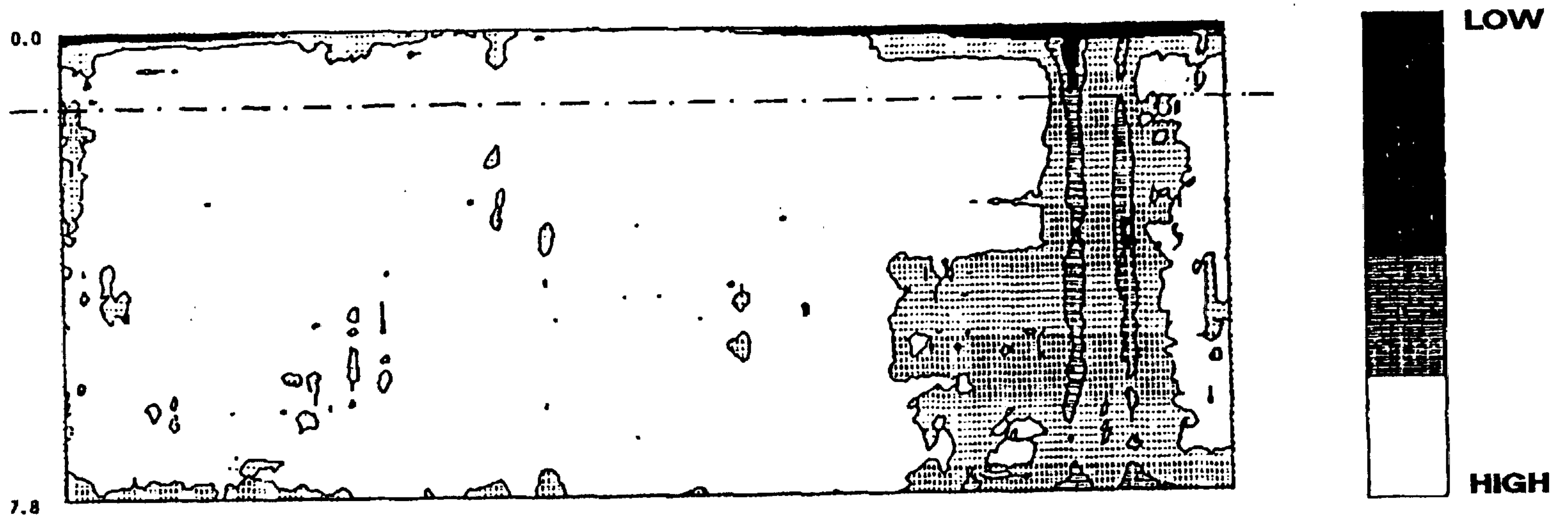

ULTRASONIC ATTENUATION (DB)

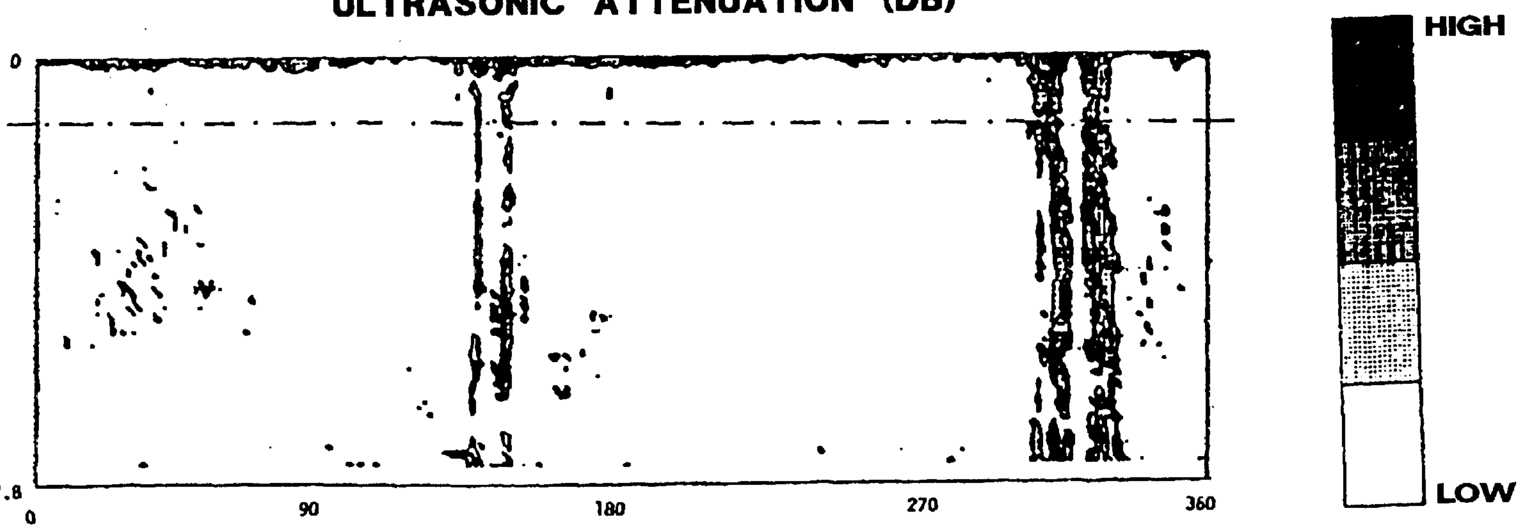

PROCEDURE

DETERMINE VALUES OF NDE DATA AT INTEGRATION POINTS

DETERMINE VALUES OF MATERIAL PROPERTIES BASED ON NDE INDICATIONS

IF MULTIMODE NDE DATA IS BEING CONSIDERED THEN DETERMINE COMPOSITE AVERAGE OF EACH MATERIAL PROPERTY

TRANSFER MATERIAL PROPERTIES TO ANALYSIS CODE

REALITIES

MUST MATCH GEOMETRY OF PART TO GEOMETRY OF ANALYSIS MODEL

CARE MUST BE TAKEN WITH HOW NDE VOXELS ARE USED TO INTERPOLATE VALUES AT INTEGRATION POINTS

A SUBSTANTIAL EFFORT WILL BE REQUIRED TO DETERMINE CORRELATIONS BETWEEN NDE INDICATIONS AND ANALYSIS INPUT

IF MULTIMODE NDE DATA IS REQUIRED THEN WEIGHTING OF EACH TYPE OF DATA MUST BE DETERMINED

MATCH GEOMETRIES OF PART AND MODEL

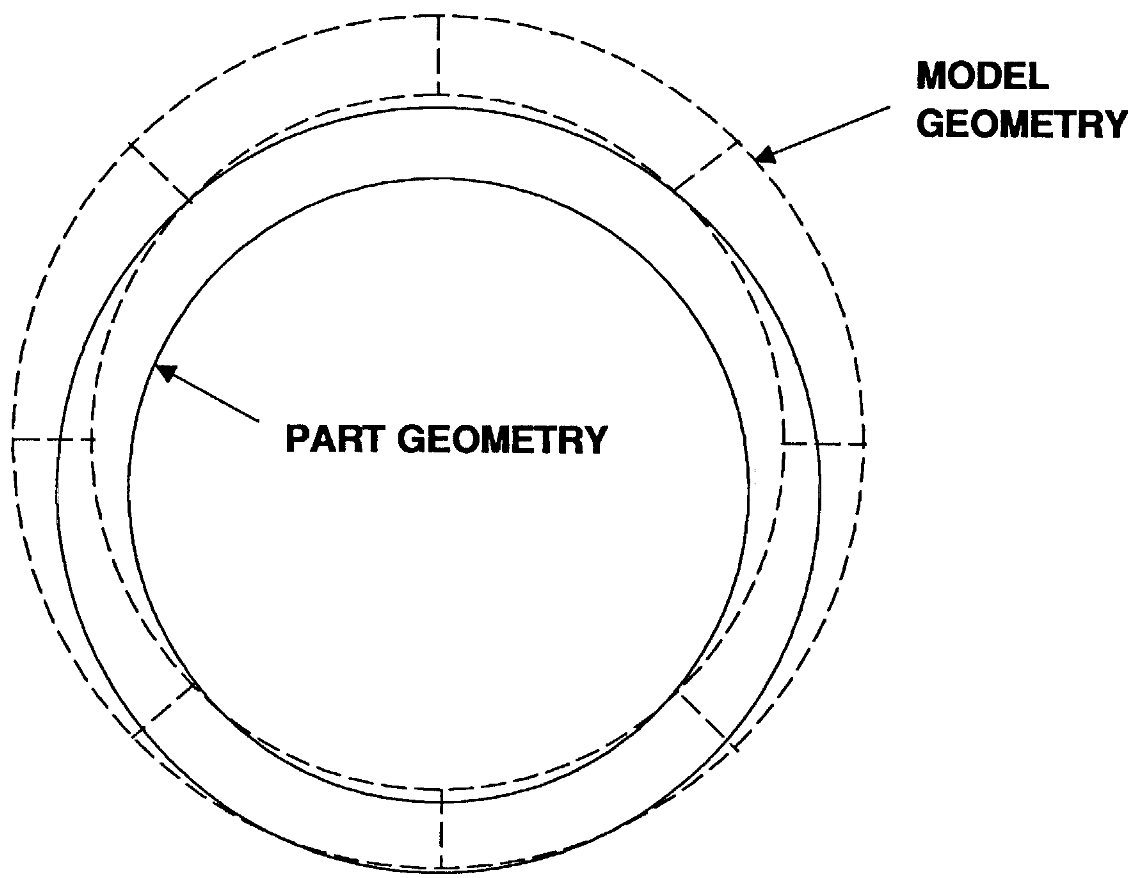

NDE VOXELS - FINITE ELEMENT MESH OVERLAY

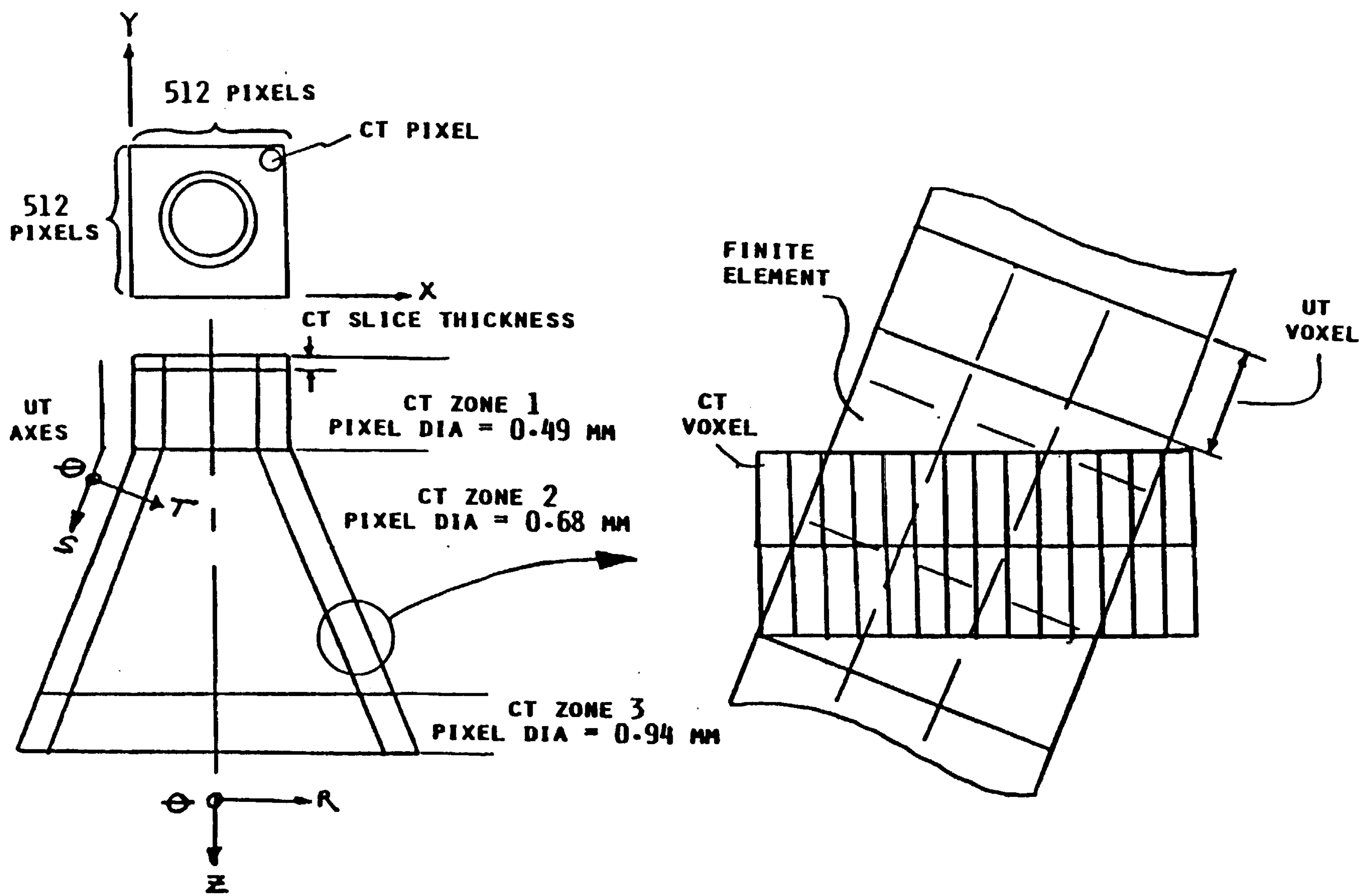

SUMMARY

- DEMONSTRATED A METHODOLOGY FOR INCORPORATING QUANTITATIVE NDE DATA IN FINITE ELEMENT ANALYSIS

- CORE OF REMAINING PROBLEM IS THE DEVELOPMENT OF CORRELATIONS BETWEEN NDE INDICATIONS AND MATERIAL PROPERTIES

- IF PROBLEM REQUIRES MULTIMODE NDE DATA, THE RELATIVE IMPORTANCE OF EACH DATA TYPE MUST BE ESTABLISHED

ADVANCED TECHNIQUES FOR EXAMINATION OF COATINGS

Robert W. McClung, Consultant
C. V. Dodd and W. A. Simpson, Jr.
Oak Ridge National Laboratory
Oak Ridge, Tennessee 37831

ornl

Proceedings for
NDE for Aerospace Requirements Conference
Huntsville, Alabama

COATINGS OF ONE MATERIAL ON ANOTHER TO PROVIDE DESIRED SURFACE PROPERTIES ARE A VITAL PART OF INDUSTRY

- Especially important for critical components
- Allows less expensive materials for structure
- Coatings provide resistance to corrosion, abrasion, erosion, contact stresses, and other environmental attack (e.g., temperature or chemical)
- Protection may not be attainable through other fabrication methods
- Applications include textile, paper, petrochemical, and metal-processing, as well as aerospace industries

ALTHOUGH COATINGS ARE WIDELY USED, USE WOULD INCREASE WITH BETTER ABILITIES TO ASSURE INTEGRITY AND PROPERTIES

- A major problem for many coatings is poor or uncertain adherence of coating to substrate with thermal cycles (or other stress)

- Other properties of concern include thickness, lack of bond, delamination, flaws (porosity, cracks, etc.) microstructure, and homogeneity

- Relative importance of above properties can vary with type of coating and the service environment

- Nondestructive testing (NDT) techniques are beneficially used to evaluate many of these properties of coatings after fabrication and service; advances are needed for improved quantitative data

A WIDE VARIETY OF NDT TECHNIQUES ARE CURRENTLY USED FOR EXAMINATION OF COATINGS; A NON-EXHAUSTIVE LISTING INCLUDES:

- Thickness: electromagnetic (eddy-current and magnetic methods), ultrasonic, optical (for transparent coatings), penetrating radiation (e.g., x-ray fluorescence, beta backscatter), thermal
- Lack-of-bond: thermal, ultrasonic, acoustic, optical holography
- Flaws: electrical continuity, fluid penetrant, ultrasonics, optical holography, thermal

PROBLEMS AFFECTING CURRENT NDT PRACTICE FOR SOME APPLICATIONS INCLUDE:

- Thickness
  - variations in electrical or magnetic properties of coating or substrate affect eddy-current and magnetic techniques
  - inhomogeneities in coating or substrate can affect penetrating-radiation techniques
  - ultrasonic technique requires adequate thickness for resolution and acoustic mismatch between coating and substrate
  - IR thermal techniques can be affected by relative emissivity

- Lack of bond
  - IR thermal techniques can be affected by emissivity
  - bond must be stressed for optical holography
  - ultrasonic techniques require adequate thickness for resolution

- Flaws
  - electrical continuity requires electrical contact with substrate and completely-through flaw
  - ultrasonics and holography may be useful for cracks or other linear flaws; probably not for porosity
  - fluid penetrant affected by natural background of acceptable porosity
  - optical holography requires application of stress

- Adherence
  - with few exceptions, techniques are unavailable for quantitative nondestructive evaluation of coating adherence

RECENT ADVANCES IN NDT TECHNOLOGY OFFER IMPROVED CAPABILITY OR POTENTIAL TO OVERCOME SOME OF THE PROBLEMS FOR COATING EVALUATION

- Multi-frequency and pulsed multiple-parameter eddy-current technology provides the capability to correct for variations in electrical and magnetic properties of coating and substrate
  - two- and three-frequency instruments that simultaneously measure phase and magnitude of all frequencies and process in nonlinear algorithms to correct for variables and solve for 4-6 unknowns (e.g., thickness, conductivity, permeability, etc.)
  - pulsed (and magnetic-saturation) instruments as another approach for ferromagnetic materials for multiparameter analysis

- High-temperature probes offer potential for application to process control

- Ultrasonic guided boundary waves (interface waves) are being investigated by ORNL and others for evaluation of interfaces in bonded structures
  - models developed at ORNL for three-layer interfaces for ceramic joints
  - transmission along interface offers potential for for evaluation and analysis of interface properties (e.g., bond strength)

COATINGS ARE EXPECTED TO BE INCREASINGLY USED TO INCREASE COMPONENT LIFE

- Nondestructive testing will play a vital role for process control, fabrication acceptance, and in-service inspection

- Improved NDT technology will increase the role for both NDT and coatings

N91-18198

An Automatic Gore Panel Mapping System

John D. Shiver, Norman N. Phelps,
and Dr. Michael E. Jackson
Martin Marietta Manned Space Systems
Marshall Space Flight Center

I. Introduction

The External Tank (ET), which supplies fuel for the main engines of the Space Shuttle, is comprised of three tanks: the oxygen, hydrogen, and inner tanks. The four domes which form the ends of the hydrogen and oxygen tanks are constructed by welding oblate, shperoidical metal sections called gore panels. These panels are chemically milled over large areas to lower the ET total weight. The weight of the raw material used to construct the oxygen and hydrogen tanks is 32,415 pounds. The final weight after chemical milling is 11,730 pounds, which is the result of a sixty-four percent weight reduction of the chem-milled parts. The Automatic Gore Mapping System is being developed to reduce the time and labor costs associated with maufacturing the External Tank. Presently, the chem-milled panels are manually scanned with an ultrasonic contact probe and mapped for thickness. The ultrasonic contact probe requires the application of couplant to the area of the part that is to be measured for thickness. To scan one panel manually during the entire production cycle requires an extimated 6.5 man days. Since chemical milling a gore panel is tedious and time consuming, NASA is funding a project that will automate this process. A workcell has been constructed at the Productivity Enhancement Facility at the Marshall Space Fight Center to develop a system that can scan the panels automatically. The automated system under development measures, stores, and computes the thickness of gore panels under computer control. As a result of the improved reliability of this system, the quality of the panels will be enhanced. This system is also being developed because of its potential applications of inspecting other manufactured parts.

II. Present Chem Milling Processes/Procedures

The stretch-formed panels are initially checked for visual damage, stamp approval, and material type. The severity of the lueder lines is also observed. Lueder lines are valleys and peaks that occur in the metal as a result of stretch-forming. Stretch-forming also causes the panels to be tapered - thicker on the ends than in the middle in an attempt to make the panel as uniform as possible. The panel is then cleaned and the rough areas are sanded and the gouge pits are filled. The panel is then chem milled once more to try to make it even more uniform. The panel is then cleaned with a tap rinse and a deoxidizing cleaning agent. The panel is manually sprayed with a green transparent maskant and allowed to cure for several hours. The panel is then placed into a template where the design for that particular panel is scribed. The design is scribed manually with a sharp blade. The maskant is then peeled form the area that is to be chem milled first. The panel is chem milled and then rinsed. The next section of maskant is removed and the panel is then chem milled and rinsed again. These steps are repated until all the maskant is removed. A four inch grid is placed on the panel across the lueder lines. Using the grid, the panel is manually mapped for thickness. The thickness is measured ultrasonically with a point-to-point contact probe using water as couplant. The out-of-tolerance areas are outlined in 0.003 inch increments. The panel is then masked and cured again. The map lines are scribed and the highest area is peeled away. Three thousandths of an inch is chem milled from the exposed area. The panel is then cleaned and the next section of maskant is removed. Once again threee thousandths of an inch is chem milled from the panel. The removal of three thousandths is done after each section of maskant is removed until all the maskant is gone. The panel then goes through its final inspection. The surface is checked for chem milled defects. The chem milled line configuration is also inspected.

III. The Automated Gore Mapping System

A robotic system, that will replace the present method of mapping gore panels, is presently under development at the Productivity Enhancement Facility at Marshall Space Flight Center. The funding for this system is provided by NASA. The system is comprised of a Cincinnati Milacron T3-776 robot, a Krautkramer-Branson WDM ultrasonic thickness measurement device, a Packard Bell AT computer, and an end-of-arm-tool. The key part of the system is the ultrasonic measurement device. This device can measure the thickness of gore panels with an accuracy of +/- 0.01 inch. The sensor used with the device is a rubber-faced two-pieced transducer. A few drops of couplant is applied at the interface of the two pieces of the sensor. This supply of couplant will last several days. The sensor is installed on the end-of-arm-tool which is installed on the robot. The robot is an electrically driven, computer controlled, six axis, articulated arm.

The end-of-arm-tool (EOAT) consists of a rotating segment, retracting stem, microswitch, and an air cylinder. The rotating segment assures that the sensor is perpendicular to the panel. Four rubber stubs on the end of the segment press against the panel and four springs on the edge of the segment allow the simi-sphere segment to rotate. When the rotating segment is perpendicular, the stem of the EOAT retracts. The retracting allows for a microswitch to be triggered. The robot controller senses this signal, stops the robot, and then signals the robot to pop the sensor onto the panel. A 1.5 inch stroke, spring loaded, air cylinder is used to pop out the sensor. The Krautkramer-Branson emits a sound pulse a predetermined number of times. After this time period, if the Krautkramer-Branson does not lock onto a thickness reading, it signals the AT computer. In return the AT computer signals the robot controller to redo that particular point. At the next point, the process is repeated. After the gore panel has been completely scanned, a color-coded thickness contour of the out-of-tolerance regions on the panel can be generated and displayed on the AT computer. Three complete scans have been performed on one gore panel. All three scans are identical.

The Automatic Gore Mapping System has been simulated on a Silicon Graphics 3120 computer. The simulation of the system have been performed on Deneb's IGRIP and SILMA's Cimstation simulation packages. Using these packages, the most efficient workcell configuration can be obtained. The cycle time of the system can also be optimized. The packages also allow for less robot downtime, because the robot can remain in cycle while the operator sits in an office environment and simulates the workcell. The simulation is translated into robot code and then downloaded to the robot controller.

IV. FUTURE RESEARCH AND CONCLUSIONS

Further development of the Automatic Gore Mapping System is still in process. The down loading of the simulation of the system has to be performed to verify that the simualtion package will translate the simulation code into robot code. Also a simualtion of this system has to be programmed for a gantry robot instead of the articulating robot that is presently in the system. It was discovered using the simualtion package that the articulation robot cannot reach all the points on some of the panels, therefore when the system is ready for production, a gantry robot will be used. Also a "hydrosensor" system is being developed to replace the point-to-point contact probe. The hydrosensor will allow the robot to perform a non-contact continuous scan ot the panel. It will also provide a faster scan of the panel because it will eliminate the in-and-out movement required for the present end effector. The system software is currently being modified so that the hydrosensor will work with the system. The hydrosensor consists of a Krautkramer-Branson transducer encased in a plexiglass nozzle. The water stream pumped through the nozzle is the couplant for the probe. Also, software is being written so that the robot will have the ability to draw the contour lines on the panel displaying the out-of-tolerance regions. Presently the contour lines can only be displayed on the computer screen. Research is also being performed on improving and automating the method of scribing the panels. Presently the panels are manually scribed with a sharp knife. The use of a low power laser or water jet is being studied as a method of scribing the panels. The contour drawing pen will be replaced with scribing tool and the robot will then move along the contour lines. With these developments the Automatic Gore Mapping Systems will provide a reduction in time and labor costs associated with manufacturing the External Tank. The system also has the potential of inspecting other manufactured parts.

V. ACKNOWLEDGEMENTS

This work was funded by NASA contract NAS8-30300 under Technical directive 1.6.3.6/3.6.2.1-673-R3. The writers would like to thank the many NASA and University of Alabama at Huntsville personnel for their assistance and guidance during this project.

VI. REFERENCES

[1] Gilliam, D., Shiver, J.D., Workman, G.L. "Advantages of Off-Line programming and Simulation for Industrial Application." Special report of the Tenth Conference on Space and Military Applications of Automation and Robotics, Huntsville, AL, June 21-22, 1988.

[2] Langworth, E.M., Assistant to the president, Aerochem, Inc. 1885 North Batavia Street, Orange, CA.

Report Documentation Page

Field	Value
1. Report No.	NASA CP-3091
2. Government Accession No.	
3. Recipient's Catalog No.	
4. Title and Subtitle	Second Conference on NDE for Aerospace Requirements
5. Report Date	December 1990
6. Performing Organization Code	
7. Author(s)	Kenneth W. Woodis, Craig C. Bryson, Gary L. Workman, Compilers
8. Performing Organization Report No.	
9. Performing Organization Name and Address	George C. Marshall Space Flight Center Marshall Space Flight Center, Alabama 35812
10. Work Unit No.	M-646
11. Contract or Grant No.	
12. Sponsoring Agency Name and Address	National Aeronautics and Space Administration Washington, D.C. 20546
13. Type of Report and Period Covered	Conference Publication
14. Sponsoring Agency Code	

15. Supplementary Notes

The Second Conference on NDE for Aerospace Requirements was jointly sponsored by the Marshall Space Flight Center and The University of Alabama in Huntsville. It was held August 22-24, 1989, at the Huntsville Marriott. This document is the proceedings from that conference and provides copies of those presentations submitted for publication.

16. Abstract

Nondestructive evaluation and inspection procedures must constantly improve rapidly in order to keep pace with corresponding advances being made in aerospace materials and systems. In response to this need, the 1989 Conference on NDE for Aerospace Requirements was organized to provide a forum for discussion between the materials scientists, systems designers, and NDE engineers who produce current and future aerospace systems. It is anticipated that problems in current systems can be resolved more quickly and that new materials and structures can be designed and manufactured in such a way as to be more easily inspected and to perform reliably over the life cycle of the system.

17. Key Words (Suggested by Author(s))	18. Distribution Statement
nondestructive evaluation for aerospace systems, nondestructive inspection techniques	Unclassified-Unlimited Subject Category: 18

19. Security Classif. (of this report)	20. Security Classif. (of this page)	21. No. of pages	22. Price
Unclassified	Unclassified	280	A13

NASA FORM 1626 OCT 86

For sale by the National Technical Information Service, Springfield, VA 22161-2171

NASA-Langley, 1990